

UPDATED RESEARCH FOR COLLISION DAMAGE AND REPAIR OF PRESTRESSED CONCRETE BEAMS

Final Report

Prepared for the
National Cooperative Highway Research Program
Transportation Research Board
of
The National Academies

Kent A. Harries, Ph.D., F.ACI, P.Eng.
Jarret Kasan, Ph.D.
University of Pittsburgh, Pittsburgh PA

Richard Miller, Ph.D., FPCI, P.E.
Ryan Brinkman
University of Cincinnati, Cincinnati OH

May 2012

The information contained in this report was prepared as part of NCHRP Project 20-07, Task 307,
National Cooperative Highway Research Program.

SPECIAL NOTE: This report **IS NOT** an official publication of the National Cooperative Highway
Research Program, Transportation Research Board, National Research Council, or The National
Academies.

EXECUTIVE SUMMARY

Collisions between over-height vehicles and bridges are becoming more commonplace. Recent catastrophic collapses have led to a re-evaluation of the condition of many prestressed structures resulting in bridges being posted and, in some cases, emergency decommissioning of structures. Collision damage, however, is generally far from catastrophic. Nonetheless, sound repair techniques are critical if additional damage (typically related to corrosion) is to be mitigated.

The objectives of NCHRP 20-07/Task 307 are to: i) develop criteria to evaluate whether to repair or to replace a prestressed concrete girder damaged by a vehicular impact; ii) identify the gaps in the available information and practices related to repair of collision damage of prestressed girders; and iii) prepare a recommend practice report guide. The primary deliverable of this project is the *Guide to Recommended Practice for the Repair of Impact-Damaged Prestressed Concrete Bridge Girders*. The *Guide* is provided as Appendix A of this report. The *Guide* serves to update the 1985 *NCHRP Report 280: Guidelines for Evaluation and Repair of Prestressed Concrete Bridge Members* which remains a primary reference for this topic.

The report identifies, using multiple examples, the nature of impact related damage. An extensive review of literature covering inspection, assessment and subsequent repair methods for impact-damaged prestressed concrete girders is presented in Chapter 1. The emphasis of this review is on fiber-reinforced polymer (FRP) based repair techniques that have been developed since the publication of *NCHRP Report 280*.

An approach to rating impact damaged girders consistent with AASHTO bridge rating procedures is presented. Additionally, a minimum residual strength below which repair is not recommended is established. These approaches lead to establishing criteria for both the ‘repair or replace’ and ‘repair or do nothing’ decisions.

Nine repair techniques are described; four are generally recommended as being practical for repairing impact damaged prestressed concrete girders: externally bonded carbon fiber reinforced polymer (EB-CFRP); externally bonded post-tensioned CFRP (bPT-CFRP); post-tensioned steel (PT-steel); and internal strand splicing. In addition, external repairs in combination with strand splicing are discussed.

In order establish limitations associated with repair methods, three prototype structures and over 440 individual damage and repair scenarios were considered. From these analyses and designs, damage classifications based on strand loss and limitations of repair techniques are established. Other practical geometric constraints associated with repair techniques are also described and quantified.

TABLE OF CONTENTS

EXECUTIVE SUMMARY	3
LIST OF FIGURES	8
LIST OF TABLES	9
ACKNOWLEDGEMENTS	10
CHAPTER 1 BACKGROUND	11
1.1 Introduction.....	11
1.2 Objective of NCHRP 20-07 Task 307	12
1.3 Nature of Impact Damage to Prestressed Concrete Bridge Elements	12
1.3.1 Factors Affecting Impact Damage	12
1.3.2 Examples of Impact Damage	17
1.3.3 Examples of Impact Damage and its Repair	17
1.3.4 Examples of Impact Damage and <i>Temporary</i> Repair	17
1.4 Assessment Techniques for prestressed concrete members	32
1.4.1 Visual and Manual Inspection.....	33
1.4.2 Surface Potential Survey/Half-Cell Potential Survey	33
1.4.3 Remnant Magnetism	33
1.4.4 Acoustic Emission.....	34
1.4.5 Linear Polarization.....	35
1.4.6 Electrical Resistance	35
1.4.7 Fiber Optic Sensors.....	36
1.4.8 Impact-Echo	36
1.4.9 Electro-Chemical Impedance Spectroscopy (AC Impedance).....	36
1.4.10 Surface Penetration Radar.....	36
1.4.11 Magnetic Field Disturbance	37
1.4.12 Electrical Time Domain Reflectometry (ETDR)	37
1.4.13 Magneto-Elastic	37
1.4.14 Computed Tomography (CT).....	37
1.4.15 Radiography	37
1.4.16 New Prototype Instrument for Measuring Remaining Prestress.....	38
1.4.17 Flat Jack Method.....	38
1.4.18 Nebraska Method	38
1.4.19 Hole Drilling Strain Gage Method.....	38
1.5 Repair, Rehabilitation and Retrofit Techniques for Prestressed Concrete Elements	39
1.5.1 Conventional Repair Methods	39

1.5.2 Refined Damage Classifications	48
1.5.3 Emerging Repair Materials and Methods	49
1.5.4 Case Studies	64
1.5.5 Aesthetic Repairs	68
1.6 Survey of Current State of Practice	71
CHAPTER 2 RESEARCH PROGRAM AND FINDINGS	73
2.1 Research Approach	73
2.1.1 Analysis of Girders	74
2.1.2 Assessment of Efficacy of Repair	75
2.1.3 Removal of Strands to Affect Damage Spectra	76
2.2 Prototype Structures	76
2.2.1 Adjacent Box Girder Prototype AB	76
2.2.2 Spread Box Girder Prototype SB	77
2.2.3 I-Girder Prototype IB	79
2.2.4 Prototype and Repair Combinations	80
2.3 Limitations of Repair Techniques	83
2.3.1 Residual Capacity and Strengthening Limits	83
2.3.2 Limitations Associated with Girder Geometry	84
2.3.3 Limitations Associated with Repair Techniques	86
2.4 Results of Parametric Study	91
2.4.1 AB Prototype	91
2.4.2 SB Prototype	93
2.4.3 IB Prototype	95
2.5 Damage Location Along Span	103
2.5.1 Strand loss near supports	103
2.6 Synthesis of Parametric Study	104
2.6.1 Maximum Effect of CFRP Repair Techniques	105
2.6.2 Hybrid Repairs with Strand Splices	109
CHAPTER 3 RECOMMENDATIONS AND CONCLUSIONS	110
3.1 Guide to Recommended Practice for the Repair of Impact-Damaged Prestressed Concrete Bridge Girders	110
3.2 Gaps in Existing Knowledge and Need for Further Research	110
REFERENCES	111
NOTATION	120
APPENDIX A - <i>Guide to Recommended Practice for the Repair of Impact-Damaged Prestressed Concrete Bridge Girders</i>	122
APPENDIX B – AB Prototype Design Example	160

APPENDIX C – SB Prototype Design Example	172
APPENDIX D1 – IB Prototype Design Example	184
APPENDIX D2 – IB 3-3-2 Hybrid Repair Design Example	198
APPENDIX D3 – IB 3-3-2 PT-Steel Design Example	204
APPENDIX E – Survey Responses	212

LIST OF FIGURES

Figure 1 Examples of damage associated with vehicle impact.....	11
Figure 2 Examples of typical damage due to vehicle impact.....	12
Figure 3 Continuum of corrosion damage (Naito et al. 2006 and Harries 2006).....	14
Figure 4 Typical corrosion damage following impact-related damage.....	15
Figure 5 Repair methods presented in Shanafelt and Horn (1980).....	42
Figure 6 Strand splices (Shanafelt and Horn 1980).....	43
Figure 7 ABITB stressing gage (ABITB 2005).....	46
Figure 8 Schematic representations of CFRP applications.....	52
Figure 9 EB-CFRP and P-CFRP specimens tested by Wight et al. (2001).....	54
Figure 10 FRP Prestressing systems.....	55
Figure 11 Nonmetallic anchoring systems (Kim et al. 2008a).....	56
Figure 12 Mechanical anchorage (Bolduc et al. 2003).....	57
Figure 13 Gradual CFRP prestress force anchorage (Kotynia et al. 2011).....	58
Figure 14 Sika CarboStress PT-CFRP system (SIKA 2008b).....	59
Figure 15 S&P FRP Systems PT-CFRP system (S&P 2011).....	59
Figure 16 Schematic of externally bonded and NSM CFRP techniques.....	60
Figure 17 Brownsbarn Bridge (Pakrashi et al. (2010).....	65
Figure 18 Strand splice repair of exterior AASHTO I-girder.....	66
Figure 19 Exterior AASHTO I girder patched repair confined with GFRP August 2006.....	68
Figure 20 Strand splicing and patch repair sequence.....	71
Figure 21 Schematic representation of design space for impact repair.....	73
Figure 22 AB Prototype bridge and girder.....	77
Figure 23 SB Prototype bridge and girder.....	78
Figure 24 IB prototype bridge and girder (Yang et al. 2011).....	79
Figure 25 Repair of prototype IB girder (Yang et al. 2011).....	81
Figure 26 Contribution to capacity of repaired girder from EB-CFRP material.....	85
Figure 27 Anchorage of post-tensioned repair systems.....	85
Figure 28 Strand splice hardware and potential interferences.....	89
Figure 29 Results of parametric study of AB girders repaired with EB-CFRP.....	93
Figure 30 Results of parametric study of AB girders repaired with PT-CFRP.....	93
Figure 31 Results of parametric study of SB girders repaired with EB-CFRP.....	94
Figure 32 Results of parametric study of SB girders repaired with PT-CFRP.....	95
Figure 33 Results of parametric study of IB girders repaired with EB-CFRP.....	96
Figure 34 Results of parametric study of IB girders repaired with PT-CFRP.....	97
Figure 35 Results of parametric study of IB girders repaired with NSM-CFRP.....	97
Figure 36 Hybrid strand splice and fabric CFRP repair of IB 3-3-2.....	98
Figure 37 Schematic representation of rating factors for IB 3-3-2 hybrid repair.....	98
Figure 38 Bolster design for PT-Steel repair of IB 3-3-2.....	99
Figure 39 Moment envelopes for AB 3-2-0.....	104
Figure 40 Theoretical maximum number of severed prestressing strands, n_{max} , that can be replaced by CFRP based on the relative contribution to moment capacity.....	108
Figure 41 Theoretical maximum number of severed prestressing strands, n_{max-PT} , whose prestress force can be replaced by bPT- CFRP.....	109

LIST OF TABLES

Table 1 Summary of assessment techniques.....	32
Table 2 Repair selection criteria proposed by Shanafelt and Horn (1980).....	44
Table 3 Comparison of beam-end numerical ratings and overall ratings	47
Table 4 Damage classification metrics proposed by Harries et al. (2009).....	48
Table 5 Sample repair matrix.....	74
Table 6 Comparison of inventory rating factors for AB 3-2-0 prototype presented in Appendix B.	76
Table 7 Prototype material properties.....	82
Table 8 Repair scenarios considered in this study.....	83
Table 9 Appropriateness of repair technique by girder geometry.....	84
Table 10 Properties of available preformed FRP materials.....	86
Table 11 Results of parametric study for AB prototype girder.....	100
Table 12 Results of parametric study for SB prototype girder.....	101
Table 13 Results of parametric study for IB prototype girder.....	102
Table 14 Maximum strand loss that can be fully restored ($RF_D \geq 1.0$) for prototype structures.....	104
Table 15 Approximate values of α and β	106
Table 16 Maximum number of severed prestressing strands, n_{max} , that can be replaced by CFRP.....	107

ACKNOWLEDGEMENTS

This study was requested by the American Association of State Highway and Transportation Officials (AASHTO), and conducted as part of National Cooperative Highway Research Program (NCHRP) Project 20-07. The NCHRP is supported by annual voluntary contributions from the state Departments of Transportation. Project 20-07 is intended to fund quick response studies on behalf of the AASHTO Standing Committee on Highways. The report was prepared by Drs. Kent A. Harries and Jarret Kasan of the University of Pittsburgh and Dr. Richard Miller and Mr. Ryan Brinkman of the University of Cincinnati. The work was guided by a task group included Alexander K. Bardow (Massachusetts DOT), Issam Harik (University of Kentucky), Bruce V. Johnson (Oregon DOT), Bijan Khaleghi (Washington State DOT), William N. Nickas (Precast/Prestressed Concrete Institute), and Benjamin A. Graybeal (Federal Highway Administration). The project was managed by Waseem Dekelbab, NCHRP Senior Program Officer.

The authors wish to acknowledge the following for their direct contributions to the present work including providing many of the photographs presented:

Lou Ruzzi, PennDOT District 11

Tim Bradberry, TXDOT

Kelly Breazeale, TXDOT

Tim Keller, ODOT

Daniel Tobias, ILDOT

Sreenivas Alampalli, NYDOT

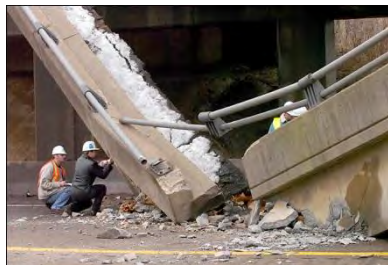
DISCLAIMER

The opinions and conclusions expressed or implied are those of the research agency that performed the research and are not necessarily those of the Transportation Research Board or its sponsoring agencies. This report has not been reviewed or accepted by the Transportation Research Board Executive Committee or the Governing Board of the National Research Council.

CHAPTER 1 BACKGROUND

1.1 Introduction

Collisions between over-height vehicles and bridges are becoming more commonplace (Fig. 1). Recent catastrophic collapses including Lake View Drive onto I-70 in Washington PA (Fig. 1a) and the McIlvaine Road vehicle collision only 8 miles east of Lake View Drive (Fig. 1b) have led to a re-evaluation of the condition of many prestressed structures. These evaluations have resulted in bridges being posted and, in some cases, emergency decommissioning of structures. Collision damage, however, is generally far from catastrophic (Fig. 1c) although sound repair techniques are critical if additional damage (typically related to corrosion) is to be mitigated.

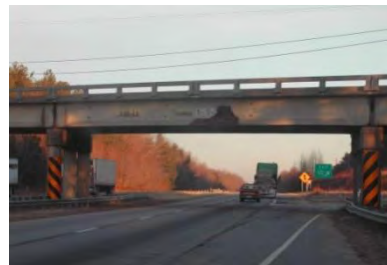


a) Lake View Drive collapse onto I-70. Impact damage led to significant strand loss, subsequent corrosion and eventual collapse under girder self-weight.

[Pittsburgh Post-Gazette]



b) Impact damage to fascia beam of McIlvaine Road over I-70. Entire bridge was demolished within 24 hours. [PennDOT]



c) Bridge over I-26 north of Columbia SC showing evidence of significant vehicle impact.

[Harries]

Figure 1 Examples of damage associated with vehicle impact.

Although there are many research and case studies addressing repair of prestressed bridge girders, there is little comprehensive guidance available. NCHRP Project 12-21, completed in 1985 and published as *NCHRP Report 280: Guidelines for Evaluation and Repair of Prestressed Concrete Bridge Members* (Shanafelt and Horn 1985) remains the most comprehensive national study to address the evaluation and repair of prestressed bridge members. A 1996 Texas study (Feldman et al. 1996) and a 2004 Wisconsin study (Tabatabai et al. 2004) have updated the earlier guides, but are limited in scope: the TXDOT study addresses only impact damage while the WIDOT study focuses primarily on corrosion mitigation techniques at girder ends in cases where strengthening or structural retrofit is largely unnecessary. Extant studies are necessarily out-of-date: i) they do not address the present state of the now 25-50 year-old prestressed concrete infrastructure and the inherent deterioration associated with this aging; ii) they do not address some of the newer methods of assessing the structural capacity and, importantly, residual prestress forces; iii) they are not consistent with present evaluation practices (AASHTO 2011); and, iv) they do not address some of the newer methods of retrofit including those using FRP materials and prestressed FRP materials.

To partially address these deficiencies, Harries et al. (2009) prepared a detailed report for Pennsylvania DOT entitled *Repair Methods for Prestressed Bridges*. While directed primarily at post-NCHRP Report 280 repair methods and focusing heavily on prestressed box girder structures, this PennDOT project and report forms a strong foundation for the present proposed study. Harries et al. provided: i) a detailed review of assessment techniques; ii) an extensive review of repair/rehabilitation and retrofit techniques including those addressed in NCHRP Report 280 and developed subsequently; iii) results from a North American survey of current state of practice; iv) 22 prototype repair examples; and v) a set of best practices recommendations. While the Harries et al. report provides a sound foundation for the present

study, it is limited in scope, provides only cursory guidance, and falls short of the objectives of NCHRP 20-07/Task 307.

1.2 Objective of NCHRP 20-07 Task 307

The objectives of NCHRP 20-07/Task 307 are to: i) develop criteria to evaluate whether to repair or to replace a prestressed concrete girder damaged by a vehicular impact; ii) identify the gaps in the available information and practices related to repair of collision damage of prestressed girders; and iii) prepare a recommend practice report guide.

1.3 Nature of Impact Damage to Prestressed Concrete Bridge Elements

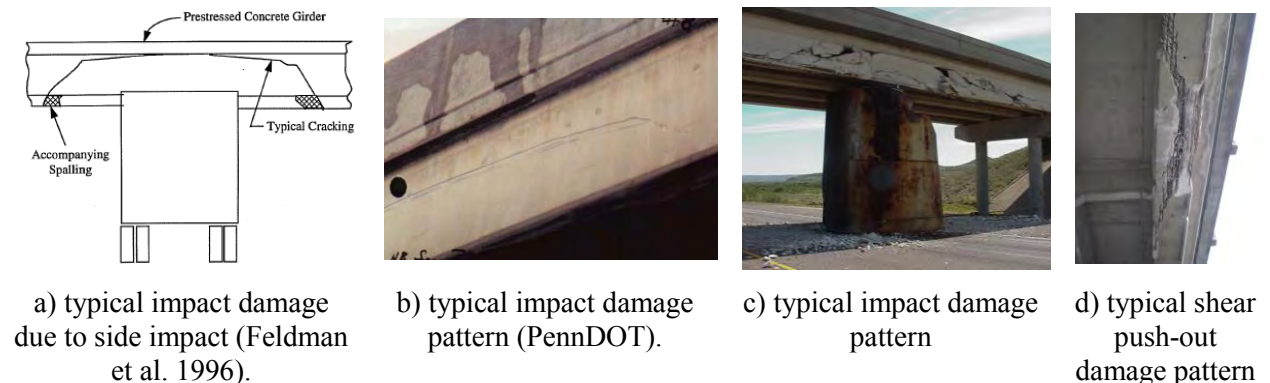
In a previous study (Harries et al. 2009), the authors categorized and provided examples of sources of damage observed in prestressed concrete bridge girders as follows:

- I. Impact by over-height vehicle
- II. Environmental distress/aging including freeze/thaw and water-induced
- III. Construction error or poor practice associated with previous repair
- IV. Construction error associated with appurtenance mounting
- V. Poor maintenance practice
- VI. Construction error
- VII. Load-related damage other than impact including the effects of natural disasters
- VIII. Extreme events such as natural disaster, fire or explosion.

The focus of this report is impact damage, although the repair methods described may also be employed for damage from other sources. Additionally, as will be described other factors including environmental exposure and construction error may compound the effects of vehicle impact.

1.3.1 Factors Affecting Impact Damage

Impact damage is usually readily apparent and varies from scrapes to structural collapse. Examples of impact damage are provided at the end of this section and are arranged, approximately, in order of severity from most severe to minor damage. Feldman et al. (1996) identified a commonly occurring damage pattern associated with side impact. The impact causes a torsion-induced shear cracking pattern in the exterior (or fascia) girder as shown in Figure 2a. In cases where the impact is more direct, this pattern becomes more of a shear push-out (Figure 2d). A discussion of damage classification is provided in Section 1.5.2. The following sections address additional factors affecting the nature of damage *in the context of repair*.



[Courtesy of the Texas Department of Transportation, © 2007 All rights reserved.]

Figure 2 Examples of typical damage due to vehicle impact.

1.3.1.1 Corrosion Damage Subsequent to Impact

Left uncorrected, minor damage (nicks and scrapes) may progress to becoming more significant as corrosion becomes manifest. Eventually corrosion can lead to section loss of the strand and resulting loss of prestress and member capacity. This continuum of corrosion damage is shown schematically in Figure 3. In general, the progression of corrosion-related damage tends to be exponential in time. Examples of typical corrosion damage observed following impact-related damage are shown in Figure 4. Repairing such damage must be accompanied by mitigating the damage where possible.

The source of corrosion-inducing chlorides may vary. Certainly, chlorides from de-icing salts may be introduced from the bridge deck as a result of poor drainage, damaged joints or other sources of damage. Adjacent box girder structures having a non-composite deck, for instance, may experience deck drainage through virtually every longitudinal joint. Leaking water then tends to ‘wick’ along the girder soffit affecting a large region of potentially susceptible concrete (Harries 2006). Chlorides may also be introduced as a result of spray from traffic passing beneath the bridge, also affecting the entire soffit region. Box girders may also be susceptible to chloride ingress from the top of the bottom flange if water is able to penetrate the girder cells (Naito et al. 2011). Based on observations and anecdotal evidence, this latter source is believed to be rare.

Susceptibility to corrosion and impact damage is compounded in cases where concrete cover is less than prescribed due to strand or reinforcing steel placement errors (observed by Harries 2006, Naito et al. 2006 and Naito et al. 2011). Naito et al. (2011) performed a destructive evaluation of several girders built in the late 1960’s and found that 92% of all strands had less cover than required. The clear cover varied from a maximum of 1.75 in. to a minimum of 0.69 in. (44.5 to 17.5 mm). Having such reduced cover provides chlorides a shorter path to the prestressing strands and thus a greater likelihood for corrosion damage. Additionally, reduced cover may lead to greater strand damage in an impact event.

1.3.1.2 Adjacent Strands

The strength capacity of a girder suffering impact damage may change significantly. If a prestressed concrete structure is impacted by a truck and only one strand is visible and severed the damage may be worse than what is apparent. Small strand spacing results in little concrete between strands. In this case, there may be insufficient concrete surrounding the adjacent strand(s) to allow the prestressing force of these strands to be transferred into the structure. As a result, a portion or all of the prestressing force near the impact may be ineffective. It may be prudent to disregard a portion or all of the contribution from surrounding strands at the affected section in a repair design.

1.3.1.3 Strand ‘Redevelopment’

Damaged strands in larger spans or long girders may be ‘redeveloped’ if there is sufficient undamaged length remaining. Conventional practice conservatively neglects any severed strand along the entire length of the girder in the analysis of the structure (Harries 2006). However, Kasan and Harries (2011) have shown that, away from the affected section, a severed strand ‘redevelops’ prestressing force in a manner consistent with the transfer length. They recommend that the transfer length of 60 strand diameters ($60d_b$) be used to redevelop severed strand once it re-enters sound concrete.

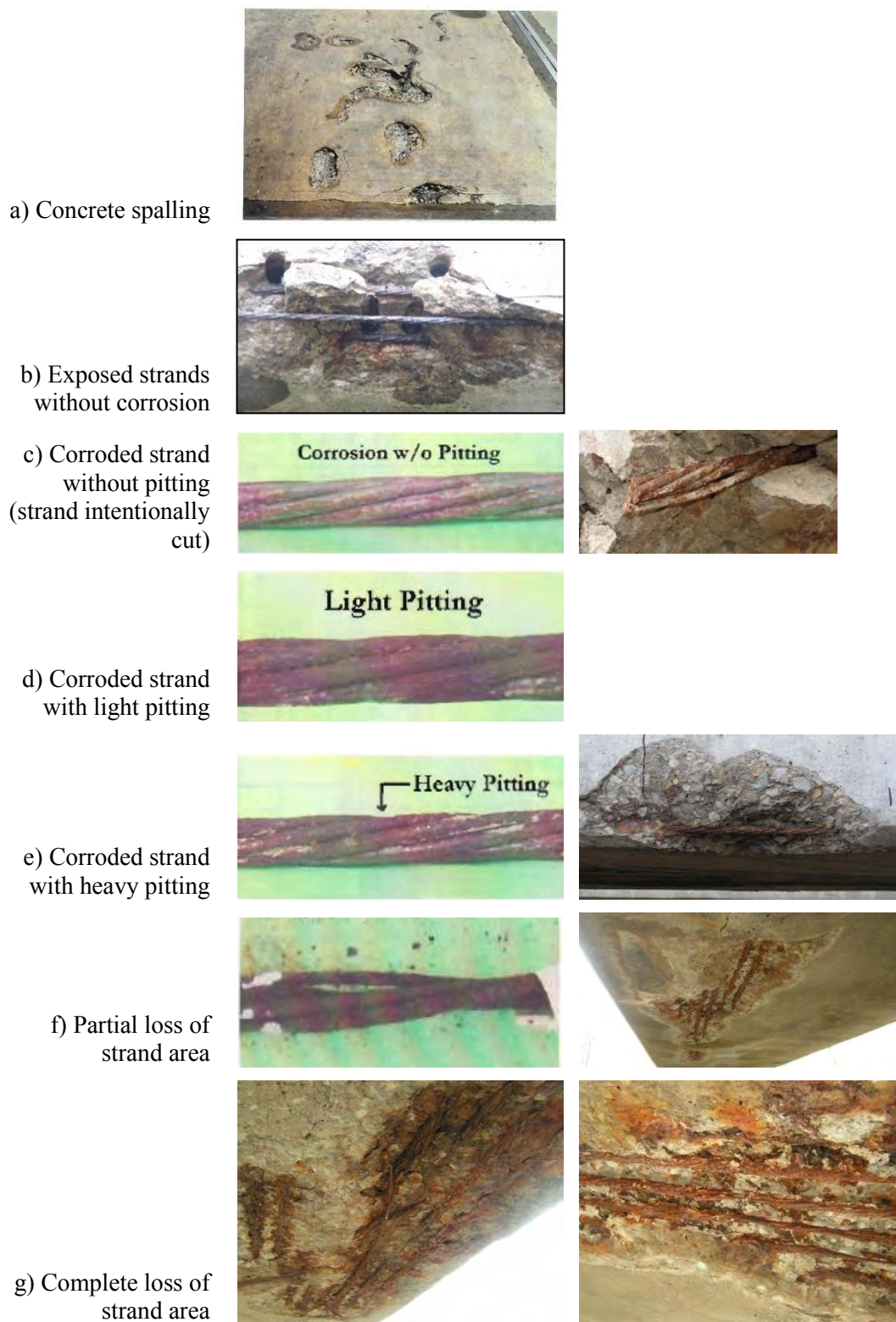
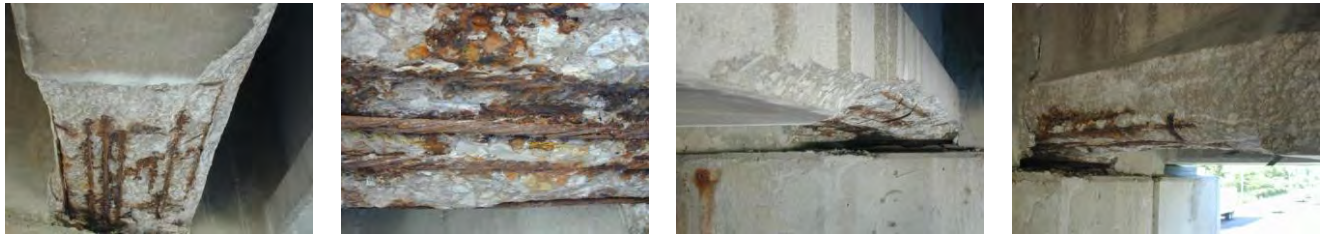


Figure 3 Continuum of corrosion damage (Naito et al. 2006 and Harries 2006).



a) AASHTO I-girder [photos: ILDOT]



b) AASHTO I-girder [photos: ILDOT]



c) Adjacent box girder [photos: Harries]

Figure 4 Typical corrosion damage following impact-related damage.

1.3.1.4 Unanticipated Composite Action

Exterior adjacent box girders often have a composite barrier wall resulting in an asymmetric section and load condition; and have strand loss (due to vehicle impact) on their lower exterior corner. There are a number of documented cases (e.g.: Harries 2009) of exterior AB girders rolling away from the bridge. Examples of such damaged girders are provided at the end of this Section. These effects individually (and more so in combination) result in a rotation of the principal axes of the section. As a result, the capacity of the girder to resist moment applied about its geometric horizontal axis will be reduced beyond what is predicted using a typical plane sections analysis due to the biaxial nature of the bending. In adjacent box bridges, this effect is most pronounced in exterior girders since interior girders are restrained from rotation by adjacent girders (Harries 2006). The effect of strand loss eccentricity and the resulting biaxial response to loading was observed by Miller and Parekh (1994) and Di Ludovico et al. (2007) and found to be negligible for double-tee girders.

This behavior becomes significant when performing load rating of the structure. Occasionally, the girder and barrier wall are assumed to be composite and a sections analysis is performed about the horizontal axis. Doing so will overestimate the true vertical capacity since it does not account for the biaxial response of the section (Kasan and Harries 2012a). Additionally, many adjacent box bridges have deteriorated or non-existent shear keys, resulting in the girders behaving independently (Harries 2006) and a corresponding increase in the transverse distribution factor (from 0.3 to 0.5 for adjacent box girders, for instance). Kasan and Harries (2012) present an analytical approach shown to capture anticipated eccentric behavior where it exists.

1.3.1.5 Asymmetric Loss of Prestressing Strands

Impact damage often results in asymmetric loss of prestressing strands, typically only affecting strands on one side of the girder. In most cases (including those presented here), effects resulting from asymmetric strand loss have not been taken into account (NCHRP 280). However, Kasan and Harries (2012a) performed an analytical study to capture the reduction in capacity when considering asymmetric strand loss in AB girders which are behaving compositely with their barrier wall/curb slab assembly. The asymmetric loss of strands and the composite action of the girder and their barrier wall/curb slab assembly (both of which result in an inclination of the neutral axis from the horizontal) result in a capacity reduction when performing an analysis about the original (horizontal) neutral axis compared with the actual rotated neutral axis. When considering the rotated neutral axis, the critical tension elements (in the exterior soffit corner) are typically those which are damaged by impact. Conventional uniaxial analyses do not account for the loss of critical tension elements and thus overestimates the actual member capacity. The study conducted by Kasan and Harries (2012a) has quantified this effect for AB structures only. Therefore, it should be noted that asymmetric effects are not typically accounted for in girder analysis, but studies have been conducted to quantify these effects which can be leveraged for other girder types.

1.3.1.6 Lateral Deflections and Twist of Girders

The asymmetric analysis method described in Kasan and Harries (2012a) does not specifically calculate the lateral stresses resulting from asymmetric strand loss. To do so, sweeping lateral curvature of the girder should be considered. Generally, if sweep is within the standard tolerance for prestressed concrete girders, lateral stresses can be ignored (Shanafelt and Horn 1985). However, lateral sweep is seldom caused by impact-damage but rather is a result of fabrication, storage or construction errors. Lateral sweep due to vehicle impact is typically abrupt and localized to the area near the impact.

Permanent twist or rotation can be caused by vehicle impacts or faulty manufacturing, storage or construction. Twist due to impact loading will generally crack the girder longitudinally at the bottom of the top flange (Figure 2) and at diaphragm locations. Permanent twist due to impact loading will be concentrated in the area of impact. Permanent twists may be accompanied with abrupt lateral offsets at the bottom of the girder (Figure 2d).

1.3.1.7 Effect of Diaphragms on Impact Damage

Many prestressed structures utilize intermediate diaphragms between beams for lateral stability. When a girder is struck by an over-height vehicle, the diaphragms transfer the impact load to the adjacent members. It was the goal of Yang et al. (2010) to determine if diaphragms transfer loads in a beneficial manner or simply extend the damage to girders beyond the impact region. Through the use of a finite element model of a 3-beam I-girder bridge, it was found that the strain energy transferred from the truck to the bridge with intermediate diaphragms was less than the energy transmitted to the bridge without intermediate diaphragms, indicating that the bridge with intermediate diaphragms experienced less vibration after impact. This suggests that structures with intermediate diaphragms performed favorably, by spreading the impact load to adjacent girders.

Yang et al. (2010) also aimed to determine which structural arrangement (with or without diaphragms) yielded less damage to the impacted girder. They showed that the shallower the intermediate diaphragm depth, the more vulnerable (more induced damage) the system became due to large deformation and rotation of the girder. Essentially, the girder flange will rotate about the diaphragm girder interface, and thus the shallower the diaphragm, the greater the lever arm and thus the greater the force and damage. Therefore full depth intermediate diaphragms were recommended. For a long bridge, multiple and distributed intermediate diaphragms resisted impact better by effectively transferring large deformations to other girders and the deck, reducing the damaged areas and absorbing more kinetic energy. Based on the model simulation, an optimized intermediate diaphragm spacing can be determined for a particular

loading (impact in this instance), and it was recommended that spacing intermediate diaphragms at 25 ft. (7.6 m) to 40 ft. (12 m) for bridges with a span of 100 ft. (30 m) or longer improves impact protection.

1.3.2 Examples of Impact Damage

The following pages provide examples of impact damage arranged, approximately, in order of severity from most severe to minor damage. The outcome of the damage, repair or replace girder/bridge is noted where known. Additional notes on the images are provided in some cases.

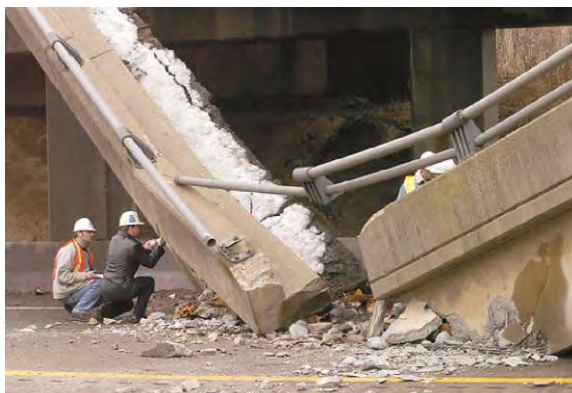






1.3.3 Examples of Impact Damage and its Repair

Following the examples noted above, further examples of impact damage and its subsequent repair are provided.

1.3.4 Examples of Impact Damage and *Temporary* Repair

Following the examples noted above, an example of impact damage and a temporary repair conducted by Illinois DOT is provided.

1.3.2 Examples of Impact Damage

			
<p>Lake View Drive bridge over I-70, Washington PA. Exterior girder collapsed December 26, 2005 under self-weight load only. Adjacent Box Girder; entire bridge demolished and replaced [Pittsburgh Post Gazette]</p>	<p>An I-45 overpass sits on the cab of a tractor trailer rig after collapsing when it was hit by the vehicle near Richland, Texas, Sunday, Sept. 8, 2002. <i>Impact was to pier column.</i> AASHTO I-girder; clearly, span was replaced [AP Photo/Donna McWilliam]</p>	<p>Soffit and fascia of McIlvaine Road bridge over I-70 damaged by vehicle October 18, 2010. Adjacent Box Girder; entire bridge was demolished and replaced [PennDOT D12-0]</p>	
			
<p>Vehicle impact to Sgt. Bluff bridge in Iowa, March 17, 2005. AASHTO I-girder; assume entire bridge was replaced [ODOT]</p>			



Exterior girder FM479 over Kerr Road, San Antonio TX.
 AASHTO I-girders; reported that entire bridge was demolished and replaced
 [Courtesy of the Texas Department of Transportation, © 2007 All rights reserved.]



RM215 over IH10, Pecos Co. TX.
 AASHTO I-girders; reported that only exterior girder was replaced
 [Courtesy of the Texas Department of Transportation, © 2007 All rights reserved.]



SH 183 at LP12, Dallas TX
 AASHTO I-girder; reportedly repaired
 [Courtesy of the Texas Department of Transportation, © 2007 All rights reserved.]

SH185 over US59
 AASHTO I-girder; reportedly repaired
 [Courtesy of the Texas Department of Transportation, © 2007 All rights reserved.]



Impact damage to SC bridge structure
AASHTO I-girder; bridge shown in service
[Harries]



12th Street over IH35, Austin TX
AASHTO I-girder; strands appear intact (fig b), repair shown in fig d
[Courtesy of the Texas Department of Transportation, © 2007 All rights reserved.]



FM3351 over IH10
AASHTO I-girder; reportedly repaired
[Courtesy of the Texas Department of Transportation, © 2007 All rights reserved.]



LP363, Temple TX
AASHTO I-girder; reportedly repaired
[Courtesy of the Texas Department of Transportation, © 2007 All rights reserved.]



Lufkin TX
AASHTO I-girder; reportedly repaired
[Courtesy of the Texas Department of Transportation, © 2007 All rights reserved.]



US54 at Altura Ave.
AASHTO I-girder; reportedly repaired
[Courtesy of the Texas Department of Transportation, © 2007 All rights reserved.]



US59 over LP287 (note previous repair material in fig b)
 AASHTO I-girder; reportedly repaired
 [Courtesy of the Texas Department of Transportation, © 2007 All rights reserved.]

US271 over LP286
 AASHTO I-girder; reportedly repaired
 [Courtesy of the Texas Department of Transportation, © 2007 All rights reserved.]



Impact damage to AASHTO I-girder
 [ILDOT]



US59 over US79
 AASHTO I-girder; reportedly repaired
 [Courtesy of the Texas Department of Transportation, © 2007 All rights reserved.]



LP301 over IH30
 AASHTO I-girder; reportedly repaired
 [Courtesy of the Texas Department of Transportation, © 2007 All rights reserved.]

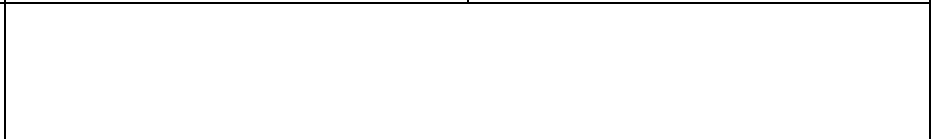


SH 302 at SP450
 AASHTO I-girder; reportedly repaired
 [Courtesy of the Texas Department of Transportation, © 2007 All rights reserved.]

IH20WB at CF1150
 AASHTO I-girder; reportedly repaired
 [Courtesy of the Texas Department of Transportation, © 2007 All rights reserved.]



US B67 over US 67
 AASHTO I-girder; reportedly repaired
 [Courtesy of the Texas Department of Transportation, © 2007 All rights reserved.]



		
<p>March 17, 2011</p>	<p>September 28, 2011</p>	<p>April 20, 2012 little additional damage was noted over the (relatively mild and snow-free) winter of 2011-12</p>
<p>Crawford Lane bridge over I-70 damaged by vehicle impact March 15, 2011. Adjacent Box Girder; single strand severed (arrow) [Kasan]</p>		
		
<p>fascia girder</p>	<p>1st interior girder</p>	<p>2nd interior girder</p>
<p>I-670 in Ohio AASHTO I-girders [ODOT]</p>		



Guardrail impact.
reported by source as box beam
[ODOT]

1.3.3 Examples of Impact Damage and its Repair



FM 1788 over IH20
AASHTO I-girder
[Courtesy of the Texas Department of Transportation, © 2007 All rights reserved.]



IH-35 at Kirnwood
AASHTO I-girder
[Courtesy of the Texas Department of Transportation, © 2007 All rights reserved.]



IH-35 at Corinth
AASHTO I-girder
[Courtesy of the Texas Department of Transportation, © 2007 All rights reserved.]



SH6 over SH30
 AASHTO I-girder
 [Courtesy of the Texas Department of Transportation, © 2007 All rights reserved.]



IH40 at Shamrock
 AASHTO I-girder
 [Courtesy of the Texas Department of Transportation, © 2007 All rights reserved.]



2006: vehicle impact #1



2007: vehicle impact #2



2008: vehicle impact #3

LP12 at Irving
AASHTO I-girder
[Courtesy of the Texas Department of Transportation, © 2007 All rights reserved.]



US183 over IH20
 AASHTO I-girder
 [Courtesy of the Texas Department of Transportation, © 2007 All rights reserved.]



Virginia Street
 AASHTO I-girder
 [Courtesy of the Texas Department of Transportation, © 2007 All rights reserved.]

1.3.4 Example of Impact Damage and *Temporary* Repair



1.4 Assessment Techniques for prestressed concrete members

A review of non-destructive testing and evaluation (NDT/NDE) techniques for assessing prestressed concrete elements was undertaken. The following sections summarize these techniques. A brief summary of the appropriateness of each method concludes each section. The sections are arranged approximately in the order of their current degree of utility for assessing prestressed girders *in situ*. Some techniques are clearly still in the development stage. Table 1 provides an indication of the utility of each approach – appropriate for inspection or long term monitoring – and the degree to which the methods are developed for bridge applications. “At speed” inspection refers to vehicle mounted systems that operate as they transit the bridge structure.

Table 1 Summary of assessment techniques.

method	inspection	at-speed inspection	traffic closure necessary	destructive evaluation	suitable for long-term monitoring	<i>in situ</i> applications	deployable in 2012	utility
visual	yes	no	occasionally	occasionally	no	yes	yes	excellent
surface potential	yes	no	occasionally	contact with steel req'd	no	yes	yes	very good
remnant magnetism	yes	yes	occasionally	no	no	yes	yes	good
acoustic emission	yes	no	occasionally	no	yes	yes	yes	good
linear polarization	yes	no	no	contact with steel req'd	yes	yes	yes	yields limited data
electrical resistance	yes	no	no	contact with steel req'd	yes	yes	yes	yields limited data
fiber optic	no	no	no	no	yes	yes	yes	excellent
impact echo	yes	no	yes	no	no	yes	yes	yields limited data
AC impedance	yes	no	no	contact with steel req'd	yes	no	no	yields limited data
radar	yes	in some applications	occasionally	no	no	limited	limited	poor
magnetic field	yes	no	occasionally	no	no	no	no	poor
ETDR	yes	no	occasionally	no	no	yes	yes	yields limited data
magneto-elastic	yes	no	no	no	no	no	no	none
CT	yes	no	probably	no	no	no	no	none
radiography	yes	no	probably	no	no	no	no	none
Civjan et al. 1998	yes	no	yes	yes	no	no	no	unproven: strand stress
flat jack	yes	no	yes	yes	no	no	yes	limited; prestress
Nebraska test	yes	no	yes	yes	no	no	yes	limited; prestress
hole-drilling	yes	no	yes	minimal	no	no	yes	none

Notes:

1. inspection methods are intended for discrete deployment as different from long-term monitoring methods that remain in *in situ*.
2. at-speed inspection refers to vehicle mounted systems that operate as they transit the bridge structure.
3. traffic closures may be required for equipment or may be required because traffic will result in ‘noise’ in data obtained. “occasionally” indicates that traffic closure is required when decks are inspected.
4. destructive evaluation methods (e.g.: pulling concrete cores) require subsequent patching.
5. *in situ* applications implies that there are documented demonstrations of the method used in prestressed bridge applications
6. deployable in 2012 implies that there are commercially available systems appropriate for bridge applications on the market.
7. utility refers to the question “can the method be practically used in the assessment of prestressed concrete bridges *today*?”

1.4.1 Visual and Manual Inspection

In general, visual inspection is the only practical triage tool; locations requiring further non-destructive or destructive evaluation are identified. Nonetheless, a skilled inspector, familiar with the structure she is inspecting will still provide a remarkably accurate assessment of the condition of the structure although is unlikely to be able to accurately quantify many damage types.

Shanafelt and Horn (1980 and 1985) categorize physical damage into 3 separate categories: minor, moderate, severe. Detailed assessment of damage such as damage caused by corrosion of strands or the remaining effective prestress was not mentioned. The initial damage inspection is conducted visually with the help of some tools such as a chipping hammer, magnifying glass, ultrasonic test equipment, concrete coring equipment, etc

A simple method of assessing the condition of concrete is to tap the surface with a hammer and listen to the resulting tone (Mehta and Monteiro 2006). A high frequency pitch indicates a sound concrete whereas a lower frequency pitch indicates the presence of flaws. This simple method combined with visual inspection of concrete surface for cracks extending over the reinforcement length may provide preliminary information about the structure. However, it is dependent on the skill level of the operator and does not provide information about the extent of damage.

The disadvantage of visual inspection is its local nature. Except in the presence of significant damage, only information about the cover concrete and outermost layers of steel may be assessed. Sections that are chipped during inspection must be repaired afterwards, which might provide a focal point for future corrosion.

For multi-strand tendons, the ‘screw-driver-test’ (Walther and Hillemeier 2008) tests the state of the tendon by trying to wedge a flat-head screw driver between strands. Nonetheless, only a limited number of wires can be visually inspected. With great care, the screw-driver test may be conducted on individual strands.

1.4.2 Surface Potential Survey/Half-Cell Potential Survey

Half-cell or electrode potential mapping is a widely accepted method for detecting corrosion of steel embedded in concrete (Ali and Maddocks 2003). The entire surface is mapped by recording the surface potentials with respect to a reference electrode. Locations with higher negative potentials indicate areas of corrosion. However, this correlation does not always hold and surface potentials are greatly influenced by surface conditions. It is not possible to distinguish between reinforcement and prestressing strands.

The corrosion potential of the steel in concrete can be measured as the voltage difference between the reinforcement and the reference electrode in contact with the concrete surface (Mehta and Monteiro 2006). Measured potentials have been assigned to certain corrosion probabilities in ASTM C876. By moving the reference electrode, a relative potential map can be made which shows areas that are more susceptible to corrosion. This is a quick and inexpensive method that may be used during planning of areas that need repair. However, results may be affected by the degree of humidity of concrete, oxygen content near the reinforcement, existence and extent of microcracks, or electrical stray currents. Due to these reasons, ASTM has specified certain conditions where the technique should not be applied. It should be recognized that results of this method are not quantitative. Connection of the equipment to the steel reinforcement is required.

The surface potential survey/half-cell potential survey is a well-established standardized technique. While cumbersome, it is presently most viable and widely used *in situ* alongside visual and other manual forms of inspection.

1.4.3 Remnant Magnetism

Remnant magnetism is useful to get information about the location of prestressing steel fractures and the degree of damage to a strand. The prestressing steel strands are magnetized up to saturation to remove

their magnetic history. This process is performed by an electromagnet along the direction of the tendon. Fractures and breaks in the prestressing tendons are detectable but the size of the defect or loss of section is not (Ali and Maddocks 2003). Limitations of the method are related to the density of the reinforcement present and the minimum degree of damage that is sought (Scheel and Hillemeier 2003). The method can be applied on the vertical face or the bottom face of a member. The magnetic properties of the steel change with different levels of prestressing. Fracture can be detected even if it is screened by other wires or if the resulting gap in the steel is relatively small. Measurement speed can be increased by magnetizing the tendons by using a large mobile magnet and then scanning the magnetic flux of the entire surface.

Walther and Hillemeier (2008) evaluated the remnant magnetism technique on prestressed concrete decks. The tendons were magnetized with an electromagnet placed on the surface of concrete and then the magnetic leakage fields are monitored for any irregularities which might be caused by fractures in wires. Individual fractured wires can be detected even if they are inside a bundle of several intact strands. When testing tendons from the upper surface, it is possible to speed up the process with the use of a large mobile magnet to magnetize several tendons of lengths up to 11.5 ft. (3.5 m) at the same time. The development and the applicability of a test vehicle and the large magnet were shown together with the experimental data. The measuring speed has been increased by several magnitudes which allow testing without severe disruption to traffic.

Taffe et al. (2010) described a mobile system (similar to that of Walther and Hillemeier 2008) used to detect fractures and voids in a prestressed concrete deck. This equipment, in conjunction with specialized software, can provide data which identify the location of the prestressing steel. In doing so, the absence of prestressing steel can be seen, thus indicating a damaged strand. The resolution is approximately 0.8 in. (20 mm). This process can be performed quickly; up to 43,000 ft.² (4,000 m²) can be covered in one shift. While there are still some concerns regarding false positive readings (where the equipment suggests a fracture which does not occur), additional time can be spent in these areas and will likely improve results. When considering the local nature of impact damage, it is likely that this technique will not be needed to review a large area, but rather only the affected girders. Therefore, the area under investigation will be well defined and the possibility of false positives reduced.

Commercially available systems are primarily aimed at detection of flaws/damage in prestressed slabs. Available systems could be readily adapted to high-speed applications on bridge soffits. Regardless, this technique is very promising in near-term.

1.4.4 Acoustic Emission

The acoustic emission (AE) technique is a noninvasive, nondestructive method that analyzes noises (“events”) that are created when materials (i.e. concrete or prestressing steel) deform or fracture. Events occurring inside the structure create waves that are collected at the surface by receivers (Ali and Maddocks 2003 and Mehta and Monteiro 2006). Continuous monitoring is carried out with sensors. Monitoring can be used to identify new cracks but will not provide information on previously existing damage.

The method is applicable for real-time health monitoring of a bridge or a girder (De Wit 2004 and Ramadan et al. 2007). AE was very successfully used to quantify and precisely locate damage to two prestressed box girders tested to failure (Harries 2006).

AE monitoring was performed on an elevated portion of the I-565 interstate highway in Huntsville, Alabama to investigate the feasibility of using AE testing to assess the performance of prestressed concrete bridge girders (Hadzor 2011). Additionally, this work used AE testing to evaluate the effectiveness of the fiber-reinforced polymer (FRP) repair used on damaged portions of the girders by comparing pre- and post-repair results. Because support conditions varied between pre- and post-repair conditions, this comparison was unable to draw any conclusions. Regardless, AE monitoring of the

girders prior to and after the repair yielded independent, but informative results, confirming the usefulness of AE monitoring for prestressed girders as well as FRP repairs.

AE is a viable method of continuous structural health monitoring. Alternate approaches using known applied loads (trucks) have been demonstrated to be viable methods of inspection (as different from monitoring). The methods are very promising and viable for ‘problem structures’, although some technical hurdles remain before wide-spread deployment is practical. Again, it is important to reiterate that AE methods are presently ‘baseline’ techniques, that is, they are unable to capture damage occurring before monitoring is initiated. Some studies have been initiated on ‘non-baseline’ damage assessment using AE-based methods, but these remain in the research stage (Kim et al. 2006; Sohn et al. 2008).

1.4.5 Linear Polarization

In this method, the corrosion rate of a metal is measured from its polarization resistance (Mehta and Monteiro 2006). This is determined by applying a small DC voltage. This method is widely used both in the field and for research. The reference provides average values for resistance, which are correlated to corrosion. The advantage of this method is that commercial equipment is available to measure polarization resistance of existing structures in the field and also the results can be obtained quickly. There are also some limitations to this technique. The whole reinforcing bar is polarized and a single value is determined as the resistance, which is essentially an average result for all steel in the vicinity. This method also enables rapid corrosion rate measurement and is useful for measuring low rates of corrosion, less than 2.5 microns/year (Ali and Maddocks 2003), but the problem here is that it assumes corrosion to be uniform throughout the reinforcement section which is not true for the usual case (Ali and Maddocks 2003 and Mehta and Monteiro 2006). Therefore, localized corrosion in the form of pitting is averaged over the entire strand length. Also, the method assumes that concrete resistivity is low whereas it is usually high. Especially in conditions where concrete is dry, this assumption may lead to significant error.

Ali and Maddocks (2003) also point out that measurement of the polarization resistance in large concrete structures requires further investigation especially in the presence of corrosion mitigation measures that limit current spread in the strand. Additionally, probes cannot distinguish between reinforcement and prestressing steel.

As part of a long-term experimental program performed by Suh et al (2007), it was necessary to monitor corrosion inside concrete specimens. In order to decrease the time required to corrode the strands, either a constant current or voltage was applied, or the specimens were initially produced by using permeable concrete with high w/c ratios or by casting specimens with inclusion of chlorides. Three different techniques were employed to monitor corrosion and determine the effectiveness of several FRP materials on corrosion prevention. Half-cell potential measurement, linear polarization measurements and soil resistance. Although unexpected fluctuations were obtained, they are useful for approximate results and in understanding the general trend and increase in corrosion.

Broomfield (1994) acknowledged that this method is useful for lab testing but some modifications are required for field testing. Regardless, the linear polarization method can be viable to obtain general condition assessment of strand in structure but is unable to address critical aspect of localization of damage and thus its use in assessing impact (and associated corrosion) damaged prestressed concrete structures is not anticipated.

1.4.6 Electrical Resistance

Electrical resistance of the steel strands is being used to detect corrosion (Ali and Maddocks 2003). Since resistivity is constant for a given steel sample, change in electrical resistivity must be caused by a change in cross-section, most probably due to corrosion. As the section gets smaller, electrical resistivity increases. It is assumed that all wires undergo the same amount of corrosion. A drawback of the method is that short circuits at the anchorage points or within the structure (stirrups) affect results.

The resistivity of concrete when exposed to an electrical current is highly correlated to the amount of ions in the concrete and the state of the reinforcement (Mehta and Monteiro 2006). Highly resistive concrete has little possibility of corrosion. Therefore it is possible to assess the degree corrosion by determining the resistivity of the section. CEB-192 (1998) has estimated values for concrete resistivity depending on the amount of corrosion rate.

Similar to linear polarization, this method has limited usefulness *in situ* and its use in the immediate future to assess impact (and associated corrosion) damaged prestressed concrete structures is not anticipated.

1.4.7 Fiber Optic Sensors

The basic idea of the stranded optical fiber sensor is to measure the degree of attenuation of light due to microbending (Hariri and Budelmann 2001). In a wire, as the strain or stress increases, so does the amount of attenuation. Analysis of the ratio of light input to output when compared to a reference wire enables the determination of internal stress levels of the wire. Fiber optic sensors have been demonstrated to be a reliable and durable method for assessing displacement or strain. Hardware is not inexpensive at this time.

1.4.8 Impact-Echo

The impact-echo method relies on a stress pulse introduced in the structure by a small impact and the reflected stress wave collected by a nearby transducer. The time of travel is calculated from the reflected stress wave and the corresponding frequencies denote locations of reinforcement or voids. The main difference from radar is the use of low frequency waves (up to 60 kHz) which addresses some problems related to non-homogeneity of concrete. Although the method is relatively successful in locating voids and reinforcement, it is not suitable for the use of assessing corrosion (Ali and Maddocks 2003).

Watanabe et al. (2005) used the impact echo technique with a scanning technique called “stack imaging of spectral amplitudes based on impact-echo” (SIBIE) to detect voids in grouted post-tensioning ducts. Laboratory specimens were tested with impact tests from steel balls. Elastic waves emitted by the impact were recorded with an accelerometer. Subsequent tests varied the location of the impactor and the sensor in order to scan the member. It was found that when the impactor was located over a duct, a void could be detected. Zein et al. (2008) demonstrated impact-echo method to determine deterioration of decommissioned 40-year-old Interstate girders subject to fatigue loads in a laboratory environment. Apparent deterioration of concrete modulus as function of load correlated well with physical measures of accumulated damage (strain and displacement). Despite these successful laboratory demonstrations, the impact-echo method is not practical for field implementation.

1.4.9 Electro-Chemical Impedance Spectroscopy (AC Impedance)

This method measures the polarization resistance as well as assessing the physical processes in concrete and concrete-steel interface (Mehta and Monteiro 2006). Small amplitude AC signals are introduced into the concrete and the time lag and the phase response are investigated in the response. Although this method has been used in laboratories, its use is limited for field applications. The necessary equipment is bulky and complex. Similar to the polarization resistance technique, the results are average values over an area and therefore assume uniform corrosion of reinforcement, which is rare. Also, physical connection to the reinforcement is required which might require some amount of concrete removal and patching work. Although this is a powerful method being able to separate the individual processes at different layers, it is still too complicated for practical use. This approach is currently impractical for field application.

1.4.10 Surface Penetration Radar

Surface penetrating radar works on the principle of reflection of high frequency electromagnetic pulses from interfaces between materials with different dielectric constants such as steel, concrete and voids (Ali and Maddocks 2003). The transducer is passed over the section to locate the position and depth of

tendons. However, this technique can only give relative results and is not suitable for detecting corrosion. It should be used together with destructive methods for an estimation of tendon loss. This technique is not well suited to assessing state of deterioration/damage although appropriate for identifying *in situ* conditions if these are not known.

1.4.11 Magnetic Field Disturbance

The magnetic field disturbance method consists of applying a constant magnetic field to the member and scanning all assessable surfaces for any abrupt change in the field which might indicate a flaw in the strands (Ali and Maddocks 2003). This method is able to detect corrosion and strand failures but is limited in its resolution and accuracy. Each type of defect: pitting, notches, loss of section, etc. has its own unique signature which enables the user to distinguish between them. However, stirrups and other metallic objects embedded in the structure may hide the actual metal loss or defects and lead to errors (Ali and Maddocks 2003). The detectable defect size is 5% loss of section when there are no stirrups. When stirrups are present, there is a significant loss in resolution, and the detectable defect size increases to 40% loss of section when the stirrups are spaced at 400 mm. With further decrease in the spacing of stirrups, the method loses its capacity to give accurate results. A high level expertise is required to interpret the results. Furthermore, *a priori* knowledge of the structure such as locations of reinforcement is required to be able to interpret results. This approach is currently impractical for field application, although improvements in resolution are expected to improve its viability.

1.4.12 Electrical Time Domain Reflectometry (ETDR)

The method is used to detect, locate and identify the sizes of voids filled with air or water in post-tensioned ducts (Okanla et al. 1997) although provides little other useful data. ETDR is not used for corrosion assessment, although results can be used to direct further investigation.

1.4.13 Magneto-Elastic

The magnetoelastic measurements correlate the magnetic flux density at saturation of the strand to its stress level (Hariri and Budelmann 2001). A formulation is given to predict stress, however, the constants need to be calibrated before testing. Method requires extensive calibration and is not yet viable for *in situ* application.

1.4.14 Computed Tomography (CT)

Computed tomography measures the attenuation of an incident beam that travels in a straight path in an object (Ali and Maddocks 2003). Computed tomography using x-rays, electrical impedance tomography, and backscattering microwave imaging are methods applicable to concrete (Mehta and Monteiro 2006). X-ray computed tomography shows promise in detection of cracks and in locating reinforcing steel in moderate size structures. However, it requires elaborate work and is costly for setup and operation. Electrical impedance tomography is fast, inexpensive, easy to use, and has the potential for locating reinforcing steel, water-filled fractures, and may provide some information about corrosion around reinforcement. Microwave imaging can be used to locate reinforcing steel within 2.5 in (64 mm) of the surface. Although it is limited to shallow sections, it is fast, simple and relatively inexpensive.

This technique is currently impractical for field application. The method can only be used when there is significant loss of section due to corrosion. Surface temperature variations and other climatic conditions affect results. The resolution limit of 0.04 in. (1 mm) and also the contrast resolution should be improved in order to use it for corrosion determination. Data collection and processing is slow.

1.4.15 Radiography

Radiographic examination involves the use of a powerful radiation source to produce x-rays (Ali and Maddocks 2003). Access to both sides of the structure is required in this method. Visualization may be achieved by either radiographs or real-time imaging. For radiographs, radiographic film is exposed for up to 30 minutes. The practical limit of concrete thickness for this method is 24 in. (600 mm). For real-time

imaging, French Scorpion System is available. While yielding tremendous results, this approach is currently impractical for field application. Application of radiographic techniques has also been reported by Petrou et al. (2000) in conjunction with freshly placed concrete.

The following four approaches have been proposed for assessing the existing prestress in concrete girders.

1.4.16 New Prototype Instrument for Measuring Remaining Prestress

Civjan et al. (1998) developed a prototype instrument to estimate the remaining prestress in the strands. A lateral force is applied on the strands and the corresponding lateral displacement is measured. During experimental testing of the research project, the instrument was calibrated for 0.5 in. 7-wire strand with exposed lengths of 1.5 to 3.75 ft. (4.9 to 12.3 m). Overall, the prototype instrument for estimating stress levels in prestressing strands performed very well. It was seen that with the use of this device, measurements can be conducted quickly and inexpensively. Furthermore, the test results were within 10% of actual stress levels. With this method, the induced prestress during repair works such as strand splicing or preloading can also be monitored and checked for adequacy. However, further experimentation with different types of strands, number of wires and exposure lengths is necessary before field application since all of these factors may affect results. The suitable calibration charts must be present before actual testing. Although a promising tool, it is not known if further development or commercialization has been undertaken. Method is most appropriate for QC/QA of spliced repairs.

1.4.17 Flat Jack Method

Turker (2003) developed the 'flat-jack method' to assess stress in a member. The distance between two points on the surface is precisely measured. Afterwards, a slit is cut into the concrete in between these two points in a direction perpendicular to the stress to be determined. The local stress in the structure is relieved due to the slit and so the relative distance between the two points decreases, for the case of compression. Then, a hydraulic jack is inserted into the slit and pressure is applied until the distance between the two points is equal to the initial distance. The pressure on the jack is equal to the internal stress in the structure. The advantage of this method is that the elastic modulus of concrete is not used to measure the *in-situ* stress. The disadvantage is that the stress distribution applied by the jack might be different than the internal stress, which might lead to an error. This method is partially destructive and may be complicated to apply *in situ*. Nonetheless, the method may be appropriate in certain circumstances.

1.4.18 Nebraska Method

The Nebraska method was developed to measure the effective prestress in prestressed concrete bridge girders (Turker 2003). A cylindrical hole having a diameter of 1 in. is drilled into the concrete and then a crack is induced in the hole. This crack extends in the direction parallel to the main axis of stress. Then, external force is applied perpendicular to the direction of the crack and the stress necessary to close the crack is determined. This value is then related to the effective prestress. Although special hardware has been developed to clamp to the underside of the bridge girders, it may still be difficult to apply this method in situations where the geometry does not allow it. So, its applicability is limited in this sense. The method has limited application and calibration is not certain, hence this method is not anticipated to be practical for *in-situ* assessment.

1.4.19 Hole Drilling Strain Gage Method

This is a widely used method to determine the residual stresses near the surface of isotropic, linearly elastic materials (ASTM E837). A small diameter hole is drilled in an elastic material to relieve strains which are measured by an attached three-gage rosette. A hole is drilled in the center of the strain rosette either completely through the section or to a depth exceeding 40% of the diameter of the strain gage. The method is reported to give good results when the material is isotropic, the internal stresses do not vary greatly, and when the structure is more like a large plate compared to hole size (Turker 2003). However,

the method is not applicable to concrete due to its heterogeneous nature. The theoretical solution of the problem is presented in detail in Turker, but experimental verification is needed before application. Known (unpublished) experimental application as yielded marginal results. This approach is currently impractical for field application.

1.5 Repair, Rehabilitation and Retrofit Techniques for Prestressed Concrete Elements

A review of repair, rehabilitation and retrofit techniques suitable for impact-damaged prestressed concrete bridge elements was carried out. NCHRP 12-21 project identified many repair methods to restore strength and serviceability to prestressed concrete girders. The resulting *NCHRP Reports 226* and *280* (Shanafelt and Horn 1980 and 1985) provided a synthesis of a significant amount of research assessing the viability of each repair method. The technologies discussed in these reports and related subsequent research is referred to as ‘conventional repair methods’ in this report. These methods include: strand splicing, external steel post-tensioning, metal sleeve splicing and beam coatings.

NCHRP Reports 226 and *280* are summarized in Section 1.5.1.1. Literature pertaining to conventional repair technologies reported subsequent to NCHRP 12-21 are described in Sections 1.5.1.2 to 1.5.1.4. Section 1.5.2 discusses impact damage classification refined since NCHRP 12-21. Section 1.5.3 focuses on repair techniques developed *since* the NCHRP 12-21 study, focusing on existing and emerging methods and philosophies for repairing prestressed concrete structures, such as the use of fiber reinforced polymers (FRP) and stressed FRP systems. Case studies employing prestressed girder repair techniques are discussed in Section 1.5.4. Finally, a review of aesthetic repair and patching techniques is provided in Section 1.5.5.

1.5.1 Conventional Repair Methods

1.5.1.1 Review of NCHRP 12-21 Project

NCHRP Report 226 (Shanafelt and Horn 1980) focused on providing guidance for the assessment, inspection and repair of damaged prestressed concrete bridge girders. Suggestions were given for standardized inspection including proper techniques, tool and forms. The authors emphasized the need to separate damage assessment tasks (inspection) from engineering assessment tasks (load rating, etc.).

Often the decision to replace or the repair method chosen was not appropriate for the level of damage, resulting in inefficient and improper repair actions. A damage classification system, allowing users to quantify the damage present was proposed. Damage was quantified into one of the three categories:

MINOR damage was defined as concrete with shallow spalls, nicks and cracks, scrapes and some efflorescence, rust or water stains. Damage at this level does not affect member capacity. Repairs are for aesthetic or preventative purposes.

MODERATE damage includes larger cracks and sufficient spalling or loss of concrete to expose strands. Moderate damage does not affect member capacity. Repairs are intended to prevent further deterioration.

SEVERE damage is any damage requiring structural repairs. Typical damage at this level includes significant cracking and spalling, corrosion and exposed and broken strands.

Minor and moderate damage can be repaired via patching and painting; guidelines were provided for these tasks. Since minor and moderate damage do not require structural repairs, emphasis was placed on severe damage.

In *Report 226*, eleven different repair methods were developed for the severe damage condition and were discussed in detail; none however was demonstrated or tested. Repair methods considered were external post-tensioning, metal sleeve splicing (to avoid confusion, this method will be referred to as ‘steel jacketing’ in the present work), strand splicing, combinations of these methods, and replacement.

Each repair technique was evaluated to provide an overview of the processes and advantages and limitations of the method. Guidelines were proposed based on service load capacity, ultimate load

capacity, overload capacity, fatigue life, durability, cost, user inconvenience and speed of repairs, aesthetics and range of applicability. Evaluation of the repair techniques based on these parameters was conducted using a value-engineering process. Topics to be considered for future research were identified; these were particularly associated with the proposed splice repairs. Some of the repair techniques presented needed to be tested and evaluated for strength and fatigue loading. *NCHRP Report 226* considered the following repair methods:

Preload Most repairs proposed in *Report 226* make use of preloading, during girder repair. Preload is the temporary application of a vertical load to the girder during repair. The preload is provided by either vertical jacking or, more conventionally a loaded vehicle. If the damage has caused a loss of concrete without severing strands, preloading during concrete restoration can restore strength of the girder without adding prestress. In this case, preloading may be used to restore partial or full prestress to the repaired area; effectively reducing tension in the repaired area during live load applications. It is for this reason that preloading was recommended for most repairs, particularly those including patching. Care should be taken when preloading a structure so as to not overload the structure or cause damage from excessive localized stresses from the preloading force. Additionally, it is very difficult to keep the preload force from distributing to adjacent undamaged girders, further affecting the uncertainty of this method.

It must be noted that Shanafelt and Horn, in *Report 226*, addressed relatively small prestressed elements having only 16 strands. In this case, the preload required to affect the post-tensioning force is relatively small, similar in scale to a parking garage structure. As elements become larger – as for a bridge – the level of preload required becomes very large and often impractical to apply. The effectiveness of preload is improved with reduced dead-to-live load ratios; however these are not typical in concrete structures.

External post-tensioning is done using steel rods, strands or bars anchored by corbels or brackets (typically referred to as ‘bolsters’) which are cast or mounted onto the girder; typically on the girder’s side (although occasionally on the soffit). The steel rods, strands or bars are then tensioned by jacking against the bolster or preload (which will be discussed later). Examples of this method are shown in Figure 5. Splice 1 (*Report 226* designation) used Grade 40 reinforcing bars, Splice 2 used Grade 60 steel rods encased in PVC conduits as a corrosion resisting measure and Splice 4 used a corbel that was continuous over the entire length of the girder for corrosion protection of six post-tensioned 270 ksi strands. Post-tensioning force of Splice 1 is nominal and is induced by preload only. Today, Splice 2 details would generally be accomplished by using high strength (150 ksi) post-tensioning bars (such as Williams or Dwydag products). In this case, post-tensioning force may be induced by jacking or preload or a combination of both. For Splice 4, post-tensioning force will typically be induced by jacking. An advantage of Splice 4 is that it can also be designed as a ‘harped’ system (king- or queen-posted), resulting in greater efficiency, particularly with respect to restoring excessive vertical deflection of the girder. In this case, both bolsters and deviators must be attached to the beam.

Design of external post-tensioned repair systems is relatively straight forward using simple plane sections analysis (recognizing that the post-tensioning bar is unbonded). The attachment/interface of the bolsters however requires significant attention. These elements are ‘disturbed regions’ subject to large concentrated compression forces. Additionally, sufficient shear capacity along the interface between the bolster and existing beam must be provided to transfer the post-tensioning force. Effective shear transfer often requires the bolster themselves to be post-tensioned (transversely) to the girder to affect adequate ‘friction’ forces along the interface. Finally, the design of the bolsters and interface must consider the moments induced by the eccentric post-tensioning forces.

Steel jacketing is the use of steel plates to encase the girder to restore girder strength. With this repair technique, post-tensioning force can only be applied by preloading. Splice 3 shown in Figure 5d, employs a steel jacket. Generally, this method of repair will also require shear heads, studs or through bars to affect shear transfer between the steel jacket and substrate beam. Steel jacketing is felt to be a very cumbersome technique. In most applications, field welds will be necessary to ‘close’ the jacket (since the

jacket cannot be ‘slipped over’ beam ends in most applications). Additionally, the jacket will need to be grouted in order to make up for dimensional discrepancies along the beam length. Neither of these details is addressed in *Report 226*.

Strand splices are designed to reconnect severed strands. Methods of reintroducing prestress force into the spliced strand are preloading, strand heating and torqueing the splice; the latter is most common, essentially making the splice a turnbuckle of sorts. Strand heating is a method in which the strand is heated, the strand splice secured to the strand and, as the strand is allowed to cool, it shrinks, thus introducing tension back into the strand. Strand heating of conventional high-strength prestressing strand does not appear to provide any reasonable prestrain because either a long length of strand must be heated; or a short length of strand must be heated to a high temperature. The former is impractical in a bridge girder and the latter will affect the material properties of the strand. Thus, Strand heating is not recommended.

Commercially available strand splices have couplers connected to reverse threaded anchors; as the coupler is turned, both anchors are drawn toward each other, introducing a prestress in the attached strand (see Figure 6a). Schematic examples of strand splices are shown in Figures 6b-d. Splice 6 utilizes strand chucks to splice the strands and strand heating to induce tension (recall that the methods in *Report 226* were not tested in relation to this work). Splice 7 uses a strand splice that has a coupler nut in the middle which connects to a steel transfer plate and then to the strands.

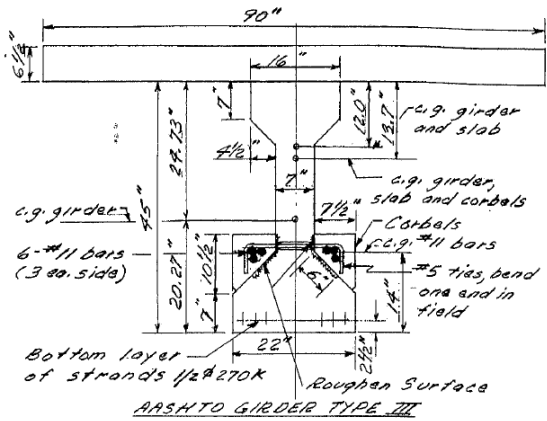
Repair techniques may be combined. Combination of repair techniques will allow the user to employ the advantages of each repair method. For example, Splice 5, shown in Figure 5e, uses post-tensioning in conjunction with steel jacketing to restore girder strength. The post-tensioning addresses girder serviceability while the steel jacket restores the girder’s ultimate capacity.

NCHRP Report 226 provided the selection matrix shown in Table 2, for selecting repair methods for prestressed girders. Guidelines presented for each repair method are as follows. The ‘number of strands’ that may be spliced must be placed in context: the prototype girders considered in this study only had 16 strands.

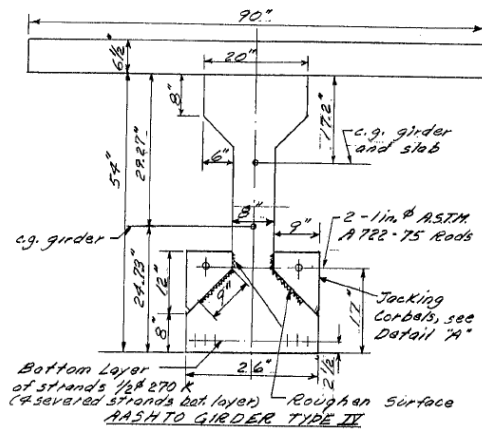
External Post-tensioning: replacing the loss of more than 6-8 strands may be difficult, but this method can be used to restore strength and durability to damaged girders and add strength to existing bridges.

Strand Splicing: this method is good for repair of a few strands but is limited by the geometry of the strand splice and concrete cover.

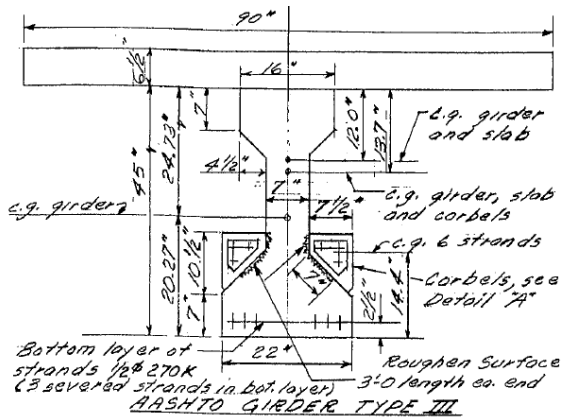
Steel Jacketing: this method was successfully used to replace the loss of 6 strands, but is not very common.



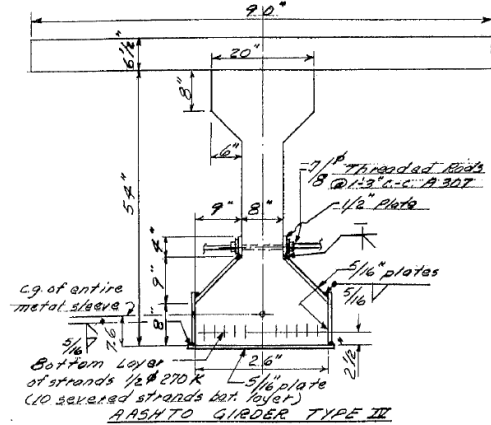
a) Splice 1: mild reinforcing steel anchored by bolster. PT provided by preload.



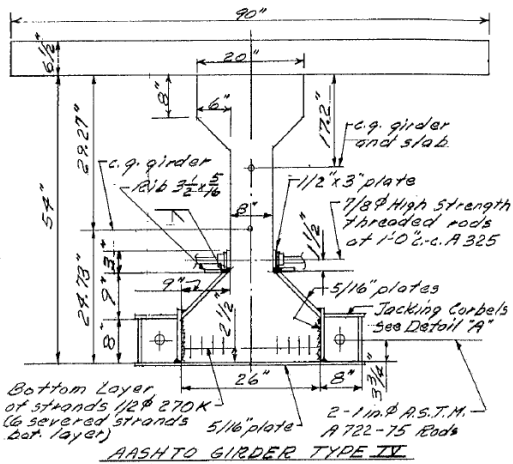
b) Splice 2: PT anchored by bolster. Bar is usually mounted in duct or greased sleeve to affect environmental protection.



c) Splice 4: PT strand in continuous bolsters. Strand may be harped. PT provided by jacking. Unbonded strand in a greased sleeve is conventionally used.



d) Splice 3: Steel jacket repair method

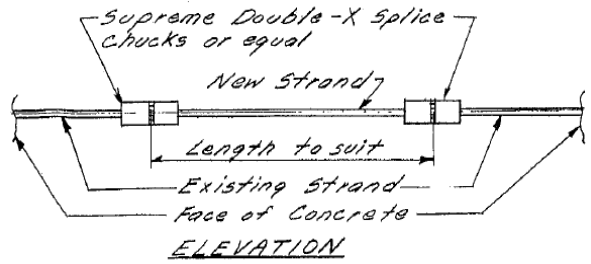


e) Splice 5: Combination of repair methods

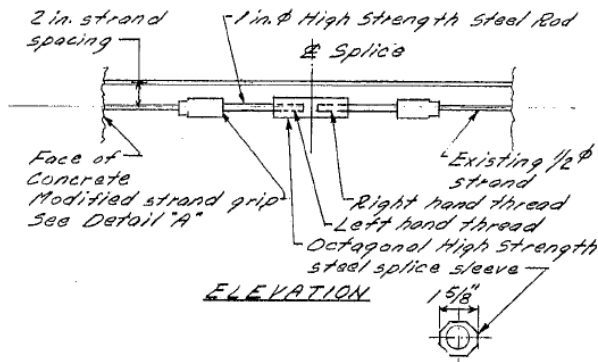
Figure 5 Repair methods presented in Shanafelt and Horn (1980).



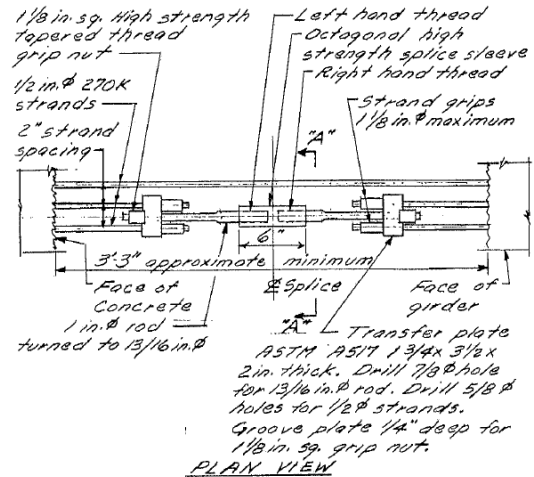
a) strand splices *in situ*
 [Courtesy of the Texas Department of Transportation, © 2007 All rights reserved.]



b) Splice 6: Strand chucks used to splice strand. Prestressing reintroduced by heating strand during installation.



(b) Splice 7: 'Turnbuckle' style strand splice. Coupler draws strand ends together.



a) Splice 8: Multiple strand 'turnbuckle' style strand splice.

Figure 6 Strand splices (Shanafelt and Horn 1980).

Table 2 Repair selection criteria proposed by Shanafelt and Horn (1980).

Damage Assessment Factor	Repair Method			
	External PT	Strand Splicing	Steel Jacket	Girder Replacement
Behavior at Ultimate Load	Excellent	Excellent	Excellent	Excellent
Overload	Excellent	Excellent	Excellent	Excellent
Fatigue	Excellent	Limited	Excellent	Excellent
Adding Strength to Non-Damaged Girders	Excellent	N/A	Excellent	N/A
Combining Splice Methods	Excellent	Excellent	Excellent	N/A
Splicing Tendons or Bundled Strands	Limited	N/A	Excellent	Excellent
Number of Strands Spliced	Limited	Limited	Many	Unlimited
Preload Required	Perhaps	Yes	Probably	No
Restore Loss of Concrete	Excellent	Excellent	Excellent	Excellent
Speed of Repair	Good	Excellent	Good	Poor
Durability	Excellent	Excellent	Excellent	Excellent
Cost	Low	Very Low	Low	High
Aesthetics	Fair ¹	Excellent	Excellent	Excellent

N/A: not applicable

¹can be improved to excellent by extending corbels on fascia girder

The second phase of the NCHRP 12-21 project, and the focus of *NCHRP Report 280*, (Shanafelt and Horn 1985) was to provide a practical user's manual for the evaluation and repair of damaged prestressed concrete bridge members. Significantly, some of the repair methods presented in the earlier *Report 226* were load tested and suggestions for their implementation are given. It is important to note that the girders were never loaded to their ultimate capacity. All tests were conducted on a single girder with artificial damage and one of the repair techniques applied.

Ten different load tests were conducted on a single I-girder to measure the behavior of each repair:

1. Load girder up to 75% of the calculated ultimate load capacity;
2. Add concrete corbels and post-tension high-strength bars and load;
3. Disconnect high-strength bars and load (same as load test 1 but girder is now cracked);
4. Break out specified concrete to sever 4 strands (25% of the total 16 strands) and load;
5. Splice 4 strands with single strand splice and patch and load;
6. Reconnect post-tension high-strength bars (same test as test 5 but with external post-tensioning);
7. Disconnect bars, break out concrete and sever the four strands spliced in test 5 and load;
8. Patch the girder and tension the external bars;
9. Disconnect bars, break out patch, sever 2 more strands for a total of 6 and splice them with a steel jacket and load;
10. Load the steel jacketed girder to 100% of the calculated ultimate moment capacity.

While the tests of each repair technique generally demonstrated a sound response, that fact that: a) there was no control specimen with which to compare results; and b) the repairs were sequential and thus the degree of damage was necessarily incremented between tests affected the ability to draw conclusions from this test program. Although a significant amount of test data is provided, few conclusions are or can be drawn.

In 1996, Feldman et al. (1996) effectively updated the NCHRP 12-21 project to include the contemporary state-of-practice. Feldman et al. focused exclusively on impact damage to prestressed concrete bridge girders and appropriate repair methods for the same. The report recommended a number of best practices associated with preloading, patching material selection and reporting practices. Nonetheless, it was determined from survey data, that little repair work was done for minor damage, patching was typical for moderate damage and girder replacement was most typical in cases of severe damage.

The following sections describe literature on conventional methods of repair developed since the publication of *NCHRP Reports 226* and *280*.

1.5.1.2 Strand Splicing

In repairing a few damaged strands, strand splicing provides an efficient, quick and simple solution. Strand splices reconnect broken strands and allow the strand to be re-tensioned. However, interactions between spliced strands and girder behavior where multiple strand splices are used should be explored. Strand splice tensioning based on the torque wrench method (i.e.: applying a specified torque to a strand splice coupler) was found to be unsatisfactory due to a variation in friction stresses along the splice and thus a variation of stress induced into the strand (Labia et al. 1996). The ‘turn of the nut’ method which uses the displacement between strand chucks or splice ends and strand modulus to calculate stress was found to be more easily accomplished and reliable (Labia et al. 1996 and Olson et al. 1992). This method is analogous to the method of assuring appropriate prestress in a strand as it is jacked by measuring the elongation of the strand. Testing has shown that strand splices can restore original girder strength (Labia et al. 1996). It should also be noted that the strand splice threaded rods should be thoroughly cleaned and lubricated to prevent the possibility of splice malfunction or failure (Zobel et al. 1996).

In some instances, the size and shape of the strand splices has been found to be problematic. Beam geometries and the amount of concrete cover limit the use of strand splices. Often, strands are too closely spaced or concrete cover is too small to accommodate the strand splice. Additionally, turnbuckle strand splices have a much larger axial and flexural stiffness than the strands themselves (Zobel et al. 1996). This affects girder behavior, particularly if the splice repair is not symmetric in the girder cross section. Olson et al. (1992) reported a strand splice-repaired test girder that failed in tension at less than 82% of the original girder capacity. Possible reasons cited for the tension failure include: a) increased strand damage during the fatigue program: the stress ranges may have been magnified on the undamaged side of the girder; b) the turnbuckle splices may have worked as anchors on the damaged side of the girder; or c) a combination of the two factors. Additionally, the wedge anchorages of the splice are stress raisers and, in combination with the increased flexural stiffness of the splice, this detail could be a source of fatigue related strand failures (Zobel et al. 1996). Earlier than anticipated failure of test girders using the strand splices is cause for concern.

It is important that the strength of the strand splices be assured. Zobel and Jirsa (1998) studied the performance of various strand splice repairs. All splices provided a minimum strength of 85% of the nominal strength of the strand. From this study, strand splices are recommended: a) when ultimate flexural strength of the girder with the remaining undamaged strands is greater than the factored design moment, repair by internal strand splices could be used to reduce the range of stress imposed on the other strands; and b) if fatigue is not a major concern. In any case, repairing more than 10-15% of the total number of strands within a single girder is not recommended (Zobel and Jirsa 1998). Rao and Frantz (1996) showed that fatigue in damaged prestressed box girders was not a significant concern.

There is a single known commercially available strand splice available today. The ‘Grabb-it Splice’ utilizes a reverse threaded coupler. This splice has two factors negatively affecting its use: First, the prestress force that may be developed is limited to 39.5 kips which is only $0.956f_{pu}$ for 0.5 in. strand (Law Engineering 1990) whereas the splice strength should be at least 15% greater than the strand strength to minimize the possibility of splice failure (Labia et al. 1996). Secondly, the splice diameter of 1.625 in.

potentially affects concrete cover and strand spacing requirements. In any event, the large diameter requires such splices to be staggered along the length of a member (Grabb-it technical literature 2008).

The Alberta Infrastructure and Transportation Department (ABITD 2005) provides additional guidance with respect to the evaluation and acceptance criteria of- and procedure for restressing severed prestressing strands. ABITB suggests that severed prestressing strands be stressed to an effective prestress of 60% of ultimate strand strength (f_{pu}). This procedure includes chipping and removal of unsound concrete and application of the stressing gage and tensioning device. It is also acknowledged that strand splices must be staggered in order to avoid confusion and congestion. Additionally, draped and harped strands should be returned to their original position and the use of deflection brackets may be used.

The ABITD stressing gage consists of a 17 in. (430 mm) long steel rod mounted on a steel plate with hook bolts (sub-assembly “C” in Figure 7), an 18 in. (457 mm) long plastic tube, and a dial gauge mounted on a second steel plate with hook bolts (sub-assembly “D” in Figure 7). Sub-assembly C is mounted on the strand using the hook bolts. The plastic tube placed over the steel rod and sub-assembly D is mounted to the strand at the other end of the tube. The plastic tube must be fitted over the two sub-assemblies and each pushed tightly against the ends of the tube, as the hook bolts are tightened. The gage is oriented so that it can be read during the stressing operation. This gage verifies the amount of prestressing force which has been restored by reading the ‘strain’ over the 17 in. gage length.

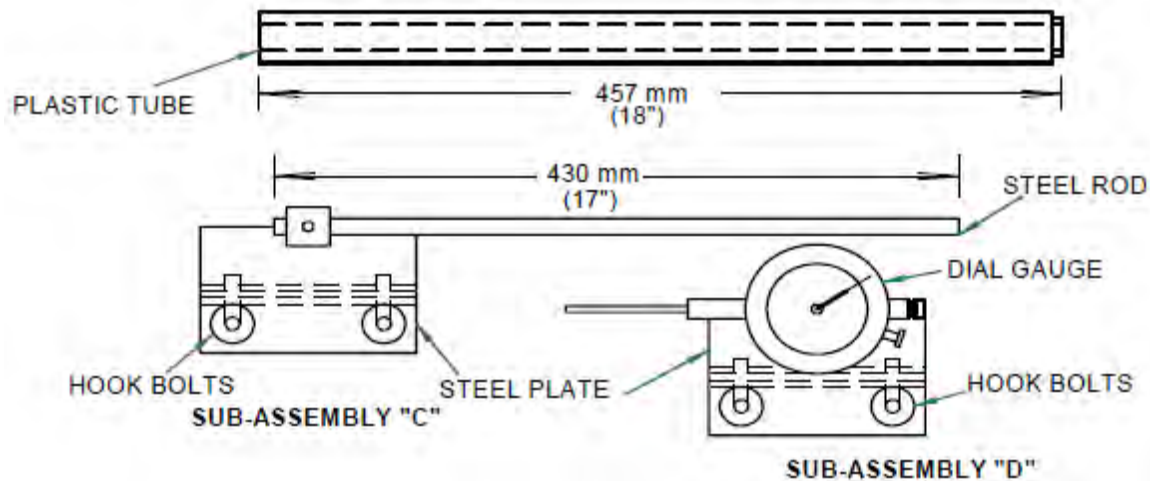


Figure 7 ABITB stressing gage (ABITB 2005).

The Alaska DOT (AKDOT 2007) has a repair guidance document that largely follows the Alberta guidance document. AKDOT acknowledges that 0.6 in. strands cannot be retensioned or spliced with the splice techniques described due to splice size availability.

1.5.1.3 Post Tensioning

Post tensioning can be used to help restore prestress as well as girder strength. This method of repair allows the design to be customized to restore strength and serviceability (Daly and Witarnawan 1997). For example, in the adjacent box (AB) beam bridge examined in Preston et al. (1987), the original strand pattern was determined to meet a particular concrete stress requirement. Therefore, it was important for the repair to restore bottom fiber prestress in a manner consistent with the original design intent. The post tensioned repair utilized four post tensioned 0.5 in. diameter, epoxy coated, low-relaxation strands installed 2 in. below the beam soffit, each tensioned and anchored at 21.5 kips. The total depth of the repair was 3 in. Some issues arose when seating the post-tensioning strands as the losses were greater than expected and thus the induced tensile force needed to be increased to account for these losses. Nonetheless, the ultimate capacity of the girder was restored as well as some of the lost prestressing force.

The same concept can be used with carbon fiber reinforced polymer (CFRP) instead of steel as the post tensioning material. El-Hacha and Elbadry (2006) examined the use of post tensioned 7-wire CFRP cables (CFCC) for strengthening of concrete beams. The experiment showed comparable results to steel post-tensioned repairs. The post-tensioning force created a stiffer beam and thus a stiffer load-deflection response.

1.5.1.4 Corrosion Mitigation

When considering the repair of corroded strand, it is important to consider the source of corrosion. For example, corrosion initiated because of cracks in the beam requires repair of the cracks to arrest further corrosion. Prestressing strand is more susceptible to corrosion than lower grades of steel (due both to the composition of prestressing steel and the increased surface area-to-cross section area ratio of a seven wire strand), therefore prestressed concrete beams are susceptible to corrosion, especially at beam ends. Since prestressed strands are anchored in the beam ends, strand corrosion in this area can be detrimental to girder performance. Tabatabai et al. (2004) focused on the repair of the beam end region (within the last two feet of the beam). A protective coating was put on some beam ends before the experimental accelerated corrosion program began to see how this would affect strand corrosion rates. Beam ends were then subjected to wet/dry cycles of salt-water sprays together with an impressed electric current to accelerate the corrosion process. After an initial exposure of six months, all but one of the untreated beam ends was protected using CFRP wrapping or painted with a protective coating. The corrosion process was then allowed to continue for an additional year. It was concluded that surface treatments and coatings are effective in the short term, but not in the long term unless the coating is applied prior to chloride contamination. As expected, a patch repair having no initial protection performed the worst. Table 3 compares beam end ratings and illustrates the most effective mitigation measure.

**Table 3 Comparison of beam-end numerical ratings and overall ratings
(adapted from Tabatabai et al. 2004).**

Beam End	Description	Chlorides ¹	Cracking ¹	Corrosion ¹	Overall Rating ¹
1A	epoxy coated from day 1	1	2	3	6
1B	epoxy coated after 6 mo. exposure	2.5	4	7	13.5
2A	no treatment applied	2	6	5.5	13.5
2B	patch repair after 6 months exposure	8	7	8	23
3A	silane sealer applied from day 1	1	5	3.5	9.5
3B	silane sealer applied after 6 mo. exposure	2	8	5.5	15.5
4A	polymer coating applied after 6 mo. exposure	4.5	3	6	13.5
4B	FRP wrap applied after 6 mo. exposure	2.5	1	7	10.5
5A	polymer resin coating applied from day 1	1	1	2	4
5B	FRP wrap applied from day 1	1.5	1	2	4.5

¹ Individual criterion ratings were based on 1–8 scale, 1 indicating best effect, 8 indicating worst effect. The overall ranking was based on a scale of 3 to 24 with 3 indicating the best condition and 24 indicating the worst condition.

Studies have shown that FRP composite wraps are effective at mitigating future corrosion damage by excluding chloride-bearing water from the concrete (Tabatabai et al. 2004 and Klaiber et al. 2004).

Active cathodic protection (impressed current systems) are also effective at mitigating corrosion, but are not commonly used due to high maintenance and monitoring costs and method complexity (Broomfield and Tinnea 1992, Bennett and Schue 1998 and Tabatabai et al. 2004). Additionally, prestressing steel is particularly susceptible to cracking due to hydrogen embrittlement. If an active cathodic protection system is installed and operated in such a way that the magnitude of polarization is excessive, then atomic hydrogen may be generated at the surface of the steel and embrittlement may occur (Bennett and Schue 1998).

Passive cathodic protection (embedded anodes) installed in concrete patches is an effective method of mitigating corrosion in prestressed concrete members. (Vector 2012).

1.5.2 Refined Damage Classifications

NCHRP Report 226 (Shanafelt and Horn 1980) established three damage classifications defined previously. Based on the potential for more effective retrofit of more heavily damaged members, Harries et al. (2009) proposed further division of the ‘severe’ category as follows:

MINOR: Concrete with shallow spalls, nicks and cracks, scrapes and some efflorescence, rust or water stains. Damage at this level does not affect member capacity. Repairs are for aesthetic or preventative purposes.

MODERATE: Larger cracks and sufficient spalling or loss of concrete to expose strands. Damage does not affect member capacity. Repairs are intended to prevent further deterioration.

SEVERE I: Damage requires structural repair that can be affected using a non- prestressed/post-tensioned method. This may be considered as repair to affect the STRENGTH (or ultimate) limit state (ULS).

SEVERE II: Damage requires structural repair involving replacement of prestressing force through new prestress or post-tensioning. This may be considered as repair to affect the SERVICE limit state (SLS) in addition to the ultimate limit state (ULS).

SEVERE III: Damage is too extensive. Repair is not practical and the element must be replaced.

Damage may be quantified in a variety of ways. Table 4 may be viewed as a guide for both selecting a method by which to quantify damage to prestressed members and for quantifying the damage.

Table 4 Damage classification metrics proposed by Harries et al. (2009).

Damage Classification	SEVERE I	SEVERE II	SEVERE III
Repair philosophy	ULS only	ULS and SLS	-
Action	non PT repair	PT repair	replace
Live load capacity replacement	up to 5%	up to 30%	100%
Ultimate load capacity replacement	up to 8%	up to 15%	100%
Replace lost strands	2-3 strands	up to 8 strands	>8 strands
Vertical Deflection	loss of camber	up to 0.5%	>0.5%
Lateral Deflection (Sweep) (Shanafelt and Horn 1985)	within construction tolerance		permanent lateral deflection exceeding construction tolerance

Defining damage based on the number of strands lost is not felt to be rational in so far as this value does not take into account the contribution of an individual strand to the member capacity. That is; 4 strands missing from a girder having only 16 strands is significant, whereas 4 strands missing from a girder having 72 strands may not require immediate repair. Classification by girder deflection, while likely an excellent indicator of performance, is felt to be impractical to establish in the field.

Harries et al. (2009) presented additional guidance based on the reported practice of the Washington State DOT as to when girder replacement is required. This guidance would correspond to the threshold between SEVERE II and SEVERE III. Replacement is required in cases where:

1. Over 25% of the strands have been severed.
2. The bottom flange is displaced from the horizontal position more than ½” per 10’ of girder length.

3. If the alignment of the girder has been permanently altered by the impact.
4. Cracks at the web/flange interface remain open.
5. Abrupt lateral offsets may indicate that stirrups have yielded.
6. Concrete damage at harping point resulting in permanent loss of prestress.
7. Severe concrete damage at girder ends resulting in permanent loss of prestress.

Items 3-7 are additional qualitative considerations for determining SEVERE III level damage. It is clear that the determination of the degree of damage in this case is largely a matter of engineering judgment.

For instance, considering item 2 (permanent lateral deflections (sweep) resulting from impact) Shanafelt and Horn (1985) suggest that when the permanent sweep exceeds the standard tolerance (reported as 1/8 in. per 10 ft.) the design either i) calculate the torsional and flexural stresses induced and use these in making repair calculations; or ii) consider jacking the bottom flange into allowable alignment and maintaining this with an added diaphragm. If the girder cannot be restored to being essentially straight, it should it is replaced (Table 4).

The Michigan DOT (Ahlborn 2005) uses an inspection handbook for adjacent box girder structures which illustrates typical forms of distress for this bridge type. Types of distress are described:

1. Map cracks.
2. Hairline cracks.
3. Spalling or delamination.
4. Narrow cracks with water or corrosion.
5. Water stains at joints.
6. Longitudinal cracks on deck.
7. Medium cracks without water.
8. Evidence of displacement between beams.
9. Medium cracks with water or corrosion.
10. Wide cracks with water or corrosion.
11. Spalling with exposed or corroded reinforcement.
12. Shear or flexure cracking.

1.5.3 Emerging Repair Materials and Methods

Many emerging repair technologies employ the use of Fiber Reinforced Polymer (FRP) materials. FRP materials consist of a polymer matrix reinforced with a high performance fiber. Fiber materials may be aramid (AFRP, uncommon in North American practice), carbon (CFRP), glass (GFRP), or high performance steel (SFRP) or hybrids of these. A list of applicable national and international specifications and guides pertaining to the use and design of FRP composite repairs for strengthening, repair and rehabilitation is as follows:

United States:

National Cooperative Highway Research Program (NCHRP) - *Recommended Construction Specifications and Process Control Manual for Repair and Retrofit of Concrete Using Bonded FRP Composites* – Report 609 (2008).

National Cooperative Highway Research Program (NCHRP) - *Bonded Repair and Retrofit of Concrete Structures Using FRP Composites: Recommended Construction Specifications and Process Control Manual* – Report 514 (2008).

American Concrete Institute (ACI) Committee 440 - *ACI 440.2R-08 Guide for the Design and Construction of Externally Bonded FRP Systems for Strengthening Concrete Structures* (2008)

Concrete Repair Manual, 3rd Ed. - published jointly by American Concrete Institute (ACI) and International Concrete Repair Institute (ICRI) (2008).

International (available in English):

Canadian Standards Association (CSA) - S806-02(R2007): *Design and Construction of Building Components with Fibre-Reinforced Polymers* (2007).

Concrete Society (Great Britain) - *Design Guidance for Strengthening Concrete Structures Using Fibre Composite Materials* - Technical Report No. 55 (2004).

International federation for Structural Concrete (fib) (European Union) - *Externally Bonded FRP Reinforcement for RC Structures* (2001).

Japan Society of Civil Engineers (JSCE) - Concrete Engineering Series 41: *Recommendations for Upgrading of Concrete Structures with Use of Continuous Fiber Sheets* (1998).

Consiglio Nazionale delle Ricerche (CNR - Italy) - *Guidelines for Design, Execution and Control of Strengthening Interventions by Means of Fibre-reinforced Composites*: CNR-DT200/204 (2004).

1.5.3.1 Externally Bonded Non Post-Tensioned CFRP Retrofit (EB-CFRP)

Carbon fiber reinforced polymer (CFRP) strips adhesively bonded to prestressed concrete girders can restore or increase the flexural capacity of damaged girders, control cracking if it is present and reduce deflections under subsequent load. This application is shown schematically in Figure 8b. The use of externally bonded (EB) CFRP strips to restore flexural capacity of damaged girders is well documented (Scheibel et al. 2001, Tumialan et al. 2001, Klaiber et al. 2003, Green et al. 2004, Reed and Peterman 2004, Wipf et al. 2004, Reed and Peterman 2005 and Reed et al. 2007). In most cases, repairs performed as expected and designed.

Green et al. (2004) investigated the behaviors of four different CFRP systems: two wet lay-up systems from different manufacturers, a fabric pre-impregnated with resin (prepreg), and a spray layed-up application. For the various repairs, the experimentally observed capacities ranged from 91-108% of the unrepaired, undamaged control girder. These values were slightly lower than the theoretically predicted capacities which were in the range of 96-114% of the original girder capacity. Beam deflections for such CFRP-repaired prestressed girders have been shown to be reduced on the order of 20 to 23% (Klaiber et al. 2003 and Green et al. 2004, respectively). Often, to improve the resistance of the CFRP debonding from the concrete, transverse U-wrapped CFRP strips were used to help 'hold' the CFRP and underlying concrete patch in place (Scheibel et al. 2001, Tumialan et al. 2001, Klaiber et al. 2003, Green et al. 2004, Reed and Peterman 2004, Wipf et al. 2004, Reed and Peterman 2005 and Rosenboom et al. 2011). Suggestions for good detailing of CFRP repairs, including CFRP development length, plate and splice staggering, U-wraps and encapsulation of the patch and additional reinforcement to account for shrinkage and transverse flexural cracking of the patch are provided in Rosenboom et al. (2011). Additional confinement of the concrete patch is helpful to mitigate the possibility of a 'pop out' failure of the patch, where the newly placed patch material breaks away from the girder, as well as shrinkage and flexural cracking in the patch. This will be described in Section 1.5.5.8.

1.5.3.1.1 CFRP strips versus wet-layed up CFRP

CFRP materials for EB applications may take the form of preformed strips or wet layed-up fabrics. Strips are generally unidirectional fiber reinforced plates having a very high fiber volume ratio; thus they are axially very stiff and strong. Strips are bonded to the prepared concrete substrate using conventional structural adhesives. Wet layed-up fabrics are saturated *in situ*. Typically, a layer of epoxy resin is placed on the prepared concrete substrate as a 'primer' layer and the dry CFRP fabrics are overlaid onto this, an additional layer of saturant is applied and the material is worked to ensure complete epoxy wet-out of the fiber. Additional layers are applied in the same fashion. The resulting CFRP material generally has a lower stiffness and strength based on the area of the resulting CFRP plate. Wet layed-up applications are suitable for column wrapping and U-wrap applications, however are falling out of favor for beam flexural strengthening for the following reasons:

1. Preformed strips have exceptional quality control in their fabrication whereas wet lay-up is accomplished overhead *in situ*.
2. Preformed strips are considerably more durable under typical exterior environments (Cromwell et al. 2011, among others; see Section 1.5.3.5).
3. The bond performance, in particular, of preformed strips has been observed to be twice as good as wet laid-up materials; that is, CFRP strain at debonding failure – typically the dominant limit state – is twice as high for strips. (Harries and Shahrooz 2011; see Section 1.5.3.5).
4. ‘Sag’ of CFRP strips is not observed during bonding with conventionally used adhesive materials whereas sag is often observed in large wet laid-up applications.
5. Adhesive bonding is a regularly conducted construction task and has minimal requirements for containment. Wet lay-up is a specialized skill usually requiring special clothing and containment in cases where the resin may enter a water course.
6. Bonding preformed strips is reported to be significantly less expensive – requiring less surface preparation, labor and time than wet lay-up methods.
7. Only preformed strips are practical if the CFRP is to be prestressed or post tensioned.

1.5.3.2 External Prestressed (P-CFRP) and Post-Tensioned (PT-CFRP) CFRP Retrofit

A parallel can be drawn between prestressed and non prestressed CFRP retrofits and prestressed and conventionally reinforced concrete beams. Prestressing the reinforcing steel in the latter application precompresses the concrete in the tension zone of the girder. As the beam is loaded, it must first ‘undo’ the compressive stress induced by the strands resulting in a more durable (fully-prestressed members do not crack under service loads) and stiffer concrete member. The benefits of stressing CFRP strips prior to application are similar to those of using a prestressed strand in a concrete beam. The four main advantages of using a stressed CFRP repair are (Nordin and Taljsten 2006): a) better utilization of the strengthening material; b) smaller and better distributed cracks in concrete; c) unloading (stress relief) of the steel reinforcement; resulting in d) higher steel yielding loads. Conventionally used CFRP materials have about 1.5 times the tensile capacity of 270 ksi steel prestressing strand and a Young’s modulus about 75% of that of steel, meaning they can reach a higher strain. Stressing the CFRP for the repair can reintroduce prestressing force, lost due to damage or strand loss, back into the beam allowing for redistribution and a decrease of stresses in the strands and concrete (Kim et al. 2008b). Thus when reloaded, the stress levels in the remaining strands will be reduced as compared to the unrepaired beam. In other words, prestressed CFRP systems create an active load-carrying mechanism which ensures that part of the dead load is carried by the CFRP sheets whereas non prestressed CFRP strips can only support loads applied after installation of the CFRP on the structure (Wight et al. 2001, El-Hacha et al. 2003, Kim et al. 2008a and Kim et al. 2008c). Loading that follows prestressed CFRP placement will result in greater CFRP strains meaning that: a) the material is used in the most efficient manner; and b) the CFRP strip is effective immediately upon loading, resulting in an increase in flexural capacity.

There are three approaches to prestressing or post-tensioning (the terms are used inconsistently in the literature) CFRP. The following terminology is adopted to clarify the types of prestressed CFRP systems. Figure 8 provides a schematic representation of each approach.

Prestressed CFRP (P-CFRP): The CFRP is drawn into tension using external reaction hardware and is adhesively bonded to the concrete substrate while under stress (Figure 8c). The stress is maintained using the external reaction until the bonding adhesive is cured. The reacting stress is released and the ‘prestress’ is transferred to the substrate concrete. This method of prestressing is susceptible to large losses at stress transfer and long term losses due to creep of the adhesive system. As a result, only relatively low levels of prestress may be achieved. Additionally, details (such as FRP U-wraps) must be provided to mitigate debonding at the termination of the CFRP strips. P-CFRP systems are analogous to prestressed concrete systems where the stress is transferred by bond to the structural member.

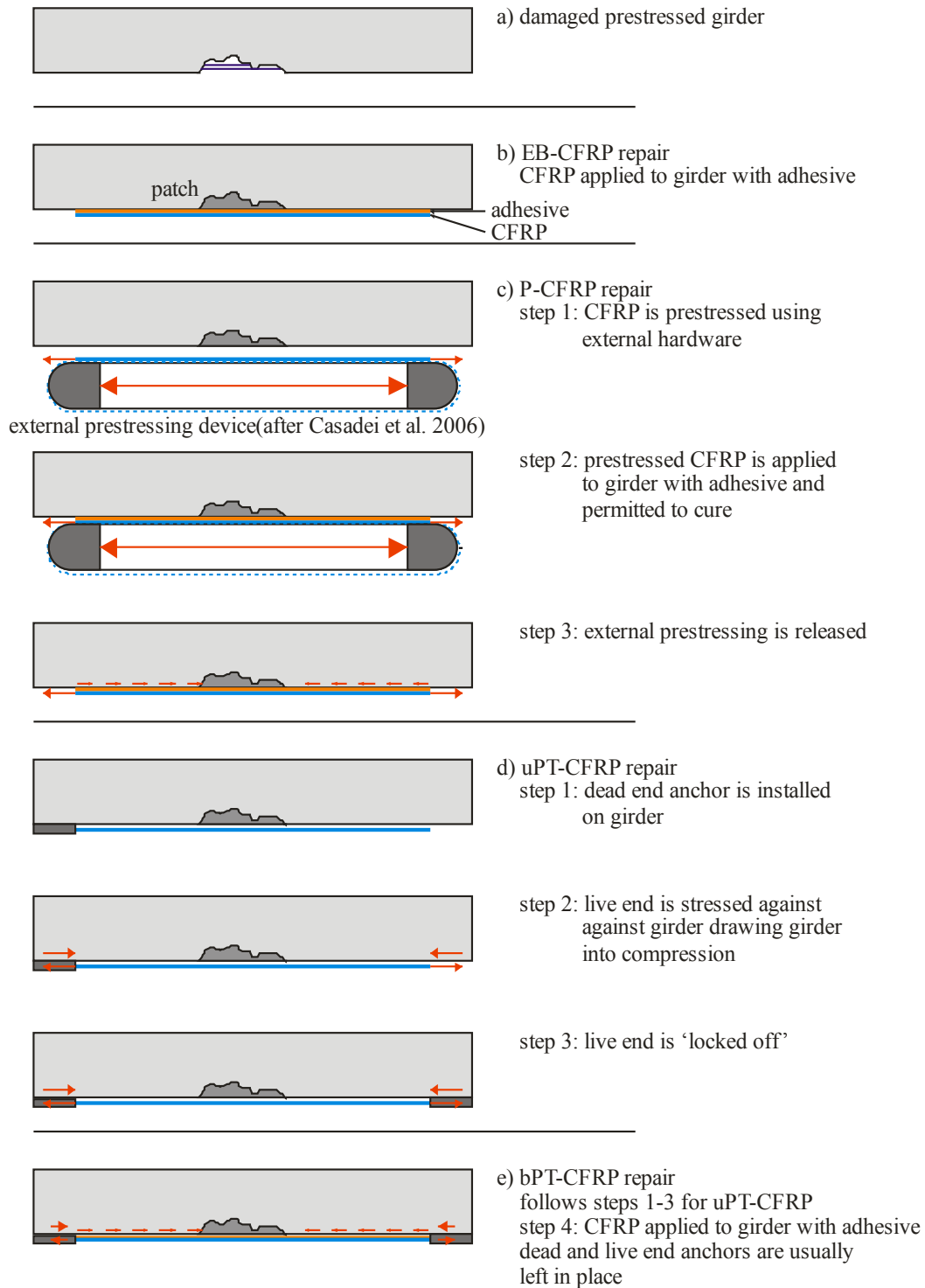


Figure 8 Schematic representations of CFRP applications.

Unbonded post-tensioned CFRP (uPT-CFRP): The CFRP is drawn into tension using the member being repaired to provide the reaction. The stress is transferred to the member by mechanical anchorage only (Figure 8d). Typically a hydraulic or mechanical stressing system will be used to apply the tension after which it will be 'locked off' at the stressing anchorage. This method of post-tensioning is susceptible

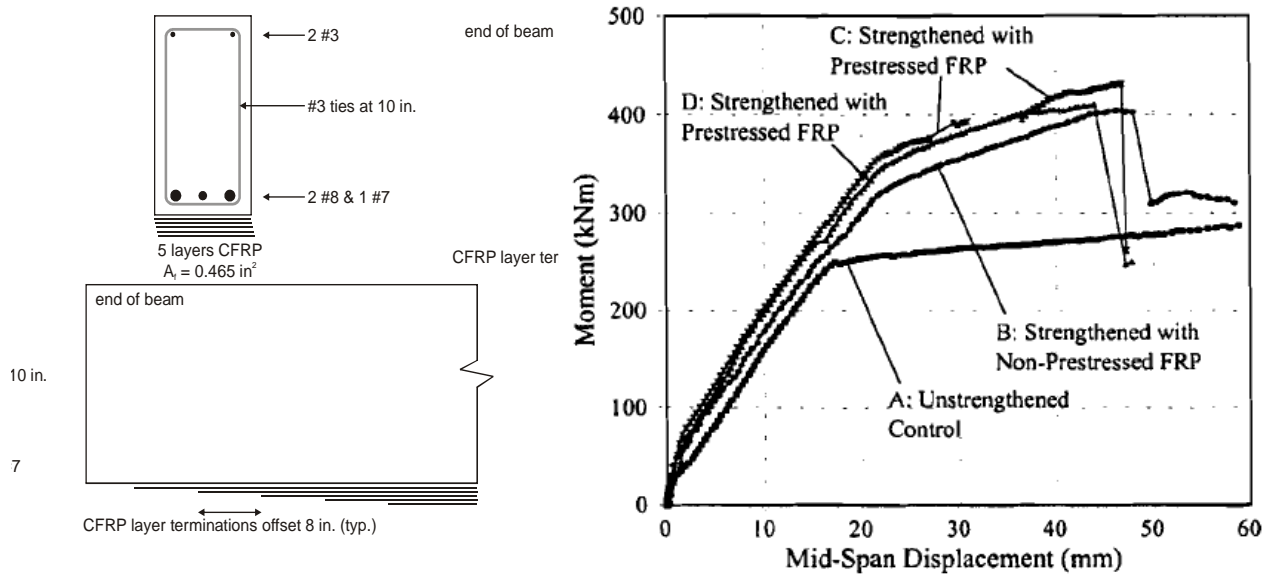
to losses during the ‘locking off’ procedure. Depending on the anchorage method, long term losses due to creep in the anchorage are a consideration. Such systems must be designed with sufficient clearance between the CFRP and substrate concrete to mitigate the potential for fretting. uPT-CFRP systems are analogous to conventional unbonded steel post tensioning systems.

Bonded post-tensioned CFRP (bPT-CFRP): The CFRP is stressed and anchored in the same fashion as the unbonded systems. Following anchorage, however, the CFRP is bonded to the concrete substrate resulting in a composite system with respect to loads applied following CFRP anchorage (Figure 8e). Since the adhesive system is not under stress due to the post-tension force, adhesive creep is not as significant a consideration with this system (Wang et al. 2012b). The bonding of the CFRP may also help to mitigate creep losses associated with the anchorage (Wang et al 2012b). bPT-CFRP systems are analogous to conventional bonded steel post tensioning systems.

Another advantage of using P-CFRP or PT-CFRP systems is the potential for the restoration of service level displacements or performance of the structure. These systems have a confining effect on concrete (and, significantly, any patch material) because they place the concrete into compression. Therefore, a delay in the onset of cracking and a reduction of crack widths (only in bonded systems) has been found when this technique is used (Wight et al. 2001, El-Hacha et al. 2003, Kim et al. 2008a, Kim et al. 2008c and Yu et al. 2008b, Wang et al. 2012b).

The results reported by Wight et al. (2001) are used here to illustrate the effects of EB-CFRP retrofit of prestressed concrete beams and to contrast this with P-CFRP. Figure 9a shows the cross section of the test specimens used by Wight et al. Four beams were tested: one specimen (A) was not strengthened with CFRP (to serve as a control), one (B) was strengthened with EB-CFRP sheets and the remaining two (C and D) used P-CFRP sheets. Each strengthened member was strengthened with 5 layers of CFRP sheets (where each subsequent layer was 7.87 in. (200 mm) shorter than the preceding layer and centered on the tension face of the specimen) for a total of 0.47 in² (300 mm²) of CFRP, having a reported modulus of $E_f = 18,130$ ksi (125 GPa), at midspan. Figure 9b summarizes the experimentally observed load-deflection behavior. As seen in Figure 9b, there is a 30% increase in mid-span moment capacity for the EB-CFRP beam (B) as compared to the control beam (A). The capacity of the P-CFRP beams (C and D) were approximately 40% greater than the control. Additionally, both bonded CFRP repair methods resulted in a cracking load 150% greater than that of the control specimen. The increase in cracking load is attributed to the addition of prestress-induced compressive force back into the member which makes the beam stiffer than before the repair.

It is important to consider the stiffness of the repaired girder. Honorio et al. (2002) performed load tests on two full-scale prestressed concrete double-T beams. After obtaining the undamaged member response, one stem was intentionally damaged, one strand (of six strands in the stem) severed and the beam load tested again. This process was repeated after severing a second strand, providing member behavior for undamaged and 1-strand and 2-strands severed cases for both beams. The damaged stems were then repaired; one member was repaired using EB-CFRP strips and the other with P-CFRP strips. It was observed that unequal load sharing between the stems of the beams occurred and the repaired stems attracted more load than the undamaged stem. The EB-CFRP repaired stem attracted 67% of the applied truck load affecting the performance of the repaired beam. While this issue may not be as significant in larger (more redundant) structures due to better load sharing between girders, it must be acknowledged for smaller structures in which the repaired girder stiffness may affect the live load distribution.



a) Specimen cross sections and elevations

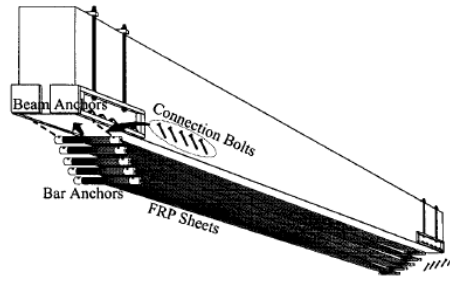
b) Moment –displacement plots

Figure 9 EB-CFRP and P-CFRP specimens tested by Wight et al. (2001).

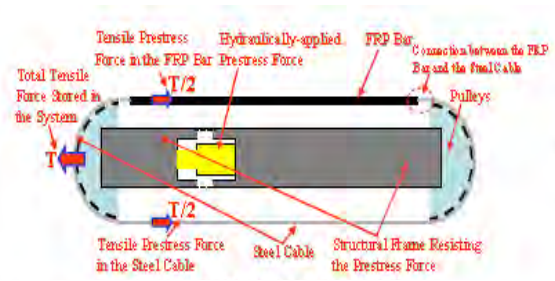
1.5.3.2.1 Prestressing CFRP

There are significant challenges associated with prestressing CFRP strips. CFRP materials have highly orthotropic material properties. The transverse stiffness and strength of unidirectional CFRP strips and fabric systems may be orders of magnitude less than the longitudinal properties that make these materials good alternatives for prestressing in the first place. This makes CFRP materials difficult to ‘grip’ in order to prestress. One solution proposes post tensioning the CFRP strip against the girder end, as seen in Figure 10a (Wight et al. 2001 and El-Hacha et al. 2003). This method proposes that the strips are permanently anchored at one end of the beam (the ‘dead end’) while jacking forces are introduced at the other, movable or ‘jacking’ end. Steel rollers are connected to each end of the strip to permit anchorage. Rollers attached to the jacking end are connected to steel prestressing strands which are connected to a hydraulic ram (jack). The movable end rollers are jacked to the desired extended position and permanently anchored. This approach results in either an uPT-CFRP or bPT-CFRP system.

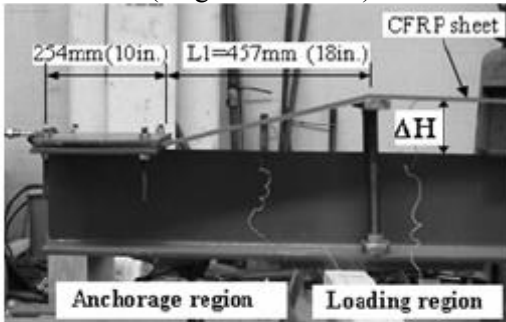
Alternative prestressing techniques include using indirect methods where the sheets are stressed in a jacking or prestressing frame independent of the beam. Prestressing force is induced by either jacking the sheet against a frame thus increasing its length (Casadei et al. 2006) or by deflection controlled loading (Yu et al. 2008a) as seen in Figures 10b and c, respectively. After prestressing by either method, the frame is moved to the girder to allow the strip to be bonded. Once bonded, the prestress force is removed from the frame and transferred (by bond) to the girder, resulting in a P-CFRP system.



a) Proposed direct prestressing system (Wight et al. 2001)



b) Proposed indirect prestressing system (Casadei et al. 2006)



c) Proposed deflection controlled indirect prestressing system (Yu et al. 2008a)

Figure 10 FRP Prestressing systems.

1.5.3.2.2 CFRP Bond and Anchorage

In P-CFRP applications, the prestressing force in the CFRP must be transferred into the girder through bond. The capacity of the CFRP-to-concrete bond is typically the dominant limit state in bonded systems. In bonded FRP-to-concrete applications, ‘bond’ refers to the entire FRP-adhesive-concrete interface. In quality FRP applications, ‘bond failure’ should describe a cohesive failure through the concrete substrate (i.e.: the weakest plane in the interface). This failure is dominantly a horizontal concrete shear failure although, due to concrete cracking and resulting local distortions direct tension can reduce the shear capacity locally. At concrete cracks occurring in a shear span (i.e.: in the presence of a moment gradient), the tension-reduced bond shear capacity occurs to the side of the crack having lower moment. Debonding will therefore propagate in the direction of decreasing moment. This type of debonding is referred to as intermediate crack (IC) debonding. Debonding failure occurring in the FRP or adhesive or at either interface is an indication of a poor FRP application.

Additionally, most high performance epoxy adhesives suitable for CFRP applications exhibit significant creep and are therefore unsuitable for maintaining a large prestress force without additional anchorage. If mechanical anchors are left in place, the system is a post-tensioned CFRP system (which can be bonded or unbonded). Permanent anchors can be used to resist the prestressing force and reduce the chance of debonding and peeling failures (Wight et al. 2001, El-Hacha et al. 2003, Kim et al. 2008a and Yu et al. 2008b). Anchors at the ends of the CFRP strips reduce the shear deformation that occurs within the adhesive layer associated with the prestress force minimizing the possibility of unwanted bond failure (El-Hacha et al. 2003). The ability of any FRP system to transfer shear, regardless of anchorage or adhesive used, is limited by the shear capacity of the concrete substrate. ACI 440.2 (2008) recommends that the shear stress transferred is limited to 200 psi in any event.

El-Hacha et al. (2003) tested three different metallic anchors including a round bar, elliptical bar and a flat plate anchor. The results indicated that a flat plate anchor was the most efficient anchor, likely due to the minimized load eccentricity between CFRP and anchorage. Furthermore, reinforcement of the anchor

zone with CFRP U-wrap resulted in greater failure loads. When the CFRP U-wrap was used in conjunction with the anchorage, failure occurred away from the anchor zone. Although these results seem promising, there are concerns about galvanic corrosion of the anchor when steel and CFRP strips are in direct contact. Mitigation of galvanic corrosion is conventionally addressed by providing an insulating layer, often E-glass (Cadei et al. 2004). This layer is softer than the CFRP and therefore affects the efficiency of the stress transfer. Similarly, Galal and Mofidi (2009) tested an anchorage system which employed steel bolts, angles and plates to anchor CFRP to reinforced concrete T-beams. The anchorage system is fairly similar to those discussed in the PT-CFRP anchorages in that the FRP is wrapped around a steel plate which is then connected to an anchor plate (in this case a steel angle). However, this anchorage system does not include a live end anchor. Moreover, the anchor plate (steel anchor) is located in the corner of the beam-to-column interface. It is for this reason that this specific anchorage is not likely to be utilized in bridge girder repair; however, simple modifications could be made to adapt this system for bridge applications.

U-wrapped CFRP strips have been employed as an alternative to metallic anchorage systems (Kim et al. 2008a, Kim et al. 2008b and Yu et al. 2008b). Many nonmetallic mechanical anchoring systems for the CFRP U-wraps have been explored (Kim et al. 2008a and Kim et al. 2008b) including (see Figure 11): a) CFRP U-wrap; b) mechanical anchorage; c) prestressed CFRP U-wrap with mechanical anchorage; and d) CFRP wrap anchored systems. Test results indicated that: a) beams with nonmetallic anchors exhibited a pseudoductile failure due to the contribution of CFRP anchors, b) beams with mechanically anchored U-wraps and side sheets exhibited a capacity close to that of the control beam; and c) beams fitted with nonmetallic anchors displayed better stress redistributions compared to the beam with steel anchors (Kim et al. 2008b). Thus the ‘stiffness’ of the anchorage system tends to affect the repair behavior.

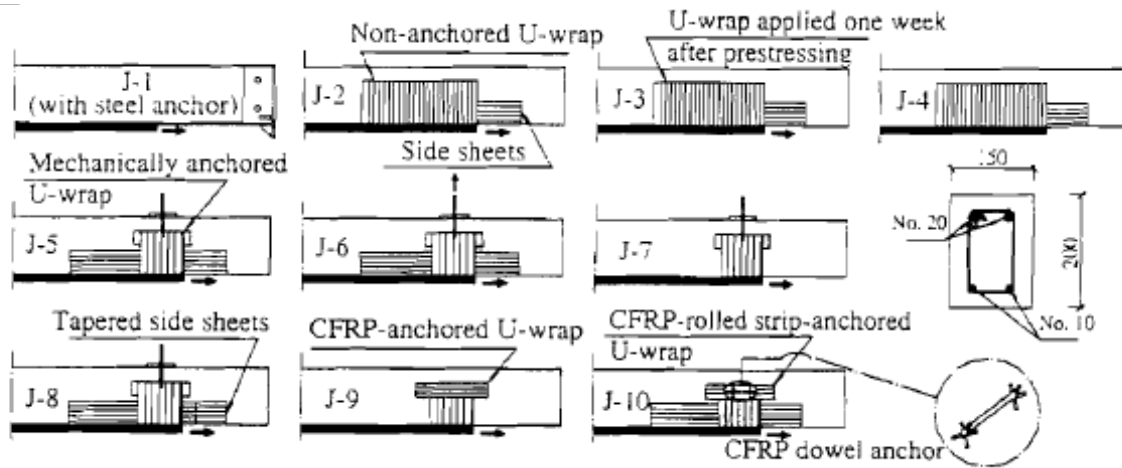


Figure 11 Nonmetallic anchoring systems (Kim et al. 2008a).

Another system, proposed by Bolduc et al. (2003), utilized mechanical (steel) anchors to transfer force from the CFRP to the beam when the epoxy bond fails. These anchors are shown in Figure 12. This arrangement did not behave as anticipated and the CRFP strip ripped away from the anchors because the strip was unable to generate the shear resistance necessary to resist anchor tear-out. It is believed that increasing the clamping force on the strip will increase the effectiveness of similar anchors as was demonstrated by Curtis et al. (2002).

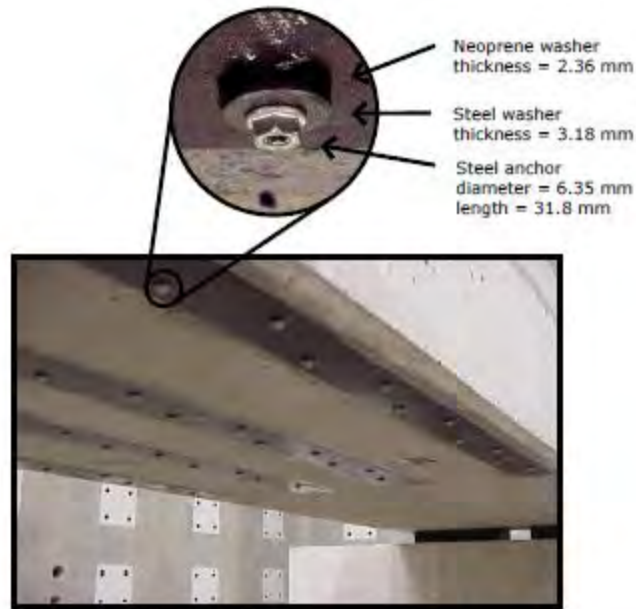


Figure 12 Mechanical anchorage (Bolduc et al. 2003).

It has been shown that when an anchorage system is used, the anchored prestressed sheets fail at a greater load than the unanchored prestressed sheets since anchorage greatly reduces the occurrence of ‘end peel debonding’ failure of the repair (Wight et al. 2001, El-Hacha et al. 2003, Kim et al. 2008a, Kim et al. 2008b and Yu et al. 2008b).

A unique approach to ‘anchoring’ P-CFRP did not use anchors at all, but rather gradually reduced the prestressing force of the strip until the force was zero at the ends of the strip (Aram et al. 2008). The concept behind this was that peeling failure of the strip could be avoided if the force at the strip termination is zero. Results show that this ‘gradient anchorage’ method was not effective and IC debonding failure occurred because the strip was anchored in a region of higher load-induced stress, rather than at the beam ends. Kotynia et al. (2011) performed a similar study on reinforced concrete slabs. CFRP strips were gradually anchored to the beam near the beam ends, with the strip terminating at a distance approximately 1.1 times the depth of the slab away from the support. In the anchorage zone, the strip was incrementally anchored, stepwise releasing 20% of the prestressing force, as shown schematically in Figure 13. This anchorage process provided better CFRP bonding behavior than that used by Aram et al. (2008) effectively mitigating plate-end debonding.

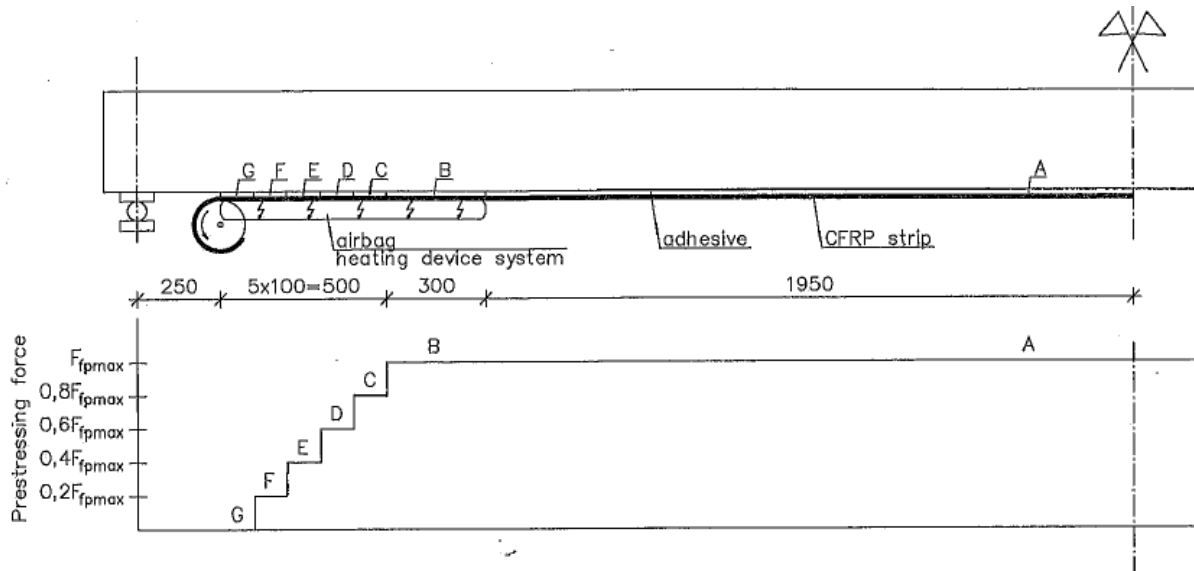


Figure 13 Gradual CFRP prestress force anchorage (Kotynia et al. 2011).

1.5.3.2.3 Commercially Available PT-CFRP systems

There are only two known commercially available ‘standardized’ PT-CFRP system: one manufactured and distributed by SIKA Corporation and the other by S&P FRP Systems. Both are marketed primarily in Europe. The SIKA CarboStress system (Sika 2008b) is shown in Figure 14. The anchorage has a capacity of 67 kips (300 kN) and is intended for a maximum applied prestress force of 45 kips (200 kN). Material properties of the CFRP strips are given later in Table 7. This system is comprised of CFRP strips with ‘potted’ CFRP anchorages referred to as ‘stressheads’ manufactured on each end. These stressheads are captured by steel anchorages mounted on the concrete (Figure 14a) or by the jacking hardware (Figures 14b and d). One anchor is the fixed or ‘dead’ end (Figure 14a) while the other is the jacking end (Figure 14b). The jacking end stresshead connects into a movable steel frame which connects to a hydraulic jack, thus allowing the strip to be stressed. Once the desired stress level is reached, the jack can be mechanically locked to retain the stress in the CFRP or the CFRP strip can be anchored by ‘clamps’ (Figure 14c) near the jacking end. Anchor points can also be located at discrete intervals along the beam. The stress in the strips can vary according to structural need and is limited to the tensile strength of the strip (in many cases, the strength of the beam at the anchor location controls the amount of prestress force that can be applied). The S&P system (S&P 2011) works similarly to the SIKA system, but uses a different proprietary jacking system. An example of the dead and live end anchors for the S&P system can be seen in Figure 15a and b, respectively.



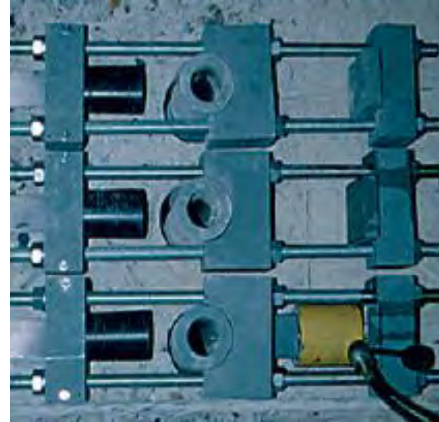
(a) dead end anchor



(b) jacking end anchor in movable frame



(c) multiple live end anchors at one location



(d) stress head system

Figure 14 Sika CarboStress PT-CFRP system (SIKA 2008b).



a) dead end anchor



b) live end anchors and jacking system

Figure 15 S&P FRP Systems PT-CFRP system (S&P 2011).

1.5.3.3 Near Surface Mounted CFRP Reinforcement

Near-surface mounted (NSM) CFRP repairs provide an alternative to externally bonded repairs. The NSM technique places the CFRP in the cover concrete of the member (see Figure 16). This protects the material from impact forces and environmental exposure (Nordin et al. 2002). Similar to external CFRP repairs, an

NSM repair can be prestressed if serviceability is a concern or non prestressed if ultimate capacity is the only design consideration. It is noted, however, that prestressing NSM applications is very difficult and has only been demonstrated in laboratory applications using a stressing procedure that is not practical for use in the field (Nordin et al. 2002 and Casadei et al. 2006). An NSM CFRP repair is completely enclosed in epoxy, making it possible to achieve higher bond strength as compared to external strip bonding due to the larger surface area which is bonded. Additionally, an NSM application engages more cover concrete and is able to transfer greater stresses into the concrete substrate (Quattlebaum et al. 2005). Since bond capacity is typically the limit state associated with EB repairs, NSM repairs will typically require less CFRP material due to the enhanced bond characteristics. NSM repairs are sensitive to the amount of concrete cover and are not a viable option when cover is not sufficient. ACI 440 (2008) requires NSM slots to have a clear spacing at least twice the slot depth and an edge distance at least four times the slot depth as shown in Figure 16. Laboratory studies have shown that both prestressed and non prestressed NSM repairs have been successful in restoring ultimate girder capacity (Nordin et al. 2002 and Casadei et al. 2006).

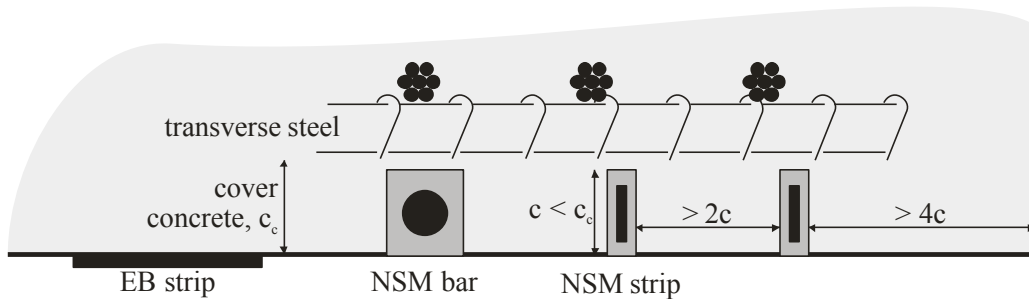


Figure 16 Schematic of externally bonded and NSM CFRP techniques.

1.5.3.4 Fatigue of CFRP and CFRP bonded to concrete

FRP materials, particularly CFRP, exhibit excellent performance when subject to fatigue loads. In conditions of tension fatigue where environmental effects are not affecting behavior, CFRP composite behavior is dominated by the strain-limited creep-rupture process. Plotted on a semi-log S-N curve (S is linear scale; N is log scale), CFRP composites exhibit strength degradation due to tensile fatigue on the order of 5 to 8% per decade of logarithmic cycles (Curtis 1989). Mild steel, by comparison, degrades at approximately 20% per decade. Additionally, CFRP composites generally do not exhibit a clearly defined endurance limit under conditions of tension fatigue.

Fatigue performance of CFRP has been shown to be relatively unaffected by changing fiber type (e.g.; one carbon fiber for another) but the S-N response may shift significantly as the matrix composition is changed (Curtis 1989; Boller 1964). Fiber orientation relative to loading direction (Boller 1964) and laminate architecture in multi-directional FRP composites (Davis et al. 1964) can also significantly affect fatigue behavior. Further, reduced fiber volume has been shown to result in a reduced rate of strength degradation with cycling (Tanimoto and Amijima 1975). It has also been shown that the fatigue life of CFRP bars depends on the mean stress and the stress ratio. Higher mean stress or a lower stress ratio causes a reduction in fatigue life (Rahman and Kingsley 1996; Saadatmanesh and Tannous 1999). Increased ambient temperature, is known to be detrimental to the fatigue performance of FRP materials (Adimi et al. 1998; Agarwal and Broutman 1990).

O'Neill et al. (2007) investigated the behavior of typical adhesive systems subject to fatigue conditioning. The adhesives considered all had measured monotonic shear capacities between 12 and 16 MPa (1750 - 2320 psi) although their shear stiffnesses differed by a factor of twenty. Fatigue conditioning consisted of 1000 cycles at stress ranges from 10% to 60% of the monotonic shear capacity followed by a monotonic test to failure. Degradation of the ultimate shear stress was apparent for all adhesive types tested. The authors conclude that for relatively low fatigue stress ranges, a stiffer adhesive will exhibit minimal

degradation. At higher stress ranges, however, degradation should be expected and a softer adhesive will provide greater ductility and may be expected to behave in a more predictable manner.

In some previously reported studies of FRP-retrofitted reinforced concrete flexural members (Heffernan 1997; Masoud et al. 2001; Quattlebaum et al. 2005; Aidoo et al. 2004 and 2006), although the stress range (S) in the primary longitudinal reinforcing steel is reported to be reduced in the FRP-retrofitted beams, there is no corresponding increase in the fatigue life (N). In these cases, it would appear that the stress range in the reinforcing steel, while initially reduced due to the presence of the additional FRP reinforcement, subsequently returned to the stress range corresponding to the unretrofitted control specimens. Debonding of the FRP retrofit material in the vicinity of the high flexural stresses is believed to explain this behavior.

Other studies (Barnes and Mays 1999; Shahawy and Beitleman 1999) demonstrated both a significant reduction in longitudinal steel stress and corresponding increase in fatigue life with the application of FRP reinforcing material. Meier et al. (1993) report that the hybrid glass/carbon FRP material used in their study was able to bridge cracks resulting from the fracture of the primary longitudinal reinforcement in the beams tested. In this case, fatigue loading was continued beyond steel fracture until eventual fatigue failure of the hybrid FRP reinforcing. These results are a clear indication of sound bond between the concrete and FRP.

The different results obtained in different studies appear to be associated with FRP-to-concrete bond and/or the nature of the FRP-concrete interface. In all previously reported studies, some extent of debonding of the FRP material from the concrete substrate was observed. Once debonding occurs, stress carried by the FRP is redistributed back to the internal reinforcing steel in the regions of debonding. Thus improvement in fatigue performance is only affected as long as the FRP is adequately bonded to the concrete.

Papakonstantinou et al. (2001) demonstrated that the fatigue behavior of the existing primary reinforcing steel will govern the eventual fatigue performance of FRP retrofitted concrete beams. In this study, the stress level applied to the internal steel reinforcement was maintained constant for both retrofitted and unretrofitted specimens. No discernable difference in behavior between retrofitted and unretrofitted specimens having the same reinforcing steel stress levels was observed. Of course, the applied load to obtain the same steel stress in the retrofitted specimens was increased. (Additionally in this study of short beam specimens, FRP anchorage was ensured by “pinning” the GFRP material beneath the beam supports.)

Heffernan (1997), on the other hand, states that FRP retrofitted beams should exhibit improved fatigue characteristics over similar unretrofitted beams having identical initial steel stresses. This conclusion stems from the observations that concrete softens with cycling (Neville 1975), requiring redistribution of applied stresses to the tensile reinforcement. The additional tensile reinforcement, in the form of the FRP retrofit material, will clearly carry some of the redistributed stresses thus relieving the steel reinforcement and prolonging its fatigue life. Heffernan estimates that this increase in fatigue life will be approximately 2%. Such an increase in fatigue life is too small to capture with certainty in a reasonably sized test program.

Bolduc et al. (2003) concluded that fatigue loading did not reduce the effectiveness of a CFRP repair. In fact, higher plate strain at failure was observed as compared to statically loaded CFRP-repaired members. Nonetheless, Bolduc et al. acknowledged that the surface preparation for the fatigue loaded member was more significant (great surface roughness) than the other specimens, which is believed to effect the results. The findings reported by Miller et al. (2006) support the conclusions of Bolduc et al. Miller et al. investigated fatigue loading of an impact-damaged AASHTO Type II girder, repaired with grout and longitudinal and U-wrapped CFRP sheets. Under fatigue loading, no cracking was observed in the patch area and thus it is believed that the patch performed better than the undamaged member. Additionally, a final static test was performed on the girder to determine its ultimate moment capacity. The repaired

girder exhibited similar stiffness as the undamaged member. U-wraps and longitudinal CFRP did not delaminate prior to crushing of the concrete at ultimate load.

Kotynia et al. (2011) tested reinforced concrete slabs with gradually anchored prestressed CFRP strips (described later) under both static and cyclic loading. The cyclic loading was also performed at elevated temperatures. Temperatures up to 75°C did not affect the bond quality. However, above 100°C, above the glass transition temperature of the CFRP, the typically-observed gradual loss of bond (slip) between concrete and FRP was accelerated. Regardless, strengthening with prestressed CFRP strips was found to increase the fatigue durability of the slabs.

Most studies clearly indicate that the performance of externally bonded CFRP systems deteriorate when subject to fatigue loading. Additionally, even very low stress ranges result in some degree of degradation suggesting that there is no (or at least a very low) endurance limit below which fatigue-induced degradation is no longer a concern. Harries et al. (2006) reported the results of a series of tests conducted on decommissioned interstate girders. They report that 2 million cycles resulting a fatigue stress range in the CFRP as low as $0.04f_{tu}$ appears to have affected the ultimate performance of the member.

1.5.3.5 Environmental Durability of FRP Systems

The dearth of information and uncertainty associated with the durability performance of FRP materials is recognized as being the primary impediment to broader adoption of these materials in civil infrastructure applications (Karbhari et al. 2003; Porter and Harries 2007). Nonetheless, properly installed and maintained FRP systems are as robust as any construction material when subject to typical bridge structure environments. ‘Durability’ is defined as a material’s “ability to resist cracking, oxidation, chemical degradation, delamination, wear, and effects of foreign object damage for a specified period of time, under the appropriate load conditions, under specified environmental conditions.” (ACI 440 2007). This all-encompassing definition has been broadly adopted making studies of durability remarkably diverse and each one necessarily specific.

A complete review of studies of FRP durability is well beyond the scope of the present report. A concise review of durability issues associated with FRP intended for use in civil infrastructure is presented in ACI 440 (2007). In environmental conditions typical of bridge structures, hydrothermal effects (the combined effects of moisture or humidity and heat) are dominant in the degradation processes of FRP materials (Anstice and Beaumont 1982). Along with moisture absorption, chemicals in solution may exacerbate deleterious effects. Salts and the high alkalinity of concrete pore water are common environments in which FRP materials must perform. It is also well established that the constituent components of FRP systems, themselves, must be compatible. Environmental degradation can be significantly accelerated in cases where the fiber and resin are incompatible (Karbhari and Engineer 1996). Water absorbed by the FRP matrix can result in physical changes to the matrix (including plasticization and a reduction in glass transition temperature) which result in a breakdown of the resin matrix and the protection it provides the encased fibers. While carbon fibers (CFRP) are relatively inert, glass fibers (GFRP) are susceptible to moisture extracting ions from the glass (corrosion of glass) and to chemical attack; glass also degrades when exposed to UV radiation (sunlight). Water absorption is also known to affect FRP-to-concrete bond, usually to a greater degree than it does the FRP properties themselves (Wan et al. 2006).

Effects of environmental exposure on in situ FRP properties are handled in design by using so-called ‘knockdown factors’ that are applied to reduce the material properties appropriately. In ACI 440.2R (2008), the environmental exposure factor is termed C_E and takes a value of 0.85 for CFRP in an aggressive environment or for exterior exposure. The knockdown factors are essentially additional material resistance factors and are understood to consider the ‘life of the repair system’ which is often described as being 50 years. The C_E factor is applied to FRP strength (i.e., $C_E f_{tu}$) and strain capacity ($C_E \epsilon_{tu}$) but not modulus; according to ACI 440, “... the modulus of elasticity... is typically unaffected by environmental conditions.” The results of an extensive study (Cromwell et al. 2011) which addressed 64 permutations of FRP material, test method, and environmental conditioning, concluded that both the

FRP strength (f_{fu}) and modulus (E_f) are affected by environmental exposure. Additionally, all data indicate that the stress-strain behavior of the FRP remains linear, in which case the strain capacity (ϵ_{fu}) is largely unaffected by exposure. Cromwell et al. also clearly indicate a difference in performance between preformed and hand laid-up CFRP with the manufactured preformed CFRP plate or strips demonstrating superior durability. This difference between manufactured and hand laid-up materials reflects issues of quality control and should not be surprising.

A significant issue with the ACI 440.2R (2008) guidelines is that the C_E factor is only applied to FRP material properties and no exposure factor is applied when determining the capacity for the FRP-to-concrete. For most flexural applications and many shear applications, limitations associated with bond will control the design of the FRP. Cromwell et al (2011) clearly showed that environmental exposure has a greater effect on bond than on FRP strength or modulus. Additionally, effects on bond capacity are more pronounced in hand laid-up fabric applications, again likely reflecting quality control issues.

Based on the findings of Cromwell et al. (2011), an alternative approach to environmental knockdown factors is proposed. Factors associated with material properties remain dependent on the FRP material with values of 0.90 and 0.80 proposed for CFRP and GFRP, respectively. It is also proposed that these factors be applied to both FRP strength (i.e., $C_E f_{fu}$) and modulus ($C_E E_f$) values. Strain capacity will, therefore, remain unchanged since the combinatorial effects of reducing both the stress and modulus equally result in unchanged strain (i.e., $\epsilon_{fu} = C_E f_{fu} / C_E E_f$). In addition, factors to be applied to bond capacity are proposed as 0.90 for preformed CFRP and 0.50 for fabric systems regardless of material (no tests of preformed GFRP were conducted although such a product is rarely used in North America). Based on the conditioning performed by Cromwell et al., it is believed that the proposed factors are appropriate for exterior bridge exposure. The factors can likely be relaxed for interior exposure and environment-specific factors need to be developed for specified 'aggressive' environments.

1.5.3.6 FRP Applications During Live Loading

In practice, there are many situations under which deteriorated structures are subjected to continuous transient vehicles loads (Moy 2000). Since many FRP applications are located on the underside of the bridge, it is particularly beneficial if the FRP strengthening can be implemented without interrupting the traffic on the bridge. Under such conditions, however, there is a need to confirm whether a reliable bond of the FRP to the concrete substrate can be achieved under conditions of continuous vehicle loading acting during the installation and, perhaps more importantly, the cure of the FRP. Nonetheless, there has been comparatively little research conducted to investigate the effects of transient loads during the installation and cure of FRP composites on the performance of FRP-strengthened RC structures. Where these studies exist, the results are contradictory. The following summarize a number of studies addressing the development of FRP bond subject to cyclic loading during cure. Many such studies refer to steel substrates rather than concrete. These studies remain informative in the context of the present work since such loading during cure affects primarily the adhesive component of the interface (Moy, 2000).

MacDonald (1981) performed tests on single-lap shear steel specimens subjected to cyclic movement while the resin was curing. The cycles were intended to represent highway traffic conditions. Each specimen was subjected to cycles with a frequency of 1 Hz while the resin was curing and for several days afterwards to give a minimum of 500,000 cycles with a strain range of 50 microstrain at full cure. Two different types of epoxy were used. The results showed that an average reduction in strength of 16% was present with a stiffer resin while there was no reduction in strength with a more flexible resin. The difference in resin modulus may account for the variation in performance of the two resin systems. Stiff resins, while required for efficient stress transfer are known to have relatively poor fatigue performance in comparison to 'softer' resins (O'Neill et al. 2007). Barnes and Mays (2001) also tested steel and CFRP lap joint specimens with results similar to those of MacDonald (1981). It was found that vibration during cure caused a progressive reduction in strength with increasing strain levels. An 8% strength reduction for steel joints was found when transient loading during cure resulted in steel strains of 50 microstrain. Moy

(2007) considered steel beams having bonded CFRP and recommended the use of enhanced curing techniques to minimize the cure time and thus any impact of transient loads during the cure.

Another testing program reported in Barnes and May (2001) included the adhering of a thin plate to a steel I-section beam. A steel beam was chosen to assure the failure plane occurred in the adhesive layer. Transient loads at 2 Hz, resulting in varying levels of strain, were introduced to the specimens for 48 hours. At the end of this time period, the specimens were tested to failure. The results from this study showed that although the strength of the plated beams decreased with increasing amplitude of cyclic strain, there was an unexpected strength increase as compared with the control specimens. The researchers concluded that a possible explanation for this strength increase was that the heat generated during the transient loading may have affected some post-cure for the adhesive. At a rate of 2 Hz, however, this explanation is believed to be unlikely (O'Neill et al. 2007).

Barnes and Mays also tested larger scale concrete beams having both steel and CFRP adhered plates. Load cycles at a frequency of 1Hz and a strain range of 150 microstrain were applied to the beams for 48 hours and the beams were tested to failure 7 days after strengthening. It was reported that the ultimate load capacity of the plated beams was not affected by transient loading during curing of the adhesives.

Wang et al. (2012) reported an experimental study of eight reinforced concrete beams strengthened with wet lay-up carbon fiber sheets subjected to simulated vehicle loading during installation and curing. The effectiveness of the EB-CFRP system installed under simulated transient loads (frequency of 1 Hz varying from 30% to 50% of the load-carrying capacity of the unstrengthened beams) was verified. Good composite action between CFRP sheets and concrete substrate was demonstrated by monitoring the strain development in the FRP sheets during the transient loading cycles. The bonding layer achieved good cure and the CFRP became composite with the concrete during the transient loading portion of the test. Compared to a control beam strengthened under a sustained load of 30% of the load-carrying capacity of the unstrengthened beam, those beams strengthened under simulated transient loads exhibited greater load-carrying capacity. This may indicate a creep-related behavior and/or a prestressing effect being introduced to the CFRP cured under conditions of sustained load and transient load, respectively.

Reed et al. (2005) reported a study similar to that of Wang et al. (2012a). They concluded that cycles applied during FRP cure (0.33 Hz at various load levels over 48 hours) have a minimal effect on the ultimate strength of the FRP-reinforced beams. However, the load cycling seemed to increase the eventual ductility of the specimens over those not exposed to load cycles. Specimens in this study were also subject to 100,000 load cycles prior to FRP installation which may have impacted the apparent ductility. Meier et al. (2003) also reported no difference in the load-carrying capacity, mid-span deflection and CFRP strains in tests of a bonded EB-CFRP plate system with or without oscillating loading during curing of the adhesive.

1.5.4 Case Studies

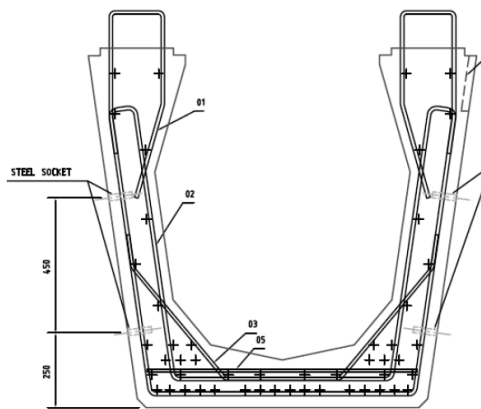
There is a relative dearth of published studies of repairs of impact-damaged prestressed concrete bridge structures. The following sections describe both published material and, in some cases, unpublished information made available to the research team. In the latter cases, information that may identify the bridge described has been removed.

1.5.4.1 Preloading Repair

Pakrashi et al. (2010) discuss the repair of the impact damage Brownsbarn Bridge, near Dublin, Ireland, which was struck by a low loader carrying an excavator. The Brownsbarn Bridge (see Figure 17a) is a two span continuous slab – girder bridge comprising six precast prestressed U8 concrete beams (approximately 1200 mm (47 in.) deep U-girder) connected by a continuity diaphragm (similar to that of spread box beam bridges). Interestingly, this impact damage did not significantly affect the exterior girder, but rather the fourth interior (Figure 17b). The exterior girder lost one prestressing strand and had

minimal concrete damage. The interior girder was significantly damaged as an appreciable volume of concrete was damaged and many strands exposed, although none were severed (Figure 17b).

The preloading technique was employed to repair the damaged girders. The repair proceeded by loading the bridge using concrete blocks in 20 ton increments up to 120 tons. Unsound concrete in the vicinity of the damage was then removed by Hydrodemolition (Figure 17c). Following this, the girder was patched using a high strength cementitious material, and 12 hours was provided to allow for curing (Figure 17d). The preload was finally removed in similar 20 ton increments. Based on instruments installed during the repair, the preload operation appeared to result in a prestrain in the patch material on the order of 120 microstrain. While this repair method is not practical for all structures, it proved itself both a useful and rapid repair method in the case of the Brownsbarn Bridge. It is important to note that extreme care regarding the damaged section properties must be taken when considering the use of the preloading technique so as not to overstress the member. The Brownsbarn Bridge is a prototypical example of a preloaded patch repair.



a) U8 girder cross section (approximately 1200 mm deep)



b) damage to fourth interior girder



c) damaged region following hydrodemolition



d) completed repair

Figure 17 Brownsbarn Bridge (Pakrashi et al. (2010).

1.5.4.2 Strand Splice Repair

In addition to the number of previously discussed studies which utilized strand splices, there are a number of States which employ this technique (see Section 1.6). Implementation of the strand splice repair technique is based on strand displaced length and will be discussed in greater detail in Task 2.2. This repair technique can be used to splice a wide number of strands (Toenjies 2005 and Enchayan 2010) and is easily used in conjunction with other external repair techniques, including externally bonded CFRP strips (Toenjies 2005). Photos of typical strand splice repair sequence are shown in Figure 18.

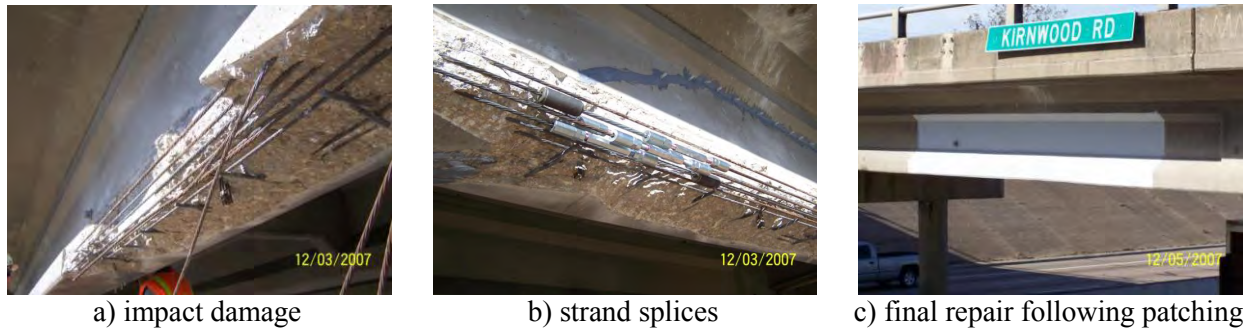


Figure 18 Strand splice repair of exterior AASHTO I-girder.

[Courtesy of the Texas Department of Transportation, © 2007 All rights reserved.]

1.5.4.3 EB-CFRP Repair

Tumialan et al. (2001) discussed an I-girder bridge (bridge number A10062) located at the interchange of Interstates 44 and 270 in St. Louis County, Missouri, which was damaged by an over-height truck. Inspection of the damage revealed that two prestressing strands (of 20 total) were severed due to the impact, resulting in an approximately 8% reduction in flexural moment capacity. Upon review of the techniques available at that time, the authors chose externally bonded CFRP to restore the girder capacity. The repair technique restored ultimate capacity of the girder and was considered to be economical due to minimal traffic disruption (the CFRP was installed in approximately two hours).

Similarly, Schiebel et al. (2001) reported the repair design and application of bridge number A4845, which was also impacted by an over-height vehicle. EB-CFRP was employed to restore the 11 girders damaged (various severity of damage) in the accident to their original undamaged capacity. This study also examined the bond strength between the CFRP and girder and found it to be of sufficient quality at the time of the repair, validating the assumptions used in design. Both Tumialan et al. and Schiebel et al. present detailed calculations for the repairs executed.

Klaiber et al. (2003) reported an I-girder bridge carrying IA Highway 65 over IA Highway 6, near Altoona, Iowa, was damaged by vehicle impact. Damage occurred to the exterior and first interior girder. Interestingly, the damage to the exterior girder was mostly concrete spalling while the damage to the first interior girder was more severe, exposing five prestressing strands and severing two. All damaged girders were patched. The first interior girder was repaired with four EB-CFRP strips longitudinally, bonded to the girder soffit. After curing, several CFRP U-wraps were placed on and around the patched area. Strain gages were mounted to all beams of the damaged span and the structure was load tested. While all deflections were fairly small, the CFRP repair reduced live load deflections by upwards of 20% in some cases.

1.5.4.4 PT-CFRP Repair

An improperly designed drainage system on a bridge allowed storm water to flow through a gap at the sidewalk-girder interface resulting in several beams being exposed to deleterious materials, mostly chlorides from de-icing salts for the 25 year life of the bridge (Sika 2008a). It is estimated that upwards of 25% of the prestressing strands were damaged or lost from the adjacent box girder structure. An extensive concrete repair and waterproofing was undertaken in order to mitigate further deterioration and the Sika CarboDur StressHead system was employed to apply a bPT-CFRP repair. According to Sika (2008a), this is the first time a PT-CFRP system was used in North America to strengthen a bridge. While not an impact damage, this case study provides a quality example of the use of PT-CFRP as a viable repair technique. Additionally, the source of deterioration (corrosion) is also of concern regarding impact damage and thus this repair scenario is applicable to the topic at hand.

Main Street Bridge, located in Winnipeg, Canada was frequently struck by heavy trucks. Impact loads had resulted in exposure and severing of prestressing strands and concrete spalling. An analysis of the damaged girder revealed that it no longer satisfied Canadian Highway Bridge Design Code (2006) requirements based on insufficient flexural load capacity and serviceability. Daily traffic on the roadway below was considerable and thus the repair needed to be performed quickly. The repair, reported by Kim et al. (2008c) utilized a custom-fabricated tensioning system to stress the strips, and included an epoxy interface between the CFRP and repair girder, thus resulting in a bPT-CFRP repair. Epoxy was applied between the CFRP and girder interface, stressing operations were performed and end anchors were bolted to the jacking plates to retain the induced stress. During the repair operations, traffic flow was maintained. The bPT-CFRP repair was able to restore approximately 8% of the undamaged cracking moment and 18% of the undamaged nominal moment. However, in load rating the repaired structure, it was found that the live load carrying capacity remained below unity – largely due to the very conservative estimate of 30% CFRP prestressing loss (which is thought to be too great owing to the use of end anchors). Regardless, this repair allowed the structure to remain in service and, in a worst-case scenario, may require posting.

Herman (2005) reports an application of bPT-CFRP on two prestressed concrete box girder bridges. The intended repair of the prestressed concrete box girders was to restore flexural capacity as well as replace some of the lost prestressing forces; employment of the Sika Carbostress system as the repair technique proved successful at restoring flexural capacity and prestressing force. Additionally, this method saved monetary and material resources and minimized construction time and traffic closures.

1.5.4.5 Combined Repair Methods

The case studies described above utilized only one of the possible repair techniques. Yang et al. (2011) discuss Texas DOT's (TXDOT) use of multiple techniques to repair impact damaged prestressed girders through discussion of four different damaged structures (some structures were impacted two or even three times). Most repairs employed a combination of preloading, strand splicing and externally bonded CFRP strips or fabric. The use of these repair techniques has been successful and beneficial to TXDOT due to decreased service disruptions and reduced repair costs (as compared to girder replacement); many structures are repaired within one week. One repair has been in place for 5 years without any sign of deterioration or delamination. Equally significant, TXDOT claims to have repaired more than 30 girders to date with CFRP (often in combination with the methods previously suggested). Interestingly, TXDOT has also used CFRP as “sacrificial” reinforcement for structures likely to experience impact after being repaired at least once. As seen in Figure 19b, CFRP is placed on the girder flange leeward to the direction of traffic to help minimize the effect of truck impact in highly vulnerable structures (those having been previously impact by vehicles). One example is an I-girder which has repaired three separate times with CFRP (see Figure 19).

One of the case studies presented by Yang et al. is presented as a prototype example structure (Section 2.2.3) in this study. The field repair conducted for this bridge is summarized in Section 2.2.3.2 and Figure 25.

1.5.4.6 Susceptibility of Repairs to Further Damage

Considering the increasing use of FRP applications and the consequent likelihood of subsequent impact damage to the repair (see Figure 19), attention is now turning to damage tolerance of FRP repairs. In general, FRP applications result in a tougher and more damage-tolerant concrete structure (as described above), nonetheless, impact can result in loss of FRP capacity. In a recent study, Kirby and Orton (2011) concluded that impact pressure less than 3000 psi (21 MPa) applied by a cylindrical loading tup resulted in no reduction in the tension capacity of CFRP applied to a concrete substrate. These results are difficult to translate to highway bridge impacts but provide some guidance to the level of impact load that may result in CFRP damage.



a) 2007 impact to previously repaired region



b) second repair confined with CFRP



c) 2008 impact to twice-repaired region



d) strand splice repair



e) completed third repair

Figure 19 Exterior AASHTO I girder patched repair confined with GFRP August 2006

[Courtesy of the Texas Department of Transportation, © 2007 All rights reserved.]

1.5.5 Aesthetic Repairs

A review of methods to affect aesthetic repairs to prestressed concrete elements is provided here. These repairs are typically necessary to address defects that occur during fabrication, shipping, handling or erection of a member but can also be used to correct impact damage. Aesthetic repair methods are also often required as a final step in a structural repair. These methods are well established and extensive guidance on their application are reported in the *Manual for the Evaluation and Repair of Precast, Prestressed Concrete Bridge Products* (PCI MNL-137-06) published by the Precast/Prestressed Concrete Institute (PCI). The *ICRI/ACI Concrete Repair Manual* also provides guidance on concrete aesthetic repairs.

1.5.5.1 Patching

No matter how much care is exercised in placing and curing concrete, defects occur that require patching. Patching requires the removal of all unsound concrete. It is usually a good idea to remove slightly more concrete rather than too little, unless it affects the bond of prestressed strands. The chipped area for patching should at least be 1 in. deep and should have edges as straight as possible, at right angles to the surface. Tapered edges of a patch will break or the thinner sections will weather and spall easily. The use of air driven chipping guns or a portable power saw for cutting concrete is recommended for removal of concrete but care should be taken to make sure that the reinforcement or the strands are not damaged. When patching prestressed elements, preloading the elements is often recommended in order to slightly ‘prestress’ the patch to resist ‘pop-out’ (Shanafelt and Horn 1985; Feldman 1996). Clearly, this is not always possible in *in situ* repairs.

There are six main methods for patching. Their selection will depend on the size of the patch and limitations of each method. Considerations in patch material selection include i) rheology of the patch material (the material must thoroughly fill or pack into the void being patched); ii) bond strength to *in situ* concrete and steel reinforcement traversing patch; iii) compressive and tensile strength of patch material;

and, iv) durability of the patch material. Given that the volume of many patches is small, the benefit of using a high quality prebagged repair material is likely warranted and represents only a small incremental cost in the entire patching operation. The six methods are described briefly in the following sections. Greater detail may be found in *PCI Manual 137* (2006).

1.5.5.1.1 Drypack Method

The drypack method should be used for the repair of newly placed concrete in which holes have a depth nearly equal to the smallest dimension of the section, such as in the case of core or bolt holes. The drypack method should not be used on shallow surfaces or for filling a hole that extends entirely through the section or member.

In order to apply the drypack, the surface must be wetted to a 'saturated-surface dry' condition. When there is no excess water, a bond coat is applied. The bond coat is made up of cement and fine sand in a 1:1 ratio (a small amount of water is used to make a very stiff paste). This coat is applied evenly to the patch surface. Then, the drypack is prepared by using cement and sand in ratios of 1:1 to 1:3 by volume (again, with a small amount of water). Since the material amounts dealt with are relatively small volume proportioning is used instead of weight. The drypack mix is then placed in layers having a maximum thickness of 0.5 in. Each layer is tamped separately and thoroughly. The finished patch should be well-cured for durability and strength.

1.5.5.1.2 Mortar Patch Method

This method is used in concrete members with shallow defects, which require a thin layer of patching material. Honeycombs, surface voids or areas where concrete has been pulled away with the formwork require mortar patching.

Surface preparation, mix design and application are very similar to drypack patching. The main difference is, since mortar patching is applied to shallow defects, the patch itself is more susceptible to the effects of shrinkage or poor bond strength especially near its edges. The use of mixes richer than the 1:3 cement to sand ratio exacerbate the effects of shrinkage whereas leaner mixes will result in poor strength.

1.5.5.1.3 Concrete Replacement Method

This method consists of replacing the defective concrete with machine-mixed concrete that will become integral with the base concrete. Concrete replacement is preferred when there is a void going entirely through the section, or if the defect goes beyond the reinforcement layer, or in general if the volume is large.

All unsound concrete should be chipped off for initial preparation. If there is reinforcement in the area, at least 1 in. of space should be provided around it. Any displaced or cut-off reinforcement should be repaired providing as much overlap as possible when tying in new reinforcement. A bond coat is then applied to the entire patch area. The repair concrete should be placed while this bond coat is still tacky. The initial layer of concrete should have a slump of around 3 in. with each consecutive layer having lower slump. Each layer should be vibrated by an immersion-type vibrator or a hammer from outside of the form if a vibrator is not available. The patch should then be moist cured for as long as possible.

1.5.5.1.4 Synthetic Patching

There can be some cases where Portland cement patches are difficult or impractical to apply. These situations include patching at freezing temperatures or patching very shallow surface defects. Two synthetic materials useful under such circumstances are epoxy and latex based products.

Epoxies can be used as a bonding agent, a binder for patching mortar, an adhesive for replacing large broken pieces, or as a crack repair material. Small deep holes can be patched with low-viscosity epoxy and sand whereas shallower patches require higher viscosity epoxy and are more expensive. It is suggested that epoxy mortars be used only in situations where exceptional durability and strength are

required. Although they offer excellent bond and rapid strength development, they are hard to finish and usually result in a color difference between the patch and the base concrete, clearly showing the repaired section, unless precautions are taken against it.

Latex materials are used in mortar to increase its tensile strength, decrease its shrinkage and improve its bond to the base concrete, thus helping to avoid patch failure due to differential shrinkage of the patch. Because of its good bonding qualities, it was found that latex was especially useful in situations where feathered edges cannot be avoided.

1.5.5.1.5 Prepackaged Patching Compounds

There are many commercial patching products available. There are several points to consider when using such products:

1. A good patching material should have an initial setting time of 10 – 15 minutes and a final setting time of 20 – 45 minutes. Cements with setting times other than these should be avoided.
2. Some products must be used in small amounts because they generate excessive amounts of heat which can lead to shrinkage and poor durability, and therefore are not suitable for general purpose patching.
3. A concrete patch should have a compressive strength at least equal to the base concrete. The compressive strength claimed by many products is based on very low water-cement ratios. For practical applications however, the compressive strength was found to be lower than Type 1 Portland cement mortar.

1.5.5.1.6 Epoxy Injection

Epoxy injection methods have been used to repair cracks or fill honeycombed areas of moderate size and depth. Only appropriately trained personnel should carry out such repairs.

Before injection, the crack must be properly sealed at its surface in order to accommodate the pressure required to completely fill the void. In most applications, sealing the crack surface with an epoxy paste is adequate. The area adjacent to the crack should be sound, clean, dry and free of dirt or oil. Epoxy injection ports need to be located based on crack length and depth. Although there are no exact values or rules, rules-of-thumb suggest that ports should not be placed closer than 8 in. For cracks narrower than 0.007 in., locate ports on both faces of a crack in order to verify complete injection. For larger cracks, reverse ports are not required.

Usually, the maximum pressure the seal or the injection equipment is capable of sustaining is used to reduce the time required to fill the crack and to ensure full penetration. Pressures used in conventional applications range from 40 – 500 psi; most commonly in the range of 75 – 200 psi.

The injection process should continue until either the adjacent port expels the resin or until the pumping motion of the equipment stops. The process should be repeated for each adjacent port in a logical path until refusal is reached at the last port.

1.5.5.2 Patch Confinement

As described previously, preloading structures during the patching operation can draw the patch material into compression thereby mitigating effects of patch shrinkage, cracking and pop-out. Preload, however is often impractical. As an alternative, both CFRP and GFRP materials have been used to confine patches. An example repair sequence involving strand splicing, patching and patch confinement is shown in Figure 20. The externally applied FRP affords some protection to the patch and, significantly, provides some continuity or ‘bridging’ between the patch and surrounding concrete. Because all GFRP systems and most epoxy resin systems are susceptible to damage from UV light exposure, FRP systems applied to exterior girders in particular require a final protective top coat. This is also often done for aesthetic reasons. FRP applications used to confine patches have been found to be very robust (Harries 2001), even serving to reduce damage caused by subsequent vehicle impacts (Figure 19).

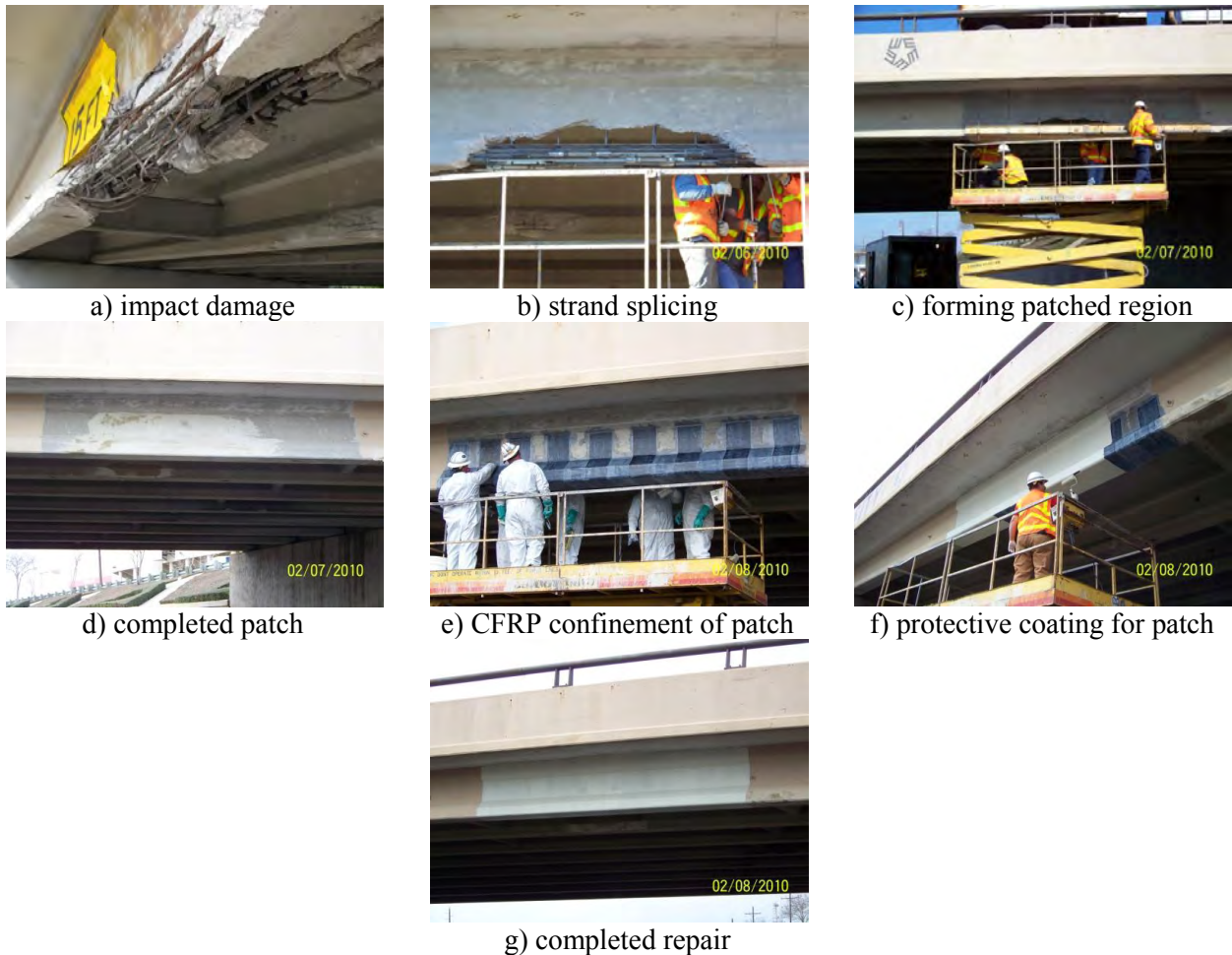


Figure 20 Strand splicing and patch repair sequence.
 [Courtesy of the Texas Department of Transportation, © 2007 All rights reserved.]

1.6 Survey of Current State of Practice

A survey of current practice was disseminated to all US State DOTs in late 2011. A copy of the survey instrument and accompanying letter is provided in Appendix E. Twenty four (24) responses were received; to this, four (4) non-duplicate responses from an essentially identical survey conducted in 2008 (Harries et al. 2009) were added (the latter are noted with an asterisk (*) in Appendix E. All responding jurisdictions are noted in the response to Question 4. The complete responses to the survey are transcribed in Appendix E. In Appendix E, boxed numbers indicate the number of respondents indicating the given responses (with the exception of Question 4). Many surveys had multiple responses to a given question. Where comments are provided, these are prefaced by the two letter state identifier. Comments have not been edited although some typographical errors have been corrected. Key findings resulting from this survey are as follows:

As should be expected, load capacity is the dominant consideration when selecting a repair method. Durability of the repair and interruption of service were also major considerations; time to make the repair was a moderate consideration and cost of the repair was not considered as significant. These responses are interpreted as indicating that non-invasive repair techniques or those that limit bridge closure are preferred. The expected durability and/or life extension imparted by the repair is a consideration indicating that repair philosophies recognize that bridge structures in the United States will be expected to serve beyond their intended design life.

Most reported impact-related damage is classified as minor damage (defined as: concrete cracks and nicks; shallow spalls and scrapes not affecting tendons). Despite anecdotal evidence to the contrary, few respondents reported corrosion resulting from previous impact damage as a significant source of damage. For minor damage, often no repair action is taken. While ‘no action’ may seem an initially prudent response for ‘minor damage’, such damage is unlikely to remain ‘minor’. The dominance of minor damage in the survey responses suggests an opportunity to deploy preventative measures addressing this level of damage in order to prevent the damage from worsening through ongoing deterioration mechanisms (primarily corrosion).

Moderate damage (defined as: large concrete cracks and spalls; exposed, undamaged tendons) was also broadly observed and was generally reported to be repaired using surface concrete patching techniques. Two jurisdictions reported using carbon fiber reinforced polymer (CFRP) materials in patching operations of moderate damage if similar materials were already being used on site to repair significant damage. Significant damage (exposed and damaged tendons; loss of portion of cross section) was reported relatively rarely. In such cases, “load bearing repairs” were generally reported. All existing methods of strand repair offered in Question 11 were reported with similar frequency, indicating no dominate or preferred method of repair. This additionally suggests that, as may be expected, repair methods and designs are site-specific. Nonetheless, Grabb-It splices are specifically cited by about one half of respondents. About one half of respondents also indicated that girder preloading is used to induce compression into concrete patch.

Severe damage (damage severe enough to result in girder distortion or misalignment), was rarely reported and the consensus was that such damaged girders would be replaced. Few respondents indicated specific criteria by which they make the “repair or replace” decision for impact-damaged prestressed girders. One jurisdiction, for instance, conducts no analytical assessment or load rating but simply replaces the girder if 3 or more strands are ruptured and repairs the girder if only 1 or 2 strands are ruptured. Texas, on the other hand, takes an approach similar to that described in this work: An operational rating factor (ORF) and load rating (OLR) for the damaged girder is established. If $ORF < 1.0$ or $OLR < HS20$, a structural repair is done to restore ORF to unity or OLR to HS20; otherwise, only a non-structural patch repair is conducted.

In most reported cases, load rating of the damaged girders was conducted using available (often in-house) software. The inspection, on which these models are based, however, is almost exclusively visual. Few jurisdictions report the use of NDE methods (hammer sounding is the only method specifically reported). This finding reflects a number of stressors on the bridge inspection process, but significantly the fact that prestressed structures are very difficult to inspect in the first place. Additionally, this finding suggests the need for more efficient NDE methods for prestressed structures are required.

Although there was little consensus on repair methods or practices, all respondents identified their repairs as successful. One respondent noted that FRP-based repairs were particularly effective. A few respondents noted the need to preload patch repairs to ensure durability and, particularly, performance in the event of subsequent impacts. Some respondents apparently believe that replacing the girder is the best alternative for prestressed concrete elements.

CHAPTER 2 RESEARCH PROGRAM AND FINDINGS

2.1 Research Approach

Previous studies have clearly indicated that ultimately the decision to repair or replace a collision-damaged prestressed concrete structure must be made on a case-by-case basis. Nonetheless, basic criteria - sometimes structure-type specific and sometimes universal - may be established. The objective of this work is to develop this guidance.

A parametric approach varying the degree of damage to the girder and considering different repair techniques is used to investigate the ‘design space’ for each repair technique. Physical limitations of the repair methods are also investigated to define the design space. The design space for each repair method is then described by the spectra of damage to which the method may be effectively applied. The spectra of damage may be envisioned as having two thresholds as shown in Figure 21: the ‘no repair – repair’ threshold and the ‘repair – replace’ threshold.

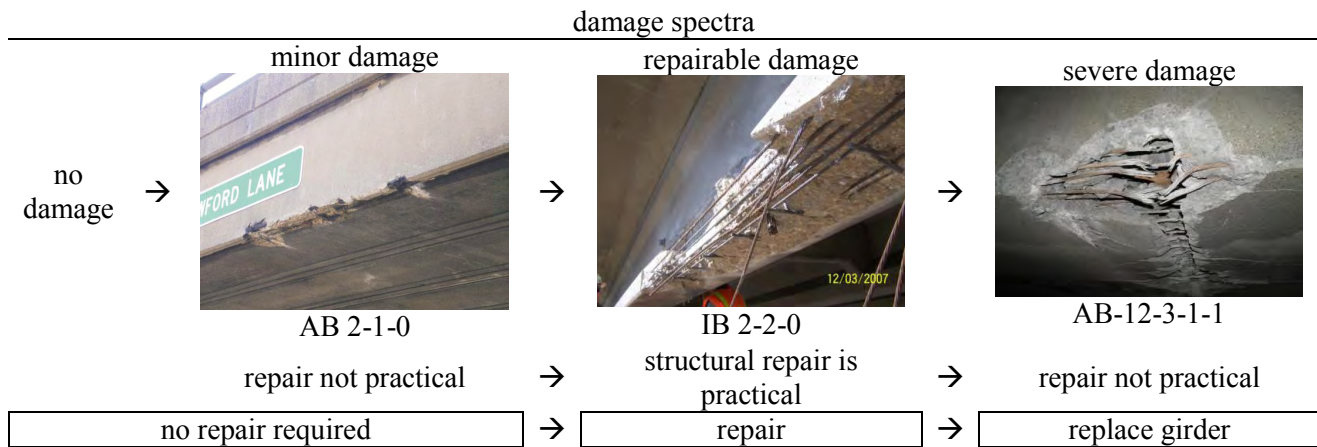


Figure 21 Schematic representation of design space for impact repair.

The approach taken, described in detail in the following sections, focuses on impact damage *requiring structural repair*. The basic steps of the approach are as follows:

1. Select prototype structure and determine undamaged capacity (Section 2.2)
2. Apply damage spectra (Section 2.1.3) and determine residual capacity of damaged girder
3. Select repair method (Section 2.3) and determine physical limitations of repair method thereby defining the ‘maximum’ capacity that the repair technique is able to develop (these are described for each repair method in Section 2.4).
4. Design repairs for range of damage (Section 2.3) and assess efficacy of repair (Section 2.1.2).
5. Identify ‘no repair-repair’ and ‘repair-replace’ thresholds for each structure type and repair method (Section 2.6).

This approach will result in a matrix of repair techniques and levels of damage for each prototype adjacent box girder (AB), spread box girder (SB) and I-girder (IB) (Section 2.2). A specific example (dark shaded in Table 5) is presented in its entirety in Appendices B through D. Additional examples of the design of specific repair techniques (light shaded in Table 5) are also presented. The remaining cases will be carried out and presented only in the matrices. Each combination of repair method and damage level will be described in terms of both the repaired girder capacity, C_R , and resulting normalized rating factor, RF_R , (see Section 2.1.2). The matrices will also report the undamaged (C_0 and RF_0) and damaged (C_D , RF_D) capacity and rating factors. Section 2.3 presents the results from all such analyses. Interpretation of this data, presented in Section 2.4, will inform the selection of repair thresholds for each girder type and repair technique.

Table 5 Sample repair matrix.

undamaged capacity $C_0, RF_0 = 1.0$		Damage Spectrum (see Section 2.1.3)					
		MINOR					SEVERE III
		C_{D1}, RF_{D1}	C_{D2}, RF_{D2}	C_{D3}, RF_{D3}	C_{D4}, RF_{D4}	...	C_{Dn}, RF_{Dn}
← Repair	Method 1	C_R, RF_R	C_R, RF_R	C_R, RF_R	C_R, RF_R		C_R, RF_R
	Method 2	C_R, RF_R	C_R, RF_R	C_R, RF_R	C_R, RF_R		C_R, RF_R
	Method 3	C_R, RF_R	C_R, RF_R	C_R, RF_R	C_R, RF_R		C_R, RF_R
	...						
	Method m	C_R, RF_R	C_R, RF_R	C_R, RF_R	C_R, RF_R		C_R, RF_R

2.1.1 Analysis of Girders

For each prototype structure described in Section 2.2, a representative worked example is presented. In these examples, the undamaged and damaged girder capacity is determined in a manner consistent with the *AASHTO LRFD Bridge Design Specifications* (2010) and the *AASHTO Manual for Bridge Evaluation* (2011). Repairs are designed, and the capacity of the repaired girders determined, based on appropriate standards and practices as noted in the examples. Fiber reinforced polymer (FRP) repairs and subsequent repaired girder capacities are based on the methods described by ACI 440 (2008).

In order to analyze the girders rapidly and consider various levels of damage, the undamaged girder cross section and all damaged and repaired sections are analyzed using a commercially available non-linear fiber sectional analysis software package XTRACT (TRC 2002). While XTRACT can perform moment-curvature (M- ϕ) and axial load-moment interaction (P-M) analyses about the horizontal (x) and vertical (y) axes, its ‘orbit analysis’ tool additionally permits an M_x - M_y failure surface to be generated based on specified failure criteria. This latter capacity is employed in this work since the nature of the applied impact damage (Section 2.1.3) results in a small eccentricity in the section behavior. This effect is described at length by Kasan and Harries (2012a). XTRACT provides both customizable analysis reports and an interactive mode to view results. All data is easily exported in text format for further processing. XTRACT is not able to run ‘batch jobs’ and thus multiple scenarios (as done for this study) require individual runs and data processing. The ease of use (particularly in editing models) of XTRACT however makes up for the necessity of this ‘brute force’ approach for multiple analyses.

In XTRACT, the section geometry is ‘drawn’ and an automated discretization procedure divides this into triangulated fiber elements. The concrete fiber element size for all models was 1 in., which is felt to be adequate given the complexity and size of the section. Mild steel and prestressing strand are modeled as individual fiber elements and are located exactly as they occur in the section. Customized non-linear stress-strain relationships are defined for all materials as described in Section 2.2.

In order to establish valid comparisons over a range of prototype structures and analyses, user-defined material failure criteria must be established. In essence, these criteria are ‘allowable strains’ or ‘performance criteria’ which no fiber in the section may exceed and are selected based on the limit state being investigated. In the present analyses, the ultimate capacity of under reinforced (i.e.: section response controlled by steel) prestressed girders girder is desired, thus criteria related to the ultimate capacity were selected (Table 7). The concrete ‘failure strain’ was selected to represent concrete crushing ($\epsilon_{cF} = 0.003$). Prestressing strand strain ($\epsilon_{pF} = 0.010$) was selected as being sufficient to develop close to the ultimate capacity of the strand (develop at least 1586 MPa = 230 ksi) while respecting the under-reinforced nature of the member. In addition, since the objective this work is repair, it is thought appropriate to consider performance where the primary prestressing strands have some reserve capacity. The mild steel strain was selected to be very high ($\epsilon_{sF} = 0.035$) so as not to affect the outcome of the analysis. In the sections considered, the mild steel (located only in the compression flange) does not play a significant role in the behavior and its failure (if the concrete and strand were still adequate) would not

be catastrophic. A sensitivity analysis (Kasan and Harries 2012a) was conducted to ensure that the criteria selected did indeed maximize girder capacity. Where applicable, CFRP ‘failure strain’ (ϵ_{IF}) was selected, in each case, to capture the debonding limit state for this linear elastic material. That is, the contribution of the CFRP is limited by the strain at which it debonds from the substrate concrete rather than by its ultimate strain (see Section 2.3.2.1).

Due to the simplifications and inherent conservativeness of code-prescribed calculations of capacity, capacities determined using XTRACT will generally be marginally greater than those determined using the AASHTO equations. This marginal difference can be seen in Table 6 and does not affect the outcome of this study since relative capacities of the undamaged, damaged and repaired girders are of interest. The modeling approach and XTRACT-based analysis used in this study has been extensively reported by the authors (Harries 2006, Harries et al. 2009, Kasan and Harries 2012a) and validated against full-scale test results (Kasan and Harries 2012b).

2.1.2 Assessment of Efficacy of Repair

AASHTO *Evaluation Manual* (2011) Eq. 6A.4.2.1-1 provides the basis for AASHTO girder rating factor, RF:

$$RF = \frac{C - \gamma_{DC}DC - \gamma_{DW}DW \pm \gamma_P P}{\gamma_{LL}(LL + IM)} \quad (\text{Eq. 1})$$

Where C is the structural capacity, DC, DW, LL and IM are load effects prescribed in the AASHTO *LRFD Bridge Design Specifications* (2010), and the values of γ are LRFD load factors prescribed in Table 6A.4.2.2 of the *Evaluation Manual* (2011). These factors differ for inventory and operational rating levels. The term P represents the effects of other permanent loads on the structure and, for convenience, is neglected in the examples presented.

Application of Equation 1 requires an entire bridge design in all cases. Since the objective of this work is to address the degree of strengthening of individual girder elements, a variation of this equation is used (Kasan 2012). If it assumed that the capacity of the as-built girder corresponds exactly to $RF_0 = 1$; that is: $C_0 = \gamma_{DC}DC + \gamma_{DW}DW + \gamma_{LL}(LL+IM) \pm \gamma_P P$, and the existing or damaged capacity is C_D , then the normalized rating factor for the damaged structure is:

$$RF_D = \frac{C_D - \gamma_{DC}DC - \gamma_{DW}DW \pm \gamma_P P}{C_0 - \gamma_{DC}DC - \gamma_{DW}DW \pm \gamma_P P} \quad (\text{Eq. 2})$$

Therefore analyses are effectively normalized by the AASHTO-prescribed inventory RF value (Eq. 1) and the normalized undamaged girder rating factor $RF_0 = 1.0$. This formulation removes the need to calculate LL, which is a function of specific bridge geometry (*AASHTO LRFD* Section 4.6). This normalized approach is illustrated in Table 6, showing the results of the rating exercise for the AB 3-2-0 prototype example presented in Appendix B. If RF for the as-built structure is known (RF_0), then the C_0 term in Equation 2 may be replaced with $RF_0 C_0$. In either case, ratings may proceed since the focus of the study is to consider the capacity of the repaired girder (C_R) relative to C_D and a target capacity C_0 (or another specified capacity). A rating factor less than unity based on Equation 2 does not necessarily imply structural deficiency as is the case when a rating factor less than unity is found from Equation 1. A value of less than unity from Eq. 2 simply indicates that the girder capacity is lower than the original design capacity. Thus, the decision to repair, replace or do nothing to an individual girder must still be made in the context of the entire structure.

Table 6 Comparison of inventory rating factors for AB 3-2-0 prototype presented in Appendix B.

	M_0 (kft)	M_D (kft)	M_R (kft)	RF_0	RF_D	RF_R
<i>AASHTO Evaluation Manual</i> approach (Eq. 1)	3511	3218	3562	2.31	2.02	2.36
XTRACT analysis (Eq. 2)	3573	3275	3698	1.00	0.88	1.05

2.1.3 Removal of Strands to Affect Damage Spectra

As shown schematically in Figure 21, a spectra of damage – represented by the number of strands removed from the prototype girder section analysis – is considered for each prototype. This spectra intentionally ranges from MINOR damage through SEVERE III (see Section 1.5.2) in order to investigate the complete design space of each repair technique.

Strand damage or loss associated with vehicle impact is most likely to occur at the outboard web-soffit corner of exterior girders. Thus removing strands beginning at the outboard web-soffit corner and progressing toward the inboard direction is appropriate to model impact damage. This type of damage is well represented in Sections 1.3.2 and 1.3.3 and shown in Figure 21. In the analyses conducted, strands were removed from the prototype girder cross sections in this manner. The multi-digit identification of each analysis indicates the number of strands removed from each layer beginning with the lowest (closest to soffit). For example the extant damage to the AB prototype (Section 2.2.1 and Appendix B), AB 3-2-0, indicates 3 strands removed from the lower layer, 2 from the second and none from the third, for a total of 5 strands removed from the AB prototype. In all cases the strands were removed from the outboard side and progressed inward. Even if vehicle impact is not the source of damage, removing strands in this manner represents a worst-case scenario since it results in the greatest girder cross section eccentricity. Each prototype was subjected to multiple levels of damage in order to capture the member behavior through a range of damage levels as indicated in the analysis results summaries presented in Section 2.4. In no case did the level of damage considered exceed that which would result in failure due to dead load of the member (i.e.: all damaged girders were still able to support their own self-weight).

2.2 Prototype Structures

Impact damage is most prevalent among ‘conventional’ prestressed bridges – those having typical spans and, often, minimal vertical clearance. This is clearly illustrated in Sections 1.3.2 and 1.3.3. Three representative prototype structures were selected for extensive parametric study: an adjacent box girder (AB), a spread box girder (SB) and an I-girder (IB) span. The AB and SB girders are decommissioned girders available to the author while the IB girder is a repair case study reported in the available literature.

2.2.1 Adjacent Box Girder Prototype AB

Prototype Girder AB is based on the exterior girder of a decommissioned adjacent box (AB) girder bridge structure available to the authors. The bridge was erected in 1960 and demolished and replaced in 2011; the fascia beam shown in Figure 22 was provided for testing (Harries 2012). The bridge spans 85’-4” with a skew of 68.5°. The bridge consists of 12 AB girders and has an out-to-out dimension of 49’-6” as shown in Figure 22a. The exterior girder was load tested over an unskewed simple span of 81’-2”;

thus all analyses utilized this span. As shown in Figure 22b, each AB girder is 48 in. wide by 42 in. deep. The primary prestressing consists of 57 - 3/8” diameter Grade 250 low-relaxation strands. Based on observed *in situ* conditions and the plan for a load test, a 3 in. composite deck is added to the girder making the overall depth 45 in. Impact damage (approximately 45 in. long) is evident centered approximately 28 ft. from the girder end (Figures 22c and d) at a location above the right lane of the carriageway passing beneath the bridge. The damage shown in Figure 22d, and the identification of this girder is AB 3-2-0 (see Section 2.1.3 for explanation of method of damage identification).

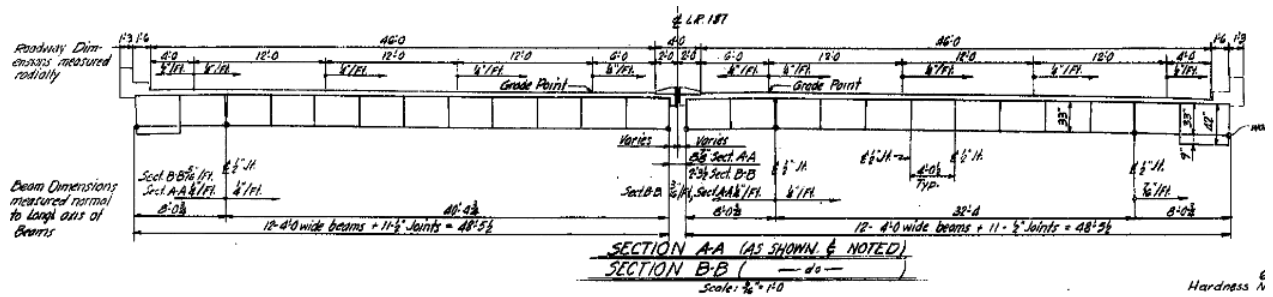
An example of the determination of capacity of the undamaged (i.e.: AB 0-0-0) and damaged (AB 3-2-0) prototype in addition to the subsequent EB-CFRP repair and assessment of the repaired capacity is

provided in Appendix B. A wide range of damage (Section 2.2.4) and different repair techniques are also considered for this prototype as presented Section 2.4.

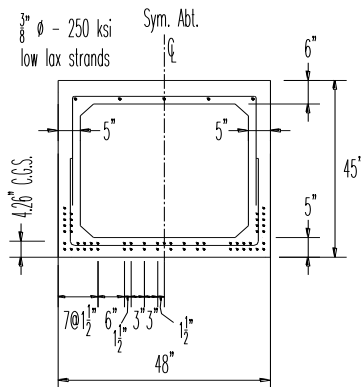
2.2.1.1 Modeling Prototype AB Girder

The example in Appendix B was completed using member capacities calculated using AASHTO (2010) methods, supplemented by ACI 440 (2008) analysis methods for the CFRP. In subsequent analyses summarized in Section 2.3, in order to rapidly analyze the girders at various damage levels, the undamaged girder cross section and all damaged and repaired sections were analyzed using a commercially available non-linear fiber sectional analysis software package XTRACT (TRC 2002) as described in Section 2.1.1.

Material properties for prototype AB are modeled as indicated in Table 7. Concrete properties were modeled after design strength values of the prototype AB girder (American Marietta 1960). Girders of this vintage utilized Grade 250 strand and Grade 40 mild steel reinforcement, hence their use in this study. All strands were assumed to be initially stressed to $0.7f_{pu}$ (175 ksi) and to retain $0.57f_{pu}$ after all losses (based on the AASHTO 2010 prestress loss calculations), resulting in an effective prestress of 142.4 ksi. CFRP material and geometric properties are based on manufacturer's data for Sika CarboDur strips (preformed CFRP strips) (Sika 2011). These properties were used for convenience; the use of Sika-reported material properties should not be interpreted as an endorsement of these products.



a) section of AB prototype bridge.



b) AB prototype girder section.



c) prototype girder *in situ* (photo from PennDOT inspection report dated August 8, 2007).



d) impact damage location (boxed location in c).

Figure 22 AB Prototype bridge and girder.

2.2.2 Spread Box Girder Prototype SB

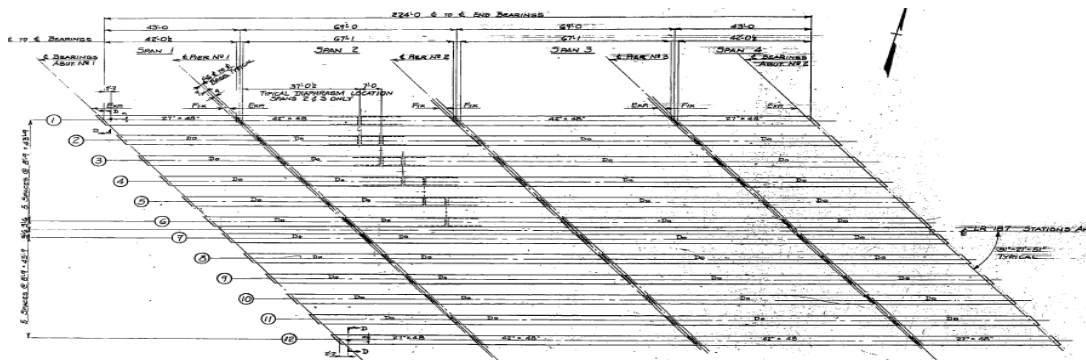
Prototype Girder SB is based on the exterior girder of a decommissioned spread box (SB) girder bridge structure (Figure 23) available to the authors. The bridge, erected in 1962, was demolished and replaced in 2011; the fascia beam shown in Figure 23c was provided for eventual testing. The bridge spans 69 feet with a skew of 51.5° . Each bridge in the dual span structure consists of 6 – 48 by 42 in. box girders

located 8'-9" on center and has an out-to-out dimension of 50'-8". The composite deck is 7.5 in. deep and a 0.5 in. haunch is provided making the overall SB girder depth 50 in. (Figure 23b). The primary prestressing consists of 68 - 3/8" diameter Grade 250 low-relaxation strands. As seen in Figure 23c, Impact damage is evident at a location above the carriageway passing beneath the bridge. This damage has been exacerbated by the fact that it is immediately beneath an active deck drain (Figure 23d). The damage shown in Figure 23 and the identification of this girder is SB 4-2-0 (see Section 2.1.3 for explanation of method of damage identification). This girder also showed significant spalling and corrosion at its pier support; the extent of this damage would likely render this span unrepairable. However, for the sake of this study, this additional deterioration is not considered.

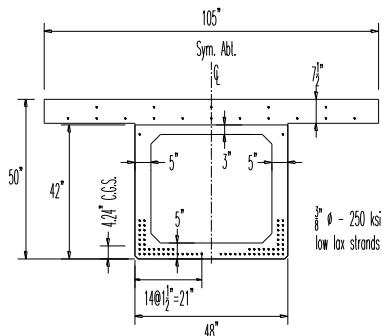
An example of the determination of capacity of the undamaged (i.e.: SB 0-0-0) and damaged (SB 6-4-0) prototype in addition to the subsequent PT-CFRP repair and assessment of the repaired capacity is provided in Appendix C. Structurally, SB and AB girders are similar although because of access to the webs, additional repair techniques may be available for SB girders.

2.2.2.1 Modeling Prototype SB Girder

The example in Appendix C was completed using member capacities calculated using either AASHTO- or ACI-prescribed analysis methods. In subsequent analyses summarized in Section 2.3, in order to rapidly analyze the girders at various damage levels, the undamaged girder cross section and all damaged and repaired sections were analyzed using a commercially available non-linear fiber sectional analysis software package XTRACT (TRC 2002) as described in Section 2.1.1. Material properties for the prototype SB girder are the same as those used for the AB girder and are given in Table 7 and discussed in Section 2.2.1.1. The PT-CFRP material properties are based on manufacturer's data for Sika CarboStress system (Sika 2008b). This system uses the same CFRP material as the EB system, although the geometry of the strip is different as indicated in Table 7.



a) plan of SB prototype bridge.



b) SB prototype girder section.



c) prototype girder *in situ* (photo from PennDOT inspection report dated August 8, 2007).



d) impact damage location (boxed location in c).

Figure 23 SB Prototype bridge and girder.

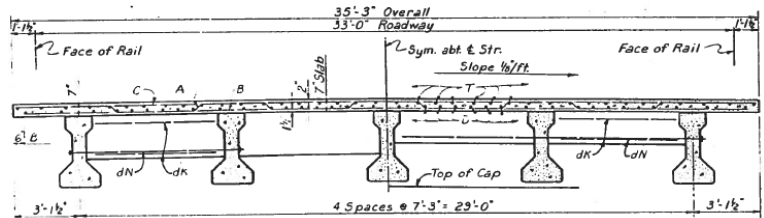
2.2.3 I-Girder Prototype IB

Prototype Girder IB is based on the exterior girder of a bridge impact and repair reported by Yang et al. (2011). The bridge was erected in 1967, and impacted and repaired in 2004. The bridge, shown in Figure 24, spans 84'-8" and consists of 5 - 40 in. deep 'Type C' girders spaced at 7'-3". The Texas Type C girder falls between an AASHTO Type II and Type III in terms of section properties and is commonly used for spans between 40 and 90 feet with normal concrete strengths. The bottom flange is slightly larger than the AASHTO Type girders, accommodating up to 74 strands. The composite deck is 7 in. deep. The primary prestressing consists of 32 - 0.5" diameter Grade 270 low-relaxation strands, 8 of which are harped as shown in Figure 24c. The resulting strand profile results in a 10 foot length of girder having 32 straight strands at midspan. The damaged region was restricted to about an 8.5 ft length and was located near a diaphragm (Figure 24d). The damage shown in Figure 24d and the identification of this girder is IB 3-3-2 (see Section 2.1.3 for explanation of method of damage identification). The damaged beam had no additional deflection due to the loss of strands – an important indication that lateral support from the diaphragms and deck allowed the superstructure to redistribute the stresses to undamaged beams.

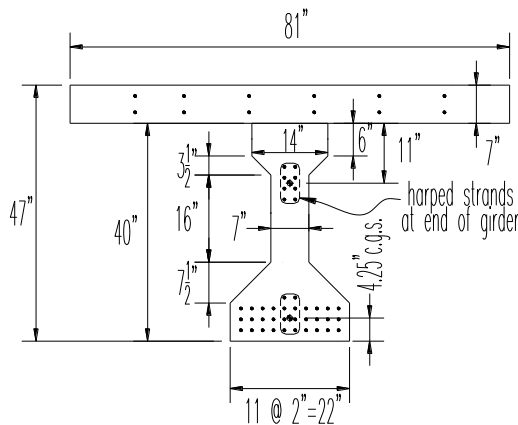
An example of the determination of capacity of the undamaged (i.e.: IB 0-0-0) and damaged (IB 3-3-2) prototype in addition to the subsequent NSM-CFRP repair and assessment of the repaired capacity is provided in Appendix D1. A summary of the actual repair executed for this structure, reported by Yang et al. (2011) is summarized in Section 2.2.3.2. The same IB 3-3-2 prototype is used to demonstrate the design of the repair described by Yang et al. (Appendix D2) and to demonstrate a PT-steel repair example (Appendix D3).



a) IB Prototype bridge.



b) section of IB prototype bridge.



c) IB girder section.



d) damage to exterior girder.

Figure 24 IB prototype bridge and girder (Yang et al. 2011).

2.2.3.1 Modeling Prototype IB Girder

The example in Appendix D was completed using member capacities calculated using either AASHTO- or ACI-prescribed analysis methods. In subsequent analyses summarized in Section 2.3, in order to rapidly analyze the girders at various damage levels, the undamaged girder cross section and all damaged and repaired sections were analyzed using a commercially available non-linear fiber sectional analysis software package XTRACT (TRC 2002) as described in Section 2.1.1. Material properties for the prototype IB girder are given in Table 7 and discussed in Section 2.2.1.1.

2.2.3.2 In situ Repair of Prototype IB Girder

Yang et al. (2011) report the repair that was carried out on the IB prototype bridge. The ‘step-by-step’ process of the repair is documented in Figure 25. The repair involved splicing five strands and the installation of a preloaded shotcrete patch. This operation was completed in 3 days. Following 5 days to permit the patch to cure, EB-CFRP was applied. This material was installed in two phases and spliced near the patch location to permit one lane of traffic to pass beneath the bridge during the CFRP installation. CFRP U-wraps were installed to ‘confine’ the longitudinally spliced CFRP. The entire CFRP installation including a final top coat was completed in 2 days. Yang et al. report this repair to have cost \$25,800 in 2004. To the author’s knowledge, this repair remains in place and in good condition. This *in situ* repair provides a benchmark for the parametric study reported in subsequent sections. Additionally, the design of this repair is demonstrated in Appendix D2.

2.2.4 Prototype and Repair Combinations

As described in Section 2.1, each prototype will be considered with a number of different repair techniques. Table 8 summarizes all cases considered and indicates which examples are included in their entirety in the Appendices to this report. Damage identification is described in Section 2.1.3. Discussion of viable repair techniques is presented in the following sections. In this study, it is assumed that damage occurs at the critical section for moment and that the objective of the repair is to restore the undamaged capacity of the girder. A brief discussion of the effect of damage location along the span is presented in Section 2.5. The objective of restoring the undamaged girder is arbitrary; other objectives that may still satisfy bridge rating objectives may be defined although these do not affect the discussion presented in the following sections.



a) five strands were spliced



b) strand splices were tensioned



c) preload applied prior to patching



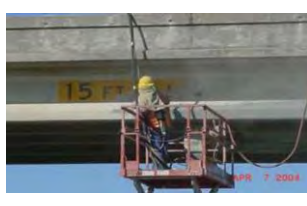
d) sandblasting in preparation for patching



e) shotcrete patch



f) epoxy injection of cracks



g) sandblasting to prepare surface



h) application of primer



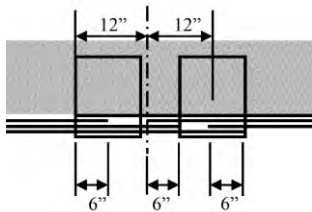
i) application of saturant



j) application of first ply of CFRP



k) U-wraps at CFRP splice



l) CFRP splice details



m) direct pull-off test



n) application of top coat



o) completed repair

Figure 25 Repair of prototype IB girder (Yang et al. 2011)

Table 7 Prototype material properties.

	Girder and Deck Concrete	Grade 250 Prestressing Steel	Grade 270 Prestressing Steel	A615 Gr. 40 Reinforcing Steel	EB-CFRP Strip	PT-CFRP Strip	CFRP Fabric Laminate	
reference material	-	-	-	-	Sika (2011) Carbodur S512	Sika (2008b) Carbostress	SikaWrap Hex 103C (Sika 2010) (laminate properties)	
prototype analyses	all	AB an SB	IB	all	all EB-CFRP and NSM-CFRP	all PT-CFRP	IB 3-3-2 (Section 2.4.3.1)	
modulus of elasticity (ksi)	$E_c = 4,227$	$E_p = 28,500$	$E_p = 28,500$	$E_s = 29,000$	$E_f = 23,200$	$E_f = 23,200$	$E_f = 10,300$	
effective initial prestress (ksi)	-	$f_{pi} = 142.4$	$f_{pi} = 153.8$	-	-	$f_{fi} = 0.5f_{fu} = 203$	-	
tensile yield strength (ksi)	-	-	-	$f_y = 40$	-	-	-	
tensile ultimate stress (ksi)	-	$f_{pu} = 250$	$f_{pu} = 270$	$f_u = 70$	$f_f = 406$	$f_f = 406$	$f_f = 123$	
diameter of strand or thickness of CFRP (in.)	-	$d_b = 0.375$	$d_b = 0.5$	-	$t_f = 0.047$	$t_f = 0.094$	$t_f = 0.040$	
width of individual CFRP strip (in.)	-	-	-	-	$b_{f1} = 2$	$b_{f1} = 2.4$ in. stresshead = 4.6 in.	$b_f = 18$	
tensile ultimate strain	-	$\epsilon_{pu} = 0.0430$	$\epsilon_{pu} = 0.0430$	$\epsilon_{su} = 0.1200$	$\epsilon_{fu} = 0.017$	$\epsilon_{fu} = 0.017$	$\epsilon_{fu} = 0.012$	
compressive strength (ksi)	$f'_c = 5.5$ $f'_c = 6.8$ (IB girder only)	-	-	-	-	-	-	
strain at f'_c	$\epsilon_c = 0.0028$	-	-	-	-	-	-	
crushing strain	$\epsilon_{cu} = 0.0060$	-	-	-	-	-	-	
spalling strain	$\epsilon_{sp} = 0.0070$	-	-	-	-	-	-	
ultimate compressive strain ($f'_c = 0$)	$\epsilon_{cmax} = 0.0080$	-	-	-	-	-	-	
failure criteria used in analysis	AB and SB	$\epsilon_{cF} = 0.003$	$\epsilon_{pF} = 0.010$	$\epsilon_{pF} = 0.010$	$\epsilon_{sF} = 0.035$	$\epsilon_{fF} = 0.0059$ (Eq. 3)	$\epsilon_{fF} = 0.0127$ (Eq. 4)	-
	IB					$\epsilon_{fF} = 0.0066$ (Eq. 3) $\epsilon_{fF} = 0.0102$ (NSM)	$\epsilon_{fF} = 0.0131$ (Eq. 4)	$\epsilon_{fF} = \frac{0.010}{\sqrt{n}}$ (Eq. 3)

Table 8 Repair scenarios considered in this study.

Prototype (Section 2.2)	Repair	Damage Considered (Section 2.1.3)	
AB (Section 2.2.1)	EB-CFRP	1-0-0, 2-1-0, 3-2-0 (Appendix B), 4-2-0, 4-2-2, 5-3-0, 4-2-2-2-2, 6-3-1, 6-4-1, 4-2-2-2-2, 6-3-2-2, 6-5-2, 7-5-2, 6-5-2-2, 6-5-2-2-2	Figure 29
	PT-CFRP	4-2-2, 5-3-0, 6-3-1, 6-4-1, 4-2-2-2-2, 6-3-2-2, 6-5-2, 7-5-2, 6-5-2-2, 8-7-2, 8-7-2-2, 10-9-2-2	Figure 30
SB (Section 2.2.2)	EB-CFRP	1-0-0, 2-0-0, 3-1-0, 4-2-0, 6-4-0, 8-6-0, 12-8-0, 4-3-2, 4-3-2-2, 6-4-2, 6-5-2-2, 10-8-0, 12-8-2, 12-8-2-2	Figure 31
	PT-CFRP	6-4-0 (Appendix C), 8-6-0, 12-8-0, 4-3-2, 4-3-2-2, 6-4-2, 6-5-2-2, 10-8-0, 12-8-2, 12-8-2-2, 14-8-2-2	Figure 32
IB (Section 2.2.3)	EB-CFRP	1-0-0, 2-0-0, 3-0-0, 2-1-0, 2-2-0, 3-1-0, 4-0-0, 3-2-0, 5-0-0, 2-2-2, 3-3-0, 6-0-0, 2-2-1, 3-3-1, 7-0-0, 3-3-2, 8-0-0, 3-3-3	Figure 33
	NSM-CFRP	1-0-0, 2-0-0, 3-0-0, 2-1-0, 2-2-0, 3-1-0, 4-0-0, 3-2-0, 5-0-0, 2-2-2, 3-3-0, 6-0-0, 2-2-1, 3-3-1, 7-0-0, 3-3-2 (Appendix D1), 8-0-0, 3-3-3	Figure 34
	PT-CFRP	1-0-0, 2-0-0, 3-0-0, 3-1-0, 5-0-0, 2-2-2, 7-0-0, 3-3-2, 8-0-0, 3-3-3	Figure 35
	Yang et al. (Section 2.2.3.2)	3-3-2 (Appendix D2) strand splicing restores capacity to 2-1-0; fabric-CFRP restores capacity to 0-0-0.	Section 2.4.3.1
	PT-Steel	3-3-2 (Appendix D3)	Section 2.4.3.2

2.3 Limitations of Repair Techniques

The selection of impact-damage repair techniques must necessarily account for mechanical and geometric constraints associated with the overall bridge, the girder to be repaired, and the repair itself. The following sections address these limitations. In this discussion, a number of assumptions are made, the most important of which is that since this report addresses impact damage, the repair technique must not encroach upon the vertical clearance below the bridge. Therefore, for example, although remarkably efficient at restoring and enhancing capacity, post-tensioned king- or queen-posted systems are not considered. Furthermore, as described in Section 1.5.1, steel jacket repairs are thought to be very cumbersome and impractical and will therefore not be considered further. CFRP repair techniques address most of the drawbacks of steel jackets and will remain the primary focus of this study. Table 9 provides a summary of the limitations of repair techniques described in the following sections.

2.3.1 Residual Capacity and Strengthening Limits

External repair techniques (CFRP and PT-Steel) are subject to damage from subsequent impact (see Section 1.5.4.6), fire or, in rare cases, vandalism. Therefore limits to the strengthening effect of a repair should be considered (ACI 440-2R 2008) – the girder must safely carry some level of load in the event the repair fails. The residual capacity of the unstrengthened girder (i.e.: the damaged capacity C_D ; see Equation 2) should safely resist an expected nominal load. There is no specific guidance for this unique load case provided by AASHTO. ACI 440-2R provides a ‘strengthening limit’ requiring that the existing (damaged) capacity of the member exceed the sum of $1.1DL + 0.75LL$. ACI 440-2R justifies these load factors as follows: “A dead load factor of 1.1 is used because a relatively accurate assessment of the existing dead loads of the structure can be determined. A live load factor of 0.75 is used to exceed the statistical mean of yearly maximum live load factor of 0.5, as given in ASCE 7-05. The minimum

strengthening limit $[1.1DL + 0.75LL]$ will allow the strengthened member to maintain sufficient structural capacity until the damaged FRP has been repaired.”

Making a similar argument and in the absence of alternate guidance, for an external repair to an impact-damaged prestressed girder to be viable:

$$C_D \geq 1.1DC + 1.1DW + 0.75(LL+IM) \quad (\text{Eq. 3})$$

2.3.2 Limitations Associated with Girder Geometry

Bonded repair techniques may be applied to accessible regions of the girder soffit and web(s). Soffit repairs are more efficient since these necessarily place the repair material as far from the member neutral axis as possible. However, soffit repairs must not encroach on the vertical clearance below the bridge. It is felt that an envelope of 1 inch for such repairs is reasonable unless other remedial action is taken such as lowering the roadway elevation beneath the bridge. Only externally bonded CFRP (EB-CFRP) or post-tensioned CFRP (PT-CFRP) repairs are suitable for soffit applications in most cases. Fully bonded CFRP applications (EB-CFRP or bPT-CFRP) also improve the resilience of the member in the event of a subsequent vehicle impact (Figure 19). Post tensioned steel (PT-steel) applications will generally have a higher profile and may be susceptible to brittle and catastrophic failure in the event of a subsequent impact making them inappropriate for soffit applications. For adjacent box (AB) structures, only the soffit is available for external repair.

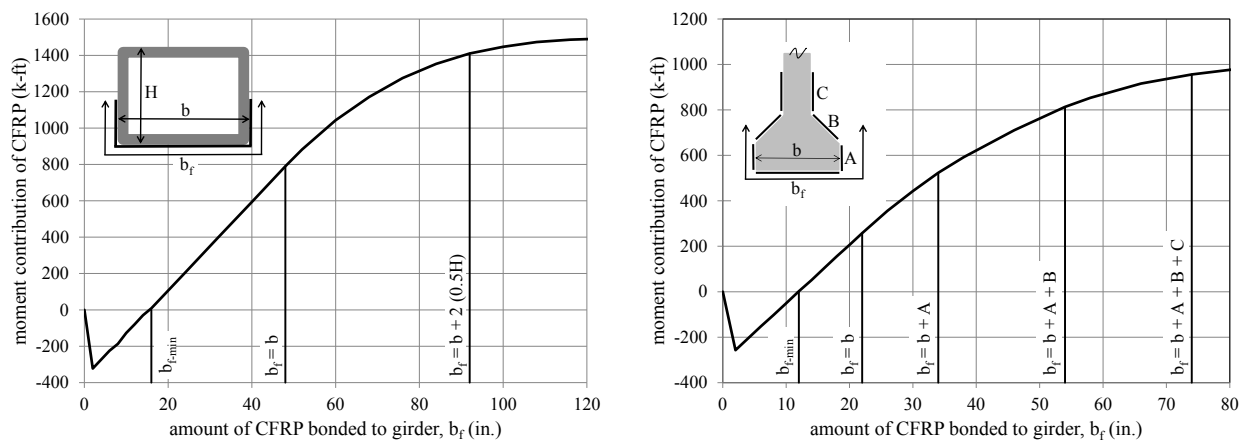
Table 9 Appropriateness of repair technique by girder geometry.

Repair technique	dominant limit state and/or primary design consideration (Section 2.3.2)	Girder type (Section 2.3.1)		
		Adjacent box (AB) and slab bridges	Spread box (SB) bridges	I-girder (IB) and similar bridges
all external techniques	failure/loss of repair material	$C_D \geq 1.1DC + 1.1DW + 0.75(LL+IM)$		
EB-CFRP	debonding	soffit only: $b_f \leq b$	soffit and web although reduced efficiency on web	soffit and bulb although reduced efficiency on bulb
uPT-CFRP	anchorage of PT forces	soffit only: $b_f \leq \approx 0.5b$		
bPT-CFRP	anchorage of PT forces and debonding			
NSM-CFRP	geometry of slots and debonding	soffit only: $b_f \leq \approx 0.5b$		
PT-Steel	anchorage of PT forces	not appropriate due to vertical clearance encroachment	web or between girders	web above bulb or between girders
strand splicing	geometry/spacing of repaired strands	limited applicability – isolated strands		appropriate

For bridge systems where the girder webs are accessible (SB and IB), bonded repair to the webs is feasible and does help to address the potential damage associated with subsequent impacts. However, as the repair material is located closer to the neutral axis of the member, its structural efficiency and therefore contribution to the load carrying capacity of the girder is diminished, requiring more material to be used to accomplish the same strengthening objective. Furthermore, for bonded repairs, the failure limit state is typically debonding of the CFRP which must be understood to occur *at the extreme tension element* of the member. As a result, failure occurs when material bonded at, or closest to the soffit debonds. Once debonding initiates in this fashion, load is redistributed to the internal prestressing strand and the CFRP located away from the soffit – driving a progressive debonding failure of this latter material. This behavior results in further diminished efficiency of material bonded to the web away from the soffit since the CFRP strain is limited *at the level of the soffit*. This effect is shown by example in Figure 26. In this figure, the moment capacity that may be restored to prototypes SB 6-4-0 and IB 3-3-2 is

shown as a function of the amount of EB-CFRP installed. The incremental moment (slope) is constant as material is added to the soffit ($b_f \leq b$, where b_f is the width of CFRP provided and b is the width of the concrete soffit available). However, as additional material is added up both sides of the web, the incremental effect is increasingly diminished as the additional material approaches the girder neutral axis. Additionally, there is a minimum amount of CFRP, b_{fmin} , below which the repair does not increase the capacity of the member since debonding of CFRP occurs prior to the damaged member capacity being achieved. This will be discussed in Section 2.3.2.1.

External post-tensioned systems are more easily used in bridge systems where the webs are accessible. PT-steel systems in particular, may be attached to the girder webs using bolsters (Figure 27a) or be located between girders, anchored to new or existing diaphragms (Figure 27b). In these cases, installation of king- or queen-post to harp the PT strand is feasible and may be used to improve the efficiency of the repair (the example shown in Figure 27b shows a small degree of harping between the anchorage and subsequent diaphragm supports).



a) SB 6-4-0 with EB-CFRP

b) IB 3-3-2 with EB-CFRP

Figure 26 Contribution to capacity of repaired girder from EB-CFRP material.



a) PT-steel anchored to girder using steel bolster bolted through girder web (second PT bolster on back of web). [DYWIDAG Systems International]



b) PT-CFRP anchored and harped by diaphragms [Mamlouk and Zaniewski *Materials for Civil and Construction Engineers* 2011]

Figure 27 Anchorage of post-tensioned repair systems.

2.3.3 Limitations Associated with Repair Techniques

2.3.3.1 EB-CFRP

For a variety of reasons described in Section 1.5.3.1.1, preformed CFRP strips are preferred over wet laid-up CFRP for flexural repair. Preformed strips are available from a variety of manufacturers in discrete sizes and a number of ‘grades’ of CFRP: high strength (HS), high modulus (HM) and ultra high modulus (UHM). Properties of each of these are provided in Table 10. Preformed UHM-GFRP (glass FRP) is also commercially available; however this material is relatively soft and not well suited for flexural repair. HS-CFRP is the most readily available material and most commonly used for concrete repair applications. Although greater material efficiency may be realized using the higher modulus varieties, the reduced stress and strain capacity make catastrophic CFRP rupture more likely, reducing the stress allowable in design (see Equation 3).

Table 10 Properties of available preformed FRP materials.

	HS-CFRP	HM-CFRP	UHM-CFRP	UHM-GFRP
Tensile modulus, E_f (ksi)	23200	30000	44000	6100
Tensile strength, f_{tu} (ksi)	406	420	210	130
Rupture strain, ϵ_{fu}	0.017	0.014	0.005	0.021
Typically available strip thickness, t_f (in.)	0.047	≈ 0.05	≈ 0.05	0.075
Typically available strip widths, b_{fl} (in.)	2 ¹ , 3 and 4	4	4	2 and 4

¹ used in this study, see Table 7

The dominant limit state for bonded CFRP applications is debonding of the CFRP from the substrate concrete. It is important to note that in a sound CFRP application, debonding failure is characterized as a cohesive failure through a thin layer of cover concrete immediately adjacent the CFRP. Because of this, it is difficult to affect debonding capacity through adhesive selection (provided the adhesive is adequate to affect the concrete failure) since the failure is governed by the substrate concrete whose properties remain unaffected in a repair. Guidance such as that provided by ACI 440 (2008) or NCHRP *Report 609* (2008) are intended to ensure a sound CFRP application in which design progresses considering the debonding limit state.

Debonding imparts a level of pseudo ductility to the failure and is preferred to CFRP rupture. In the design of bonded FRP systems, the strain carried by the FRP is limited to a value corresponding to the strain to cause debonding, defined as (ACI 440 2008):

$$\epsilon_{fd} = 0.083 \sqrt{\frac{f'_c}{nE_f t_f}} \leq 0.9\epsilon_{fu} \quad (\text{ksi units}) \quad (\text{Eq. 4})$$

Where f'_c = concrete substrate compressive strength

E_f = tension modulus of elasticity of CFRP

t_f = thickness of one ply/layer CFRP

n = number of layers of CFRP

ϵ_{fu} = rupture strain of CFRP strip

the leading coefficient 0.083 is taken as 0.41 for MPa units

Using preformed strips, the effectiveness of a repair is maximized by first maximizing the coverage of the CFRP on the soffit of the structure; i.e.: maximizing the width of the CFRP application, b_f . As can be seen from Equation 4, additional layers of CFRP (n) or additional CFRP thickness (nt_f) are not proportionally effective as the debonding strain falls as a function of the square root of the thickness. Thus doubling the CFRP by applying a second layer only increases the capacity of the CFRP by 141%. Three layers, result in only a 173% increase in capacity over a single layer. The reduced effectiveness of thicker CFRP

applications stems from the nature of the interface stresses: ideally, debonding is a Mode II failure¹. Thicker CFRP impart an increasing Mode I component to the interface stresses which dramatically reduced the toughness of the debonding interface (Wan et al. 2004). Additional layers of CFRP also introduce additional adhesive interfaces which a) may exhibit an adhesive or cohesive failure; and b) will effectively soften the apparent axial stiffness of the gross CFRP section. Finally, Equation 3 is empirical and calibrated based on a large data set² where the average value of nt_f was 0.042 in. and the greatest value was 0.102 in. It is unknown how appropriate Equation 3 is for nt_f greater than 0.1 in. For these reasons, the use of multiple layers of CFRP is discouraged and will not be considered in this work.

Because bond capacity does not permit the full utilization of the CFRP, when small amounts of CFRP are used, these may debond prior to providing any enhancement of the *ultimate* capacity of the girder. In this work, this effect is reported as a capacity below the damaged girder capacity (noted as an **x** in Figures 29 to 36).

Clearly, this is not the case (the bonded material does not reduce the girder capacity); the capacity at the *debonding limit state* is below the damaged girder capacity. In an externally bonded system, the debonding limit state is taken as being critical since once the bond fails, the girder is no longer strengthened. This effect is shown in Figure 26 as a ‘negative’ strengthening effect for small amounts of CFRP (small b_f values). In Figure 26a, for instance, no strengthening effect from EB-CFRP is observed until at least 8 strips ($b_f > 16$ in.) are used.

2.3.3.2 NSM-CFRP

For near-surface mounted applications (NSM-CFRP; see Section 1.5.3.3), bond is improved and ACI 440 (2008) prescribes a debonding strain of $\varepsilon_{fd} = 0.7\varepsilon_{fu}$. However, the improved bond effectiveness is often negated by the limited amount of material that may be applied in this manner: Slots for NSM reinforcing should be spaced at least twice their depth apart and have an edge distance of at least four times their depth (ACI 440 2008). Slots must not encroach on the internal reinforcing steel; for typical prestressed concrete structures, slots will not exceed 1 in., and may be better specified to be 0.75 in. in depth. The CFRP inserted into the slot is necessarily shorter than the slot depth although typically two plies of preformed CFRP will be used in each slot. For prestressed concrete applications described in this work, NSM-CFRP will typically consist of 2-0.5 in. strips inserted into slots spaced at 1.75 in. This provides 50% of the material that an EB-CFRP application provides at a greater cost in terms of resources and installation time. The improved bond behavior will normally not improve the CFRP efficiency the required 200% just to ‘break even’ in capacity. As such NSM repairs are not recommended as being efficient for repairs in the positive bending region of a structure. The significant advantage of NSM techniques is that they may be used in the negative moment region of a structure and remain protected from wear and abrasion. This is not an application considered in this work focusing on repair of impact damaged prestressed concrete elements.

2.3.3.3 PT-CFRP

The advantages of prestressing a CFRP repair are a) that the CFRP becomes active and replaces some of the prestress force lost due to internal strand loss; and b) the CFRP debonding strain is effectively increased by the level of prestress in the CFRP:

$$\varepsilon_{fd} = 0.083 \sqrt{\frac{f'_c}{nE_f t_f}} + \kappa \varepsilon_{fu} \leq 0.9 \varepsilon_{fu} \quad (\text{ksi units}) \quad (\text{Eq. 5})$$

¹ Modes I and II refer to the traditional fracture mechanics definitions of ‘opening’ (CFRP peeling) and ‘shear’ displacements, respectively, of plane-strain crack opening.

² The dataset used to calibrate Equation 3 is unpublished but is available to Dr. Harries who chaired the task group that developed and calibrated Equation 3.

Where κ is the effective level of prestress in the CFRP. Losses are relatively significant in PT-CFRP systems (Wang et al 2012b). Based on relatively limited available data, κ should remain less than 0.50 for bPT-CFRP (Figure 8e) and 0.30 for uPT-CFRP (Figure 8d) systems (Harries et al. 2009). Due to the stressing equipment required, prestressed CFRP (P-CFRP; shown schematically in Figures 8c and 10b) is not considered to be practical for bridge structures and is not considered further. Furthermore, for bridges or other applications subject to significant transient loads, uPT-CFRP is not recommended. uPT-CFRP strips will be located against the substrate concrete and therefore be subject to abrasion or fretting damage associated with differential displacement between the concrete substrate and unbonded CFRP strip. This situation must be remediated as the CFRP materials do not have a great resistance to abrasion. Bonding this interface addresses this issue. For this reason, only bPT-CFRP will be considered further.

Anchorage of PT-CFRP is usually provided by proprietary anchorage hardware which in turn is anchored to the concrete substrate (see Section 1.5.3.2.3 and Figure 14). The CFRP-to-anchor connections may rely on adhesive bond, friction or bearing of a preformed CFRP ‘stresshead’ (Figure 14a). The proprietary anchor, in turn, is secured to the concrete substrate. Anchor bolts (seen in Figure 14a) and shear keys are conventional methods of transferring the force. For anchorages bolted to the concrete substrate, the recommendations ACI 318 (2011) Appendix D for bolting to concrete should be followed and great care must be taken to ensure that installed bolts do not interfere with sound internal prestressing strand or other reinforcement. For anchorages relying on a shear key arrangement, the key should be designed to carry 100% of the prestress force and bolts should be provided to carry any uplift caused by moment and to keep the shear key fully engaged. Pipe-type shear key inserts, as are occasionally used with the system shown in Figure 14 are impractical for prestressed members in regions where strand is present. Anchorage requirements such as available space and bolt spacing may affect the amount of post-tensioned CFRP that may be installed.

Due to their size, adjacent anchorages must be staggered longitudinally (analogous to staggering reinforcing steel lap splice locations) if a large amount of CFRP is required. Additionally, based on commercially PT-CFRP systems, the minimum transverse spacing of the CFRP strips is typically twice the strip width. Thus the coverage of PT-CFRP on the girder soffit is $b_f \leq 0.5b$. This latter issue diminishes some of the effectiveness of PT-CFRP although some systems (SIKA 2008b) utilize a thicker CFRP strip than is available for EB-CFRP (see Table 7).

2.3.3.4 Strand splicing

Strand splicing is well established and an effective means of restoring steel continuity and prestress force to severed strands (Shanafelt and Horn 1980 and 1985). Commercially available strand splices are reportedly adequate to develop $0.96f_{pu}$. Typically, a re-tensioning operation will aim to restore $0.60f_{pu}$ which will generally be close to the long-term effective prestress in a strand. Commercially available splices (shown in Figure 28a) are available for strand diameters up to 0.5 in.³.

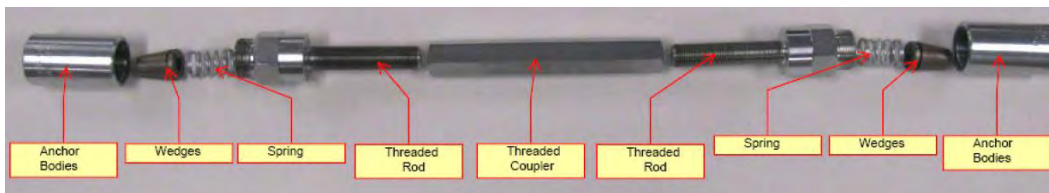
Limitations pertaining to the use of strand splices are based on the physical dimensions of the splices and spacing of the strands to be spliced. Often, prestressing strands are spaced at 1.5 in. on center. Anchor bodies (Figure 28a) have a diameter of 1.625 in. irrespective of spliced strand size. When repairing adjacent strands, splices must be staggered (Figure 28b) to avoid interference (Figure 28c). The specified stagger must accommodate the ‘stroke’ of the splice coupler; a minimum spacing of 2 in. is recommended (Figure 28b). Installation of splices for exterior strands also results in reduced concrete cover at the splice location unless section enlargement is also affected. Reduced cover may affect durability and result in a region more susceptible to cracking. Clear spacing between splices and adjacent bonded strands is also reduced (Figure 28c) which may affect bond performance and increase the development length of the adjacent strand (Kasan and Harries 2011).

³ The primary North American manufacturer of strand splices has indicated that a 0.6 in. variety will be commercially available in the near future.

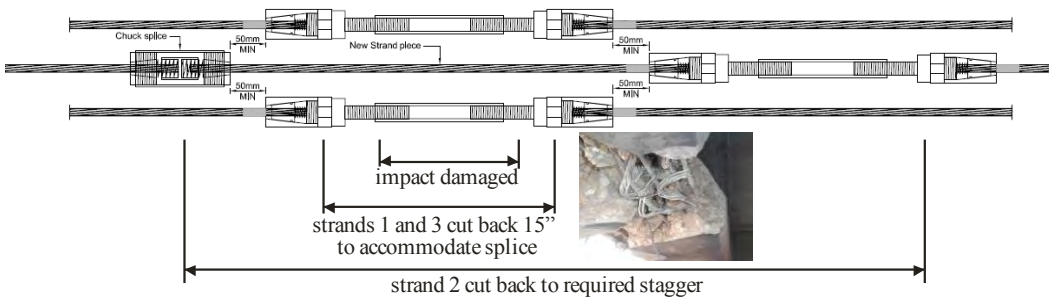
Additionally, chuck splices, having a diameter of 2 in. are used to allow for removal of damaged strand and to shift the location of the splice to accommodate staggering and reduce congestion (Figure 28b). Chuck splices must also be staggered and not coincide with strand splice locations in order to avoid interferences. Staggering strand splices often requires the removal of additional strand and its surrounding concrete. Finally, strand splices and chuck splices also interfere with transverse reinforcement where it is present. This may require removal of the transverse steel and replacement with grouted or epoxied hairpins. In some cases, FRP U-wraps (see Sections 1.5.3.2.2 and 1.5.5.8) may be designed to restore the confinement and shear capacity lost by the removal of transverse steel (ACI 440 2008).

Considering interferences, strand splicing is practical for relatively few severed strands but becomes increasingly cumbersome for significant damage – particularly for the case of adjacent damaged strands. For this reason, as is done in the case described in Section 2.2.3.2, a combination of external repair and strand splicing may be appropriate where a large number of strands are damaged, particularly if this damage is confined to a short length of the girder (such as is shown in Figures 1b, 20 and 24).

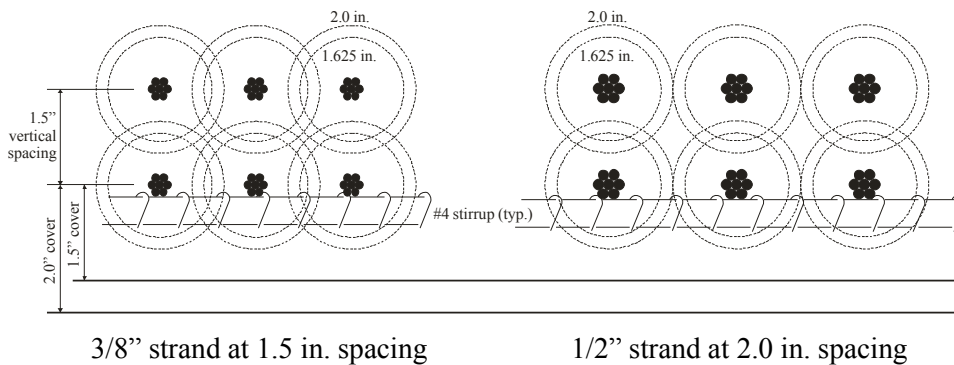
Finally it must be emphasized that strand splicing requires sound strands. Any corroded region of strand must be removed back to ‘bright steel’. Thus if impact damage has been left unrepaired and corrosion set in (Figures 3 and 4), strand splicing may require additional strand and concrete removal.



a) components of strand splice [Prestress Supply Inc. 2011]



b) required longitudinal stagger of adjacent strand splices [Prestress Supply Inc. 2011]



c) strand splice interferences.

Figure 28 Strand splice hardware and potential interferences.

2.3.3.4.1 Strand Splice Ultimate Capacity

As reported in Section 1.5.1.2, strand splices cannot universally be relied upon to develop the ultimate capacity of the strands. Some research indicates that 100% of capacity can be restored (Labia et al. 1996) while others report that only about 80% of capacity can be restored (Olsen et al. 1992). Zobel and Jirsa (1998) report a ‘guaranteed’ strength of $0.85f_{pu}$ while the Grabb-It literature implies a capacity of $0.96f_{pu}$ for strand splices. Zobel and Jirsa also recommend that more than 10-15% of strands in a section be spliced.

Considering this discussion, it is recommended that strand splices:

1. be limited to strand diameters 0.5 in. and less
2. be able to restore *in situ* prestress forces assumed to be less than $0.70f_{pu}$.
3. be limited to developing $0.85f_{pu}$, thereby reducing their effectiveness in restoring strands. The effective number of strands restored by strand splices should be taken as $0.85n_{spliced}$ when using the approach described in Sections 2.4.3.1 and 2.6.2 and shown schematically in Figure 37.
4. be staggered (Figure 28b) when splicing adjacent strands.
5. be limited to splicing 15% of strands in a girder regardless of staggering.

2.3.3.4.2 Strand Splicing in AB and SB Girders

In general, the authors do not recommend strand splicing for impact-damaged box girders (AB and SB), particularly older girders. Anecdotal evidence has indicated significantly reduced cover concrete (as small as 0.75 in. to the center of the strand) and inconsistent strand spacing (as small as 1 in. center-to-center) in girders from the 1960’s and early 1970’s (Harries 2009). In any event, splicing adjacent strands in a box girder will result in significantly reduced concrete cover and interferences. Issues of splitting associated with strand splices cannot be adequately addressed in box girders since the top of the bottom flange (in the box void) is inaccessible. Providing new internal confinement (grouted hairpins) is impractical since these cannot be anchored in the 4 to 5 in. bottom flanges. External confinement (such as CFRP U-wraps) is also not as efficient since this confinement cannot be provided inside the box void. Section enlargement of box girders (particularly AB) is not as practical as for flanged members.

In box sections, it is felt that strand splicing is only practical for the repair of a few isolated strands. For these reasons, strand splicing will not be pursued as a practical alternative for the AB and SB impact damage repair.

2.3.3.4.3 Strand Splicing in I-girders

Strand splicing is more practically applied to ‘flanged’ members. The reduced cover, spacing and interferences with adjacent strands/splices affect development, crack control and the likelihood of splitting. For this reason, confinement of the spliced region is recommended to ensure long-term durability and performance. In flanged sections such as AASHTO I-girders and bulb tees, section enlargement, grouted or epoxied hairpins and/or CFRP (or GFRP) U-wraps may be used to confine the spliced region, control splitting cracks and replace any transverse reinforcement that may have been removed to affect the splice repair.

Splicing adjacent strands requires a longer repair region (Figure 28) and may therefore not be practical for cases of very local damage (such as is shown in Figures 1b, 20, 24 and the inset in Figure 28). In this case a hybrid approach may be efficient: repairing some strands (perhaps every second strand) with strand splices and restoring the remaining capacity with an externally bonded alternative. This is the approach reported by Yang et al (2011; Section 2.2.3.2)

2.3.3.5 PT-steel

Traditional post-tensioned steel (PT-Steel) repair techniques are well established (Shanafelt and Horn 1980 and 1985). Any degree of damage may be repaired and prestress force restored using this method. The primary design consideration is the anchorage of the PT force. Typically this is done with steel or

concrete bolsters (corbels) attached to the side of the girders (Figure 27a). In this case, the bolsters must be designed to transfer the PT force into the girder. This is accomplished through shear friction (see *AASHTO LRFD Specifications* Section 5.8.4) or through direct bearing of a shear key. Typically, the bolsters themselves will be post-tensioned onto the girder web thereby affecting a normal force (P_c in *AASHTO LRFD* Equation 5.8.4.1-3) anchoring the bolster. When adding bolsters to SB girders, the web thickness (and possible variation thereof; see Harries 2009) must be considered: Ideally, the bolsters are post-tensioned to a single web although this will likely require access inside the box. If post-tensioning the bolster through an entire box girder, this should be done at the location of an internal diaphragm in order not to affect out-of-plane bending of the web. In general, applying PT-steel repair methods to box sections is perhaps not as practical as to single web members. PT-steel may also be anchored to existing or purpose-cast diaphragms between girders as shown in Figure 27b.

Generally it will be more efficient to harp external post tensioning. This is easily done, although the attachment of the harping points to the girder requires the same attention as the end anchorages.

2.4 Results of Parametric Study

The results of the parametric study summarized in Table 8 are presented in the following sections. The approach and format follows that outlined in Section 2.1 and all rating factors are given in terms of the normalized girder rating factor given by Equation 2.

This study adopts the ‘repair objective’ of restoring the original girder capacity, C_0 , at the location of the damage; that is ensuring that $C_R \geq C_0$ or $RF_R \geq 1.0$. Different objectives are certainly possible and a repair that does not restore the original girder capacity may be acceptable, particularly if there is a great deal of overstrength (reserve capacity) in the first place (this was the case for the AB example presented in Appendix B). This decision must, however, be made on a case-by-case basis. Regardless of the goal of the repair, the trends and conclusions discussed here remain valid.

All analyses presented in this section were conducted using XTRACT as described in Section 2.1.1. Using the fiber analysis method of XTRACT is more rigorous than the AASHTO or ACI-prescribed plane sections analyses presented in Appendices B through D. The difference in results is marginal; the XTRACT-derived values are about 2% greater than those based on code approaches as is shown in Table 6 for AB 3-2-0. Finally, all assessments were carried out considering only the damaged girder; thus the normalized rating factor derived from Eq. 2 was used.

2.4.1 AB Prototype

Considering the AB prototype described in Section 2.2.1, a range of damage (Table 8) was considered. EB-CFRP and PT-CFRP repair techniques were considered at length and aspects of strand splicing repairs were also considered. Eighteen damage cases ranging from AB 1-0-0 (2% strand loss) to AB 10-9-2-2 (40% strand loss) were considered. The AB 3-2-0 case repaired with EB-CFRP is presented in its entirety in Appendix B.

As described in Section 2.3.1 and Table 9, the practical limit of the EB-CFRP repair considered is providing full CFRP coverage of the soffit: $b_f \leq b = 48$ in. The CFRP strips used (Table 7) have an individual width of 2 in., resulting in a maximum number of strips that may be located on the soffit equal to 24. To illustrate the range of EB-CFRP repair possible – and therefore to identify the range of repair objectives possible – four degrees of repair were considered corresponding to 25, 50, 75 and 100% of the greatest practical repair. Thus all damaged beams were assessed for their repaired capacity, C_R , assuming 6, 12, 18 and 24-2 in. EB-CFRP strips. Including the damaged unrepaired girders, 75 ratings were carried out. The results of these ratings are presented in Table 11 in terms of both the member moment capacity (C_0 , C_D and C_R , the undamaged, damaged and repaired capacities, respectively) and the resulting rating factors (RF_D and RF_R for the damaged and repaired scenarios). Using the normalized rating factor (Eq. 2) implies that the undamaged rating factor, $RF_0 = 1$.

The resulting damaged and repaired normalized rating factors are shown graphically in Figure 29. In this figure, each vertical line represents a damage case. The lower solid circle (●) data point on each line is the rating factor for the unrepaired damaged girder, RF_D . The higher solid circle (●) data point is the rating factor for the repair having 24-2 in. EB-CFRP strips - the maximum practical repair. Data points for each of the repairs having 6, 12 and 18 EB-CFRP strips are shown as horizontal ticks (-) along each line. Interpretation of Figure 29 (and subsequent similar Figures 30 to 35) is as follows:

Considering the AB 3-2-0 example presented in Appendix B, the damaged rating factor $RF_D = 0.88$. The repair design having the objective of restoring the original girder capacity ($RF_R \geq 1.0$) required 15 – 2 in. ($b_f = 30$ in.), resulting in a repaired rating factor of 1.05. Maximizing the repair, using 24-2 in. EB-CFRP strips, the capacity of the repaired girder could be increased well above its undamaged capacity to a rating factor $RF_R = 1.20$.

At the high end of the spectrum, AB 6-5-2-2 has a damaged rating factor of $RF_D = 0.65$; its capacity cannot be fully restored even with the maximum practical EB-CFRP strips applied. In this case, the maximum repaired $RF_R = 0.97$. Assuming the predefined objective of the ‘repair or replace’ question was that the repair must restore the original capacity of the girder, AB 6-5-2-2 could not be repaired and would require replacement. Interestingly, this conclusion is consistent with a rule-of-thumb used for prestressed girder repair: a girder must be replaced if strand loss exceeds 25% (Section 1.5.2).

It is also informative to consider the other end of the damage spectrum: a lightly damaged girder having a small amount of CFRP applied. For example, the case of the very lightly damaged AB 2-1-0, a repair consisting of only 2-2 in. strips results in a repaired rating that falls below unrepaired damaged capacity (shown as **x** in Figure 29). This result indicates that the CFRP reaches its debonding strain prior to the girder reaching its damaged capacity. In this case, the repair is ineffectual. Showing this repair below the damaged capacity (RF_D) is intended to aid in visualising the ‘minimum’ repair required to affect any increase in damaged girder capacity; clearly, in these cases, the repaired capacity and rating factors are the same as the damaged valued: $C_R = C_D$ and $RF_R = RF_D$. For AB 2-1-0, a minimum of 5-2 in. strips are required to affect an increase in capacity; fewer than this and the CFRP debonds prior to incrementing the beam capacity. This effect is shown as the ‘negative’ incremental capacity affected by repairs having very little CFRP (small b_f values) shown in Figure 26. In the case shown in Figure 26a, for instance, b_f must exceed 16 in. in order for the EB-CFRP to have any effect on the damaged girder capacity.

Using an approach such as that presented in Figure 29, defining the required repair capacity as a horizontal line at the desired capacity ($RF_R = 1.0$ was used here), one can quickly establish repair-or-replace criteria based on viable repairs that fall above this line. The same approach may also be calibrated using Eq. 1 although separating individual girder damage from global bridge performance is rather complex. The nature of repairable vehicle impact damage most often only affects exterior girders which raises a third alternative to the repair/replace decision. Exterior girders may simply be removed (physically or lane restricted so that they are not loaded) from the bridge altogether without affecting the load capacity of this bridge. Such an approach clearly, however, affects the traffic-carrying capacity of the span.

Similar data and plots were developed for the bPT-CFRP repair of the damage cases summarized in Table 8. The practical limit of the PT-CFRP repair considered is providing full CFRP coverage of the soffit: $b_f \leq \approx 0.5b = 24$ in. The CFRP strips used (Table 7) have an individual width of 2.4 in. and a stresshead dimension of approximately 4.6 in, resulting in a maximum number of strips that may be located on the soffit equal to 10. To illustrate the range of bPT-CFRP repair possible – and therefore to identify the range of repair objectives possible – five degrees of repair were considered corresponding to 10, 30, 50, 80 and 100% of the greatest practical repair. Thus all damaged beams were assessed for their repaired capacity, C_R , assuming 1, 3, 5, 8 and 10 PT-CFRP strips. Including the damaged unrepaired girders, 72 ratings were carried out. The results of these ratings are presented in Table 12 and Figure 30.

In all but the most heavily damaged case, a single bPT-CFRP strip is inadequate to improve the capacity of the damaged girder – these cases are indicated as **x** in Figure 30.

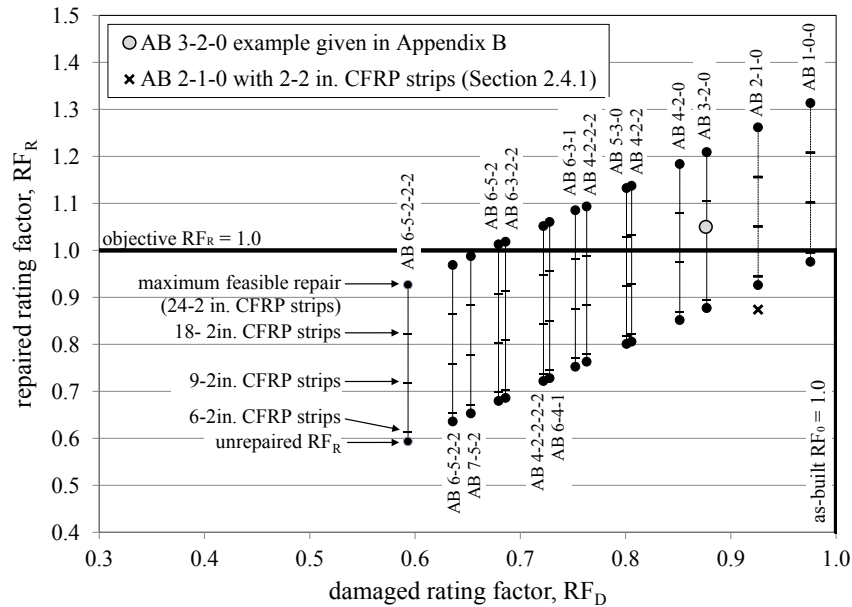


Figure 29 Results of parametric study of AB girders repaired with EB-CFRP.

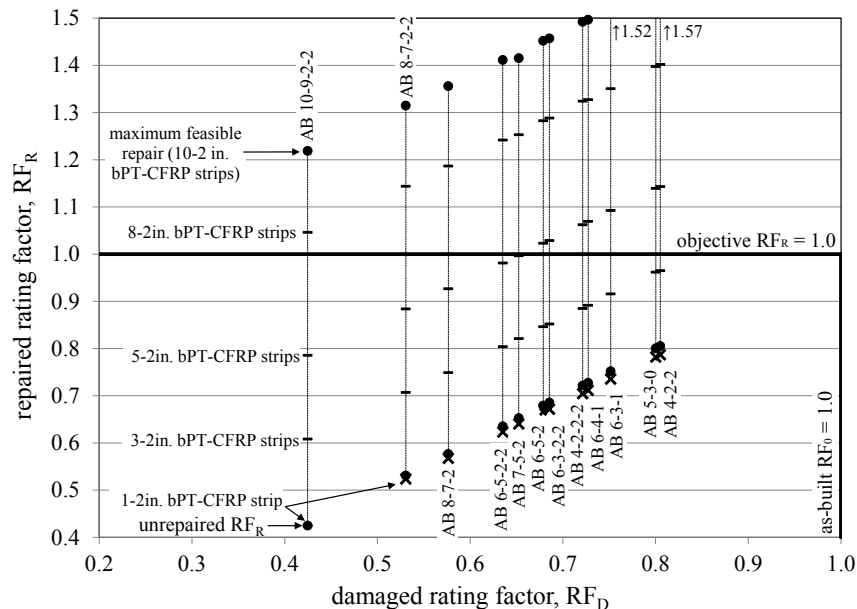


Figure 30 Results of parametric study of AB girders repaired with PT-CFRP.

2.4.2 SB Prototype

Considering the SB prototype described in Section 2.2.2, a range of damage (Table 8) was considered. EB-CFRP and PT-CFRP repair techniques were considered at length and aspects of strand splicing and PT-Steel repairs were also considered. Fifteen damage cases ranging from SB 1-0-0 (2% strand loss) to SB 14-8-2-2 (38% strand loss) were considered. The SB 6-4-0 case repaired with PT-CFRP is presented in its entirety in Appendix C. Repair capacity and ratings for EB-CFRP and PT-CFRP repairs are given in

Table 12. Figures similar to those described in Section 2.4.1 are given for EB-CFRP and PT-CFRP in Figures 31 and 32, respectively.

As described in Section 2.3.1 and Table 9, the EB-CFRP repair may extend across the soffit ($b_f = b = 48$ in.) and extend up the outside of the webs (the latter material being less effective than that on the soffit). In the example considered, it was considered practical to extend the EB-CFRP approximately half way up each web, resulting in a total coverage of $b_f = b + 2(H/2) = 48 + 2(21) = 90$ in. or 44-2 in. EB-CFRP strips (Table 7) strips. To illustrate the range of EB-CFRP repair possible four degrees of repair were considered corresponding to 25, 50, 75 and 100% of full soffit coverage (6, 12, 18 and 24-2 in. EB-CFRP strips). Two additional cases, considering the full soffit plus either 4 in. (2 strips/web) or 20 in. (10 strips/web) additional coverage up each web. Including the damaged unrepaired girders, 98 ratings were carried out. The results of these ratings are presented in Table 12 and Figure 31.

Similar data and plots were developed for the PT-CFRP repair of the damage cases summarized in Table 8. It was not felt to be necessary to extend the PT-CFRP up the webs, in which case the practical limit of the PT-CFRP repair considered is providing full CFRP coverage of the soffit: $b_f \leq \approx 0.5b = 24$ in. or 10-2.4 in. PT-CFRP strips (Table 7). Similar to the AB prototype, five repair cases having 1, 3, 5, 8 and 10 PT-CFRP strips were considered and a total of 66 ratings conducted. The results of these ratings are presented in Table 12 and Figure 32.

Behavior of the SB prototype was similar to that of the AB, although more heavily loaded, the SB girder was shorter and more heavily prestressed resulting in comparable behavior. Similar to the AB prototype, in most cases, a single bPT-CFRP strip is inadequate to improve the capacity of the damaged girder – these cases are indicated as **x** in Figure 32.

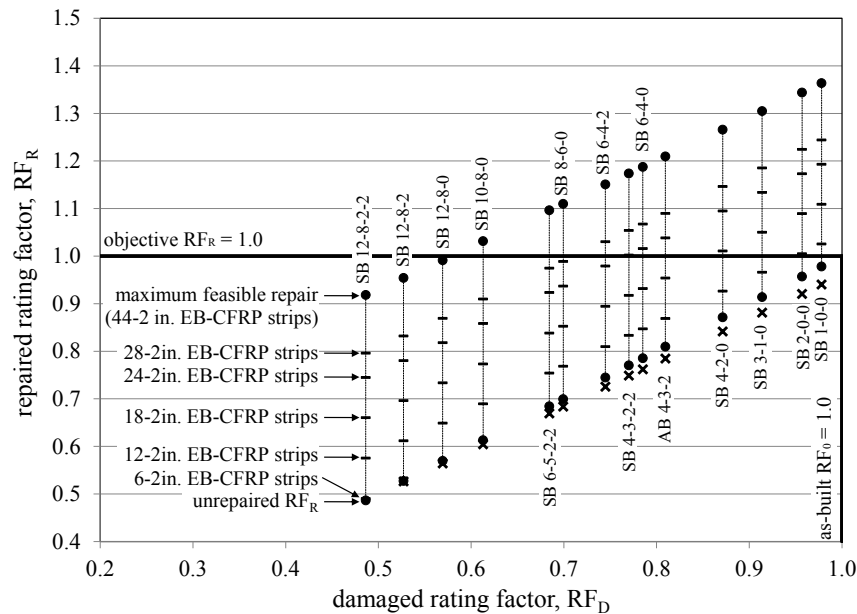


Figure 31 Results of parametric study of SB girders repaired with EB-CFRP.

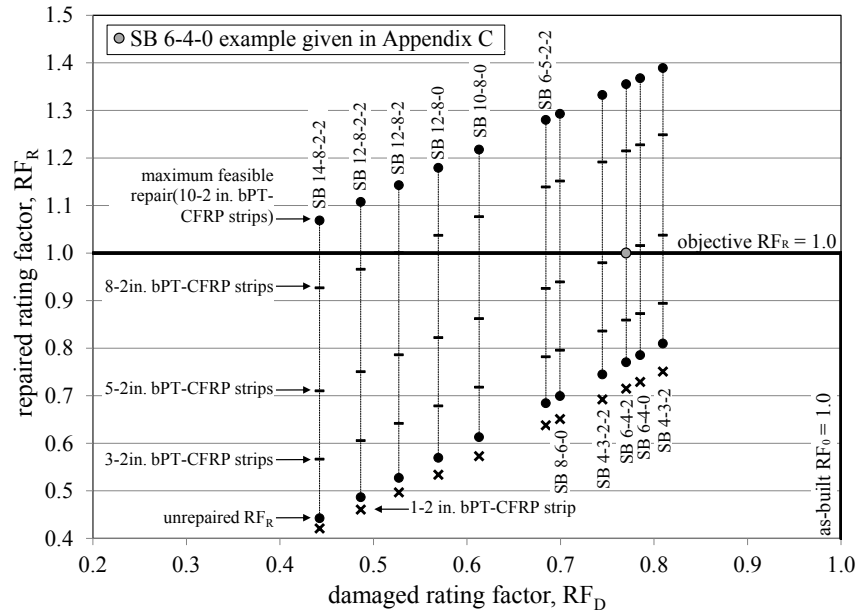


Figure 32 Results of parametric study of SB girders repaired with PT-CFRP.

2.4.3 IB Prototype

Considering the IB prototype described in Section 2.2.3, a range of damage (Table 8) was considered. EB-CFRP, PT-CFRP and NSM-CFRP repair techniques were considered at length and aspects of strand splicing and PT-Steel repairs were also considered. Eighteen damage cases ranging from IB 1-0-0 (3% strand loss) to IB 3-3-3 (28% strand loss) were considered. The IB 3-3-2 case repaired with NSM-CFRP is presented in its entirety in Appendix D1. Repair capacity and ratings for EB-CFRP, PT-CFRP and NSM-CFRP repairs are given in Table 13. Figures similar to those described in Section 2.4.1 are given for EB-CFRP, PT-CFRP and NSM-CFRP in Figures 33 through 35.

As described in Section 2.3.1 and Table 9, the EB-CFRP repair may extend across the soffit ($b_f = b = 22$ in.) and extend up the outside of the 7in. tall flange bulb (the latter material being less effective than that on the soffit), resulting in a total coverage of $b_f = 34$ in. or 17-2 in. EB-CFRP strips (Table 7) strips. To illustrate the range of EB-CFRP repair possible three degrees of repair were considered corresponding to 36, 72 and 100% of full soffit coverage (4, 8, and 11-2 in. EB-CFRP strips). One additional case, considering the full soffit plus 6 in. (3 strips/side) additional coverage up the sides of the flange bulb including the damaged unrepaired girders, 90 ratings were carried out. The results of these ratings are presented in Table 13 and Figure 33.

Similar data and plots were developed for the PT-CFRP repair of the damage cases summarized in Table 8. For the PT-CFRP repair, it was not felt to be necessary to extend the PT-CFRP up the sides of the flange bulb, in which case the practical limit of the PT-CFRP repair considered is providing full CFRP coverage of the soffit: $b_f \leq \approx 0.5b = 11$ in. or 4-2.4 in. PT-CFRP strips (Table 7). Four repair cases having 1, 2, 3 and 4 PT-CFRP strips were considered and a total of 50 ratings conducted. The results of these ratings are presented in Table 13 and Figure 34.

Finally, an NSM-CFRP technique was also demonstrated (see Section 1.5.3.3). In this case, 0.75 in. deep (to avoid interference with existing strands and transverse reinforcing steel) NSM slots are spaced at 1.75 in. Ten slots are provided along the 22 in. wide soffit, leaving an edge distance of 3 in. to avoid weakening the corner of the flange. Into each slot 2-0.047 in. wide by 0.5 in. tall (equivalent to $b_f = 1$ in.) CFRP strips (Table 7) are placed side by side. This results in equivalent CFRP coverage of $b_f = 0.5b$,

approximately half that available using EB-CFRP. Four repair cases having 3, 6, 9 and 10 NSM-CFRP strips were considered and a total of 90 ratings conducted. The results of these ratings are presented in Table 13 and Figure 35.

The IB prototype is considerably less amenable to CFRP repairs than the AB or SB prototypes. The primary reason for this is that the available surface area for CFRP coverage (b_f) of the bulb flange section is quite a bit smaller than for the box sections. A second consideration is the fact that the centroid of the prestressing steel is further from the soffit in a bulb flange than a box. Impact damage (particularly less severe damage) typically occurs at the bottom layer of strands. A severed strand in the lower layer has a proportionally greater effect on the damaged girder capacity, requiring proportionally more CFRP to restore the lost capacity. The inability of small amounts of CFRP to contribute to the repaired girder capacity (indicated as **x** in Figures 33 to 35) is more pronounced for the IB prototype.

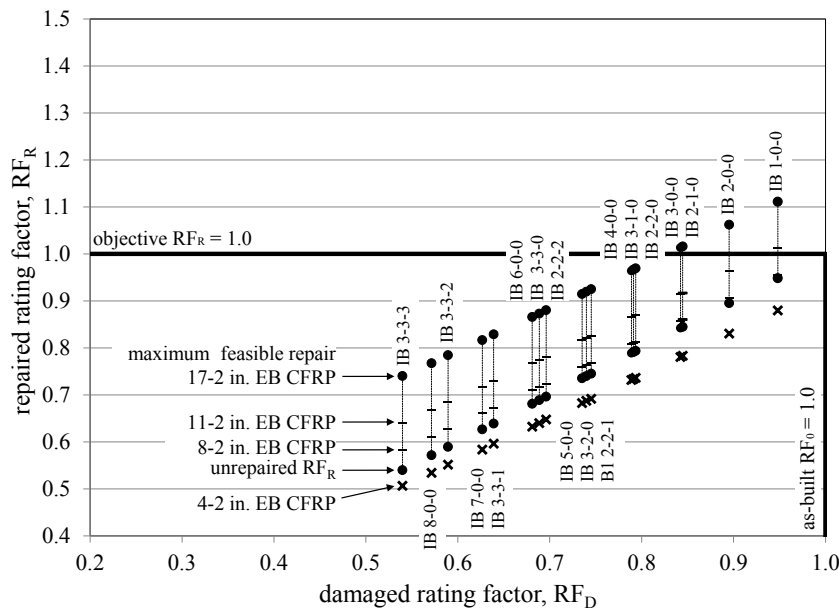


Figure 33 Results of parametric study of IB girders repaired with EB-CFRP.

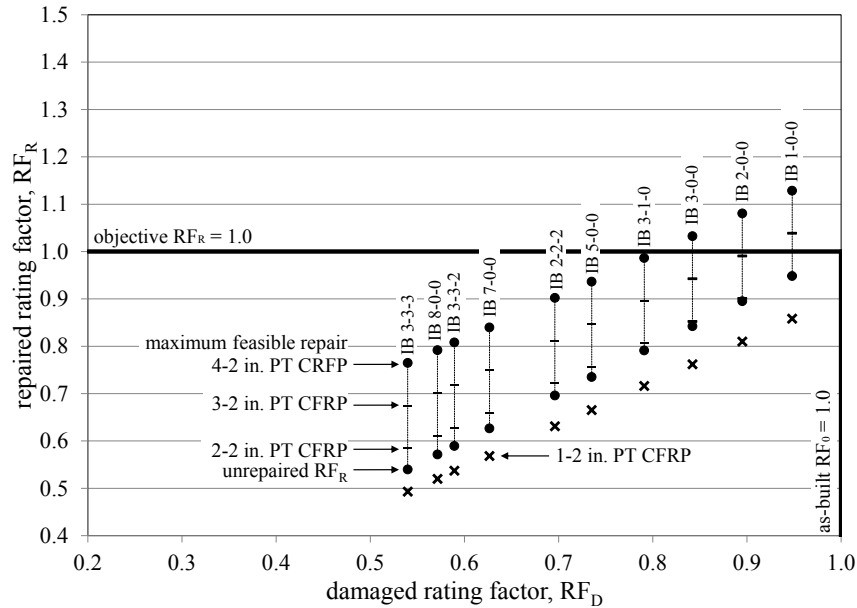


Figure 34 Results of parametric study of IB girders repaired with PT-CFRP.

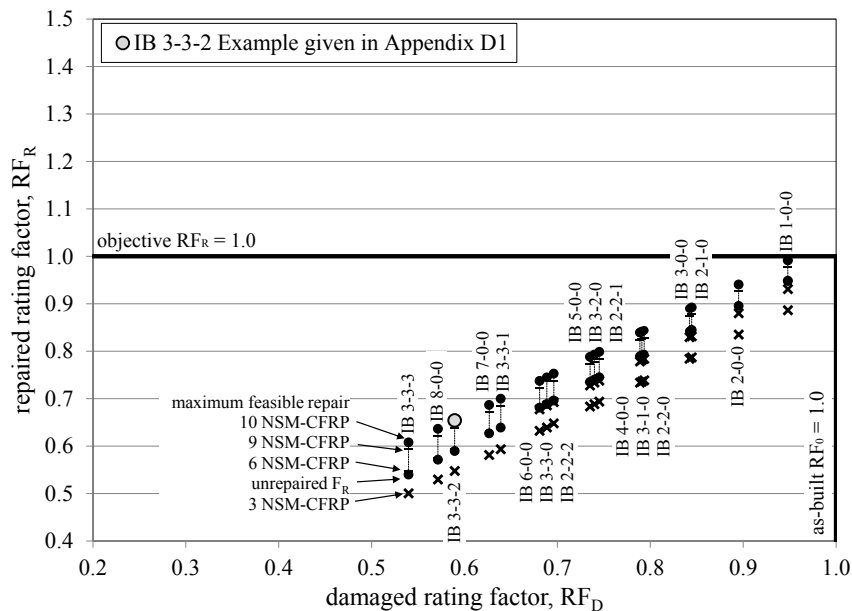


Figure 35 Results of parametric study of IB girders repaired with NSM-CFRP.

2.4.3.1 IB 3-3-2 Yang et al. (2011) Example

It is clear that the undamaged girder capacity of the IB 3-3-2 ($RF_D = 0.59$) prototype cannot be restored with CFRP techniques alone. Similarly, the nature of the impact damage (Figure 24d): adjacent strands in a relatively confined region along the beam length make splicing all eight strands less practical (Section 2.3.2.4.3). Finally, recommendations (Section 2.3.3.4.1) limit the number of splice strands in a beam to about 15% (5 strands in this case). Therefore, the solution, was to splice five strands (Figure 25a), tensioning these to a stress approximately equal to the long term effective stress in the strands (Figure 25b) thereby restoring five strands. As described in Section 2.3.2.4.1, strands splices are only approximately 85% effective under ultimate load conditions. Thus, when considering the ultimate load

carrying capacity, the damaged girder has been ‘upgraded’ by replacing an equivalent to 4 strands, resulting in the IB 2-2-0 ($RF_R = 0.79$) scenario. The remaining lost capacity can then be restored using EB-CFRP techniques. The calculations for this approach are provided in Appendix D2.

In 2004, when the repair was conducted, CFRP fabric was used. The actual repair used three layers of fabric CFRP (Figure 25j). Using the design approach described in this work, the application of four layers of fabric CFRP (Table 7) was found to restore the girder capacity to $RF_R = 0.95$. Additional layers of CFRP will only marginally increase the capacity since the reduction in debond strain (resulting from increasing nt_f in Equation 3) affects both the efficiency of the CFRP and prestressing strand at the debonding event. The resulting repair detail is shown in Figure 36. This two-stage hybrid repair approach is shown schematically in Figure 36 in terms of the damaged and repaired rating factors.

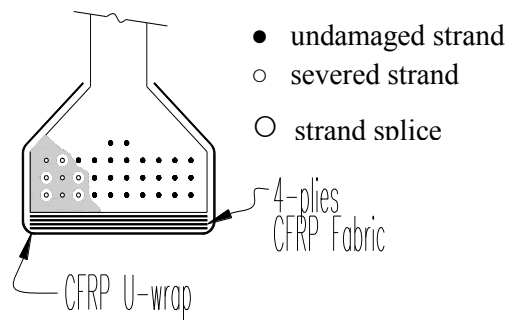


Figure 36 Hybrid strand splice and fabric CFRP repair of IB 3-3-2.

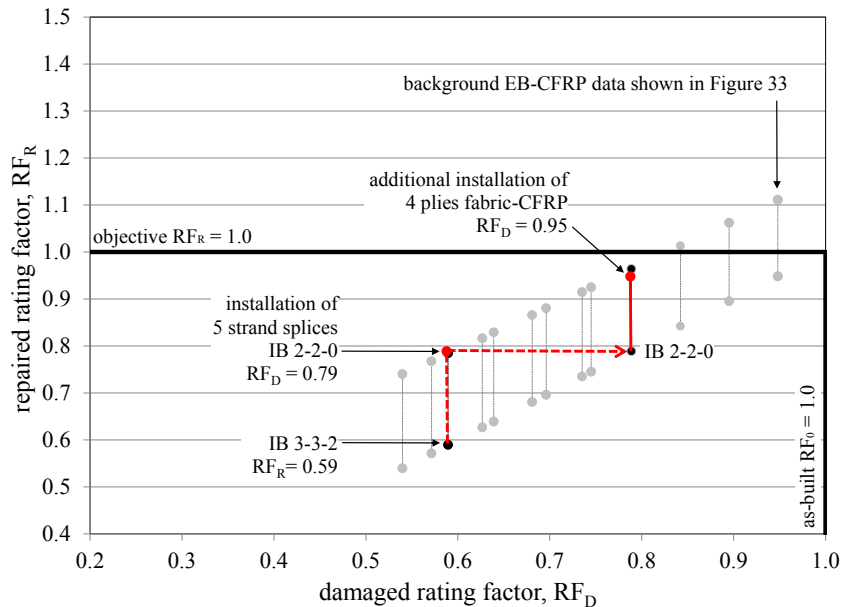


Figure 37 Schematic representation of rating factors for IB 3-3-2 hybrid repair.

The differences between the 2004 repair reported by Yang et al. (2011) and that reported here stem from two issues:

1. It is not clear from Yang et al. whether the splices were considered able to develop 100% of the strand capacity, or 85% as recommended here.

- The ACI 440 (2002) FRP debonding strain calculation used in 2004 permitted greater debonding strains to be used in design (thereby increasing the CFRP contribution). This equation was found to be unconservative in many cases and was replaced in 2008 by what is presented as Equation 3 in this work.

2.4.3.2 PT-Steel Repair of IB 3-3-2

PT-steel repairs can generally be designed to restore the full capacity, including the lost prestress force of damaged I-girders (see Section 2.3.2.5). Although covered extensively in Shanafelt and Horn (1980 and 1985), the same IB 3-3-2 prototype is used in this work to demonstrate the approach to developing a PT-steel repair. It is noted that the capacity of the IB 3-3-2 ($RF_D = 0.59$) prototype could not be repaired using CFRP methods and required a hybrid approach mixing strand splices and EB-CFRP. The PT-steel approach offers an alternative that may be attractive if the severed strands have also experienced extensive corrosion or the concrete has otherwise deteriorated making strand splicing and external bonding approaches less practical. The complete PT-steel repair design is presented in Appendix D3.

Two straight 1.375 in. diameter 150 ksi PT bars, each stressed to $0.53f_{pu} = 80$ ksi are used. These bars are anchored to bolsters partially notched into the upper slope of the bottom flange. Notching the bolsters into the flange allows the resultant PT force to be located lower in the cross section in order to have a greater effect on ultimate girder capacity. The bolster is subsequently post-tensioned through the web of the girder. The transverse PT is designed to provide sufficient clamping force to anchor the longitudinal PT force through friction, using a friction coefficient of 0.7 (AASHTO LRFD Section 5.8.4.3). An example of a simple bolster design is shown in Figure 38. The final PT-steel system resembles that shown in Figure 27a.

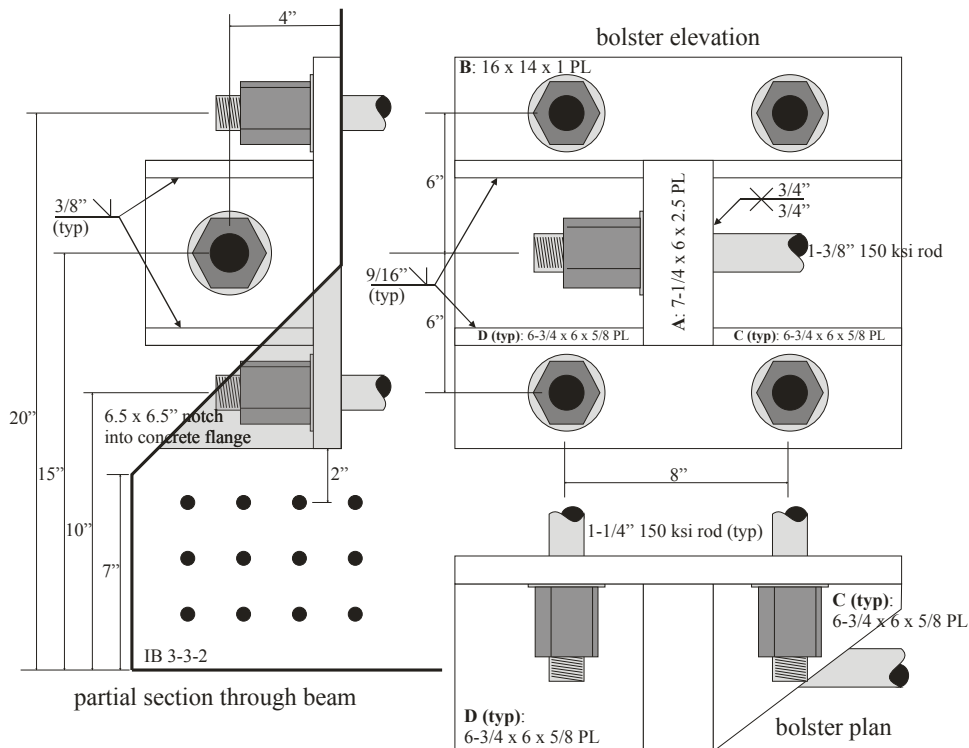


Figure 38 Bolster design for PT-Steel repair of IB 3-3-2.

Table 11 Results of parametric study for AB prototype girder.

C ₀ =3573 kft RF ₀ =1.0	AB Damage Case																	
	damage is sufficient to result in decompression under nominal dead load																	
	100	210	320	420	422	530	4222	631	641	42222	6322	652	752	6522	65222	872	8722	10922
strand loss	2%	5%	9%	11%	14%	14%	18%	18%	19%	21%	23%	23%	25%	26%	30%	30%	33%	40%
C _D (kft)	3514	3393	3275	3213	3102	3090	2998	2972	2913	2899	2811	2795	2731	2689	2586	2547	2435	2178
RF _D	0.98	0.93	0.88	0.85	0.81	0.80	0.76	0.75	0.73	0.72	0.69	0.68	0.65	0.64	0.59	0.58	0.53	0.42
C _R (kft)	EB-CFRP Repairs																	
RF _R																		
EB-CFRP 6 strips	3562 1.00	3438 0.94	3316 0.89	3253 0.87	3142 0.82	3132 0.82	3039 0.78	3015 0.77	2596 0.75	2937 0.74	2854 0.70	2840 0.70	2777 0.67	2734 0.65	2633 0.61	-	-	-
EB-CFRP 12 strips	3820 1.10	3696 1.05	3571 1.00	3511 0.97	3398 0.93	3388 0.92	3293 0.88	3270 0.88	3210 0.85	3193 0.84	3111 0.81	3096 0.80	3033 0.78	2988 0.76	2888 0.72	-	-	-
EB-CFRP 18 strips	4078 1.21	3951 1.16	3826 1.10	3764 1.08	3653 1.03	3640 1.03	3546 0.99	3526 0.98	3465 0.96	3445 0.95	3363 0.91	3350 0.91	3288 0.88	3243 0.86	3143 0.82	-	-	-
EB-CFRP 24 strips	4333 1.31	4208 1.26	4080 1.21	4018 1.18	3907 1.14	3894 1.13	3799 1.09	3780 1.09	3719 1.06	3698 1.05	3618 1.02	3604 1.01	3543 0.99	3498 0.97	3395 0.93	-	-	-
C _R (kft)	bPT-CFRP Repairs																	
RF _R																		
bPT-CFRP 1 strip	-	-	-	-	3058 0.79	3046 0.78	-	2933 0.74	2874 0.71	2858 0.70	2778 0.67	2763 0.67	2702 0.64	2660 0.62	-	2525 0.57	2418 0.52	2178 0.42
bPT-CFRP 3 strips	-	-	-	-	3490 0.96	3482 0.96	-	3370 0.92	3312 0.89	3295 0.88	3215 0.85	3202 0.85	3140 0.82	3099 0.80	-	2965 0.75	2863 0.71	2623 0.61
bPT-CFRP 5 strips	-	-	-	-	3923 1.14	3913 1.14	-	3799 1.09	3743 1.07	3726 1.06	3645 1.03	3631 1.02	3567 1.00	3529 0.98	-	3397 0.93	3293 0.88	3054 0.79
bPT-CFRP 8 strips	-	-	-	-	4550 1.40	4540 1.40	-	4426 1.35	4369 1.33	4362 1.32	4275 1.29	4261 1.28	4189 1.25	4162 1.24	-	4028 1.19	3924 1.14	3687 1.05
bPT-CFRP 10 strips	-	-	-	-	4958 1.57	4950 1.57	-	4837 1.52	4781 1.50	4770 1.49	4685 1.46	4673 1.45	4583 1.42	4573 1.41	-	4439 1.36	4339 1.31	4106 1.22
AB Girder: 42 x 48 in. box girder (BIV-48) with 3 in. composite deck. 57-3/8" 250 ksi strands										light shaded entries do not meet repair objective of RF _R ≥ 1.0 darker shaded entries are ineffectual repairs where there is insufficient CFRP to affect the damaged capacity (see Section 2.3.2.1)								

Table 12 Results of parametric study for SB prototype girder.

C ₀ =5005 kft RF ₀ =1.0	SB Damage Case														
												damage is sufficient to result in decompression under nominal dead load			
	100	200	310	420	432	640	4322	642	860	6522	1080	1280	1282	12822	14822
strand loss	2%	3%	6%	9%	13%	15%	16%	18%	21%	22%	26%	29%	32%	35%	38%
C _D (kft) RF _D	4929 0.98	4856 0.96	4707 0.91	4560 0.87	4346 0.81	4262 0.79	4210 0.77	4122 0.74	3965 0.70	3913 0.68	3666 0.61	3515 0.57	3369 0.53	3228 0.49	3076 0.44
C _R (kft) RF _R	EB-CFRP Repairs														
EB-CFRP 6 strips	4799 0.94	4730 0.92	4594 0.88	4457 0.84	4260 0.78	4182 0.76	4136 0.75	4055 0.73	3910 0.68	3861 0.67	3636 0.60	3497 0.56	3367 0.53	3242 0.49	-
EB-CFRP 12 strips	5093 1.03	5023 1.01	4887 0.97	4750 0.93	4551 0.87	4476 0.85	4428 0.83	4346 0.81	4203 0.77	4154 0.75	3930 0.69	3790 0.65	3662 0.61	3536 0.58	-
EB-CFRP 18 strips	5382 1.11	5314 1.09	5178 1.05	5042 1.01	4845 0.95	4769 0.93	4719 0.92	4639 0.89	4494 0.85	4445 0.84	4220 0.77	4083 0.73	3953 0.70	3829 0.66	-
EB-CFRP 24 strips	5673 1.19	5604 1.17	5468 1.13	5333 1.09	5137 1.04	5060 1.02	5013 1.00	4933 0.98	4787 0.94	4740 0.92	4514 0.86	4375 0.82	4244 0.78	4122 0.74	-
EB-CFRP 28 strips	5849 1.24	5781 1.22	5646 1.19	5511 1.15	5315 1.09	5238 1.07	5191 1.05	5109 1.03	4966 0.99	4918 0.97	4693 0.91	4553 0.87	4423 0.83	4299 0.80	-
EB-CFRP 44 strips	6263 1.36	6195 1.34	6059 1.30	5924 1.27	5730 1.21	5654 1.19	5607 1.17	5527 1.15	5385 1.11	5338 1.10	5114 1.03	4975 0.99	4846 0.95	4723 0.92	-
C _R (kft) RF _R	bPT-CFRP Repairs														
bPT-CFRP 1 strip	-	-	-	-	4143 0.75	4068 0.73	4019 0.72	3940 0.69	3798 0.65	3752 0.64	3528 0.57	3392 0.53	3264 0.50	3139 0.46	3001 0.42
bPT-CFRP 3 strips	-	-	-	-	4639 0.89	4564 0.87	4517 0.86	4437 0.84	4298 0.80	4250 0.78	4029 0.72	3893 0.68	3765 0.64	3640 0.61	3505 0.57
bPT-CFRP 5 strips	-	-	-	-	5134 1.04	5059 1.02	5013 1.00	4934 0.98	4795 0.94	4747 0.93	4528 0.86	4390 0.82	4265 0.79	4142 0.75	4003 0.71
bPT-CFRP 8 strips	-	-	-	-	5865 1.25	5793 1.23	5748 1.21	5668 1.19	5529 1.15	5485 1.14	5269 1.08	5133 1.04	5008 1.00	4887 0.97	4752 0.93
bPT-CFRP 10 strips	-	-	-	-	6352 1.39	6277 1.37	6233 1.36	6155 1.33	6018 1.29	5973 1.28	5758 1.22	5625 1.18	5499 1.14	5377 1.11	5243 1.07
SB Girders: 42 x 48 in. box girder (BIV-48) with 7.5 in. composite deck at 8'-9" center-to-center spacing 68-3/8" 250 ksi strands								light shaded entries do not meet repair objective of RF _R ≥ 1.0 darker shaded entries are ineffectual repairs where there is insufficient CFRP to affect the damaged capacity (see Section 2.3.2.1)							

Table 13 Results of parametric study for IB prototype girder.

C ₀ =4519 kft RF ₀ =1.0	IB Damage Case																	
																	decompression	
	100	200	300	210	220	310	400	320	500	222	330	600	221	331	700	332	800	333
strand loss	3%	6%	9%	9%	13%	13%	13%	16%	16%	19%	19%	19%	22%	22%	22%	25%	25%	28%
C _D (kft)	4380	4237	4095	4102	3964	3958	3952	3820	3808	3703	3683	3662	3834	3549	3516	3416	3368	3283
RF _D	0.95	0.90	0.84	0.84	0.79	0.79	0.79	0.74	0.74	0.70	0.69	0.68	0.75	0.64	0.63	0.59	0.57	0.54
C _R (kft)	EB-CFRP Repairs																	
RF _R																		
EB-CFRP 4 strips	4196 0.88	4063 0.83	3930 0.78	3937 0.78	3811 0.74	3803 0.73	3798 0.73	3679 0.69	3666 0.68	3573 0.65	3552 0.64	3532 0.63	3691 0.69	3434 0.60	3400 0.58	3314 0.55	3267 0.53	3193 0.51
EB-CFRP 8 strips	4400 0.96	4268 0.91	4135 0.86	4143 0.86	4017 0.81	4010 0.81	4003 0.81	3883 0.76	3870 0.76	3777 0.72	3758 0.72	3738 0.71	3896 0.77	3638 0.67	3606 0.66	3519 0.63	3473 0.61	3399 0.58
EB-CFRP 11 strips	4555 1.01	4422 0.96	4289 0.91	4295 0.92	4171 0.87	4164 0.87	4157 0.87	4039 0.82	4025 0.82	3932 0.78	3913 0.77	3893 0.77	4051 0.83	3793 0.73	3759 0.72	3674 0.69	3628 0.67	3554 0.64
EB-CFRP 17 strips	4818 1.11	4686 1.06	4555 1.01	4562 1.02	4437 0.97	4428 0.97	4422 0.96	4303 0.92	4290 0.91	4198 0.88	4178 0.87	4158 0.87	4318 0.92	4059 0.83	4026 0.82	3940 0.78	3894 0.77	3821 0.74
C _R (kft)	bPT-CFRP Repairs																	
RF _R																		
bPT-CFRP 1 strips	4183 0.86	4008 0.81	3879 0.76	-	-	3757 0.72	-	-	3620 0.67	3528 0.63	-	-	-	-	3359 0.57	3276 0.54	3229 0.52	3157 0.49
bPT-CFRP 2 strips	4381 0.95	4253 0.90	4122 0.85	-	-	3998 0.81	-	-	3863 0.76	3771 0.72	-	-	-	-	3603 0.66	3518 0.63	3474 0.61	3402 0.58
bPT-CFRP 3 strips	4623 1.04	4493 0.99	4364 0.94	-	-	4241 0.90	-	-	4107 0.85	4013 0.81	-	-	-	-	3848 0.75	3762 0.72	3717 0.70	3643 0.67
bPT-CFRP 4 strips	4864 1.13	4735 1.08	4606 1.03	-	-	4483 0.99	-	-	4348 0.94	4256 0.90	-	-	-	-	4088 0.84	4003 0.81	3959 0.79	3888 0.76
C _R (kft)	NSM-CFRP Repairs																	
RF _R																		
NSM-CFRP 3 strips	4213 0.89	4076 0.84	3939 0.78	3947 0.79	3817 0.74	3810 0.74	3803 0.73	3682 0.69	3688 0.68	3573 0.65	3550 0.64	3531 0.63	3696 0.69	3427 0.59	3394 0.58	3303 0.55	3255 0.53	3177 0.50
NSM-CFRP 6 strips	4333 0.93	4197 0.88	4061 0.83	4066 0.83	3938 0.78	3932 0.78	3923 0.78	3803 0.73	3788 0.73	3693 0.69	3674 0.69	3653 0.68	3815 0.74	3550 0.64	3517 0.63	3425 0.59	3378 0.58	3303 0.55
NSM-CFRP 9 strips	4456 0.98	4319 0.93	4182 0.87	4189 0.88	4058 0.83	4052 0.83	4046 0.82	3923 0.78	3909 0.77	3815 0.74	3794 0.73	3773 0.72	3937 0.78	3672 0.68	3638 0.67	3548 0.64	3502 0.62	3425 0.59
NSM-CFRP 10 strips	4496 0.99	4359 0.94	4223 0.89	4229 0.89	4099 0.84	4093 0.84	4087 0.84	3963 0.79	3949 0.79	3854 0.75	3833 0.74	3813 0.74	3978 0.80	3713 0.70	3678 0.69	3589 0.65	3542 0.64	3465 0.61
IB Girder: 40 in. C girder with 7 in. composite deck at 7'-3" center-to-center spacing 32-0.5" 270 ksi strands										light shaded entries do not meet repair objective of RF _R ≥ 1.0 darker shaded entries are ineffectual repairs where there is insufficient CFRP to affect the damaged capacity (see Section 2.3.2.1)								

2.5 Damage Location Along Span

Throughout the presented discussion, the focus is on restoring damaged section behavior; tacitly implying that the damaged section is also the critical section along the length of the member (i.e.: the impact damage occurs at the midspan of a simply supported girder). This approach, while common in practice, may be overly conservative. Common practice when rating impact-damaged girders is to consider the damaged section and rate this based on the beam design moment. This, implies that the contribution of a strand severed at any location is neglected in the member analysis. Kasan and Harries (2011) have clearly demonstrated that once a severed strand re-enters sound concrete, the prestress force is ‘redeveloped’ over the transfer length measured from the edge of the sound concrete. Kasan and Harries propose that the design transfer length of $60d_b$ (AASHTO 2010) is appropriate for ‘redevelopment’ of prestress force following impact damage; in fact experimental data suggested a value of about one half this prescribed value. Thus, damage is effectively ‘localized’ at a region extending the strand development length to either side of the maximum extent of the damage. The implication of this is that damage located away from the region of maximum moment may not require structural repair at least to the point of restoring the full section capacity. This distinction is most critical when rating individual girders as is done in this work (Eq. 2) since not only is the damaged section possibly removed from the critical section for moment but also the moment that must be resisted at the location of the damage is a function of the damage location.

The foregoing discussion is demonstrated by the example of the AB prototype described in Section 2.2.1. The AB 3-2-0 damage (Figure 22c) extends only about 45 in. along the span centered approximately 28 feet (0.35L) along the span from the West support. The damage is located immediately above the right lane of the carriageway passing beneath the bridge. Figure 39 shows the AB prototype moment demand and capacity envelopes. The moment demand envelope includes all dead load and lane load effects and the appropriate vehicle live load moment determined at each section (i.e.: the live load determined from an influence line analysis of the HL-93 load). As seen in Appendix B, this AB girder has considerable reserve capacity (plotted on the right-hand axis of Figure 39). The damage occurring at 0.35L is mitigated as the strands are ‘redeveloped’ into the sound concrete away from the damaged region. For the damage case of AB 3-2-0 located at 0.35L, the damage barely affects the girder capacity since the midspan (0.5L) undamaged section remains critical. Greater damage (AB 6-5-2-2 shown) clearly results in the section at 0.35L becoming the critical section. In the latter case, however, the moment demand at the damaged section (0.35L) is less than the girder design moment at 0.5L. In this example, a valid argument may be made for stabilizing (patching and corrosion mitigation measures) but not repairing (in a structural sense) the AB 3-2-0 damage case, since the overall girder performance is not compromised. For the AB 6-5-2-2 damage case, structural repair may not be required if lower margin of safety (structural reliability) is acceptable since the girder capacity remains higher than demand at all sections. This latter issue is a philosophical design issue beyond the scope of the present discussion: *to what performance level does an aging damaged bridge need to be restored?*

2.5.1 Strand loss near supports

A special case, and relatively rare in terms of likely impact damage, results in strand loss near the girder support. Near the support, strands are still not completely developed and some may be unbonded. In addition to carrying stresses due to applied moments (low near beam supports), bonded strands in this region also resist additional tensile stresses equilibrating the high shear stress in this region (AASHTO LRFD Article 5.8.3.5). Strands lost due to damage in this region are analogous to additional unbonded strands (particularly in light of the previous discussion of ‘redevelopment’). AASHTO LRFD Article 5.11.4.3 restricts the number of debonded strands to 25% of the total strands in the section. In the absence of additional guidance, this limit is appropriate for considering strand damage to this region. While beyond the scope of the present study, NCHRP Project 12-91, will develop guidance on the upper limit for debonding strands. These results will be applicable to considering strands lost due to impact damage in regions of low moment-to-shear ratios.

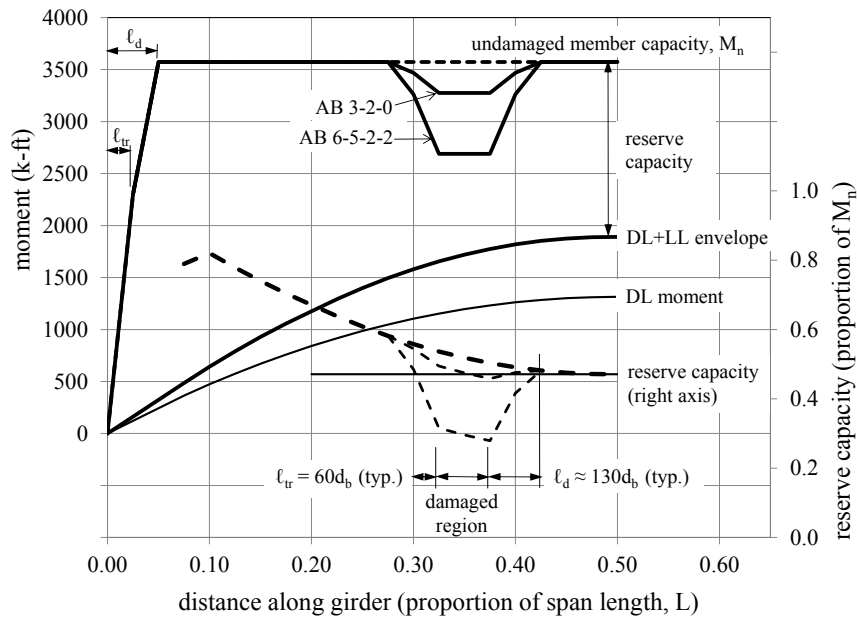


Figure 39 Moment envelopes for AB 3-2-0.

2.6 Synthesis of Parametric Study

It is evident from the variable nature of impact damage and the previous discussion of repair techniques and incremental capacity, that repair decisions and design must be executed on a case-by-case basis. Nonetheless, trends are clearly evident in Figures 29 through 35. Table 14 summarizes the maximum strand loss that could be restored for each of the prototypes. Based on the objective of restoring $RF_D \geq 1.0$, these limits would represent to threshold for the repair-or-replace decision for these girders. As a basis for comparison, the strand loss required to result in decompression of the girder (initiation of tension strains at the girder soffit under the action of nominal dead load only) is provided (see Section 2.5.1.2).

Table 14 Maximum strand loss that can be fully restored ($RF_D \geq 1.0$) for prototype structures.

	AB Prototype	SB Prototype	IB Prototype
girder detail	42 x 48 in. box girder (BIV-48) with 3 in. composite deck	42 x 48 in. box girder (BIV-48) spaced at 8'-9" with 7.5 in. composite deck	40 in. C-girder spaced at 7'-3" with 7 in. composite deck
prestressing strands	57-3/8" 250 ksi strands	68-3/8" 250 ksi strands	32-0.5" 270 ksi strands
strand loss to cause decompression	≈12 strands (21%)	≈20 strands (29%)	≈8 strands (25%)
EB-CFRP	$RF_R = 0.69$ 13 strands (23%)	$RF_R = 0.61$ 18 strands (26%)	$RF_R = 0.84$ 3 strands (9%)
bPT-CFRP	$< RF_R = 0.40$ 23 strands (40%)	$< RF_R = 0.44$ 26 strands (38%)	$< RF_R = 0.84$ 3 strands (9%)
NSM-CFRP	NSM not considered practical		$RF_R = 0.95$ 1 strands (3%)

2.6.1 Maximum Effect of CFRP Repair Techniques

Although repair designs must be considered on a case-by-case basis, it is useful to have an approximate measure of the effectiveness of the repair material in restoring moment capacity and to relate this to the *in situ* girder being repaired. By equating the nominal moment capacity contribution of the CFRP (Figure 26) to an equivalent contribution of the *in situ* prestressing strand, one arrives at the theoretical maximum number of severed prestressing strands, n_{max} , that can be replaced by CFRP based on its relative contribution to moment capacity:

$$n_{max} = \frac{E_f n t_f b_f \varepsilon_{fd} \alpha H}{f_{pu} A_p \beta H} \quad (\text{Eq. 6})$$

Where: E_f = tension modulus of elasticity of CFRP

t_f = thickness of one ply/layer of CFRP

n = number of plies/layers of CFRP.

EB-CFRP: for preformed strip it is recommended that $n = 1$ (Section 2.3.2.1)

PT-CFRP: $n = 1$

b_f = maximum width available for CFRP bonding (see Section 2.3.1):

EB-CFRP: $b_f = b$

PT-CFRP: $b_f = 0.5b$

NSM-CFRP: $b_f = (b/2 + 1)c$

b = soffit width of girder; if chamfers are present, the available soffit width should be reduced accordingly

c = depth of NSM slot

ε_{fd} = debonding strain of CFRP (see Section 2.3.2):

$$\text{EB-CFRP: } \varepsilon_{fd} = 0.083 \sqrt{\frac{f'_c}{n E_f t_f}} \leq 0.9 \varepsilon_{fu} \quad (\text{ksi units}) \quad (\text{Eq. 7})$$

$$\text{PT-CFRP: } \varepsilon_{fd} = 0.083 \sqrt{\frac{f'_c}{n E_f t_f}} + \kappa \varepsilon_{fu} \leq 0.9 \varepsilon_{fu} \quad (\text{ksi units}) \quad (\text{Eq. 8})$$

$$\text{NSM-CFRP: } \varepsilon_{fd} \leq 0.7 \varepsilon_{fu}$$

ε_{fu} = rupture strain of CFRP strip

f'_c = concrete substrate compressive strength

$\kappa = 0.3$ for uPT-CFRP (Figure 8d)

$\kappa = 0.5$ for bPT-CFRP (Figure 8e)

αH = depth from compression resultant to location of CFRP on soffit

βH = depth from compression resultant to centroid of prestressing strands

H = overall depth of girder⁴

f_{pu} = ultimate stress of prestressing strand

A_p = area of one prestressing strand

Values of α and β vary based on the section geometry and amount of prestressing provided. In lieu of member-specific calculations, the values given in Table 15 may be used as estimates of these values. The ratio α/β effectively normalizes the CFRP stress to that of the *in situ* strand accounting for section geometry. The CFRP, located at the extreme tension fiber, is more efficient at providing moment capacity to the section than the *in situ* strand due to its greater level arm to the compression resultant, αH .

⁴ Although H cancels in Equation 5, it is left in place so that both the numerator and denominator represent moment capacities.

Table 15 Approximate values of α and β .

	rectangular section	voided slab	I-girders	bulb tees	deck bulb tees	box girders
α	0.65	0.65	0.80	0.80	0.90	0.92
β^1	0.50	0.58	0.64	0.64	0.76	0.82

¹ based on values reported in Collins and Mitchell (1997) for location of top kern point

The approach described by Equation 6 was applied to standard prestressed concrete shapes described in *Appendix B: Standard Products* of the *PCI Bridge Design Manual* (PCI 2003) to establish an approximate value of n_{max} for these products. The results are shown in Table 16 and Figure 40. The values reported must be understood to be upper-bound values. ACI 440 (2008) design of CFRP flexural repairs, for instance, introduces an additional strength reduction factor, $\Psi = 0.85$, to the CFRP component of moment resistance. Furthermore, the values reported in Table 16 are normalized to 3/8" 250 ksi strand (typical of older damaged box girders); factors to normalize these results for other strands are given in the notes to Table 16.

Based on this approach, the efficiency of a CFRP repair is seen to be primarily a function of the girder surface area available for bonding and the efficiency of the CFRP: whether it is post-tensioned or not. Sections having larger soffit widths may be more efficiently repaired since b_f may be maximized. The efficiency of a given CFRP material is a function of its debonding strain; thus post tensioned applications have a significantly greater capacity for restoring capacity than do EB-CFRP systems. For the materials described in Table 7, bPT-CFRP applications are approximately twice as effective as EB-CFRP provided there is sufficient surface area available to accommodate the larger bPT-CFRP footprint. Because of geometric considerations, NSM-CFRP and EB-CFRP are about equally effective; thus it is unlikely that the additional effort required to install NSM-CFRP would be warranted. The values reported in Table 16 should be interpreted as an upper bound for the number of strands that may be repaired. As indicated in the results of the parametric study given in Section 2.4 and summarized in Table 14, these theoretical values were not achieved. Nonetheless, Eq. 5 provides an initial basis for a repair-or-replace decision. Based on the results of the parametric study and the nature of the simplifications in Equation 5, it is felt that taking 80% of the theoretical upper bound values reported is an appropriate basis for the design of impact-damage repairs.

2.6.1.1 Restoration of Prestressing Force

In addition to restoring the ultimate load carrying capacity of a member, PT-CFRP systems are able to restore some degree of prestress force lost along with severed strands. Using the same approach as described in Section 2.6.1, Equation 9 provides an approximation for the maximum amount of prestress force that can be replaced by PT-CFRP systems. Consistent with Equation 6, Equation 9 is normalized by the effective prestress force provided by a single strand ($f_{pe}A_p$) resulting in the equivalent number of strands whose prestress force can be replaced with PT-CFRP, n_{max-PT} :

$$n_{max-PT} = \frac{E_f n t_f b_f \kappa \varepsilon_{fu} \beta}{f_{pe} A_p \alpha} \quad (\text{Eq. 9})$$

Where f_{pe} is the long term effective prestress force; in lieu of calculating this value, $f_{pe} = 0.57f_{pu}$ may be used as a reasonable estimate for the long term effective prestress after all losses (based on AASHTO LRFD Section 5.9.5.3). All other values are the same as those given for Equation 5. The ratio β/α effectively normalizes the CFRP stress to that of the *in situ* strand accounting for section geometry. The CFRP, located at the extreme tension fiber, is less efficient at providing prestress to the section than the *in situ* strand. Values of n_{max-PT} are given in Table 16 and shown in Figure 41.

It is seen that PT-CFRP is less efficient at restoring lost prestress force (n_{max-PT}) than lost ultimate capacity (n_{max}). Because of the limited long term prestress force available in an uPT-CFRP system (taken as $0.30f_{fu}$), such systems perform only marginally better than EB-CFRP. Like NSM-CFRP, it is unlikely that

the additional effort required for uPT-CFRP would warrant its use. The prestress force available for a P-CFRP system is even less than a uPT-CFRP and therefore possibly less efficient than an EB-CFRP system due to geometric constraints.

Table 16 Maximum number of severed prestressing strands, n_{max} , that can be replaced by CFRP.

Shape (PCI 2003)	H (in.)	b (in.)	typical strands ³ (PCI 2003)	equivalent 3/8" 250 ksi strand ⁴						
				EB- CFRP	bPT-CFRP		uPT-CFRP		NSM- CFRP	
				n_{max}	n_{max}	n_{max-PT}	n_{max}	n_{max-PT}	n_{max}	
AASHTO I-girders	I	28	16	20	6	13	10	10	6	7
	II	36	18	30	7	15	11	12	7	8
	III	45	22	50	8	19	14	14	8	9
	IV	54	26	66	10	22	16	17	10	11
	V	63	28	80	11	24	18	18	10	12
	VI	72	28	80	11	24	18	18	10	12
	C ¹	40	22	50	8	19	14	14	8	9
Boxes	B-36	27, 33, 39	36	34	13	28	26	21	15	13
	B-48 ²	& 42	48	46	17	37	34	29	20	18
Bulb Tees	BT	54, 63 & 72	26	40	10	22	16	17	10	11
Deck Tees	-	35, 53 & 65	25	32	9	20	17	16	10	10
Slabs	S-36	12, 15, 18	36	17	13	27	26	21	15	13
	S-48	& 21	48	23	17	37	34	29	20	18

¹ IB Prototype

² AB and SB prototype

³ Typical number of strands in a section; taken as:

maximum number of strands that may be located in confines of the bottom flange or bulb;

maximum number of strands in one layer for slabs; or

⁴ to convert tabulated values to...

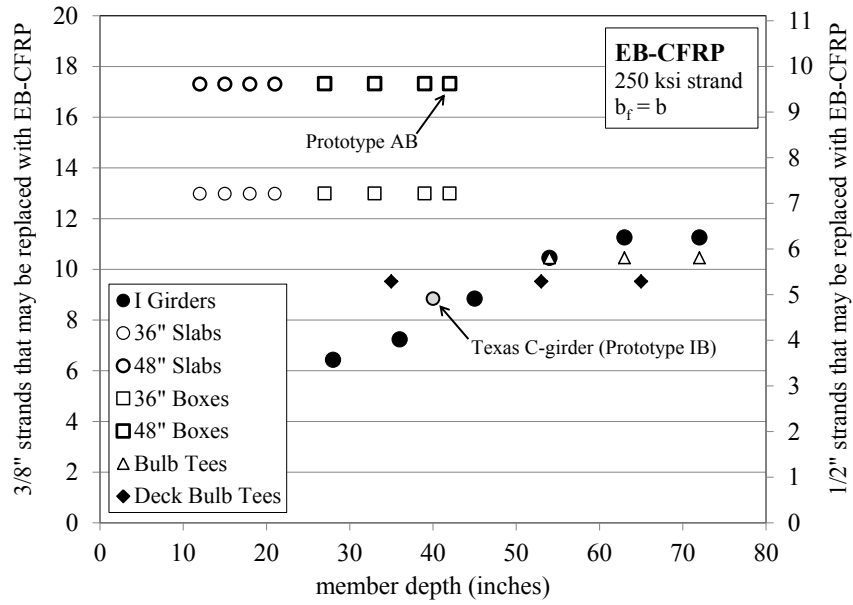
equivalent 3/8" 270 ksi strand, multiply tabulated value by $(0.080/0.085)(250/270) = 0.87$

equivalent 1/2" 250 ksi strand, multiply tabulated value by $(0.080/0.144) = 0.56$

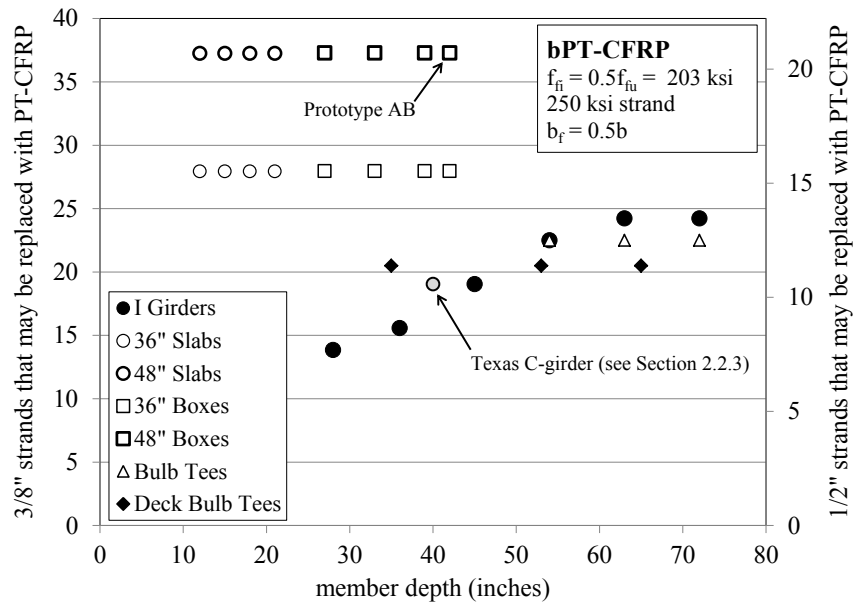
equivalent 1/2" 270 ksi strand, multiply tabulated value by $(0.080/0.153)(250/270) = 0.48$

equivalent 0.6" 250 ksi strand, multiply tabulated value by $(0.080/0.216) = 0.37$

equivalent 0.6" 270 ksi strand, multiply tabulated value by $(0.080/0.215)(250/270) = 0.34$



a) EB-CFRP



b) bPT-CFRP

Figure 40 Theoretical maximum number of severed prestressing strands, n_{max} , that can be replaced by CFRP based on the relative contribution to moment capacity.

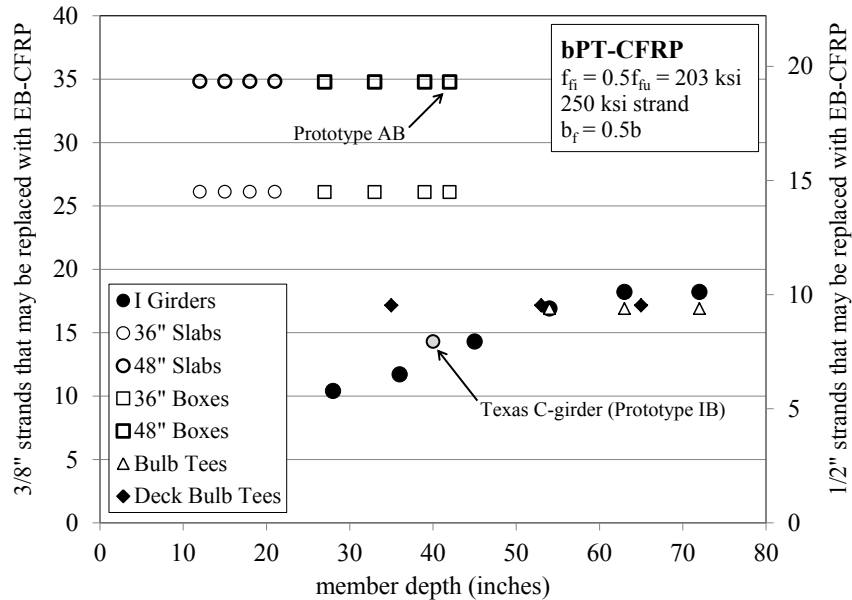


Figure 41 Theoretical maximum number of severed prestressing strands, $n_{\max-PT}$, whose prestress force can be replaced by bPT- CFRP.

2.6.1.2 Damage Threshold to Cause Decompression

The fundamental design philosophy for prestressed concrete bridge girders is to provide sufficient prestress force to avoid decompression of the extreme ‘tension’ fiber of the girder. Thus girders that are sufficiently damaged to result in decompression (particularly under the effects of dead load only as described above) should be provided with an active (PT) repair capable of restoring some degree of prestress force in addition to restoring the girder ultimate capacity. As such, the decompression load, or any other performance point defined by section stress, can be used to identify appropriate repair techniques (PT) and/or the limits of others (non PT).

2.6.2 Hybrid Repairs with Strand Splices

Limitations associated with each repair technique clearly point to the adoption of hybrid repair approaches in order to maximize the degree of damage that may be repaired.

Strand splices are internal applications and therefore may be used with most any external application (except, perhaps NSM where interference between the strand chunks and NSM slots is likely). Strand splices are reported to have the capacity to restore *in situ* prestress to all but 0.6 in. strands. Typically, *in situ* levels of long term prestress will be on the order of $0.60f_{pu}$. As reported in Section 2.3.2.4.1, strand splices cannot be relied upon to develop the ultimate capacity of the strands. Thus when considering the ultimate capacity of a section, the effectiveness of strand splicing should be reduced such that the equivalent number of strands considered in calculating the girder capacity is $0.85n_{spliced}$. Using this approach, as shown in Figure 37, the damage that must be repaired using external techniques is reduced. The use of strand splices may effectively extend the utility of other repair techniques. Additionally, since strand splices are active, they may be used to restore a degree of prestressing, avoiding decompression (Section 2.6.1.2) and permitting passive external repair techniques to be utilized.

Hybrid combinations of techniques other than strand splices will generally be inefficient since the repair stiffnesses and capacities differ resulting in multiple systems behaving in series rather than in parallel.

CHAPTER 3 RECOMMENDATIONS AND CONCLUSIONS

3.1 Guide to Recommended Practice for the Repair of Impact-Damaged Prestressed Concrete Bridge Girders

The primary deliverable of this project is the *Guide to Recommended Practice for the Repair of Impact-Damaged Prestressed Concrete Bridge Girders*. The *Guide* is provided as Appendix A. The *Guide* summarizes the findings presented in Chapters 1 and 2 of this report and utilize this report as a ‘commentary’ by reference to report sections using square brackets.

The *Guide* serves to update the 1985 *NCHRP Report 280: Guidelines for Evaluation and Repair of Prestressed Concrete Bridge Members*. This report remains a primary reference for this topic. Material repeated from *NCHRP 280* is duly cited.

3.2 Gaps in Existing Knowledge and Need for Further Research

Through the conduct of this project a number of gaps in the knowledge base have been identified; these include:

1. Although FRP-based repairs are becoming well established, there is a need for demonstration projects to both verify design assumptions and to develop a database of successful projects from which the bridge engineering community can learn and gain confidence in these still relatively novel systems. EB-CFRP systems are well established. PT-CFRP systems, on the other hand, hold great promise but have only been broadly demonstrated in Europe (and to a small extent Asia). Focus on demonstration projects should be aimed at bPT-CFRP systems.
2. Although not yet practical for deployment, P-CFRP systems have some advantages if appropriate hardware may be developed for their large scale application. Limited research in this regard has been conducted and more is warranted.
3. Self-stressing prestressed CFRP systems have also been proposed. These would garner the benefits of a bPT-CFRP system with the simpler installation effort of an EB-CFRP system (Harries 2010).
4. Studies of the efficacy of hybrid repair approaches should be conducted. The assumption that transient loads are shared between components in a hybrid system (existing beam and repair methods) at service levels needs to be validated.
5. With the use of higher strength concrete, 0.6 in. and even 0.7 in. strands are becoming more common. Methods of effectively splicing these larger strands require investigation. It is proposed that the use of different strand splice materials and geometries can make this approach more practical for greater degrees of damage to larger strand diameters.
6. Impact damage near girder ends or affecting strand harping locations need to be studied. Although not addressing impact damage *per se*, the anticipated outcomes of NCHRP 12-91 will provide some guidance related to limits of the loss of prestressing force near girder ends. The results of NCHRP 12-91 should inform updates to the present *Guide* in the regard.
7. Significant research is required in the realm of inspection and damage assessment. Automated structural health monitoring (SHM) systems hold great promise but few have reached the demonstration phase in bridge structures.
8. Portable or rapidly deployable SHM that may supplement a scheduled or impact-triggered bridge inspection (usually requiring a vehicle of known load to actuate the monitored bridge) are also a stage appropriate for demonstration projects to be implemented.

REFERENCES

- Adimi, R., Rahman, H., Benmokrane, B. and Kobayashi, K. 1998. "Effect of Temperature and Loading Frequency on Fatigue Life of a CFRP Bar in Concrete", *Proceedings of the 2nd International Conference on Composites in Infrastructure*, Tucson, Vol. 2 pp 203-210.
- Agarwal, B.D. and Broutman, L.J. 1990. *Analysis and Performance of Fiber Composites*, John Wiley and Sons.
- Ahlborn, T.M., Gilbertson, C.G., Aktan, H. and Attanayake, U. 2005 *Condition Assessment and Methods of Abatement of Prestressed Concrete Adjacent Box Beam Deterioration: Phase I*, Michigan Department of Transportation Report RC-1470. 197 pp.
- Aidoo, J., Harries, K.A. and Petrou, M.F. 2006. "Full-scale Experimental Investigation of Repair of Reinforced Concrete Interstate Bridge using CFRP Materials", *ASCE Journal of Bridge Engineering*. Vol. 11, No. 3, pp 350-358.
- Aidoo, J., Harries, K.A. and Petrou, M.F. 2004. "Fatigue Behavior of CFRP Strengthened Reinforced Concrete Bridge Girders", *ASCE Journal of Composites in Construction*, Vol. 7, No. 6, pp 501-518.
- Alaska Department of Transportation. 2007. *Prestressed Girder Repair Procedures*, August 2007, Alaska Department of Transportation, Juneau, 9 pp.
- Alberta Infrastructure and Transportation Department. 2005. *Repair Manual for Concrete Bridge Elements: Version 2.0*, Revised October 2005, Alberta Infrastructure and Transportation Department, Alberta. 27 pp.
- Ali, M. G. and Maddocks, A. R. 2003. "Evaluation of Corrosion of Prestressing Steel in Concrete Using Non-destructive Techniques", *Corrosion and Materials*, Vol. 28, No. 5-6, pp 42-48.
- American Association of State Highway and Transportation Officials (AASHTO). 2011. *Manual for Bridge Element Inspection*, 1st Edition, Washington, D.C.
- American Association of State Highway and Transportation Officials (AASHTO). 2011. *Manual for Bridge Evaluation*, 2nd Edition, Washington, D.C.
- American Association of State Highway and Transportation Officials (AASHTO). 2010. *LRFD Bridge Design Specifications*, 4th Edition and Interims, Washington, D.C.
- American Concrete Institute (ACI) and International Concrete Repair Institute (ICRI). 2008. *Concrete Repair Manual*, 3rd Edition, 2077 pp.
- American Concrete Institute (ACI) Committee 440. 2008. *ACI 440.2R-08 Guide for the Design and Construction of Externally Bonded FRP Systems for Strengthening Concrete Structures*, 76 pp.
- American Concrete Institute (ACI) Committee 440. 2007. *ACI 440R-07 Report on Fiber-Reinforced Polymer (FRP) Reinforcement for Concrete Structures*.
- American Concrete Institute (ACI) Committee 440. 2002. *ACI 440.2R-02 Guide for the Design and Construction of Externally Bonded FRP Systems for Strengthening Concrete Structures*.
- American Concrete Institute (ACI) Committee 318. 2011. *ACI 318-11 Building Code Requirements for Structural Concrete*, 503 pp.
- American Marietta Company. 1960. *L.R. 187 Bridge at STA. 316+18.25 Drawings* (4 sheets). Approved by PADOH, October 26, 1960.
- Anstice, P.D. and Beaumont, P.W.R. 1982. "Hygrothermal ageing of fibrous composites", *Proceedings of the 4th International Conference on Composite Materials*, October 1982, Tokyo, pp 1001-1107.
- Aram, M-R., Czaderki, C. and Motavalli, M. 2008. "Effects of Gradually Anchored Prestressed CFRP Strips Bonded on Prestressed Concrete Beams", *ASCE Journal of Composites for Construction*, Vol. 12, No. 1, pp 25-34.
- ASTM International. 2008. *E837-08 Standard Test Method for Determining Residual Stresses by the Hole-Drilling Strain-Gage Method*. West Conshohocken, PA.

- ASTM International. 1999. *C876-91 Standard Test Method for Half-Cell Potentials of Uncoated Reinforcing Steel in Concrete*. (withdrawn 2008). West Conshohocken, PA.
- Barnes, R.A. and Mays, G.C. 2001. "The effect of traffic vibration on adhesive curing during installation of bonded external reinforcement." *Proceedings of the Institution of Civil Engineers - Structures & Buildings*, Vol. 146, No. 4, pp 403-410.
- Barnes, R.A. and Mays, G.C. 1999. "Fatigue Performance of Concrete Beams Strengthened with CFRP Plates", *ASCE Journal of Composites for Construction*, Vol. 3, No. 2, pp 63-72.
- Bennett, J.E. and Schue, T.J. 1998. "Cathodic Protection Field Trials on Prestressed Concrete Components", *Report No. FHWA-RD-97-153*, ELTECH Research Corporation, Fairport Harbor, OH.
- Boller, K.H. 1964. "Fatigue Characteristics of RP Laminates Subject to Axial Loading", *Modern Plastics*, Vol. 41, No. 145, pp 235-244.
- Broomfield, J. P. 1994. "Corrosion Rate Measurements in Reinforced Concrete Structures by a Linear Polarization Device", *ACI Special Publication 151 Concrete Bridges in Aggressive Environments*, pp 163-182.
- Broomfield, J.P. and Tinnea, J.S. 1992. "Cathodic Protection of Reinforced Concrete Bridge Components", *Report No. SHRP-C/UWP-92-618*, Strategic Highway Research Program, National Research Council, Washington, D.C.
- Cadei, J.M.C., Stratford, T.J., Hollaway, L.C. and Duckett, W.G. 2004. "Strengthening Metallic Structures Using Externally Bonded Fibre-Reinforced Polymers", *CIRIA Pub. No. C595*. 233 pp.
- Canadian Standards Association (CSA). 2007. *CAN/CSA S806-02(R2007) Design and Construction of Building Components with Fibre-Reinforced Polymers*, 177 pp.
- Canadian Standards Association (CSA). 2006. *CAN/CSA S6-06 Canadian Highway Bridge Design Code*, 800 pp.
- Casadei, P., Galati, N., Boschetto, G., Tan, K.Y., Nanni, A. and Galeki, G. 2006. "Strengthening of Impacted Prestressed Concrete Bridge I-Girder Using Prestressed Near Surface Mounted C-FRP Bars", *Proceedings of the 2nd International Congress*, Federation Internationale du Beton, Naples, Italy.
- Civjan, S.A., Jirsa, J.O., Carrasquillo, R.L. and Fowler, D.W. 1998. "Instrument to Evaluate Remaining Prestress in Damaged Prestressed Concrete Bridge Girders", *PCI Journal*, Vol. 43, No. 2, pp 62-71.
- Collins, M.P. and Mitchell, D. 1997. *Prestressed Concrete Structures*, Response Publications, 766 pp.
- Comite Euro-International du Beton (CEB). 1989. *CEB Bulletin 192 Diagnosis and Assessment of Concrete Structures - State-of-Art Report*.
- Concrete Society Committee (CSC). 2004. "Design Guidance for Strengthening Concrete Structures Using Fibre Composite Materials", *Technical Report No. 55*", 102 pp.
- Consiglio Nazionale delle Ricerche (CNR). 2004. *CNR-DT200/204 Guidelines for Design, Execution and Control of Strengthening Interventions by Means of Fibre-reinforced Composites*, 154 pp.
- Cromwell, J.R., Harries, K.A. and Shahrooz, B.M. 2011 "Environmental Durability of Externally Bonded FRP Materials Intended for Repair of Concrete Structures", *Journal of Construction and Building Materials*, Vol. 25, pp 2528-2539.
- Curtis, K., Huber, D., and Øyen, P.E. 2002. "Use of Fiber Reinforced Polymer Composite for Strengthening of Reinforced Concrete Structures," *REU Final Report*, University of Cincinnati, Cincinnati, Ohio.
- Daly, A.F. and Witarnawan, W. 1997. "Strengthening of bridges using external post-tensioning", *Transportation Research Laboratory Report No. PA3307/97*. Berks, United Kingdom.
- Davis, J.W., McCarthy, J.A. and Schurb, J.N. 1964. "Fatigue Resistance of Reinforced Plastics", *Materials in Design Engineering*. pp 87-91.

- De Wit, M. 2004. "The Use of Acoustic Monitoring to Manage Concrete Structures". *Proceedings of the first workshop of COST 534 on NDT Assessment and New Systems in Prestressed Concrete Structures*. Zurich, Switzerland.
- Di Ludovico, M., Arena, W., Prota, A., Manni, O. and Manfredi, G. 2007. "Impacted PC Girder: Experimental Behavior and Design of FRP Strengthening", *8th International Symposium on Fiber Reinforced Polymer Reinforcement for Concrete Structures (FRPRCS-8)*, University of Patras, Patras, Greece.
- El-Hacha, R. and Elbadry, M. 2006. "Strengthening Concrete Beams with Externally Prestressed Carbon Fiber Composite Cables: Experimental Investigation", *PTI Journal*, Vol. 4, No. 2, pp 53-70.
- El-Hacha, R., Wight, R.G. and Green, M.F. 2003, "Innovative System for Prestressing Fiber-Reinforced Polymer Sheets", *ACI Structural Journal*, ACI, Vol. 100, No. 3, pp 305-313.
- Enchayan, R. 2010. "Repair of Damaged Prestressed Concrete Girder", Presentation at the AASHTO Midwest Bridge Preservation Conference, October 13, 2010, Detroit, MI.
- Feldman, L.R., Jirsa, J.O., Fowler, D.W. and Carrasquillo, R.L. 1996. "Current Practice in the Repair of Prestressed Bridge Girders", *Report No. FHWA/TX-96/1370-1*, The University of Texas at Austin, TX. 69 pp.
- Galal, K. and Mofidi, A. 2009. "Strengthening RC Beams in Flexure Using New Hybrid FRP Sheet/Ductile Anchor System", *ASCE Journal of Composites for Construction*, Vol. 13, No. 3, pp 217-225.
- Grabb-it. 2008. *Cable Splice Product Information Sheet*, Prestress Supply, Inc.
- Green P.S., Boyd, A.J., Lammert, K. and Ansley, M. 2004. "CFRP Repair of Impact-Damaged Bridge Girders Volume 1 – Structural Evaluation of Impact Damaged Prestressed Concrete I Girders Repaired with FRP Materials", *UF Project No. 4504-922-12*, University of Florida, Gainesville, FL.
- Hadzor, T.J. 2011. *Acoustic Emission Testing of Repaired Prestressed Concrete Bridge Girders*. MS Thesis, Auburn University.
- Hariri, K. and Budelmann, H. 2001. "Assessment of the Load-Capacity of Prestressed Concrete Structures by Means of Innovative Measurement Techniques", *Proceedings of the 3rd International Workshop on Structural Health Monitoring*, Stanford University, pp 474-483.
- Harries, K.A. 2012. *Proof of Concept of the OSMOS Solution for Bridge Monitoring - Full-Scale Girder Load Test*, report submitted to STRAEN Inc. January 2012.
- Harries, K.A. 2010. *United States Provisional Patent SN61/405,006 Electroactive Prestressed FRP Systems for Structural Retrofit, Application*, filed 10/20/2010.
- Harries, K.A. 2009. "Structural Testing of Prestressed Concrete Girders from the Lake View Drive Bridge", *ASCE Journal of Bridge Engineering*, Vol. 149, No. 2, pp 78-92.
- Harries, K.A. 2006. "Full-scale Testing Program on De-commissioned Girders from the Lake View Drive Bridge", *Pennsylvania Department of Transportation Report FHWA-PA-2006-008-EMG001*, 158 pp.
- Harries, K.A. 2001. *In Situ Tests on FRP Retrofit Application: I585 Northbound Bridge over SC85 Southbound in Spartanburg SC*, report to South Carolina Department of Transportation, October 2001. 5 pp.
- Harries, K.A., Kasan, J.L. and Aktas, C. 2009. "Repair Methods for Prestressed Concrete Bridges", *Report FHWA-PA-2009-008-PIT 006*, 169 pp.
- Harries, K.A. and Shahrooz, B.M. 2011. "Alternative Environmental 'Knockdown' Factors (CE) Derived from Extensive Experimental Data", *Proceedings of the Fourth International Conference on Durability & Sustainability of Fiber Reinforced Polymer (FRP) Composites for Construction (CDCC 2011) Quebec City, July 2011*.

- Harries, K.A., Zorn, A., Aidoo, J. and Quattlebaum, J., 2006. "Deterioration of FRP-to-Concrete Bond Under Fatigue Loading". *Advances in Structural Engineering - Special Issue on Bond Behavior of FRP in Structures*, Vol. 9, No. 6, pp 779-789.
- Heffernan, J. P. 1997. "Fatigue Behavior of Reinforced Concrete Beams Strengthened with CFRP Laminates", *Ph.D. Dissertation*, Department of Civil Engineering, Royal Military College of Canada, Kingston, Ontario, May 1995, 157 pp.
- Herman, T. 2005. "A Tale of Two Bridges", *Bridges*, Nov/Dec. 2005, pp 14-16.
- Honorio, U., Wight, R.G. and Erki, M.A. 2002. "CFRP Sheet for Strengthening Full-Scale Severely Damaged Concrete Structures", *4th Structural Specialty Conference of the Canadian Society for Civil Engineers*, Montreal, Quebec, Canada.
- International federation for Structural Concrete (fib). 2001. *Externally Bonded FRP Reinforcement for RC Structures*, 130 pp.
- Japan Society of Civil Engineers (JSCE). 1998. "Recommendations for Upgrading of Concrete Structures with Use of Continuous Fiber Sheets", *JSCE-Concrete Engineering Series 41*, 88pp.
- Kasan, J. 2012. "On The Repair of Impact-Damaged Prestressed Concrete Bridge Girders", *PhD Dissertation*, University of Pittsburgh, April 2012.
- Kasan, J. and Harries, K.A. 2012a (in press), "Analysis of Eccentrically Loaded Adjacent Box Girders", *ASCE Journal of Bridge Engineering*. Vol. 17.
- Kasan, J.L. and Harries, K.A. 2012b. "Assessment of Damaged Prestressed Adjacent Box Girder Bridges: A Case Study", *Proceedings of 14th International Conference on Structural Faults and Repair*, Edinburgh, June 2012.
- Kasan, J. and Harries, K.A. 2011. "Redevelopment of Prestressing Force in Severed Prestressed Strands", *ASCE Journal of Bridge Engineering*, Vol. 16, No. 3, pp 431-437.
- Karbhari, V. M.; Chin, J. W.; Hunston, D.; Benmokrane, B.; Juska, T.; Morgan, R.; Lesko, J. J.; Sorathia, U.; and Reynaud, D., 2003, "Durability Gap Analysis for Fiber- Reinforced Composites in Civil Infrastructure", *ASCE Journal of Composites for Construction*, Vol. 7, No. 3, pp. 238-247.
- Karbhari, V. M., and Engineer, M., 1996, "Investigation of Bond Between Concrete and Composites: Use of a Peeling Test", *Journal of Reinforced Plastics and Composites*, Vol. 15, pp. 208-227.
- Kim, S.D., In, C.W., Cronin, K., Sohn, H, and Harries, K.A. 2006. "Application of Outlier Analysis for Baseline-Free Damage Diagnosis", *Proceedings Smart Structures and Materials and NDE and Health Monitoring and Diagnostics*, San Diego, March 2006.
- Kim, Y.J., Wight, R.G. and Green, M.F. 2008a. "Flexural Strengthening of RC Beams with Prestressed CFRP Sheets: Development of Nonmetallic Anchor Systems", *ASCE Journal of Composites for Construction*, Vol. 12, No. 1, pp 35-43.
- Kim, Y.J., Wight, R.G. and Green, M.F. 2008b. "Flexural Strengthening of RC Beams with Prestressed CFRP Sheets: Using Nonmetallic Anchor Systems", *ASCE Journal of Composites for Construction*, Vol. 12, No. 1, pp 44-52.
- Kim, Y.J., Green, M.F. and Fallis, G.J. 2008c. "Repair of Bridge Girder Damaged by Impact Loads with Prestressed CFRP Sheets", *ASCE Journal of Bridge Engineering*, Vol. 13, No. 1, pp 15-23.
- Klaiber, F.W., Wipf, T.J., and Kash, E.J. 2004. "Effective Structural Concrete Repair – Volume 2 of 3: Use of FRP to Prevent Chloride Penetration in Bridge Columns", *Iowa DOT Project TR-428*, Iowa Department of Transportation, Ames, IA.
- Klaiber, F.W, Wipf, T.J. and Kempers, B.J. 2003. "Repair of Damaged Prestressed Concrete Bridges using CFRP", *Mid-Continent Transportation Symposium Proceedings*, Center for Transportation Research and Education, Ames, IA.

- Kotynia, R., Walendziak, R. Stoecklin, I and Meler, U. 2011. "RC Slabs Strengthened with Prestressed and Gradually Anchored CFRP Strips under Monotonic and Cyclic Loading", *ASCE Journal of Composites for Construction*, Vol. 15, No. 2, pp 168-180.
- Labia, Y., Saiidi, M. & Douglas. 1996. "Evaluation and Repair of Full-Scale Prestressed Concrete Box Girders", *Report No. CCEER-96-2*, University of Nevada, Reno, NV.
- Law Engineering. 1990. "Load Testing of Anchoring Assemblies (Grabb-it Cable Splice), Job No. 1460014400 Lab Number: E0429", *Testing Report*, March 20, 1990.
- Macdonald, M.D. 1981. "Strength of Bonded Shear Joints Subjected to Movement During Cure", *International Journal of Cement Composites and Lightweight Concrete*, Vol. 3, No. 4, pp 267-272.
- Masoud, S., Soudki, K. and Topper, T. 2001. "CFRP-Strengthened and Corroded RC Beams under Monotonic and Fatigue Loads", *ASCE Journal of Composites for Construction*, Vol. 5 No. 4, pp 228-236.
- Mehta, P. K. and Monteiro, P. J. M. 2006. *Concrete, Microstructure, Properties, and Materials*, McGraw-Hill.
- Meier, H., Clenin, R. and Basler, M. 2003. "Bridge Strengthening with Advanced Composite Systems", *ACI SP 215 Field Applications of FRP Reinforcement: Case Studies*, S. Rizkalla and A. Nanni, editors.
- Meier, U., Deuring, M., Meier, H. and Schwegler, G. 1993. "Strengthening of Structures with Advanced Composites", *Alternate Materials for the Reinforcement and Prestressing of Concrete*, J.L. Clarke, editor, Blackie Academic and Professional, Glasgow.
- Miller R.A. and Parekh K. 1994. "Destructive Testing of a Deteriorated Prestressed Box Bridge Beam", *Transportation Research Record*, 1460.
- Miller, A., Rosenboom, O. and Rizkalla, S. 2006. "Fatigue Behavior of Impact Damaged Prestressed Concrete Bridge Girder Repaired with CFRP Sheets", *Proceedings of the 7th International Conference on Short and Medium Span Bridges*, Montreal, Quebec, Canada.
- Moy, S.S.J. 2007. "CFRP Reinforcement of Steel Beams Adhesive Cure Under Cyclic Load", *Proceedings of the First Asia-Pacific Conference on FRP in Structures (APFIS 2007)*. Hong Kong, pp 1019-1024.
- Moy, S.S.J. 2000. "Early age curing under cyclic loading – an investigation into stiffness development in carbon fibre reinforced steel beams", *LINK project, Carbon Fibre Composites for Structural Upgrade and Life Extension, Validation and Design Guidance. Project Report*. University of Southampton.
- Naito, C., Jones, L. and Hodgson, I. 2011. "Development of Flexural Strength Rating Procedures for Adjacent Prestressed Concrete Box Girder Bridges", *ASCE Journal of Bridge Engineering*, Vol. 16, No. 5, pp 662-670.
- Naito, C., Sause, R., Hodgson, I., Pessiki, S. & Desai, C. 2006. "Forensic Evaluation of Prestressed Box Beams from the Lake View Drive over I-70 Bridge", *ATLSS Report No. 06-13*, Lehigh University, Bethlehem, PA. 62 pp.
- National Cooperative Highway Research Program (NCHRP). 2008. "Bonded Repair and Retrofit of Concrete Structures Using FRP Composites: Recommended Construction Specifications and Process Control Manual", *NCHRP Report 514*, 102 pp.
- National Cooperative Highway Research Program (NCHRP). 2008. "Recommended Construction Specifications and Process Control Manual for Repair and Retrofit of Concrete Using Bonded FRP Composites", *NCHRP Report 609*, 68 pp.
- Neville, A.M. 1975. *Properties of Concrete*, 2nd edition, Pitman.
- Nordin, H. and Taljsten, B. 2006. "Concrete Beams Strengthened with Prestressed Near Surface Mounted CFRP", *ASCE Journal of Composites for Construction*, Vol. 10, No. 1, pp 60-68.

- Nordin, H., Taljsten, B., and Carolin, A. 2002. "CFRP Near Surface Mounted Reinforcement (NSMR) For Pre-Stressing Concrete Beams", *Proceedings of Third International Conference on Composites in Infrastructure*, San Francisco, June 2002.
- O'Neill, A., Harries, K.A. and Minnaugh, P. 2007. "Fatigue Behavior of Adhesive Systems used for Externally-bonded FRP Applications", *Proceedings of the Third International Conference on Durability & Field Applications of Fiber Reinforced Polymer (FRP) Composites for Construction (CDCC 2007)* Quebec City, May 2007.
- Okanla, E. I., Gaydecki, P. A., Manaf, S., Burdekin, F. M. 1997. "Detecting Faults in Posttensioning Ducts by Electrical Time-Domain Reflectometry", *ASCE Journal of Structural Engineering*, Vol. 123, No. 5, pp 567-574.
- Olson, S.A., French, C.W. & Leon, R.T. 1992. "Reusability and Impact Damage Repair of Twenty-Year-Old AASHTO Type III Girders", *Minnesota Department of Transportation Research Report No. 93-04*, University of Minnesota, Minneapolis, MN.
- Pakrashi, V., Kelly, J., Harkin, J., Farrell, A., Nanukuttan, S. 2010. "Emergency Rehabilitation of Brownsbarn Bridge", *BCRI2010 Joint Symposium: Bridge and Infrastructure Research in Ireland (BRI) and Concrete Research in Ireland (CRI)*. Cork, Ireland.
- Papakonstantinou, C.G., Petrou M.F. and Harries, K.A. 2001. "Fatigue of Reinforced Concrete Beams Strengthened with GFRP Sheets", *ASCE Journal of Composites for Construction*, Vol. 5, No. 4, pp 246-253.
- Pennsylvania Department of Transportation (PennDOT). (2010). "Bridge Safety Inspection Manual", 2nd edition, *Publication 238*, Revised March 2010, Pennsylvania Department of Transportation, Harrisburg, PA. 482 pp.
- Petrou, M.F., Harries, K.A., Gadala-Maria, F. and Kolli, V.G., 2000. A Unique Experimental Method for Monitoring Aggregate Settlement in Concrete. *Cement and Concrete Research*, Vol. 30, No. 5, pp 809-816.
- Porter, M. and Harries, K.A., 2007. "Forum: Future Directions for Research in FRP Composites in Concrete Construction", *ASCE Journal of Composites for Construction*, Vol. 11, No. 3, pp 252-257.
- Precast/Prestressed Concrete Institute (PCI). 2006. "Manual for the Evaluation and Repair of Precast, Prestressed Concrete Bridge Products", *Report No. PCI MNL-137-06*. Chicago, IL. 66 pp.
- Precast/Prestressed Concrete Institute (PCI). 2003. "Bridge Design Manual", *Report No. PCI MNL-133-97*. Chicago, IL.
- Preston, H.K., Osborn, A. E. N. & Roach, C. E. 1987. "Restoration of Strength in Adjacent Prestressed Concrete Box Beams", *Report No. FHWA-PA-86-044+84-21*, Pennsylvania Department of Transportation, Harrisburg, PA.
- Prestress Supply, Inc. (PSI) 2011. *Grabb-it Cable Splice Installation Instructions*. Prestress Supply, Inc. <<http://www.prestressupply.com/LinkClick.aspx?fileticket=Sx6pxCOxgAc%3d&tabid=147>>, (accessed February 9, 2012).
- Quattlebaum, J., Harries, K.A. and Petrou, M.F. 2005. "Comparison of Three CFRP Flexural Retrofit Systems Under Monotonic and Fatigue Loads", *ASCE Journal of Bridge Engineering*. Vol. 10, No. 6, pp 731-740.
- Rahman, A. H., and Kingsley, C. Y. 1996. "Fatigue Behavior of a Fiber-Reinforced-Plastic Grid as Reinforcement for Concrete", *Proceedings of the First International Conference on Composites in Infrastructure*, Tucson, pp 427-439.
- Ramadan, S., Gaillet, L., Tessier, C., Idrissi, H. 2007. "Detection of Stress Corrosion Cracking of High-Strength Steel Used in Prestressed Concrete Structures by Acoustic Emission Technique", *Applied Surface Science*, Vol. 254, No. 8, pp 2255-2261.

- Rao, C and Frantz, G.C. 1996. "Fatigue Tests of 27-Year-Old Prestressed Concrete Bridge Box Beams", *PCI Journal*, Vol. 41, No. 5, pp 74-83.
- Reed, M.W., Barnes, R.W., Schindler, A.K. and Lee, H-W 2005. "Fiber Reinforced Polymer Strengthening of Concrete Bridges that Remain Open to Traffic", *ACI Structural Journal*, Vol. 102, No. 6, pp 823-831.
- Reed, C.E., Peterman, R.J., Rasheed, H. and Meggers, D. 2007. "Adhesive Applications Used During Repair and Strengthening of 30-Year-Old Prestressed Concrete Girders", *Transportation Research Record* 1827/2003, pp 36-43.
- Reed C.E. and Peterman, R.J. 2005. "Evaluating FRP Repair Method for Cracked Prestressed Concrete Bridge Members Subjected to Repeated Loadings Phase 1", *Report No. KTRAN: KSU-01-2*, Kansas Department of Transportation, KS.
- Reed, C.E. and Peterman, R.J. 2004. "Evaluation of Prestressed Concrete Girders Strengthened with Carbon Fiber reinforced Polymer Sheets", *ASCE Journal of Bridge Engineering*, Vol. 9, No. 2, pp 60-68.
- Rosenboom, O.A., Miller, A.D. and Rizkalla, S. (2011). "Repair of Impact-Damaged Prestressed Concrete Bridge Girders Using CFRP Materials", *ASCE Journal of Bridge Engineering*, publication pending.
- S&P FRP Systems. 2011. "FRP systems: structural strengthening", www.reinforcement.ch (accessed 10/6/11).
- Saadatmanesh, H., and Tannous, F. E. 1999. "Relaxation, Creep, and Fatigue Behavior of Carbon Fiber-Reinforced Plastic Tendons", *ACI Materials Journal*, Vol. 96, No. 2, pp 143-153.
- Saiedi, R., Fam, A. and Green, M.F. 2011. "Behavior of CFRP=Preprestressed Concrete Beams under High-Cycle Fatigue at Low Temperature", *ASCE Journal of Composites for Construction*, Vol. 15, No. 4, pp 482-489.
- Scheel, H. and Hillemeier, B. 2003. "Location of Prestressing Steel Fractures in Concrete", *ASCE Journal of Materials in Civil Engineering*, Vol. 15, No. 3, pp 228-234.
- Schiebel, S., Parretti, R. and Nanni, A. 2001. "Repair and Strengthening of Impacted PC Girders on Bridge A4845 Jackson County, Missouri", *Report No. RDT01-017*, Missouri Department of Transportation, Jackson City, MO.
- Shahawy, M. and Beitelman, E. T. 1999. "Static and Fatigue Performance of RC Beams Strengthened with CFRP Laminates", *ASCE Journal of Structural Engineering*, Vol. 125, No. 6, pp 613-621.
- Shanafelt, G.O. & Horn, W.B. 1985. "Guidelines for Evaluation and Repair of Prestressed Concrete Bridge Members", *NCHRP Report 280*, Project No. 12-21(1), Transportation Research Board, Washington, D.C., 84 pp.
- Shanafelt, G.O. & Horn, W.B. 1980. "Damage Evaluation and Repair Methods for Prestressed Concrete Bridge Members", *NCHRP Report 226*, Project No. 12-21, Transportation Research Board, Washington, D.C., 66 pp.
- Sika. 2011. *Sika Carbodur Carbon Fiber Laminate for Structural Strengthening*, Sika Corporation, USA.
- Sika. 2010. *SikaWrap Hex 103C Carbon Fiber Fabric for Structural Strengthening*, Sika Corporation, USA.
- Sika. 2008a. *Case Study: Hopkin and Clinton Street Bridge Rehabilitation*, Sika Corporation, USA.
- Sika. 2008b. *Prestressing System for Structural Strengthening with Sika CarboDur CFRP Plates*, Sika Corporation, USA.
- Sohn, H., Kim, S.D. and Harries, K.A. 2008. "Reference-Free Damage Classification based on Cluster Analysis", *Journal of Computer Aided Civil and Infrastructure Engineering*, Vol. 23, pp 324-338.

- Suh, K., Mullins, G., Sen, R., Winters, D. 2007. "Effectiveness of Fiber-Reinforced Polymer in Reducing Corrosion in Marine Environment", *ACI Structural Journal*, Vol. 104, No. 1, pp 76-83.
- Tabatabai, H., Ghorbanpoor, A. and Turnquist-Naas, A. 2004. "Rehabilitation Techniques for Concrete Bridges", *Project No. 0092-01-06*, University of Wisconsin-Milwaukee, Milwaukee, WI.
- Taffe, A., Hillemeier, B. and Walther, A. 2010. "Condition Assessment of 45-year old prestressed concrete bridge using NDT and verification of the results", www.ndt.net/search/docs.php3?showForm=off&id=9952. (accessed 10/2/11).
- Tanimoto, T. and Anijima, S. 1975. "Progressive Nature of Fatigue Damage of Glass Reinforced Plastics", *Journal of Composite Materials*, Vol. 9, No. 4, pp 380-390.
- Toenjes, C.A. 2005. "Repair of Prestressed Concrete Girders with Carbon Fiber Reinforced Polymer Wrap", Presentation at the International Bridge, Tunnel and Turnpike Association (IBTTA) Facilities Management Workshop, May 14-18, 2005, Toronto, Ontario. www.ibtta.org/files/PDFs/Toenjes_Chris.pdf. (accessed 10/6/11).
- TRC Engineers, Inc. 2002. *XTRACT: A Tool for Axial Force - Ultimate Curvature Interactions*. TRC, Rancho Cordova, CA.
- Tumialan, J.G., Huang, P., Nanni, A. and Jones, M. 2001. "Strengthening of an Impacted PC Girder on Bridge A10062 St Louis County, Missouri", *Report No. RDT01-013*, University of Missouri-Rolla, Rolla, MO.
- Turker, H. T. 2003. "Theoretical Development of the Core-Drilling Method for Nondestructive Evaluation of Stresses in Concrete Structures", *Ph.D. Dissertation*, Lehigh University.
- Vector Corrosion Technologies (Vector). 2011. *Galvasheild XP Products*. Vector Corrosion Technologies. <<http://www.vector-corrosion.com/systemsservices/galvanic/galvashield%C2%AE-xp-anodes/>>, (accessed April 5, 2012).
- Walther, A. and Hillemeier, B. 2008. "Fast NDT Localization of Prestressing Steel Fractures in P-T Concrete Bridges", *Proceedings of the 12th International Conference and Exhibition on Structural Faults and Repair*, Edinburgh, Scotland.
- Wan, B., Petrou, M.F. and Harries, K.A., 2006. "Effect of the Presence of Water on the Durability of Bond Between CFRP and Concrete", *Journal of Reinforced Plastics and Composites*, Vol. 25, No. 8, pp 875-890.
- Wan, B., Sutton, M., Petrou, M.F., Harries, K.A., and Li, N. 2004. "Investigation of Bond between FRP and Concrete Undergoing Global Mixed Mode I/II Loading", *ASCE Journal of Engineering Mechanics*, Vol. 130, No. 12, pp 1467-1475.
- Wang, W., Dai, J-G. and Harries, K.A., 2012a (in press) "Performance evaluation of RC beams strengthened with an externally bonded FRP system under simulated vehicles loads", *ASCE Journal of Bridge Engineering*
- Wang, W., Dai, J-G., Harries, K.A. and Bao, Q-H. 2012b (in press) "Prestress Losses and Flexural Behavior of Reinforced Concrete Beams Strengthened with Post-tensioned CFRP Sheets", *ASCE Journal of Composites for Construction*
- Watanabe, T., Hashimoto, C. and Ohtsu, M. 2005. "NDT for Detecting Voids in Post-Tensioning Tendon by SIBIE", *Proceedings of the 11th International Conference on Fracture*, Turin, Italy.
- Wight, R.G., Green, M.F., and Erki, M-A. 2001. "Prestressed FRP Sheets for Post-strengthening Reinforced Concrete Beams", *ASCE Journal of Composites for Construction*, Vol. 5, No. 4, pp 214-220.
- Wipf, T.J., Klaiber, F.W., Rhodes, J.D. and Kempers, B.J. 2004. "Effective Structural Concrete Repair – Volume 1 of 3: Repair of Impact Damaged Prestressed Concrete Beams with CFRP", *Iowa DOT Project TR-428*, Iowa Department of Transportation, Ames, IA.

- Yang, D. Merrill, B.D. and Bradberry, T.E. 2011. "Texas' use of CFRP repair to concrete bridges", *Recent Advances in Maintenance and Repair of Concrete Bridges: ACI SP-277*, Y. J. Kim, editor 39-48.
- Yang, M., Qiao, P., McLean, D.I. and Khaleghi, B. 2010. "Effect of Intermediate Diaphragms to Prestressed Concrete Bridge Girders in Over-height Truck Impact", *PCI Journal*, Winter 2010, pp 58-78.
- Yu, P., Silva, P.F. and Nanni, A. 2008a. "Description of a Mechanical Device for Prestressing Carbon Fiber-Reinforced Polymer Sheets-Part I", *ACI Structural Journal*, Vol. 105, No. 1, pp 3-10.
- Yu, P., Silva, P.F. and Nanni, A. 2008b. "Flexural Strength of Reinforced Concrete Beams Strengthened with Prestressed Carbon Fiber-Reinforced Polymer Sheets-Part II", *ACI Structural Journal*, Vol. 105, No. 1, pp 11-19.
- Zein, A., Gassman, S.L. and Harries, K.A. 2008. "Relationship Between Impact-Echo Response and Structural Behavior of Retrofitted Concrete Girders During Loading", *Research in Nondestructive Evaluation*. Vol. 66, No. 11, pp 1173-1181.
- Zobel, R.S. and Jirsa, J. O. 1998. "Performance of Strand Splice Repairs in Prestressed Concrete Bridges", *PCI Journal*, Vol. 43, No. 6, pp 72-84.
- Zobel, R.S. , Jirsa, J.O., Fowler, D.W. and Carrasquillo, R.L. 1996. "Evaluation and Repair of Impact-Damaged Prestressed Concrete Bridge Girders", *Report No. FHWA/TX-96/1370-3F*, The University of Texas at Austin, Austin, TX.

NOTATION

A_p	area of prestressing strand
b	width of concrete soffit
b_f	width of CFRP provided
b_{fl}	width of individual CFRP strip
c	depth of NSM slot
C	structural capacity
C_0	capacity of undamaged girder
C_D	capacity of damaged girder
C_E	environmental reduction factor (ACI 440-2R 2008)
C_R	capacity of repaired girder
d_b	prestressing strand or reinforcing bar nominal diameter
DC, DW, LL, P and IM	load effects (AASHTO <i>LRFD Bridge Design Specifications</i> (2010))
E_c	modulus of elasticity of concrete
E_f	modulus of elasticity of CFRP
E_p	modulus of elasticity of prestressing steel
E_s	modulus of elasticity of mild reinforcing steel
f_c'	compressive strength of concrete
f_{fi}	effective initial prestress of PT-CFRP
f_{fu}	ultimate tensile strength of CFRP
f_{pe}	long term effective prestress force in prestressing strand
f_{pi}	effective initial prestress of prestressing steel
f_{pu}	ultimate tensile strength of prestressing strand
f_u	ultimate tensile strength of mild reinforcing steel
H	overall depth of prestressed girder
L	length of girder
M_0	nominal moment capacity of undamaged section
M_D	nominal moment capacity of damaged section
M_R	nominal moment capacity of repaired section
n	number of plies of CFRP
n_{max}	maximum number of severed prestressing strands that can be replaced by CFRP based on its relative contribution to moment capacity
n_{max-PT}	equivalent number of strands whose prestress force can be replaced with PT-CFRP
$n_{spliced}$	number of prestressing strands spliced in a member
RF	rating factor
RF_0	normalized rating factor (Eq. 2) of undamaged girder
RF_D	normalized rating factor (Eq. 2) of damaged girder
RF_R	normalized rating factor (Eq. 2) of repaired girder
t_f	thickness of single CFRP ply or layer
αH	depth from compression resultant to location of CFRP on soffit
βH	depth from compression resultant to centroid of prestressing strands

$\gamma_{DC}, \gamma_{DW}, \gamma_P$ and γ_{LL}	LRFD load factors (Table 6A.4.2.2 of the <i>Evaluation Manual</i> (2011)).
ϵ_c'	concrete strain at f_c'
ϵ_{cF}	concrete failure strain (criteria) used in analysis
ϵ_{cmax}	ultimate concrete strain
ϵ_{cu}	concrete crushing strain
ϵ_{fd}	CFRP debonding strain
ϵ_{fF}	CFRP failure strain (criteria) used in analysis
ϵ_{fu}	ultimate tensile strain of CFRP
ϵ_{pF}	prestressing strand failure strain (criteria) used in analysis
ϵ_{pu}	ultimate tensile strain of prestressing strand
ϵ_{sF}	mild reinforcing steel failure strain (criteria) used in analysis
ϵ_{sp}	concrete spalling strain
ϵ_{su}	ultimate tensile strain of mild reinforcing steel
κ	effective prestress factor in CFRP ($0 \leq \kappa \leq 1$)
Ψ	strength reduction factor for FRP (ACI 440-2R 2008)

APPENDIX A - *Guide to Recommended Practice for the Repair of Impact-Damaged Prestressed Concrete Bridge Girders*

***GUIDE TO RECOMMENDED PRACTICE FOR THE REPAIR
OF IMPACT-DAMAGED PRESTRESSED
CONCRETE BRIDGE GIRDERS***

Prepared for the
National Cooperative Highway Research Program
Transportation Research Board
of
The National Academies

Kent A. Harries, Ph.D., F.ACI, P.Eng.
Jarret Kasan, Ph.D.
University of Pittsburgh, Pittsburgh PA

Richard Miller, Ph.D., F.PCI, P.E.
Ryan Brinkman
University of Cincinnati, Cincinnati OH

May 2012

ACKNOWLEDGEMENTS

This study was requested by the American Association of State Highway and Transportation Officials (AASHTO), and conducted as part of National Cooperative Highway Research Program (NCHRP) Project 20-07. The NCHRP is supported by annual voluntary contributions from the state Departments of Transportation. Project 20-07 is intended to fund quick response studies on behalf of the AASHTO Standing Committee on Highways. The report was prepared by Drs. Kent A. Harries and Jarret Kasan of the University of Pittsburgh and Dr. Richard Miller and Mr. Ryan Brinkman of the University of Cincinnati. The work was guided by a task group included Alexander K. Bardow (Massachusetts DOT), Issam Harik (University of Kentucky), Bruce V. Johnson (Oregon DOT), Bijan Khaleghi (Washington State DOT), William N. Nickas (Precast/Prestressed Concrete Institute), and Benjamin A. Graybeal (Federal Highway Administration). The project was managed by Waseem Dekelbab, NCHRP Senior Program Officer.

The authors wish to acknowledge the following for their direct contributions to the present work including providing many of the photographs presented:

Lou Ruzzi, PennDOT District 11

Tim Bradberry, TXDOT

Kelly Breazeale, TXDOT

Tim Keller, ODOT

Daniel Tobias, ILDOT

Sreenivas Alampalli, NYDOT

DISCLAIMER

The opinions and conclusions expressed or implied are those of the research agency that performed the research and are not necessarily those of the Transportation Research Board or its sponsoring agencies. This report has not been reviewed or accepted by the Transportation Research Board Executive Committee or the Governing Board of the National Research Council.

1 INTRODUCTION	5
1.1 Significance and Scope	5
1.2 Factors Affecting Impact Damage	5
1.2.1 Corrosion Damage Subsequent to Impact	6
1.2.2 Adjacent Strands	6
1.2.3 Strand ‘Redevelopment’	6
1.2.4 Unanticipated Composite Action	6
1.2.5 Lateral Deflections and Twist of Girders	7
1.2.6 Effect of Diaphragms on Impact Damage	7
2 INSPECTION OF IMPACT DAMAGED PRESTRESSED GIRDERS	7
3 ASSESSING (RATING) IMPACT-DAMAGED PRESTRESSED GIRDERS	8
3.1 Rating Impact Damaged and Subsequently Repaired Girders	8
3.1.1 Repair Objective	9
3.1.2 Residual Capacity and Strengthening Limits	9
3.2 Methods of Analysis	9
3.2.1 Non-composite Exterior Box Girders with Asymmetric Damage and Loading	9
3.3 Damage Classification of Prestressed Concrete Bridge Girders	10
3.3.1 ‘Repair or Replace’ Threshold	10
3.3.2 ‘Repair or Do Nothing’ Threshold	11
4 REPAIR OF PRESTRESSED CONCRETE BOX GIRDERS	11
5 REPAIR OF PRESTRESSED CONCRETE SINGLE-WEB GIRDERS	12
6 PRESTRESSED GIRDER REPAIR TECHNIQUES	12
6.1 Limitations of Repair Techniques Associated with Damaged Girder Geometry	12
6.1.1 Repair Applications During Live Loading	13
6.2 CFRP-Based Techniques	14
6.2.1 Material Selection	14
6.2.2 Environmental Durability	14
6.2.3 Fatigue	14
6.2.3.1 Fretting Associated with Fatigue Loads	15
6.2.4 Externally Bonded Non Post-Tensioned CFRP Retrofit (EB-CFRP)	15
6.2.4.1 Limit States of EB-CFRP Repairs	15
6.2.5 External Prestressed (P-CFRP) and Post-Tensioned (PT-CFRP) CFRP Retrofit	16
6.2.5.1 Prestressed CFRP (P-CFRP)	17
6.2.5.2 Unbonded post-tensioned CFRP (uPT-CFRP)	18
6.2.5.3 Bonded post-tensioned CFRP (bPT-CFRP)	18
6.2.5.4 Limit States of PT-CFRP Repairs	18

6.2.5.5 Methods of Prestressing CFRP	19
6.2.6 Near Surface Mounted CFRP reinforcement	20
6.2.6.1 Limit States of NSM-CFRP Repairs	20
6.2.7 Maximum Effect of CFRP Repair Techniques	21
6.2.7.1 Restoration of Prestressing Force.....	22
6.3 Steel-Based Techniques	22
6.3.1 PT-Steel.....	22
6.3.2 Steel Jackets	23
6.4 Strand-Splicing	23
6.4.1 Limit States of Strand Splice Repairs	23
6.4.1.1 Strand Splice Ultimate Capacity	24
6.4.1.2 Strand Splicing in Box Girders	25
6.4.1.3 Strand Splicing in Single-web Girders.....	25
6.5 Hybrid Repairs.....	25
6.6 Preloading Structural Repairs	26
7 PATCHING AND CORROSION MITIGATION.....	26
7.1 Patching.....	26
7.1.1 Drypack Method	27
7.1.2 Mortar Patch Method	27
7.1.3 Concrete Replacement Method.....	27
7.1.4 Synthetic Patching.....	27
7.1.5 Prepackaged Patching Compounds	27
7.1.6 Epoxy Injection.....	27
7.1.7 Patch Preloading	27
7.2 Patch Confinement – FRP U-Wraps	28
7.3 Corrosion Mitigation.....	28
8 SUMMARY OF FACTORS AFFECTING SELECTION OF PRESTRESSED GIRDER REPAIR TECHNIQUES	29
REFERENCES	33
NOTATION.....	34
APPENDIX I: Applicable national and international specifications and guides pertaining to the use and design of FRP composite repairs for strengthening, repair and rehabilitation.....	35

1 INTRODUCTION

Throughout this *Guide*, commentary and reference to the supporting NCHRP 20-07 Task 307 Final Report (referred to as the *Report*) are made by section number in square brackets.

This *Guide* serves to update the 1985 *NCHRP Report 280: Guidelines for Evaluation and Repair of Prestressed Concrete Bridge Members*. This report remains a primary reference for this topic. Material repeated from *NCHRP 280* is duly cited.

1.1 Significance and Scope

This document provides guidance for inspecting, assessing and repairing damage to prestressed concrete bridge girders resulting from vehicular impact. This *Guide* focuses on structural (load carrying) repair techniques rather than aesthetic or preventative repairs. Guidance for the latter is given by reference to other established sources. Similarly, the focus of this *Guide* is impact damage, although the repair methods described may also be employed for similar damage from other sources.

This *Guide* is written considering the following underlying assumptions:

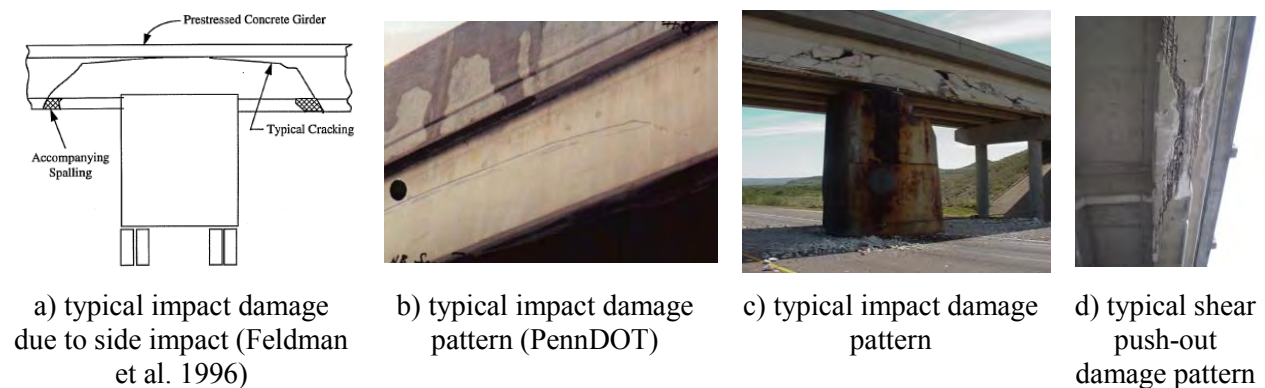
Repair methods are intended to restore all or a portion of **individual girder** capacity lost due to impact damage and subsequent impact-related deterioration. This *Guide* does not consider strengthening beyond the original undamaged girder capacity although the methods may be appropriate for this objective in some cases.

Repair methods are intended to be ‘permanent’. With proper details and maintenance the repair method becomes a permanent part of the girder and is expected to have a life equal to that of the girder. Temporary repair techniques are beyond the scope of this *Guide*.

Combinations of impact damage, bridge geometry, extant condition and material properties are necessarily unique and must be considered on a case-by-case basis. This *Guide* attempts to delineate an approach to repair of such damage emphasizing the applicability, utility and limitation of repair techniques.

1.2 Factors Affecting Impact Damage

Impact damage is usually readily apparent and varies from minor scrapes to structural collapse. The most commonly occurring damage pattern associated with side impact to prestressed concrete girders causes a torsion-induced shear cracking pattern in the exterior (or fascia) girder as shown in Figure 1a. In cases where the impact is more direct, this pattern becomes more of a shear push-out (Figure 1d). Examples of impact damage are provided in Section 1.3.2 through 1.3.4 of the *Report*.



[Courtesy of the Texas Department of Transportation, © 2007 All rights reserved.]

Figure 1 Examples of typical damage due to vehicle impact.

The following address additional factors affecting the nature of damage in the context of repair.

1.2.1 Corrosion Damage Subsequent to Impact

Left uncorrected, minor damage (nicks and scrapes) may progress to becoming more significant as corrosion becomes manifest. Eventually corrosion can lead to section loss of the strand and resulting loss of prestress and member capacity [1.3.1.1]. In general, the progression of corrosion-related damage tends to be exponential in time. Repairing such damage must be accompanied by mitigating the damage where possible.

The source of corrosion-inducing chlorides may vary. Chlorides from de-icing salts or salt-water environments may be introduced from the bridge deck as a result of poor drainage, damaged joints or other sources of damage. Adjacent box girder structures having a non-composite deck, for instance, may experience deck drainage through longitudinal joints and ‘wicking’ along the girder soffit affecting a large region of potentially susceptible concrete. Chlorides may also be introduced as a result of spray from traffic passing beneath the bridge or from a salt water environment, affecting the entire soffit region. Box girders may also be susceptible to chloride ingress from the top of the bottom flange if water is able to penetrate the girder cells, although this is believed to be rare.

1.2.2 Adjacent Strands

Impact damage to prestressed concrete girders may be more severe than visually apparent. Small strand spacing may result in insufficient concrete surrounding strands adjacent to damaged or severed strand(s) to allow the prestressing force of these undamaged strands to be transferred into the structure. As a result, a portion or all of the prestressing force near the impact may be ineffective. It may be prudent to disregard a portion or all of the contribution from surrounding strands at the affected section in a repair design [1.3.1.2].

1.2.3 Strand ‘Redevelopment’

Damaged strands in larger spans or long girders may be ‘redeveloped’ if there is sufficient undamaged length remaining. Conventional practice conservatively neglects any severed strand along the entire length of the girder in the analysis of the structure. However it has been shown that a severed strand ‘redevelops’ prestressing force in a manner consistent with the transfer length assumptions used in design (AASHTO 2010) once the damaged strand re-enters sound concrete [1.3.1.3 and 2.5].

1.2.4 Unanticipated Composite Action

Exterior adjacent box girders often have a composite barrier wall resulting in an asymmetric section and load condition; and have asymmetric strand loss concentrated on their lower exterior corner. These effects individually (and more so in combination) result in a rotation of the principal axes of the section [1.3.1.5]. As a result, the capacity of the girder to resist moment applied about its geometric horizontal axis will be reduced beyond what is predicted using a typical plane sections analysis due to the biaxial nature of the bending. In adjacent box bridges, this effect is most pronounced in exterior girders since interior girders are restrained from rotation by adjacent girders. This behavior becomes significant when performing load rating of the structure. Occasionally, the girder and barrier wall are assumed to be composite and a sections analysis is performed about the horizontal axis. Doing so will overestimate the true vertical capacity since it does not account for the biaxial response of the section [1.3.1.4].

Additionally, many adjacent box bridges have deteriorated or non-existent shear keys, resulting in the girders behaving independently and a corresponding increase in the transverse live load distribution factor (from 0.3 to 0.5 for adjacent box girders, for instance). Kasan and Harries (2012) present an analytical approach shown to capture anticipated eccentric behavior where it exists [2.1.1].

1.2.5 Lateral Deflections and Twist of Girders

Lateral sweep of a prestressed girder is seldom caused by impact-damage but rather is a result of fabrication, storage or construction errors. Lateral sweep due to vehicle impact is typically abrupt and localized to the area near the impact. Permanent twist or rotation can be caused by vehicle impacts or faulty manufacturing, storage or construction. Twist due to impact loading will generally crack the girder longitudinally at the bottom of the top flange (Figure 1) and at diaphragm locations. Permanent twist due to impact loading will be concentrated in the area of impact [1.3.1.6].

1.2.6 Effect of Diaphragms on Impact Damage

Many prestressed structures utilize intermediate diaphragms between beams for lateral stability. When a girder is struck by an over-height vehicle, the diaphragms transfer the impact load to the adjacent members. It has been shown that, in general, structures with intermediate diaphragm perform favorably when subject to impact, by spreading the impact load to adjacent girders. Nonetheless, shallow diaphragms may result in increased damage as the impacted girder flange rotates about the diaphragm; therefore full depth intermediate diaphragms are recommended. For a long bridge, multiple and distributed intermediate diaphragms resist impact better by effectively transferring large deformations to other girders and the deck, reducing the damaged areas and absorbing more kinetic energy [1.3.1.7].

2 INSPECTION OF IMPACT DAMAGED PRESTRESSED GIRDERS

All inspection should be guided by the *AASHTO Guide Manual for Bridge Element Inspection* (2011). In general, visual and manual inspection is the only practical triage tool for impact-affected prestressed concrete girders [1.4]. A significant goal of this triage is to identify locations requiring further non-destructive or destructive evaluation. A skilled inspector, familiar with the structure is able to provide a remarkably accurate assessment of the condition of the structure although is unlikely to be able to accurately quantify many damage types.

The goal of the visual inspection is to identify damages to the girder which affect the girder's load carrying ability. Visual indicators include:

- exposed/corroded/severed strands
- longitudinal and transverse cracks
- concrete spalling
- efflorescence
- rust staining
- presence of water/leakage
- longitudinal cracks on deck
- evidence of displacement between beams
- web out-of-plumbness
- relative dislocation of girder from bearing
- shear or flexure cracking

When documenting damage in the inspection report, every effort should be made to obtain photographic evidence of the damage in order to provide a visual for the assessment engineer and to provide a basis for inspection-to-inspection comparison. When documenting cracks, crack orientation and severity (width) are vital and must be documented. Other pertinent items should be noted as needed, such as a source of damage exacerbation (i.e.: improperly functioning drainage systems over the damage location). Ahlborn (2005) provides an inspection handbook for adjacent box girder structures which illustrates typical forms of distress for this bridge type.

Surface tapping and using a chipping hammer to remove loose concrete are common and recommended methods of manual inspection. With great care, the ‘screw-driver test’ (Walther and Hillemeier 2008) may be used to inspect the interior wires of prestressing strand and to assess the degree of remaining prestress [1.4.1].

Where corrosion of non-visible reinforcement or strand is suspected, the surface potential survey/half-cell potential survey [1.4.2] is a well-established standardized inspection technique (ASTM C876). While cumbersome, it is presently the most viable and widely used *in situ* approach alongside visual and other manual forms of inspection.

Remnant magnetism [1.4.3] is a useful method to get information about the location of prestressing steel fractures and the degree of damage to a strand. Presently, commercially available systems are aimed at detection of flaws/damage in prestressed slabs although could be readily adapted to high-speed applications on bridge soffits. This technique is very promising in near-term.

The acoustic emission (AE) technique is a noninvasive, nondestructive method that analyzes noises (“events”) that are created when materials (i.e. concrete or prestressing steel) deform or fracture [1.4.4]. The method is applicable for real-time health monitoring of a bridge or a girder and has been successfully used to quantify and precisely locate damage in prestressed concrete girders. Alternate approaches using known applied loads (trucks) have been demonstrated to be viable methods of inspection for structures having significant existing damage, although some technical hurdles remain before wide-spread deployment is practical. AE methods are presently ‘baseline’ techniques, that is, they are unable to capture damage occurring before monitoring is initiated.

While there are numerous other inspection techniques available to the practitioner [1.4], few are practically deployable or offer great utility for the inspection of impact damaged prestressed concrete girders.

It is stressed that inspection is not member assessment. The goal of inspection is to communicate information pertaining to the structure’s condition and damage severity and location which could affect the member’s load carrying capacity to the party responsible for assessment. Additionally, the importance of the inspection should not be overlooked as the capacity assessment relies on the information gathered during inspection.

3 ASSESSING (RATING) IMPACT-DAMAGED PRESTRESSED GIRDERS

3.1 Rating Impact Damaged and Subsequently Repaired Girders

AASHTO *Evaluation Manual* (2011) Eq. 6A.4.2.1-1 provides the basis for the bridge rating factor, RF:

$$RF = \frac{C - \gamma_{DC}DC - \gamma_{DW}DW \pm \gamma_P P}{\gamma_{LL}(LL + IM)} \quad (\text{Eq. 1})$$

Where C is the structural capacity, DC, DW, LL, IM and P are load effects prescribed in the AASHTO *LRFD Bridge Design Specifications* (2010), and the values of γ are LRFD load factors prescribed in Table 6A.4.2.2 of the *Evaluation Manual* (2011). These factors differ for inventory and operational rating levels.

Because impact damage is very often localized to one girder – usually an exterior girder – adjusting this approach to consider only the damaged girder is convenient and appropriate [2.1.2]. In this approach, the capacity of the as-built girder corresponds exactly to $RF_0 = 1$; that is: $C_0 = \gamma_{DC}DC + \gamma_{DW}DW + \gamma_{LL}(LL+IM) \pm \gamma_P P$, and the existing or damaged capacity is C_D , then the **normalized rating factor** for the damaged girder is:

$$RF_D = \frac{C_D - \gamma_{DC}DC - \gamma_{DW}DW \pm \gamma_P P}{C_0 - \gamma_{DC}DC - \gamma_{DW}DW \pm \gamma_P P} \quad (\text{Eq. 2})$$

In this manner analyses are effectively normalized by the AASHTO-prescribed inventory RF value (Eq. 1) and the normalized undamaged girder rating factor $RF_0 = 1.0$. If RF for the as-built structure is known (RF_0), then the C_0 term in Equation 2 may be replaced with $RF_0 C_0$. In either case, ratings may proceed since the objective of the rating is to consider the capacity of the repaired girder (C_R) relative to C_D and a target capacity C_0 (or another specified capacity). A rating factor less than unity based on Equation 2 does not necessarily imply structural deficiency as is the case when a rating factor less than unity is found from Equation 1. A value of less than unity from Eq. 2 simply indicates that the girder capacity is lower than its original design capacity. If the girder has excess capacity, it may still be adequate with a relative $RF_D < 1$. This situation is relatively common where identical girders are used for interior and more lightly loaded exterior girders in order to economize long-bed prestressing operations. Thus, the decision to repair, replace or do nothing to an individual girder must still be made in the context of the entire structure.

3.1.1 Repair Objective

This *Guide* is prepared on the assumption that the goal of a repair is to restore the original undamaged capacity of an impact-damaged girder (i.e.: $C_R \geq C_0$). Clearly, this may not be strictly necessary to the overall performance of the bridge. In this sense, Equation 2 is most useful in assessing the relative effect of the repair provided with respect to the individual girder capacity. These values are then considered in the overall bridge rating. The bridge rating process is necessarily unique to each bridge and beyond the scope of this *Guide*.

3.1.2 Residual Capacity and Strengthening Limits

External repair techniques are subject to damage from subsequent impact, fire or, in rare cases, vandalism. Therefore limits to the strengthening effect of a repair should be considered (ACI 440-2R 2008). The residual capacity of the unstrengthened girder (i.e.: the damaged capacity C_D) should safely resist an expected nominal load. In the absence of alternate guidance, for an external repair to be viable [2.3.1]:

$$C_D \geq 1.1DC + 1.1DW + 0.75(LL+IM) \pm \gamma_P P \quad (\text{Eq. 3})$$

If internal strand splicing is combined with external repairs (so called ‘hybrid’ repairs; see Section 6.5), the capacity of the girder considering the strand splices alone should exceed the limit given by Eq. 3.

3.2 Methods of Analysis

Due to the nature of prestressed member repairs and the need to assess the undamaged (C_0), damaged (C_D) and repaired (C_R) capacities in a consistent manner, plane sections analyses are most appropriate. Traditional Whitney stress-block approaches or fiber sections analyses satisfying strain compatibility and equilibrium are recommended. These analyses are conducted at various sections along a girder and may be ‘stitched together’ to create a capacity envelope [2.5]. Transitioning between damaged and undamaged sections may be considered using AASHTO-prescribed transfer and development lengths in the same manner as one treats the ends of girders. The transfer length may be assumed to begin at a location that a sound strand reenters sound concrete [1.3.1.3 and 2.5].

3.2.1 Non-composite Exterior Box Girders with Asymmetric Damage and Loading

Non-composite exterior box girders are generally loaded in an asymmetric manner and have some degree of asymmetric load resistance associated with typical impact patterns [1.3.1.4]. Additionally, deteriorated shear keys may result in increased live load distribution factors from those assumed in design [2.1.1]. Asymmetry results in a rotation of the neutral axis and related reduction in vertical load carrying capacity resulting from the unanticipated coupled transverse flexure. Kasan and Harries (2012) present an analytical approach shown to capture such eccentric behavior where it exists [2.1.1].

Such effects have been shown to be negligible for sections other than box girders and for interior girders that are restrained from rotation by adjacent girders.

3.3 Damage Classification of Prestressed Concrete Bridge Girders

Damage to impact-damaged prestressed concrete girders is described in a spectra ranging from minor to severe as broadly described below. Damage classification must be considered on a case-by-case basis. The classifications given in Table 1 are intended to provide approximate guidance only for the classification of damage to prestressed concrete girders.

Table 1 Damage classification for prestressed concrete girders

		strand loss	camber
MINOR	Concrete with shallow spalls, nicks and cracks, scrapes and some efflorescence, rust or water stains. Damage does not affect member capacity. Repairs are for aesthetic and preventative purposes only (<i>NCHRP 280</i>).	no exposed strands	no effect of girder camber
MODERATE	Larger cracks and sufficient spalling or loss of concrete to expose strands. Damage does not affect member capacity. Repairs are intended to prevent further deterioration (<i>NCHRP 280</i>).	exposed strands no severed strands	no effect of girder camber
SEVERE I	Damage affects member capacity but may not be critical – being sufficiently minor or not located at a critical section along the span [2.5]. Repairs to prevent further deterioration are warranted although structural repair is typically not required.	less than 5% strand loss	partial loss of camber
SEVERE II	Damage requires structural repair that can be affected using a non-prestressed/post-tensioned method. This may be considered as repair to affect the STRENGTH (or ultimate) limit state.	strand loss greater than 5%	complete loss of camber
SEVERE III	Decompression of the tensile soffit has resulted [2.6.1.2]. Damage requires structural repair involving replacement of prestressing force through new prestress or post-tensioning. This may be considered as repair to affect the SERVICE limit state in addition to the STRENGTH limit state.	strand loss exceeding 20%. In longer and heavily loaded sections, decompression may not occur until close to 30% strand loss.	vertical deflection less than 0.5%
SEVERE IV	Damage is too extensive. Repair is not practical and the element must be replaced.	strand loss greater than 35%	vertical deflection greater than 0.5%

3.3.1 ‘Repair or Replace’ Threshold

The threshold between SEVERE III and SEVERE IV essentially represents the ‘repair or replace’ criteria. In addition to the general guidance provided in Table 1, the following conditions require girder replacement [1.5.2]:

- Permanent lateral deflection exceeding standard girder tolerance (*NCHRP 280*) [1.3.1.6]
- Permanent vertical deflection from horizontal exceeding 0.5%
- Cracks at the web/flange interface that remain open indicating yield of transverse steel
- Loss of prestress at harping point [3.2 (6)]
- Loss of prestress at girder ends exceeding 25% of the total number of strands (*AASHTO LRFD 5.11.4.3*) [2.5.1]
- Damage girder capacity falling below the residual capacity given by Eq. 3 if external repair methods are used. If strand splicing is combined with external repairs, the capacity of the girder repaired with strand splices alone should exceed the limit given by Eq. 3.

3.3.2 ‘Repair or Do Nothing’ Threshold

From the perspective of structural (load bearing) repair, the threshold between SEVERE I and SEVERE II has few clear delineators and will generally be based on the judgment of the design professional. Often the loss of a few discrete strands in a section will not warrant structural repair. CFRP repair techniques have an effective lower limit of their utility. It is not practical to use a CFRP technique when damage does not exceed this limit as described in Section 6.2.4.1. [2.3.3.1]

Wherever possible, strand, whether severed or in good shape should not remain exposed to the environment as deterioration will accelerate and propagate. Exposed strand conditions should be mitigated using sound patching techniques as described in Section 7.

4 REPAIR OF PRESTRESSED CONCRETE BOX GIRDERS

Box girders include adjacent box, spread box and tub girders. Large segmental-type box girders are not within the scope of this *Guide*.

Damage classification must be considered on a case-by-case basis. Table 1 is intended to provide approximate guidance only for the classification of damage to adjacent and spread prestressed concrete box girders. MINOR and MODERATE damage does not require structural (load bearing) repair and is addressed in Section 3.3 and 7.1.

Selection of recommended repair techniques for prestressed concrete box girders is shown schematically in Figure 2. Repair techniques, their application and limitations are described in Section 6. It is generally not feasible to provide additional confinement (i.e.: CFRP U-wraps) to box girder repairs.

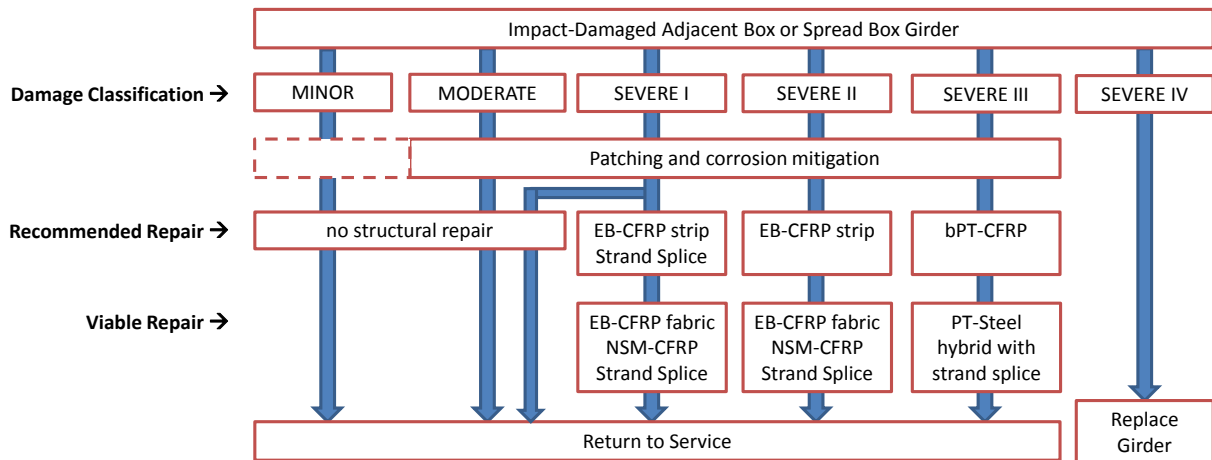


Figure 2 Repair selection flow chart for prestressed concrete box girders.

5 REPAIR OF PRESTRESSED CONCRETE SINGLE-WEB GIRDERS

Single web girders include flanged girders similar in form to AASHTO-I sections. Guidance is generally applicable to non-flanged sections such as tees and double-tees.

Damage classification must be considered on a case-by-case basis. Table 1 is intended to provide approximate guidance only for the classification of damage to single-web prestressed concrete girders. MINOR and MODERATE damage does not require structural (load bearing) repair and is addressed in Section 3.3 and 7.1.

Selection of recommended repair techniques for prestressed concrete single-web girders is shown schematically in Figure 3. Repair techniques, their application and limitations are described in Section 6. It is recommended to provide additional confinement (i.e.: CFRP U-wraps) to single-web girder repairs; this also provides confinement to any necessary concrete patches.

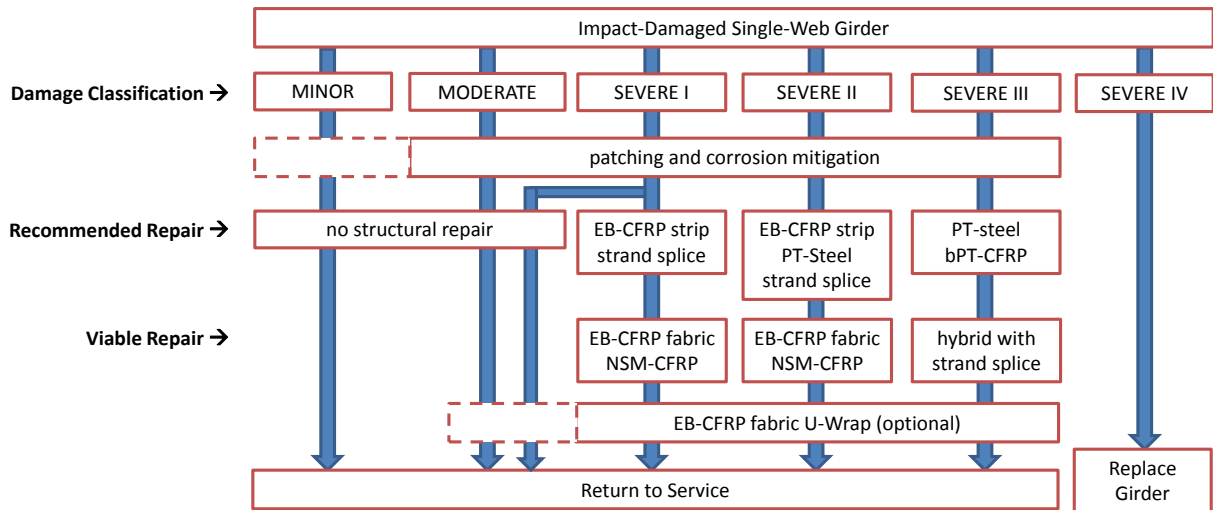


Figure 3 Repair selection flow chart for prestressed concrete single-web girders.

6 PRESTRESSED GIRDER REPAIR TECHNIQUES

The following sections describe techniques for the structural (load bearing) repair of impact-damaged prestressed concrete girders. Non-structural repair applications are described in Section 7.

6.1 Limitations of Repair Techniques Associated with Damaged Girder Geometry

Bonded repair techniques may be applied to accessible regions of the girder soffit and web(s). Soffit repairs are more efficient since these necessarily place the repair material as far from the member neutral axis as possible. However, soffit repairs must not encroach on the vertical clearance below the bridge. It is felt that an envelope of 1 inch for such repairs is reasonable unless other remedial action is taken such as lowering the roadway elevation beneath the bridge. Only externally bonded CFRP (EB-CFRP; see Section 6.2.4) or post-tensioned CFRP (PT-CFRP; see Section 6.2.5) repairs are suitable for soffit applications in most cases. Fully bonded CFRP applications (EB-CFRP or bPT-CFRP) also improve the resilience of the member in the event of a subsequent vehicle impact [1.5.4.6]. Post tensioned steel (PT-steel; see Section 6.3.1) applications will generally have a higher profile and may be susceptible to brittle and catastrophic failure in the event of a subsequent impact making them inappropriate for soffit applications. For adjacent box (AB) structures, only the soffit is available for external repair.

For bridge systems where the girder webs are accessible, bonded repair to the webs is feasible and does help to address the potential damage associated with subsequent impacts. However, as the repair material is located closer to the neutral axis of the member, its structural efficiency and therefore contribution to the load carrying capacity of the girder is diminished, requiring more material to be used to accomplish the same strengthening objective. Furthermore, for bonded repairs, the failure limit state is typically debonding of the CFRP which must be understood to occur *at the extreme tension element* of the member. As a result, failure occurs when material bonded at, or closest to the soffit debonds. Once debonding initiates in this fashion, load is redistributed to the internal prestressing strand and the CFRP located away from the soffit – driving a progressive debonding failure of this latter material. This behavior results in further diminished efficiency of material bonded to the web away from the soffit since the CFRP strain is limited *at the level of the soffit* [2.3.2].

External post-tensioned systems are more easily used in bridge systems where the webs are accessible. PT-steel systems in particular, may be attached to the girder webs using bolsters (Figure 4a) or be located between girders, anchored to new or existing diaphragms (Figure 4b). In these cases, installation of king- or queen-post to harp the PT strand is feasible and may be used to improve the efficiency of the repair (the example shown in Figure 4b shows a small degree of harping between the anchorage and subsequent diaphragm supports).



a) PT-steel anchored to girder using steel bolster bolted through girder web (second PT bolster on back of web) [DYWIDAG Systems International]



b) PT-CFRP anchored and harped by diaphragms [Mamlouk and Zaniewski *Materials for Civil and Construction Engineers* 2011]

Figure 4 Anchorage of post-tensioned repair systems.

6.1.1 Repair Applications During Live Loading

In practice, there are many situations under which deteriorated structures are subjected to continuous transient vehicles loads. Since repair applications are generally located on the underside of the bridge, it is particularly beneficial if the repair can be implemented without interrupting the traffic on the bridge.

Research on the performance of repair techniques installed under conditions of continuous vehicle loading acting during the installation are rare and their results contradictory [1.5.3.6]. It is recommended that traffic be restricted from affecting the girder being repaired during the repair installation. For externally bonded systems relying on an adhesive interface (EB-CFRP and bPT-CFRP), it is recommended that traffic be further restricted during the initial epoxy cure (typically about three hours) and for 24 hours if possible. This is not to say that a bridge must be closed during repair. Impact damage typically affects exterior girders. Closing the outside lane to traffic should be sufficient to effectively install most repairs. Limited research suggests that typical levels of transient strain does not affect epoxy cure and that only large strain excursions should be avoided. In this case, closing the affected lane to

trucks (but allowing small vehicles) is likely sufficient. In the absence of additional data, it is recommended to consult the adhesive manufacturer and follow their guidance.

6.2 CFRP-Based Techniques

Many emerging repair technologies employ the use of Fiber Reinforced Polymer (FRP) materials. FRP materials consist of a polymer matrix reinforced with a high performance fiber. Fiber materials may be aramid (AFRP, uncommon in North American practice), carbon (CFRP), glass (GFRP), or high performance steel (SFRP) or hybrids of these. A list of applicable national and international specifications and guides pertaining to the use and design of FRP composite repairs for strengthening, repair and rehabilitation are provided in Appendix I.

6.2.1 Material Selection

For highway infrastructure applications, preformed CFRP strips are preferred over wet laid-up CFRP for flexural repair. Preformed strips are available from a variety of manufacturers in discrete sizes and a number of ‘grades’ of CFRP: high strength (HS), high modulus (HM) and ultra high modulus (UHM). Properties of each of these are provided in Table 3. Preformed UHM-GFRP (glass FRP) is also commercially available; however this material is relatively soft and not well suited for flexural repair. HS-CFRP is the most readily available material and most commonly used for concrete repair applications. Although greater material efficiency may be realized using the higher modulus varieties, the reduced stress and strain capacity make catastrophic CFRP rupture more likely, reducing the stress allowable in design (see Eq. 4).

Table 3 Representative properties of available preformed FRP materials.

	HS-CFRP	HM-CFRP	UHM-CFRP	UHM-GFRP
Tensile modulus, E_f (ksi)	23200	30000	44000	6100
Tensile strength, f_{tu} (ksi)	406	420	210	130
Rupture strain, ϵ_{ru}	0.017	0.014	0.005	0.021
Typically available strip thickness, t_f (in.)	0.047	≈ 0.05	≈ 0.05	0.075
Typically available strip widths, b_{fl} (in.)	2, 3 and 4	4	4	2 and 4

6.2.2 Environmental Durability

Based on a recent study (Cromwell et al. 2011) the reduction factors (C_E) given in Table 4 are recommended for use with exterior bridge applications [1.5.3.5]. These factors are applied to both FRP strength (i.e., $C_E f_{tu}$) and modulus ($C_E E_f$) values.

Table 4 Proposed environmental reduction factors, C_E

	CFRP strips	CFRP fabric	GFRP strips	GFRP fabric
FRP Material Properties (f_{tu} and E_f)	0.90	0.90	0.80	0.80
Bond Capacity	0.90	0.50	0.90	0.50

ACI 440-2R (2008) recommends a value of $C_E = 0.85$ and $C_E = 0.65$ for CFRP and GFRP materials properties, respectively. No reduction is used for bond capacity.

6.2.3 Fatigue

FRP materials, particularly CFRP, exhibit excellent performance when subject to fatigue loads [1.5.3.4]. In conditions of tension fatigue where environmental effects are not affecting behavior, CFRP composite behavior is dominated by the strain-limited creep-rupture process. In terms of tensile S-N behavior, CFRP material degrades at a rate approximately one half that of steel (i.e.: slope of S-N curve is half that of steel). CFRP composites generally do not exhibit a clearly defined endurance limit under conditions of tension fatigue.

The performance of externally bonded (EB) CFRP systems deteriorates when subject to fatigue loading. Fatigue along the bond interface affects the FRP strain at which debonding initiates but, in a well detailed application where debonding is controlled, will not result in a significant reduction in ultimate repaired member capacity. Ductility or deformation capacity is reduced, although this is not typically a significant concern for prestressed concrete girders. Additionally, even very low stress ranges result in some degree of degradation suggesting that there is no (or at least a very low) endurance limit below which fatigue-induced degradation is no longer a concern.

Adhesive (epoxy) selection can mitigate some effects of fatigue. For relatively low fatigue stress ranges typical of prestressed girder repairs, a stiffer adhesive will exhibit minimal degradation. At higher stress ranges, however, degradation should be expected and a softer adhesive will provide greater ductility and may be expected to behave in a more predictable manner. It is noted that in terms of efficient stress transfer under static loads, a stiff adhesive is preferred. Therefore, except in cases where fatigue effects are dominant, well designed and detailed EB-CFRP systems will perform well. Post-tensioned bonded systems (bPT-CFRP, see below) further mitigate the deleterious effects of fatigue.

6.2.3.1 Fretting Associated with Fatigue Loads

A secondary effect of fatigue loads is the relative movement that occurs between the girder substrate and unbonded repair measures (uPT-CFRP and PT-steel). In such cases, unbonded repair materials must be physically isolated from the substrate girder to avoid the possibility of fretting along this discontinuous interface. When considering fretting, anticipated girder repair system deformations should be accounted for.

6.2.4 Externally Bonded Non Post-Tensioned CFRP Retrofit (EB-CFRP)

EB-CFRP systems are the recommended technique for repairing impact-damaged prestressed girders not requiring the restoration of some prestress force (SEVERE I and II).

CFRP strips adhesively bonded to prestressed concrete girders can restore or increase the flexural capacity of damaged girders, control cracking if it is present and reduce deflections under subsequent load [1.5.3.1]. This application is shown schematically in Figure 5b.

CFRP materials for EB applications may take the form of preformed strips or wet layed-up fabrics. Strips are generally unidirectional fiber reinforced plates having a very high fiber volume ratio; thus they are axially very stiff and strong. Strips are bonded to the prepared concrete substrate using conventional structural adhesives. Wet layed-up fabrics are saturated *in situ*. Typically, a layer of epoxy resin is placed on the prepared concrete substrate as a ‘primer’ layer and the dry CFRP fabrics are overlaid onto this, an additional layer of saturant is applied and the material is worked to ensure complete epoxy wet-out of the fiber. Additional layers are applied in the same fashion. The resulting CFRP material generally has a lower stiffness and strength based on the area of the resulting CFRP plate. Wet layed-up applications are suitable for column wrapping and U-wrap applications, however are not generally recommended for flexural repair for prestressed concrete girders [1.5.3.1.1]

6.2.4.1 Limit States of EB-CFRP Repairs

The dominant limit state for bonded CFRP applications is debonding of the CFRP from the substrate concrete. It is important to note that in a sound CFRP application, debonding failure is characterized as a cohesive failure through a thin layer of cover concrete immediately adjacent the CFRP. Because of this, it is difficult to improve debonding capacity through adhesive selection (provided the adhesive is adequate to result in failure in the concrete) since the failure is governed by the substrate concrete whose properties remain unaffected in a repair. Guidance such as that provided by ACI 440-2R (2008) or NCHRP *Report 609* (2008) are intended to ensure a sound CFRP application in which the design process considers the debonding limit state.

Debonding imparts a level of pseudo ductility to the failure and is preferred to CFRP rupture. In the design of bonded FRP systems, the strain carried by the FRP is limited to a value corresponding to the strain to cause debonding, defined as (ACI 440-2R 2008):

$$\varepsilon_{fd} = 0.083 \sqrt{\frac{f'_c}{nE_f t_f}} \leq 0.9\varepsilon_{fu} \quad (\text{ksi units}) \quad (\text{Eq. 4})$$

Where f'_c = concrete substrate compressive strength
 E_f = tension modulus of elasticity of CFRP
 t_f = thickness of one ply/layer CFRP
 n = number of layers of CFRP
 ε_{fu} = rupture strain of CFRP strip
the leading coefficient, 0.083, is taken as 0.41 for MPa units

Using preformed strips, the effectiveness of a repair is maximized by first maximizing the coverage of the CFRP on the soffit of the structure; i.e.: maximizing the width of the CFRP application, b_f . As can be seen from Eq. 4, additional layers of CFRP (n) or additional CFRP thickness (nt_f) are not proportionally effective [2.3.3.1].

Because bond capacity does not permit the full utilization of the CFRP, when small amounts of CFRP are used, these may debond prior to providing any enhancement of the *ultimate* capacity of the girder. In this case, the capacity at the *debonding limit state* is below the damaged girder capacity. In an externally bonded system, the debonding limit state is taken as being critical since once the bond fails, the girder is no longer strengthened. This hierarchy of failure also justifies the limit provided by Eq. 3.

6.2.5 External Prestressed (P-CFRP) and Post-Tensioned (PT-CFRP) CFRP Retrofit

A parallel can be drawn between prestressed and non prestressed CFRP retrofits and prestressed and conventionally reinforced concrete beams. The benefits of stressing CFRP strips prior to application include i) better utilization of the strengthening material; ii) smaller and better distributed cracks in concrete; iii) unloading (stress relief) of the steel reinforcement; resulting in iv) higher steel yielding loads. Another advantage of using P-CFRP or PT-CFRP systems is the potential for the restoration of service level displacements or performance of the structure. These systems have a confining effect on concrete (and, significantly, any patch material) because they place the concrete into compression. Therefore, a delay in the onset of cracking and a reduction of crack widths (only in bonded systems) is possible when this technique is used

Conventionally used CFRP materials have about 1.5 times the tensile capacity of 270 ksi steel prestressing strand and a Young's modulus about 75% of that of steel, meaning they can reach a higher strain. Stressing the CFRP for the repair can reintroduce prestressing force, lost due to damage or strand loss, back into the beam allowing for redistribution and a decrease of stresses in the strands and concrete. Thus when reloaded, the stress levels in the remaining strands will be reduced as compared to the unrepaired beam. In other words, prestressed CFRP systems create an active load-carrying mechanism which ensures that part of the dead load is carried by the CFRP whereas non prestressed EB-CFRP can only support loads applied after installation of the CFRP on the structure.

There are three approaches to prestressing or post-tensioning (the terms are used inconsistently in the literature) CFRP. The following terminology is adopted to clarify the types of prestressed CFRP systems. Figure 5 provides a schematic representation of each approach.

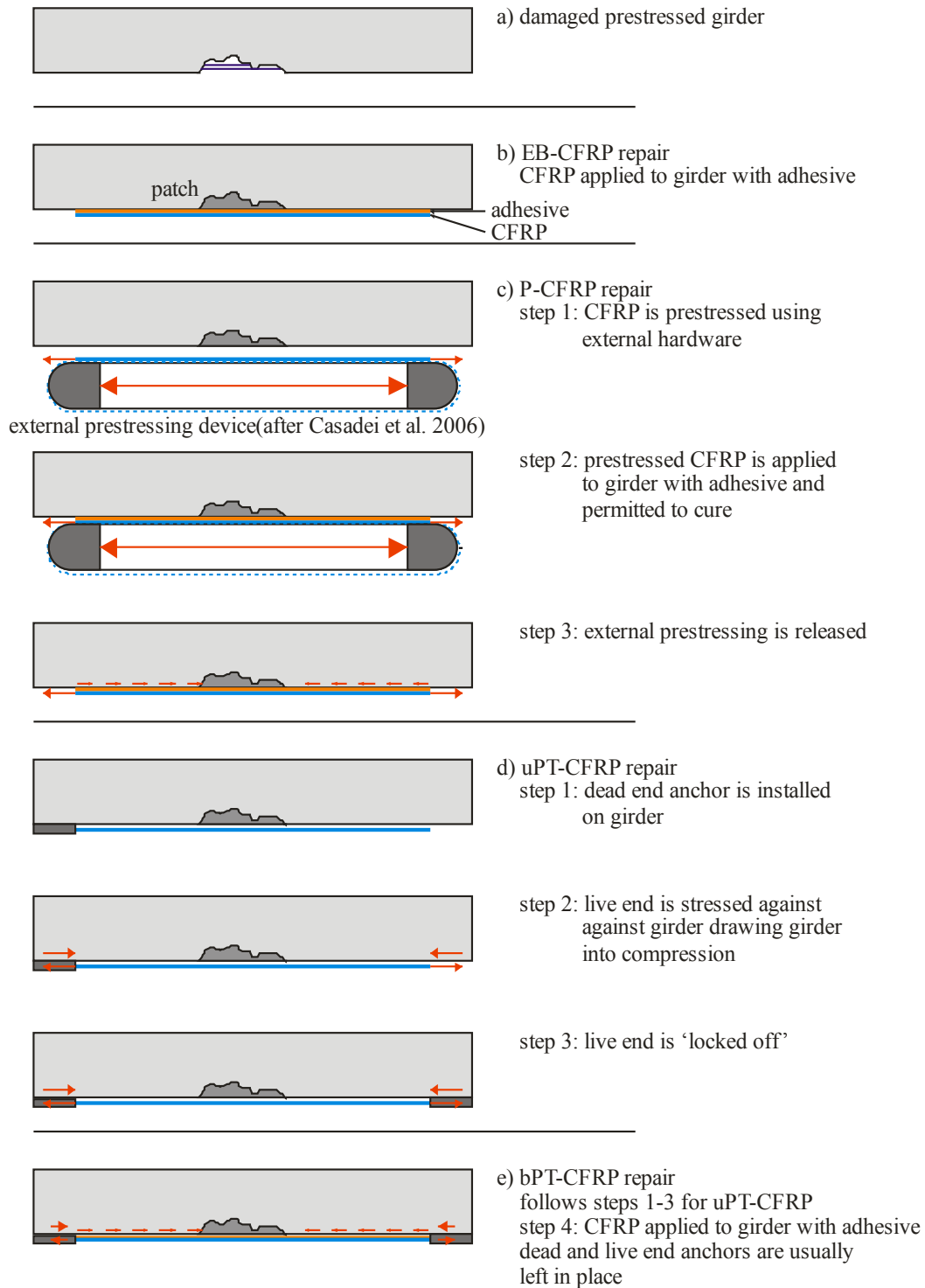


Figure 5 Schematic representations of CFRP applications.

6.2.5.1 Prestressed CFRP (P-CFRP)

Due to their only marginal improvement in performance over EB-CFRP systems and considering the complexity of their application, P-CFRP systems are not recommended as a repair method for impact-damaged prestressed concrete girders.

In a P-CFRP system, the CFRP is drawn into tension using external reaction hardware and is adhesively bonded to the concrete substrate while under stress (Figure 5c). The stress is maintained using the external reaction until the bonding adhesive is cured. The reacting stress is released and the ‘prestress’ is transferred to the substrate concrete. This method of prestressing is susceptible to large losses at stress transfer and long term losses due to creep of the adhesive system. As a result, only relatively low levels of prestress may be achieved. Additionally, details (such as FRP U-wraps) must be provided to mitigate debonding at the termination of the CFRP strips. P-CFRP systems are analogous to prestressed concrete systems where the stress is transferred by bond to the structural member.

6.2.5.2 Unbonded post-tensioned CFRP (uPT-CFRP)

Due to the increased susceptibility to fretting damage, uPT-CFRP are not recommended as a repair method for impact-damaged prestressed concrete girders. bPT-CFRP systems overcome the drawbacks of uPT-CFRP at little additional cost.

In a uPT-CFRP system, the CFRP is drawn into tension using the member being repaired to provide the reaction. The stress is transferred to the member by mechanical anchorage only (Figure 5d). Typically a hydraulic or mechanical stressing system will be used to apply the tension after which it will be ‘locked off’ at the stressing anchorage. This method of post-tensioning is susceptible to losses during the ‘locking off’ procedure. Depending on the anchorage method, long term losses due to creep in the anchorage are a consideration. Such systems must be designed with sufficient clearance between the CFRP and substrate concrete to mitigate the potential for fretting. uPT-CFRP systems are analogous to conventional unbonded steel post tensioning systems.

6.2.5.3 Bonded post-tensioned CFRP (bPT-CFRP)

bPT-CFRP systems are the recommended technique for repairing impact-damaged prestressed girders requiring the restoration of some prestress force (SEVERE III).

In this technique, the CFRP is stressed and anchored in the same fashion as the unbonded systems. Following anchorage, however, the CFRP is bonded to the concrete substrate resulting in a composite system with respect to loads applied following CFRP anchorage (Figure 5e). Since the adhesive system is not under stress due to the post-tension force, adhesive creep is not as significant a consideration with this system. The bonding of the CFRP may also help to mitigate creep losses associated with the anchorage. bPT-CFRP systems are analogous to conventional bonded steel post tensioning systems.

6.2.5.4 Limit States of PT-CFRP Repairs

The advantages of prestressing a CFRP repair are i) that the CFRP becomes active and replaces some of the prestress force lost due to internal strand loss; and ii) the CFRP debonding strain is effectively increased by the level of prestress in the CFRP:

$$\varepsilon_{fd} = 0.083 \sqrt{\frac{f'_c}{nE_f t_f}} + \kappa \varepsilon_{fu} \leq 0.9 \varepsilon_{fu} \quad (\text{ksi units}) \quad (\text{Eq. 5})$$

Where κ is the effective level of prestress in the CFRP and the remaining parameters are provided in reference to Eq. 4. Losses are relatively significant in PT-CFRP systems. Based on relatively limited available data, κ should remain less the 0.50 for bPT-CFRP (Figure 5e) and 0.30 for uPT-CFRP (Figure 5d) systems. Due to the stressing equipment required, prestressed CFRP (P-CFRP; shown schematically in Figure 5c) is not considered to be practical for bridge structures and is not considered further. Furthermore, for bridges or other applications subject to significant transient loads, uPT-CFRP is not recommended. uPT-CFRP strips will be located against the substrate concrete and therefore be subject to abrasion or fretting damage associated with differential displacement between the concrete substrate and unbonded CFRP strip (see Section 6.2.3.1). This situation must be remediated as the CFRP materials do

not have a great resistance to abrasion. Bonding this interface addresses this issue. For this reason, only bPT-CFRP are recommended.

Anchorage of PT-CFRP is usually provided by proprietary anchorage hardware which in turn is anchored to the concrete substrate (see Section 6.2.5.5). The CFRP-to-anchor connections may rely on adhesive bond, friction or bearing of a preformed CFRP ‘stresshead’ (Figure 6a). The proprietary anchor, in turn, is secured to the concrete substrate. Anchor bolts (seen in Figure 6a) and shear keys are conventional methods of transferring the force. For anchorages bolted to the concrete substrate, the recommendations ACI 318 (2011) Appendix D for bolting to concrete should be followed and great care must be taken to ensure that installed bolts do not interfere with sound internal prestressing strand or other reinforcement. For anchorages relying on a shear key arrangement, the key should be designed to carry 100% of the prestress force and bolts should be provided to carry any uplift caused by moment and to keep the shear key fully engaged. Pipe-type shear key inserts, as are occasionally used with the system shown in Figure 6, are impractical for prestressed members in regions where strand is present. Anchorage requirements such as available space and bolt spacing may affect the amount of post-tensioned CFRP that may be installed.

Due to their size, adjacent anchorages must be staggered longitudinally if a large amount of CFRP is required. Additionally, based on commercially PT-CFRP systems (see Section 6.2.5.5), the minimum transverse spacing of the CFRP strips is typically twice the strip width. Thus the coverage of PT-CFRP on the girder soffit is $b_f \leq 0.5b$. This diminishes some of the effectiveness of PT-CFRP although some systems utilize a thicker CFRP strip than is available for EB-CFRP.

6.2.5.5 Methods of Prestressing CFRP

There are significant challenges associated with prestressing CFRP strips. CFRP materials have highly orthotropic material properties. The transverse stiffness and strength of unidirectional CFRP strips and fabric systems may be orders of magnitude less than the longitudinal properties that make these materials good alternatives for prestressing in the first place. This makes CFRP materials difficult to ‘grip’ in order to prestress. A variety of solutions have been demonstrated in laboratory and ‘pilot’ applications [1.5.3.2.1 and 1.5.3.2.2] although few are practical for full scale deployment.

There are only two known commercially available ‘standardized’ PT-CFRP systems. Both systems work on the same principle, have essentially the same capacities and differ only in the proprietary nature of the jacking hardware used. An example of such a system is shown in Figure 6. The anchorage has a capacity of 67 kips (300 kN) and is intended for a maximum applied prestress force of 45 kips (200 kN). Material properties of the CFRP strips are those given for HS-CFFP in Table 2. This system is comprised of CFRP strips with ‘potted’ CFRP anchorages referred to as ‘stressheads’ manufactured on each end. These stressheads are captured by steel anchorages mounted on the concrete (Figure 6a) or by the jacking hardware (Figures 6b and d). One anchor is the fixed or ‘dead’ end (Figure 6a) while the other is the jacking end (Figure 6b). The jacking end stresshead connects into a movable steel frame which connects to a hydraulic jack, thus allowing the strip to be stressed. Once the desired stress level is reached, the jack can be mechanically locked to retain the stress in the CFRP or the CFRP strip can be anchored by ‘clamps’ (Figure 6c) near the jacking end. Anchor points can also be located at discrete intervals along the beam. The stress in the strips can vary according to structural need and is limited to the tensile strength of the strip. In many cases, the strength of the beam at the anchor location controls the amount of prestress force that can be applied.

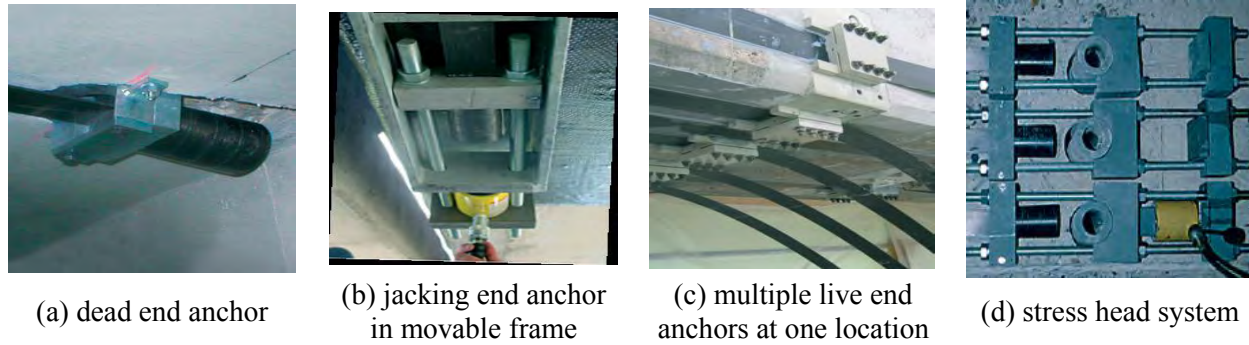


Figure 6 Components of commercially available PT-CFRP system.

6.2.6 Near Surface Mounted CFRP reinforcement

Near-surface mounted (NSM) CFRP repairs provide an alternative to externally bonded repairs. The NSM technique places the CFRP in the cover concrete of the member (see Figure 7). This protects the material from impact forces and environmental exposure. Although there is no prohibition against prestressing NSM CFRP, there is presently no practical method by which to prestress such systems. An NSM CFRP repair is completely enclosed in epoxy, making it possible to achieve higher bond strength as compared to external strip bonding due to the larger surface area which is bonded. Additionally, an NSM application engages more cover concrete and is able to transfer greater stresses into the concrete substrate. Since bond capacity is typically the limit state associated with EB repairs, NSM repairs will typically require less CFRP material due to the enhanced bond characteristics. NSM repairs are sensitive to the amount of concrete cover and are not a viable option when cover is not sufficient.

NSM repairs are not recommended as being efficient for repairs in the positive bending region of a structure (see 6.2.6.1). The significant advantage of NSM techniques is that they may be used in the negative moment region of a structure while remaining protected from wear and abrasion. Negative moment region repairs are not an application considered within the scope of this *Guide*.

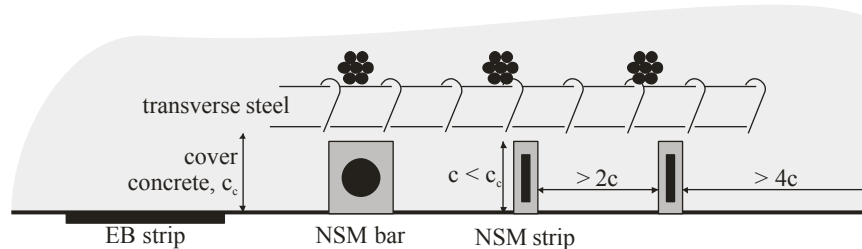


Figure 7 Schematic of externally bonded and NSM CFRP techniques.

6.2.6.1 Limit States of NSM-CFRP Repairs

For near-surface mounted applications, bond is improved over EB applications. ACI 440-2R (2008) prescribes a debonding strain of $\epsilon_{fd} = 0.7\epsilon_{fu}$. However, the improved bond effectiveness is often negated by the limited amount of strain of material that may be applied in this manner: Slots for NSM reinforcing should be spaced at least twice their depth apart and have an edge distance of at least four times their depth as shown in Figure 7 (ACI 440-2R 2008). Slots must not encroach on the internal reinforcing steel; for typical prestressed concrete structures, slots will not exceed 1 in., and may be better specified to be 0.75 in. in depth. The CFRP inserted into the slot is necessarily shorter than the slot depth although typically two plies of preformed CFRP will be used in each slot. For such typical prestressed concrete applications, NSM-CFRP will typically consist of 2-0.5 in. strips inserted into slots spaced at 1.75 in. This provides 50% of the material that an EB-CFRP application provides at a greater cost in terms of resources and

installation time. The improved bond behavior will normally not improve the CFRP efficiency the required 200% just to ‘break even’ in terms of capacity.

6.2.7 Maximum Effect of CFRP Repair Techniques

Although repair designs must be considered on a case-by-case basis, it is useful to have an approximate measure of the effectiveness of the repair material in restoring moment capacity and to relate this to the *in situ* girder being repaired [2.6.1]. By equating the nominal moment capacity contribution of the CFRP to an equivalent contribution of the *in situ* prestressing strand, one arrives at the theoretical maximum number of severed prestressing strands, n_{max} , that can be replaced by CFRP based on its relative contribution to moment capacity:

$$n_{max} = \frac{E_f n t_f b_f \varepsilon_{fd} \alpha H}{f_{pu} A_p \beta H} \quad (\text{Eq. 6})$$

Where: E_f = tension modulus of elasticity of CFRP

t_f = thickness of one ply/layer of CFRP

n = number of plies/layers of CFRP

EB-CFRP: for preformed strip it is recommended that $n = 1$

PT-CFRP: $n = 1$

b_f = maximum width available for CFRP bonding

EB-CFRP: $b_f = b$

PT-CFRP: $b_f = 0.5b$

NSM-CFRP: $b_f = (b/2 + 1)c$

b = soffit width of girder; if chamfers are present, the available soffit width should be reduced accordingly

c = depth of NSM slot

ε_{fd} = debonding strain of CFRP:

$$\text{EB-CFRP: } \varepsilon_{fd} = 0.083 \sqrt{\frac{f'_c}{n E_f t_f}} \leq 0.9 \varepsilon_{fu} \quad (\text{ksi units}) \quad (\text{Eq. 4})$$

$$\text{PT-CFRP: } \varepsilon_{fd} = 0.083 \sqrt{\frac{f'_c}{n E_f t_f}} + \kappa \varepsilon_{fu} \leq 0.9 \varepsilon_{fu} \quad (\text{ksi units}) \quad (\text{Eq. 5})$$

$$\text{NSM-CFRP: } \varepsilon_{fd} \leq 0.7 \varepsilon_{fu}$$

ε_{fu} = rupture strain of CFRP strip

f'_c = concrete substrate compressive strength

$\kappa = 0.3$ for uPT-CFRP

$\kappa = 0.5$ for bPT-CFRP

αH = depth from compression resultant to location of CFRP on soffit

βH = depth from compression resultant to centroid of prestressing strands

H = overall depth of girder

f_{pu} = ultimate stress of prestressing strand

A_p = area of one prestressing strand

Values of α and β vary based on the section geometry and amount of prestressing provided. In lieu of member-specific calculations, the values given in Table 5 may be used as estimates of these values. The ratio α/β effectively normalizes the CFRP stress to that of the *in situ* strand accounting for section geometry. The CFRP, located at the extreme tension fiber, is more efficient at providing moment capacity to the section than the *in situ* strand due to its greater level arm to the compression resultant, αH .

Table 5 Approximate values of α and β .

	rectangular section	voided slab	I-girders	bulb tees	deck bulb tees	box girders
α	0.65	0.65	0.80	0.80	0.90	0.92
β^1	0.50	0.58	0.64	0.64	0.76	0.82

¹ Collins and Mitchell (1997)

6.2.7.1 Restoration of Prestressing Force

In addition to restoring the ultimate load carrying capacity of a member, PT-CFRP systems are able to restore some degree of prestress force lost along with severed strands. Using the same approach as described by Eq. 6, Eq. 7 provides an approximation for the maximum amount of prestress force that can be replaced by PT-CFRP systems. Equation 7 is normalized by the effective prestress force provided by a single strand ($f_{pe}A_p$) resulting in the equivalent number of strands whose prestress force can be replaced with PT-CFRP, n_{max-PT} :

$$n_{max-PT} = \frac{E_f n t_f b_f \kappa \epsilon_{fu} \beta}{f_{pe} A_p \alpha} \quad (\text{Eq. 7})$$

Where f_{pe} is the long term effective prestress force; in lieu of calculating this value, $f_{pe} = 0.57f_{pu}$ may be used as a reasonable estimate for the long term effective prestress after all losses (based on *AASHTO LRFD* Section 5.9.5.3). All other values are the same as those given for Equation 6. The ratio β/α effectively normalizes the CFRP stress to that of the *in situ* strand accounting for section geometry. The CFRP, located at the extreme tension fiber, is less efficient at providing prestress to the section than the *in situ* strand.

PT-CFRP is less efficient at restoring lost prestress force (n_{max-PT}) than lost ultimate capacity (n_{max}). Because of the limited long term prestress force available in an uPT-CFRP system ($0.30f_{tu}$), such systems perform only marginally better than EB-CFRP. Like NSM-CFRP, it is unlikely that the additional effort required for uPT-CFRP would warrant its use. The prestress force available for a P-CFRP system is even less than an uPT-CFRP and therefore possibly less efficient than an EB-CFRP system due to geometric constraints.

6.3 Steel-Based Techniques

6.3.1 PT-Steel

External steel post-tensioning (PT-steel) is done using steel rods, strands or bars anchored by corbels or brackets (typically referred to as ‘bolsters’) which are cast or mounted onto the girder; typically on the girder’s side (although occasionally on the soffit) as shown in Fig. 4. The high strength steel rods, strands or bars are then tensioned by jacking against the bolster (*Report 280*). Design of PT-steel repair systems are well established using simple plane sections analysis (recognizing that the post-tensioning bar is unbonded). Any degree of damage may be repaired and prestress force restored using this method. The primary design consideration is the transfer the PT force into the girder through the bolsters. This is accomplished through design of the bolster as a bracket or corbel (see *AASHTO LRFD Specifications* Section 5.13.2.4) or through direct bearing of a shear key. Typically, the bolsters themselves will be post-tensioned onto the girder web thereby affecting a normal force (P_c in *AASHTO LRFD* Equation 5.8.4.1-3) anchoring the bolster. When adding bolsters to box girders, the web thickness (and possible variation thereof) must be considered: Ideally, the bolsters are post-tensioned to a single web although this will likely require access inside the box. If post-tensioning the bolster through an entire box girder, this should be done at the location of an internal diaphragm in order not to affect out-of-plane bending of the web. In general, applying PT-steel repair methods to box sections is perhaps not as practical as to single web members. PT-steel may also be anchored to existing or purpose-cast diaphragms between girders as shown in Figure 4b.

Generally it will be more efficient to harp external post tensioning. This is easily done, although the attachment of the harping points to the girder requires the same attention as the end anchorages. Additionally, harping points damaged in a subsequent impact may result in a catastrophic failure; therefore harping points should not be located in impact-susceptible areas. Finally, external PT-steel must be adequately protected from corrosion; grease-filled ducts/tubes are recommended. Epoxy-coated strand used for external PT-steel repairs should be provided with additional protection against corrosion.

External post-tensioning may also use CFRP cables (CFCC). These systems have proprietary anchorages that interface with conventional prestressing hardware. Such systems are rare in North American practice.

6.3.2 Steel Jackets

Due to their complexity and the fact that they are untested, steel jacket repairs are not recommended as a repair method for impact-damaged prestressed concrete girders; it is believed that CFRP repairs address all advantages of steel jackets while overcoming some of their drawbacks.

Steel jacketing is the use of steel plates to encase the girder section to restore girder strength. Generally, this method of repair will also require shear heads, studs or through bars to affect shear transfer between the steel jacket and substrate girder. Steel jacketing is felt to be a very cumbersome technique. In most applications, field welds will be necessary to ‘close’ the jacket (since the jacket cannot be ‘slipped over’ beam ends in most applications). Additionally, the jacket will need to be grouted in order to make up for dimensional discrepancies along the girder length. *Report 280* discusses steel jacket repairs.

6.4 Strand-Splicing

Strand splices are designed to reconnect severed strands. Methods of reintroducing prestress force into the spliced strand are preloading, strand heating and torquing the splice (*Report 280*); the latter is analogous to a turnbuckle. Preloading to develop prestress forces in a strand splice will generally be impractical (see Section 6.6) and strand heating is not recommended.

Strand splicing is well established and an effective means of restoring steel continuity and prestress force to severed strands. Commercially available strand splices have couplers connected to reverse threaded anchors; as the coupler is turned, both anchors are drawn toward each other, introducing a prestress in the attached strand (see Figure 8). Commercially available strand splices are reportedly adequate to develop $0.96f_{pu}$. Typically, a re-tensioning operation will aim to restore $0.60f_{pu}$ which will generally be close to the long-term effective prestress in a strand. Commercially available splices are available for strand diameters only up to 0.5 in. [2.3.3.4].

6.4.1 Limit States of Strand Splice Repairs

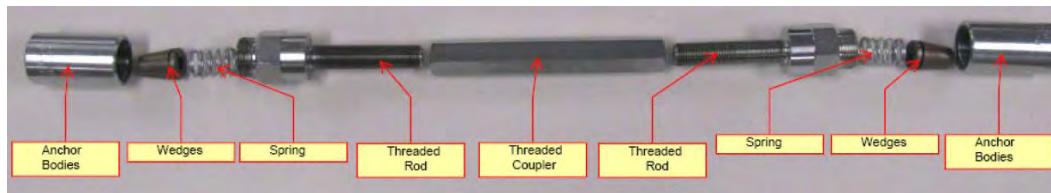
Limitations pertaining to the use of strand splices are based on the physical dimensions of the splices and spacing of the strands to be spliced. Often, prestressing strands are spaced at 1.5 in. on center. Anchor bodies (Figure 8a) have a diameter of 1.625 in. irrespective of spliced strand size. When repairing adjacent strands, splices must be staggered (Figure 8b) to avoid interference (Figure 8c). The specified stagger must accommodate the ‘stroke’ of the splice coupler; a minimum spacing of 2 in. is recommended (Figure 8b). Installation of splices for exterior strands also results in reduced concrete cover at the splice location unless section enlargement is also affected. Reduced cover may affect durability and result in a region more susceptible to cracking. Clear spacing between splices and adjacent bonded strands is also reduced (Figure 8c) which may affect bond performance and increase the development length of adjacent intact strand.

Chuck splices, having a diameter of 2 in. are used to allow for removal of damaged strand and to shift the location of the splice to accommodate staggering and reduce congestion (Figure 8b). Chuck splices must also be staggered and not coincide with strand splice locations in order to avoid interferences. Staggering strand splices often requires the removal of additional strand and its surrounding concrete. Finally, strand splices and chuck splices also interfere with transverse reinforcement where it is present. This may

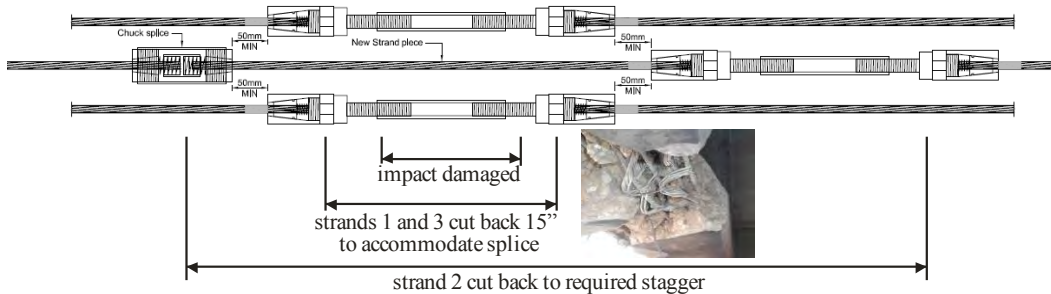
require removal of the transverse steel and replacement with grouted or epoxied hairpins. In some cases, FRP U-wraps (see Section 7.2) may be designed to restore the confinement and shear capacity lost by the removal of transverse steel (ACI 440-2R 2008).

Considering interferences, strand splicing is practical for relatively few severed strands but becomes increasingly cumbersome for significant damage – particularly for the case of adjacent damaged strands. For this reason, a combination of external repair and strand splicing (see Section 6.5) may be appropriate where a large number of strands are damaged, particularly if this damage is confined to a short length of the girder.

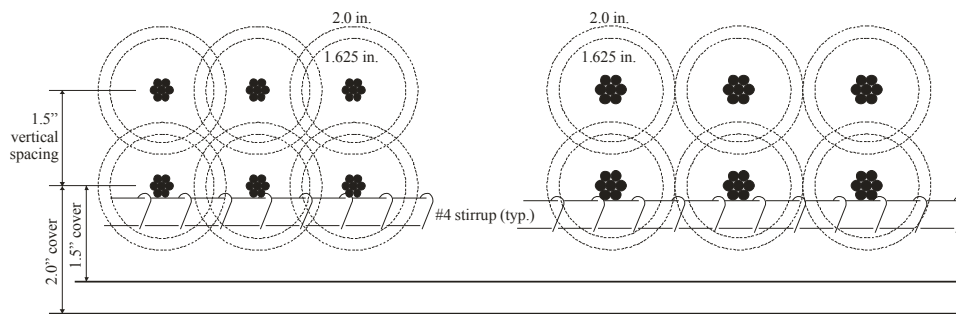
Strand splicing requires sound strands. Any corroded region of strand must be removed back to ‘bright steel’. Thus if impact damage has been left unrepaired and corrosion set in (see Section 1.2.1), strand splicing may require additional strand and concrete removal.



a) components of strand splice [Prestress Supply Inc. 2011]



b) required longitudinal stagger of adjacent strand splices [Prestress Supply Inc. 2011]



3/8" strand at 1.5 in. spacing

1/2" strand at 2.0 in. spacing

c) strand splice interferences

Figure 8 Strand splice hardware and potential interferences.

6.4.1.1 Strand Splice Ultimate Capacity

Strand splices cannot be universally relied upon to develop the ultimate capacity of the strands. Some research indicates that 100% of capacity can be restored while others report that only about 80% of

capacity can be restored. Zobel and Jirsa (1998) report a ‘guaranteed’ strength of $0.85f_{pu}$ while the available commercial literature implies a capacity of $0.96f_{pu}$ for strand splices. Zobel and Jirsa also recommend that more than 10-15% of strands in a section be spliced. Thus it is assumed that strand splices are able to restore *in situ* prestress forces assumed to be less than $0.70f_{pu}$. Furthermore, it is recommended that strand splices:

- be limited to strand diameters 0.5 in. and less
- be limited to developing $0.85f_{pu}$, thereby reducing their effectiveness in restoring strands. The effective number of strands restored by strand splices should be taken as $0.85n_{spliced}$
- be staggered (Figure 8b) when splicing adjacent strands.
- be limited to splicing 15% of strands in a girder regardless of staggering.

The Alberta Infrastructure and Transportation Department (ABITD 2005) provides additional guidance with respect to the evaluation and acceptance criteria of- and procedure for restressing severed prestressing strands. In particular, the need to calibrate the restressing operation is emphasized and guidance provided [1.5.1.2].

6.4.1.2 Strand Splicing in Box Girders

Beyond the repair of a few isolated strands, it is not recommended to use strand splicing for impact-damaged box girders, particularly older girders. Anecdotal evidence has indicated significantly reduced cover concrete (as small as 0.75 in. to the center of the strand) and inconsistent strand spacing (as small as 1 in. center-to-center) in girders from the 1960’s and early 1970’s. In any event, splicing adjacent strands in a box girder will result in significantly reduced concrete cover and interferences. Issues of splitting associated with strand splices cannot be adequately addressed in box girders since the top of the bottom flange (in the box void) is inaccessible. Providing new internal confinement (grouted hairpins) is impractical since these cannot be anchored in the 4 to 5 in. bottom flanges. External confinement (such as CFRP U-wraps) is also not as efficient since this confinement cannot be provided inside the box void. Section enlargement (‘blisters’) of box girders may be used but is not as practical as for flanged members and reduces the roadway clearance below the bridge.

6.4.1.3 Strand Splicing in Single-web Girders

Strand splicing is more practically applied to ‘flanged’ members. The reduced cover, spacing and interferences with adjacent strands/splices associated with strand splices affect development, crack control and the likelihood of splitting. For this reason, confinement of the spliced region is recommended to ensure long-term durability and performance. In flanged sections such as AASHTO I-girders and bulb tees, section enlargement, grouted or epoxied hairpins and/or CFRP (or GFRP) U-wraps may be used to confine the spliced region, control splitting cracks and replace any transverse reinforcement that may have been removed to affect the splice repair (ACI 440-2R 2008).

Splicing adjacent strands requires a longer repair region (Figure 8) and may therefore not be practical for cases of very local damage (such as is shown in the inset in Figure 8). In this case a hybrid approach may be efficient: repairing some strands (perhaps every second strand, limited to 15% of the strands in the affected section) with strand splices and restoring the remaining capacity with an externally bonded alternative. This approach is described in the following section.

6.5 Hybrid Repairs

Limitations associated with each repair technique clearly point to the adoption of hybrid repair approaches in order to maximize the degree of damage that may be repaired.

Strand splices are internal applications and therefore may be used with most any external application (except, perhaps NSM where interference between the strand chunks and NSM slots is likely). Strand splices are reported to have the capacity to restore *in situ* prestress to all but 0.6 in. strands. Typically, *in situ* levels of long term prestress will be on the order of $0.60f_{pu}$. As reported in Section 6.4.1.1, strand

splices cannot be relied upon to develop the ultimate capacity of the strands. Thus when considering the ultimate capacity of a section, the effectiveness of strand splicing should be reduced such that the equivalent number of strands considered in calculating the girder capacity is $0.85n_{\text{spliced}}$. Using this approach, the damage that must be repaired using external techniques is reduced. The use of strand splices may effectively extend the utility of other repair techniques. Additionally, since strand splices are active, they may be used to restore a degree of prestressing, avoiding decompression [2.6.1.2] and permitting passive external repair techniques to be utilized.

Hybrid combinations of techniques other than strand splices will generally be inefficient since the repair stiffnesses and capacities differ resulting in multiple systems behaving in series rather than in parallel.

6.6 Preloading Structural Repairs

Preload is the temporary application of a vertical load to the girder during repair [1.5.1.1]. The preload is provided by either vertical jacking or, more conventionally a loaded vehicle. If the damage has caused a loss of concrete without severing strands, preloading during concrete restoration can restore capacity to the girder without adding prestress. In this case, preloading may be used to restore partial or full prestress to the repaired area; effectively reducing tension in the repaired area during live load applications. Preloading is most effective for smaller prestressed girders. As elements become larger the level of preload required becomes very large and often impractical to apply. The effectiveness of preload is improved with reduced dead-to-live load ratios; however these are not typical in concrete bridge structures [1.5.4.1.1].

It is believed that preloading in order to affect or restore prestress force, while feasible, is typically impractical. Preloading in order to precompress patch repairs, however, is recommended (see 7.1.7).

Care should be taken when preloading a structure so as to not overload the structure or cause damage from excessive localized stresses from the preloading force.

7 PATCHING AND CORROSION MITIGATION

7.1 Patching

Concrete patching repairs are typically necessary to address defects that occur during fabrication, shipping, handling or erection of a member but can also be used to correct impact damage. Aesthetic repair methods are also often required as a final step in a structural repair. Sound patches are particularly important when they serve as substrates for bonded external repair measures (EB-CFRP and bPT-CFRP) and especially so if an NSM-CFRP repair crosses a patched area. Patching methods are well established and extensive guidance on their application are reported in the *Manual for the Evaluation and Repair of Precast, Prestressed Concrete Bridge Products* (PCI MNL-137-06) published by the Precast/Prestressed Concrete Institute (PCI). The *ICRI/ACI Concrete Repair Manual* also provides guidance on concrete aesthetic repairs.

Patching requires the removal of all unsound concrete. It is usually a good idea to remove slightly more concrete rather than too little, unless it affects the bond of prestressed strands. The chipped area for patching should at least be 1 in. deep and should have edges as straight as possible, at right angles to the surface. The use of air driven chipping guns or a portable power saw for cutting concrete is recommended for removal of concrete but care should be taken to make sure that the reinforcement or the strands are not damaged. When patching prestressed elements, preloading the elements is often recommended in order to slightly ‘prestressing’ the patch to resist ‘pop-out’; this is not always possible in *in situ* repairs.

The selection of a patching technique and material will depend on the size of the patch and limitations of each method. Considerations in patch material selection include i) rheology of the patch material (the material must thoroughly fill or pack into the void being patched); ii) bond strength to *in situ* concrete and steel reinforcement traversing patch; iii) compressive and tensile strength of patch material; and, iv)

durability of the patch material. Given that the volume of many patches is small, the benefit of using a high quality prebagged repair material is likely warranted and represents only a small incremental cost in the entire patching operation. The following six methods of patching are described and details of their application are found in *PCI Manual 137* (2006):

7.1.1 Drypack Method

The drypack method is suitable for holes having a depth nearly equal to the smallest dimension of the section, such as core or bolt holes. The method should not be used on shallow surfaces or for filling a hole that extends entirely through the section or member [1.5.5.1.1].

7.1.2 Mortar Patch Method

Mortar patches are used in concrete members with shallow defects, which require a thin layer of patching material such as in honeycombs, surface voids or areas where concrete has been pulled away with the formwork [1.5.5.1.2].

7.1.3 Concrete Replacement Method

The concrete replacement method consists of replacing the defective concrete with machine-mixed concrete that will become integral with the base concrete. Concrete replacement is preferred when there is a void extending entirely through the section, or if the defect goes beyond the reinforcement layer, or in general if the volume is large [1.5.5.1.3]. Concrete replacement will also provide the best substrate for eventual EB-CFRP, bPT-CFRP or even NSM-CFRP repairs.

7.1.4 Synthetic Patching

There are cases where Portland cement patches are difficult or impractical to apply. These situations include patching at freezing temperatures or patching very shallow surface defects. Two synthetic materials useful under such circumstances are epoxy and latex based products [1.5.5.1.4]. Epoxies can be used as a bonding agent, a binder for patching mortar, an adhesive for replacing large broken pieces, or as a crack repair material. Small deep holes can be patched with low-viscosity epoxy and sand whereas shallower patches require higher viscosity epoxy and are more expensive. It is suggested that epoxy mortars be used only in situations where exceptional durability and strength are required. Although they offer excellent bond and rapid strength development, epoxies are hard to finish and usually result in a color difference between the patch and the base concrete, clearly showing the repaired section, unless precautions (such as tinting) are taken. Latex materials are used in mortar to increase its tensile strength, decrease its shrinkage and improve its bond to the base concrete, thus helping to avoid patch failure due to differential shrinkage of the patch. Because of its good bonding qualities, latex is especially useful in situations where feathered edges cannot be avoided.

7.1.5 Prepackaged Patching Compounds

There are many commercial patching products available. A good patching material should have an initial setting time of 10 – 15 minutes and a final setting time of 20 – 45 minutes. Because some compounds generate excessive heat (leading to shrinkage and poor durability), they often are not suitable for general purpose patching [1.5.5.1.5].

7.1.6 Epoxy Injection

Epoxy injection methods have been used to repair cracks or fill honeycombed areas of moderate size and depth [1.5.5.1.6]. Only appropriately trained personnel should carry out such repairs.

7.1.7 Patch Preloading

Preloading (see Section 6.6) is recommended for patch operations. Preloading structures during the patching operation can draw the patch material into compression thereby mitigating effects of patch

shrinkage, cracking and pop-out. For patching operations, preload is often provided by a vehicle parked above the patch location.

7.2 Patch Confinement – FRP U-Wraps

Preload is often impractical. As an alternative, both CFRP and GFRP materials in a ‘U-wrap’ fashion may be used to confine patches and resist ‘pop-out’ failure of the patch and shrinkage and flexural cracking in the patch [1.5.5.2]. An example repair sequence involving strand splicing, patching and patch confinement is shown in Figure 9. The externally applied FRP affords some protection to the patch and, significantly, provides some continuity or ‘bridging’ between the patch and surrounding concrete. Because all GFRP systems and most epoxy resin systems are susceptible to damage from UV light exposure, FRP systems applied to exterior girders in particular require a final protective top coat. This is also often done for aesthetic reasons. FRP applications used to confine patches have been found to be very robust, even serving to reduce damage caused by subsequent vehicle impacts [1.5.4.6].

In addition to the patch confinement, U-wrapped CFRP strips may be used to help ‘hold’ the longitudinal CFRP and improve the resistance of EB-CFRP and bPT-CFRP debonding from the concrete [1.5.3.2.2].

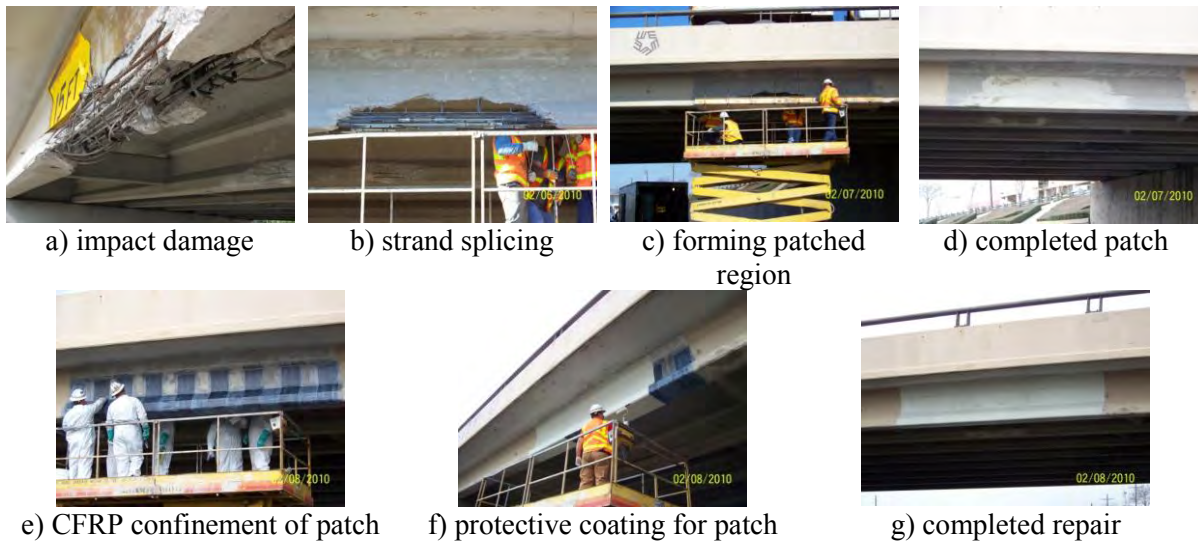


Figure 9 Strand splicing and patch repair sequence.

[Courtesy of the Texas Department of Transportation, © 2007 All rights reserved.]

7.3 Corrosion Mitigation

When considering the repair of corroded strand, it is important to mitigate the source of corrosion prior to patching and repair. Prestressing strand is more susceptible to corrosion than lower grades of steel (due both to the composition of prestressing steel and the increased surface area-to-cross section area ratio of a seven wire strand), therefore prestressed concrete beams are susceptible to corrosion, especially at beam ends. Surface treatments and coatings are effective at mitigating corrosion in the short term, but are only effective in the long term if applied prior to chloride contamination [1.5.1.4]. The addition of FRP wraps has also shown to effectively mitigate corrosion by excluding chloride bearing water [1.5.1.4].

Active cathodic protection (impressed current systems) is also effective at mitigating corrosion, but are not commonly used due to high maintenance and monitoring costs and method complexity. Additionally, prestressing steel is particularly susceptible to cracking due to hydrogen embrittlement. If an active cathodic protection system is installed and operated in such a way that the magnitude of polarization is excessive, then atomic hydrogen may be generated at the surface of the steel and embrittlement may occur.

Passive cathodic protection (embedded anodes) installed in concrete patches is an effective method of mitigating corrosion in prestressed concrete members (Vector 2012).

8 SUMMARY OF FACTORS AFFECTING SELECTION OF PRESTRESSED GIRDER REPAIR TECHNIQUES

Ultimately, repair selection must be made on a case-by-case basis. The following matrix summarizes the utility and viability of each repair method described.

Repair Selection Criteria – EB-CFRP Techniques.

Selection Criteria	EB-CFRP strips		EB-CFRP fabric ¹		NSM-CFRP ²	
	this report		this report		this report	
commercially available? ⁷	yes		yes		yes	
girder type	box girder	I-girder	box girder	I-girder	box girder	I-girder
generally recommended?	yes	yes	no	yes, if bulb to be wrapped	no	no
dominant repair limit state	CFRP bond		CFRP bond		NSM slot geometry and CFRP debonding	
damage that may be repaired	Severe I and II		Severe I		Severe I and II	
prestress steel that may be replaced	≤20% of strands	≤10% of strands	≤20% of strands	≤10% of strands	≤20% of strands	≤10% of strands
active or passive? ⁸	passive		passive		passive	
behavior at ultimate load	good		fair		good	
resistance to overload	limited by bond		limited by bond		good	
fatigue performance	limited by bond ⁹		limited by bond ⁹		uncertain	
strengthening beyond undamaged capacity?	yes		yes		yes	
combining splice methods	possible with strand splicing		possible with strand splicing		unlikely	
preload for repair ¹⁰	no		no		no	
FRP U-wrap ¹⁰	not feasible	recommended ¹¹	not feasible	recommended ¹¹	not required	
restore loss of concrete	patch prior to repair		patch prior to repair		patch prior to repair	
preload for patch ¹⁰	possibly		possibly		yes	
speed of mobilization	fast		fast		moderate	
constructability	easy		easy		difficult	moderate
specialized labor required ¹³	no		yes		no	
proprietary tools required	no		yes, saturation bath		no	
lift equipment required ¹⁴	no		no		perhaps	
closure below bridge	single lane possible		single lane possible		full carriageway closure	
time for typical repair	1-2 days		2-4 days		2-4 days	
environmental impact of repair process	dust from surface preparation		VOCs from saturant and dust from surface preparation		dust from concrete sawing	
durability	requires environmental protection		requires environmental protection		excellent	
cost	low		low		moderate	
aesthetics	good		good		excellent	
retain capacity in event of subsequent impact	good		very good		very good	

Repair Selection Criteria – PT-CFRP Techniques

Selection Criteria	P-CFRP ³		bPT CFRP		uPT-CFRP	
primary reference	this report		this report		this report	
commercially available? ⁷	no		yes		yes	
girder type	box girder	I-girder	box girder	I-girder	box girder	I-girder
generally recommended?	no	no	yes	yes	no	no
dominant repair limit state	CFRP bond		anchorage design		anchorage design	
damage that may be repaired	Severe II		Severe II and III		Severe II and III	
prestress steel that may be replaced	≤20% of strands	≤10% of strands	≤40% of strands	≤20% of strands	≤20% of strands	≤10% of strands
active or passive? ⁸	marginally active		active		active	
behavior at ultimate load	very good		very good		very good	
resistance to overload	limited by bond		good		good	
fatigue performance	limited by bond ⁹		limited by bond ⁹		excellent if fretting is mitigated	
strengthening beyond undamaged capacity?	yes		yes		yes	
combining splice methods	possible with strand splicing		possible with strand splicing		possible with strand splicing	
preload for repair ¹⁰	no		no		no	
FRP U-wrap ¹⁰	recommended ¹¹		recommended ¹¹		not feasible	
restore loss of concrete	patch prior to repair		patch prior to repair		patch prior to repair	
preload for patch ¹⁰	not required		not required		not required	
speed of mobilization	moderate		moderate		moderate	
constructability	difficult		difficult		difficult	
specialized labor required ¹³	yes		yes		yes	
proprietary tools required	yes, prestressing hardware		yes, PT anchors and hardware		yes, PT anchors and hardware	
lift equipment required ¹⁴	yes		no		no	
closure below bridge	full carriageway closure		full carriageway closure		full carriageway closure	
time for typical repair	1-2 days		1 week		1 week	
environmental impact of repair process	dust from surface preparation		dust from surface preparation		minimal	
durability	requires environmental protection		requires environmental protection		requires environmental protection and protection from fretting	
cost	moderate		moderate		moderate	
aesthetics	good		fair		fair	
retain capacity in event of subsequent impact	fair		good		none if PT impacted	

Repair selection criteria – Steel-based Techniques

Selection Criteria	PT-steel		Strand Splicing		Steel Jacket ⁴		Replace Girder
primary reference	<i>NCHRP Report 280</i>		this report and <i>NCHRP Report 280</i>		<i>NCHRP Report 280</i>		<i>LRFD Specification</i>
commercially available? ⁷	yes		yes		no		yes
girder type	box girder	I-girder	box girder	I-girder	box girder	I-girder	all
generally recommended?	no ⁵	yes	no ⁶	yes	no	no ⁴	yes
dominant repair limit state	anchorage design		geometry of strands to be spliced		geometry of girder		new design
damage that may be repaired	Severe II and III		Moderate	Severe I	Severe II		Severe IV
prestress steel that may be replaced	unlimited provided sufficient reserve capacity ¹⁵		no more than 15% of strands to $0.85f_{pu}$		uncertain		unlimited
active or passive? ⁸	active		active (can be installed passively)		passive		-
behavior at ultimate load	excellent		good but limited to $0.85f_{pu}$		uncertain		excellent
resistance to overload	excellent		poor		uncertain		excellent
fatigue performance	excellent		uncertain, thought to be poor		uncertain		excellent
strengthening beyond undamaged capacity?	yes		no		yes		-
combining splice methods	possible with any method		possible with any method		unlikely		-
preload for repair ¹⁰	no		possibly		possibly		-
FRP U-wrap ¹⁰	not required		not feasible	recommended ¹²	not required		-
restore loss of concrete	patch prior to repair		patch following repair		patch prior to repair		-
preload for patch ¹⁰	not required		yes		not required		-
speed of mobilization	moderate		fast		slow		very slow
constructability	difficult	moderate	difficult	moderate	very difficult		difficult
specialized labor required ¹³	no		no		no		no
proprietary tools required	yes, PT jacks		torque wrench		maybe		-
lift equipment required ¹⁴	yes		no		yes		yes
closure below bridge	full carriageway closure		single lane possible		full		full
time for typical repair	1 week		1-2 days		weeks		months
environmental impact of repair process	minimal		dust from concrete chipping		welding		typical erection issues
durability	requires corrosion protection		excellent		requires corrosion protection		excellent
cost	moderate		very low		moderate		high
aesthetics	fair		good	excellent	poor		excellent
retain capacity in event of subsequent impact	none if PT impacted		very good		excellent		-

Notes for Repair Selection Matrix:

1. Preformed strip CFRP materials will always out-perform fabric materials unless the repair must conform to an irregular geometry.
2. NSM repairs will generally only be used for repairs where abrasion resistance is an active concern; this will typically not be the case for impact damage repair.
3. Prestressed CFRP requires external hardware for stressing – this is felt to be impractical for bridge applications; additionally no known systems are commercially available.
4. Due to their complexity and the fact that they are untested, steel jacket repairs are not recommended; it is believed that CFRP repairs address all advantages of steel jackets while overcoming some of their drawbacks.
5. See Section 6.1.
6. See Section 6.4.1.3.
7. There are commercially available systems appropriate for bridge applications on the market in 2012 (although these may be limited).
8. Active repairs can restore some of the lost prestressing force in addition to enhancing load carrying capacity; passive repairs only affect load carrying capacity
9. See Harries et al. (2006) for a discussion of fatigue of bonded CFRP repair systems.
10. Preload may be required for the repair or simply to pre-compress associated concrete patches. U-wraps render the need to pre-compress the patch unnecessary.
11. Although data is inconclusive, U-wraps are widely believed to enhance bond performance or, at the very least to help in arresting or slowing debonding once initiated.
12. See Section 6.4.1.
13. Skills beyond those expected of a typical bridge contractor in 2012.
14. Handling equipment beyond a manlift required.
15. See Section 2.3.2

REFERENCES

- Ahlborn, T.M., Gilbertson, C.G., Aktan, H. and Attanayake, U. 2005 *Condition Assessment and Methods of Abatement of Prestressed Concrete Adjacent Box Beam Deterioration: Phase I*, Michigan Department of Transportation Report RC-1470. 197 pp.
- Alberta Infrastructure and Transportation Department. 2005. *Repair Manual for Concrete Bridge Elements: Version 2.0*, Revised October 2005, Alberta Infrastructure and Transportation Department, Alberta. 27 pp.
- American Association of State Highway and Transportation Officials (AASHTO). 2011. *Guide Manual for Bridge Element Inspection*, 1st Edition, Washington, D.C.
- American Association of State Highway and Transportation Officials (AASHTO). 2011. *Manual for Bridge Evaluation*, 2nd Edition, Washington, D.C.
- American Association of State Highway and Transportation Officials (AASHTO). 2010. *LRFD Bridge Design Specifications*, 4th Edition and Interims, Washington, D.C.
- American Concrete Institute (ACI) and International Concrete Repair Institute (ICRI). 2008. *Concrete Repair Manual*, 3rd Edition, 2077 pp.
- American Concrete Institute (ACI) Committee 440. 2008. *ACI 440.2R-08 Guide for the Design and Construction of Externally Bonded FRP Systems for Strengthening Concrete Structures*, 76 pp.
- American Concrete Institute (ACI) Committee 318. 2011. *ACI 318-11 Building Code Requirements for Structural Concrete*, 503 pp.
- ASTM International. 1999. *C876-91 Standard Test Method for Half-Cell Potentials of Uncoated Reinforcing Steel in Concrete*. (withdrawn 2008). West Conshohocken, PA.
- Casadei, P., Galati, N., Boschetto, G., Tan, K.Y., Nanni, A. and Galeki, G. 2006. "Strengthening of Impacted Prestressed Concrete Bridge I-Girder Using Prestressed Near Surface Mounted C-FRP Bars", *Proceedings of the 2nd International Congress*, Federation Internationale du Beton, Naples, Italy.
- Collins, M.P. and Mitchell, D. 1997. *Prestressed Concrete Structures*, Response Publications, 766 pp.
- Cromwell, J.R., Harries, K.A. and Shahrooz, B.M. 2011 "Environmental Durability of Externally Bonded FRP Materials Intended for Repair of Concrete Structures", *Journal of Construction and Building Materials*, Vol. 25, pp 2528-2539.
- Feldman, L.R., Jirsa, J.O., Fowler, D.W. and Carrasquillo, R.L. 1996. "Current Practice in the Repair of Prestressed Bridge Girders", *Report No. FHWA/TX-96/1370-1*, The University of Texas at Austin, TX. 69 pp.
- Harries, K.A. 2006. "Full-scale Testing Program on De-commissioned Girders from the Lake View Drive Bridge", *Pennsylvania Department of Transportation Report FHWA-PA-2006-008-EMG001*, 158 pp.
- Kasan, J. and Harries, K.A. 2012 (in press), "Analysis of Eccentrically Loaded Adjacent Box Girders", *ASCE Journal of Bridge Engineering*. Vol. 17.
- National Cooperative Highway Research Program (NCHRP). 2008. "Recommended Construction Specifications and Process Control Manual for Repair and Retrofit of Concrete Using Bonded FRP Composites", *NCHRP Report 609*, 68 pp.
- Precast/Prestressed Concrete Institute (PCI). 2006. "Manual for the Evaluation and Repair of Precast, Prestressed Concrete Bridge Products", *Report No. PCI MNL-137-06*. Chicago, IL. 66 pp.
- Prestress Supply, Inc. (PSI) 2011. *Grabb-it Cable Splice Installation Instructions*. Prestress Supply, Inc. <<http://www.prestresssupply.com/LinkClick.aspx?fileticket=Sx6pxCOxgAc%3d&tabid=147>>, (accessed February 9, 2012).

- Shanafelt, G.O. & Horn, W.B. 1985. “Guidelines for Evaluation and Repair of Prestressed Concrete Bridge Members”, *NCHRP Report 280*, Project No. 12-21(1), Transportation Research Board, Washington, D.C., 84 pp.
- Vector Corrosion Technologies (Vector). 2011. *Galvasheild XP Products*. Vector Corrosion Technologies. <<http://www.vector-corrosion.com/systemsservices/galvanic/galvashield%C2%AE-xp-anodes/>>, (accessed April 5, 2012).
- Walther, A. and Hillemeier, B. 2008. “Fast NDT Localization of Prestressing Steel Fractures in P-T Concrete Bridges”, *Proceedings of the 12th International Conference and Exhibition on Structural Faults and Repair*, Edinburgh, Scotland.
- Zobel, R.S. , Jirsa, J.O., Fowler, D.W. and Carrasquillo, R.L. 1996. “Evaluation and Repair of Impact-Damaged Prestressed Concrete Bridge Girders”, *Report No. FHWA/TX-96/1370-3F*, The University of Texas at Austin, Austin, TX.

NOTATION

A_p	area of prestressing strand
b	width of concrete soffit
b_f	width of CFRP provided
b_{fi}	width of individual CFRP strip
c	depth of NSM slot
C	structural capacity
C_0	capacity of undamaged girder
C_D	capacity of damaged girder
C_E	environmental reduction factor (ACI 440-2R 2008)
C_R	capacity of repaired girder
DC, DW, LL, P and IM	load effects (AASHTO <i>LRFD Bridge Design Specifications</i> (2010))
E_f	modulus of elasticity of CFRP
f_c'	compressive strength of concrete
f_f	ultimate tensile strength of CFRP
f_{pu}	ultimate tensile strength of prestressing strand
H	overall depth of prestressed girder
n	number of plies of CFRP
n_{max}	maximum number of severed prestressing strands that can be replaced by CFRP based on its relative contribution to moment capacity
n_{max-PT}	equivalent number of strands whose prestress force can be replaced with PT-CFRP
$n_{spliced}$	number of prestressing strands spliced in a member
RF	rating factor
RF_0	normalized rating factor (Eq. 2) of undamaged girder
RF_D	normalized rating factor (Eq. 2) of damaged girder
RF_R	normalized rating factor (Eq. 2) of repaired girder
t_f	thickness of single CFRP ply or layer
αH	depth from compression resultant to location of CFRP on soffit
βH	depth from compression resultant to centroid of prestressing strands

γ_{DC} , γ_{DW} , γ_P and γ_{LL}	LRFD load factors (Table 6A.4.2.2 of the <i>Evaluation Manual</i> (2011)).
ϵ_{fd}	CFRP debonding strain
ϵ_{fu}	ultimate tensile strain of CFRP
κ	effective prestress factor in CFRP ($0 \leq \kappa \leq 1$)

APPENDIX I: Applicable national and international specifications and guides pertaining to the use and design of FRP composite repairs for strengthening, repair and rehabilitation.

United States:

National Cooperative Highway Research Program (NCHRP) - *Recommended Construction Specifications and Process Control Manual for Repair and Retrofit of Concrete Using Bonded FRP Composites* – Report 609 (2008).

National Cooperative Highway Research Program (NCHRP) - *Bonded Repair and Retrofit of Concrete Structures Using FRP Composites: Recommended Construction Specifications and Process Control Manual* – Report 514 (2008).

American Concrete Institute (ACI) Committee 440 - *ACI 440.2R-08 Guide for the Design and Construction of Externally Bonded FRP Systems for Strengthening Concrete Structures* (2008)

Concrete Repair Manual, 3rd Ed. - published jointly by American Concrete Institute (ACI) and International Concrete Repair Institute (ICRI) (2008)

International (available in English):

Canadian Standards Association (CSA) - S806-02(R2007): *Design and Construction of Building Components with Fibre-Reinforced Polymers* (2007).

Concrete Society (Great Britain) - *Design Guidance for Strengthening Concrete Structures Using Fibre Composite Materials* - Technical Report No. 55 (2004).

International federation for Structural Concrete (fib) (European Union) - *Externally Bonded FRP Reinforcement for RC Structures* (2001).

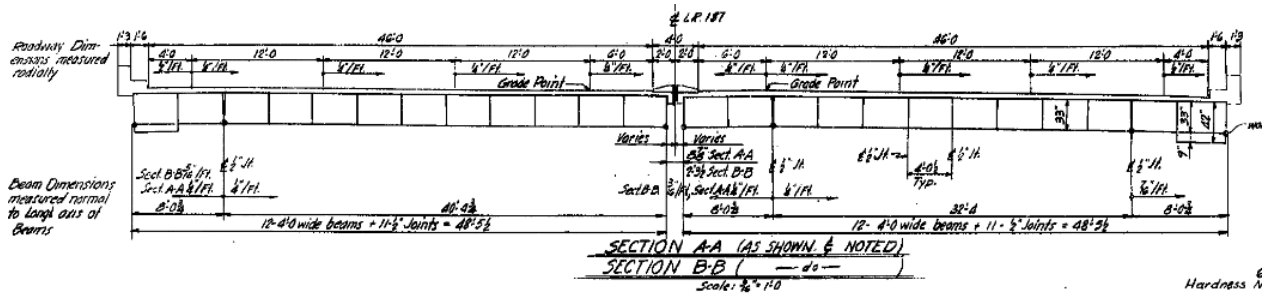
Japan Society of Civil Engineers (JSCE) - Concrete Engineering Series 41: *Recommendations for Upgrading of Concrete Structures with Use of Continuous Fiber Sheets* (1998).

Consiglio Nazionale delle Ricerche (CNR - Italy) - *Guidelines for Design, Execution and Control of Strengthening Interventions by Means of Fibre-reinforced Composites*: CNR-DT200/204 (2004).

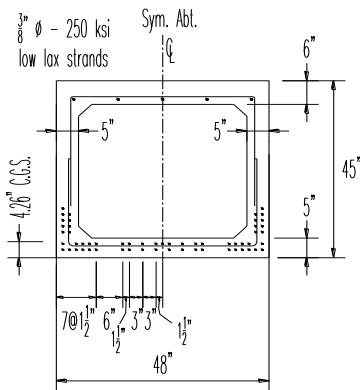
APPENDIX B – AB Prototype Design Example

Prototype Girder AB is based on the exterior girder of a decommissioned adjacent box (AB) girder bridge structure available to the authors. The bridge, erected in 1960, was demolished and replaced in 2011; the fascia beam shown in Figure B1 was provided for testing (Harries 2012). The bridge spans 85'-4" with a skew of 68.5°. The bridge consists of 12 AB girders and has an out-to-out dimension of 49'-6" as shown in Figure B1a. The exterior girder was load tested over an unskewed simple span of 81'-2"; thus all analyses utilized this span. As shown in Figure B1b, each AB girder is 48 in. wide by 42 in. deep. The primary prestressing consists of 57 - 3/8" diameter Grade 250 low-relaxation strands. Based on observed *in situ* conditions and the plan for a load test, a 3 in. composite deck is added to the girder making the overall depth 45 in. Impact damage (approximately 45 in. long) is evident centered approximately 28 ft. from the girder end (Figures B1c and d) at a location above the right lane of the carriageway passing beneath the bridge. The damage shown in Figure B1d, and the identification of this girder is AB 3-2-0.

An example of the determination of capacity of the undamaged (i.e.: AB 0-0-0) and damaged (AB 3-2-0) prototype in addition to the subsequent EB-CFRP repair and assessment of the repaired capacity is provided here.



a) section of AB prototype bridge.



b) AB prototype girder section.



c) prototype girder *in situ* (photo from PennDOT inspection report dated August 8, 2007).



d) impact damage location (boxed location in c).

Figure B1 AB Prototype bridge and girder.

GIVEN CONDITIONS Span Length: Year Built: Concrete Compressive Strength: Prestressing Steel: Mild-reinforcing steel: Number of beams: Skew:	81 ft. simple span c1960 $f'_c = 5.5$ ksi (P/S beam) 3/8 in. diameter, 250 ksi low-lax strands Grade 40 12 0 degrees	
SECTION PROPERTIES 48 in. x 42 in. adjacent box beams: $A_{cg} = 742 \text{ in}^2$ $I_x = 181,800 \text{ in}^4$ $S_b = 9,619 \text{ in}^3$ $S_t = 7,870 \text{ in}^3$	Composite Section Properties: $A_{cg,C} = 886 \text{ in}^2$ $I_{x,C} = 255,300 \text{ in}^4$ $S_{b,C} = 11,197 \text{ in}^3$ $S_{t,C} = 11,500 \text{ in}^3$	calculated from bridge drawings
STEP 1: DEAD LOAD ANALYSIS <i>Components and Attachment: DC (per girder)</i> Beam Self Weight: $\left(\frac{742'}{144} \times 0.150\right) = 0.773\text{k} / \text{ft}$ Composite Deck Slab: $\left(\frac{3'' \times 576''}{144} \times 0.150\right) \frac{1}{12 \text{ girders}} = 0.150\text{k} / \text{ft}$ Parapet (exterior): $\left(\left(\frac{42'' \times 15''}{144} + \frac{16'' \times 9''}{144}\right) \times 0.150\right) \frac{1}{12} = 0.068\text{k} / \text{ft}$ Parapet (center): $\left(\frac{0.5'' \times 24'' \times 8''}{144} \times 0.150\right) \frac{1}{12} = 0.008\text{k} / \text{ft}$ Total DC: 0.999 k/ft Moment due to DC: $M_{DC} = \frac{0.999 \times 81^2}{8} = 819.3 \text{ kft} \leftarrow$ <i>Wearing Surface: DW (per girder)</i> Asphalt thickness = 2 in.: $\left(\frac{2'' \times 576''}{144} \times 0.144\right) \frac{1}{12} = 0.096\text{k} / \text{ft}$ Moment due to DW: $M_{DW} = \frac{0.096 \times 81^2}{8} = 78.7 \text{ kft} \leftarrow$		
STEP 2: LIVE LOAD ANALYSIS Type F cross section; effective shear keys are present COMPUTE LIVE LOAD DISTRIBUTION FACTORS FOR INTERIOR GIRDERS <i>Compute Live Load Distribution Factors</i> $N_b = 12$ $k = 2.5(N_b)^{-0.2} = 2.5(12)^{-0.2} = 1.52 \geq 1.5$		LRFD T4.6.2.2.1-1 LRFD T4.6.2.2.2b-1

<p>For closed thin wall shapes:</p> <p>A_0 = Area enclosed by the centerlines of elements $A_0 = (48-2.5-2.5) \times (45-3-2.5) = 1698.5 \text{ in}^2$ S = length of a side element</p> $J = \frac{4A_0^2}{\sum_t \frac{s}{t}} = \frac{4 \times 1698.5^2}{\frac{(48-5)}{5} + \frac{(48-5)}{6} + \frac{2(45-3-2.5)}{5}} = 365,563 \text{ in}^4$	<p>LRFD C4.6.2.2.1-3</p>
<p>Distribution Factor for Moment – Interior Girders, g_{int} One Lane Loaded:</p> $g_{int,m1} = k \left(\frac{b}{33.3L} \right)^{0.5} \left(\frac{I_x}{J} \right)^{0.25} = 1.52 \left(\frac{48}{33.3(81)} \right)^{0.5} \left(\frac{255,300}{365,563} \right)^{0.25} = 0.185$ <p>Two Lanes Loaded:</p> $g_{int,m2} = k \left(\frac{b}{305} \right)^{0.6} \left(\frac{b}{12L} \right)^{0.2} \left(\frac{I_x}{J} \right)^{0.06} = 1.52 \left(\frac{48}{305} \right)^{0.6} \left(\frac{48}{12(81)} \right)^{0.2} \left(\frac{255,300}{365,563} \right)^{0.06} = 0.269$ <p style="text-align: center;">$g_{int} = g_{int,m2} = 0.269 \leftarrow$</p>	<p>LRFD T4.6.2.2.2b-1</p>
<p>Distribution Factor for Moment – Exterior Girders, g_{ext} One Lane Loaded:</p> $g_{ext,m1} = e \times g_{int,m1}$ $e = 1.125 + \frac{d_e}{30} = 1.125 \geq 1.0 \text{ with } d_e = 0$ $g_{ext,m1} = 1.125 \times 0.185 = 0.208$ <p>Two Lanes Loaded:</p> $e = 1.04 + \frac{d_e}{25} = 1.04 \geq 1.0$ $g_{ext,m2} = 1.04 \times 0.269 = 0.280$ <p style="text-align: center;">$g_{ext} = g_{ext,m2} = 0.280 \leftarrow$</p>	<p>LRFD T4.6.2.2.2d-1</p>
<p>STEP 3: MOMENT DEMAND Maximum Live Load (HL-93) Moment at MIDSPAN Design Lane Load = 523 kft Design Truck = 1182 kft Design Tandem = 545 kft IM = 33%</p> $M_{LL+IM} = LL + TRUCK * IM = 523 + 1.33 \times 1182 = 2095 \text{ kft}$ $g \times M_{LL+IM} = 0.280 \times 2095 = 586.6 \text{ kft}$	<p>LRFD T3.6.2.1-1</p>

STEP 4: COMPUTE NOMINAL FLEXURAL RESISTANCE

$$f_{ps} = f_{pu} \left(1 - k \frac{c}{d_p} \right)$$

$f_{pu} = 250$ ksi and $k = 0.28$ for low lax strands

d_p = distance from extreme compression fiber to C.G. of prestressing tendons

original cg strands = 4.3 in; $d_p = 45 - 4.3 = 40.7$ in

For rectangular section behavior:

with $A_{ps} = 57 \times 0.08 = 4.56 \text{ in}^2$; $b = 48 \text{ in}$; $f'_c = 5.5 \text{ ksi}$; and $\beta = 0.78$

Assume $A_s = A'_s = 0 \text{ in}^2$.

$$c = \frac{A_{ps} f_{ps} - A_s f_s - A'_s f'_s}{0.85 f'_c \beta_1 b + k A_{ps} \frac{f_{pu}}{d_p}} = \frac{4.56 \times 250 - 0}{0.85 \times 5.5 \times 0.78 \times 48 + 0.28 \times 4.56 \times \frac{250}{40.7}} = 6.2 \text{ in}$$

$$a = \beta_1 c = 0.78 \times 6.2 = 4.9 \text{ in} < 6 \text{ in}$$

Therefore, rectangular section behavior assumption is valid

$$f_{ps} = 250 \left(1 - 0.28 \frac{4.9}{40.7} \right) = 241.6 \text{ ksi}$$

$$M_n = A_{ps} f_{ps} \left(d_p - \frac{a}{2} \right) = 4.56 \times 241.6 \left(40.7 - \frac{4.9}{2} \right) \times \frac{1}{12} = 351 \text{ kft}$$

LRFD Eq.
5.7.3.1.1-1
LRFD Eq.
TC5.7.3.1.1-1

LRFD
5.7.2.2
LRFD Eq.
5.7.3.1.1-4

LRFD Eq.
5.7.3.2.2-1

<p>STEP 5: EFFECTIVE PRESTRESS Determine Effective Prestress, P_{pe}: $P_{pe} = A_{ps} \times f_{pe}$ Total Prestress Losses: $\Delta f_{pT} = \Delta f_{pES} + \Delta f_{pLT}$ immediately before transfer Effective Prestress: $f_{pe} = \text{Initial Prestress} - \text{Total Prestress Losses}$ Loss Due to Elastic Shortening, Δf_{pES}: $\Delta f_{pES} = \frac{E_p}{E_{ct}} f_{gcp}$ $f_{gcp} = \frac{P_i}{A} + \frac{P_i e^2}{I} - \frac{M_{De}}{I}$ Initial Prestress immediately prior to transfer = $0.7f_{pu}$. For estimating P_i immediately after transfer, use $0.90(0.7f_{pu})$. $P_i = 0.90 \times (0.7 \times 250) \times 57 \times 0.08 = 718.2$ kips $A_{cg} = 742$ in²; $I_x = 181,800$ in⁴; $e = 22.8 - 4.3 = 18.5$ in M_{sw} = moment due to self-weight of the member $M_{sw} = \frac{0.773 \times 81^2}{8} = 634$ kft $f_{gcp} = \frac{718.2}{742} + \frac{718.2 \times 18.5^2}{181,800} - \frac{634 \times 12 \times 18.5}{181,800} = 0.968 + 1.352 - 0.774 = 1.546$ ksi $K_1 = 1.0$ $w_c = 0.140 + 0.001f'_c = 0.140 + 0.001(5.5) = 0.146$ kcf $E_c = 33000K_1(w_c)^{1.5} \sqrt{f'_c} = 33000 \times 1.0 \times (0.146)^{1.5} \sqrt{5.5} = 4317$ ksi $E_p = 28,500$ ksi $\Delta f_{pES} = \frac{28,500}{4317} \times 1.546 = 10.2$ ksi ←</p>	<p>LRFD Eq. 5.9.5.1-1</p> <p>LRFD Eq. 5.9.5.2.3a-1</p> <p>LRFD T5.9.3-1 LRFD C5.9.5.2.3a</p> <p>LRFD 5.4.2.4 LRFD Eq. 5.4.2.4-1</p>
<p>Approximate Lump Sum Estimate of time-Dependent Losses, Δf_{pLT}: Includes creep, shrinkage and relaxation of steel. $\Delta f_{pLT} = 10.0 + \frac{f_{pi} A_{ps}}{A_{cg,C}} \gamma_h \gamma_{st} + 12.0 \gamma_h \gamma_{st} + \Delta f_{pR}$ with $H = 70\%$; $\gamma_h = 1.7 - 0.01H = 1.7 - 0.01(70) = 1.0$ $\gamma_{st} = \frac{5}{(1 + f'_c)} = \frac{5}{(1 + 5.5)} = 0.77$ Δf_{pR} = an estimate of relaxation loss = 2.5 ksi; $f_{pi} = 0.70 \times 250 = 175$ ksi $\Delta f_{pLT} = 10.0 + \frac{175 \times 4.56}{886} (1.0)(0.77) + 12.0(1.0)(0.77) + 2.5 = 22.4$ ksi Total Prestress Losses, Δf_{pT}: $\Delta f_{pT} = \Delta f_{pES} + \Delta f_{pLT} = 10.2 + 22.4 = 32.6$ ksi ←</p>	<p>LRFD 5.9.5.3-1</p> <p>LRFD Eq. 5.9.5.3-2 LRFD Eq. 5.9.5.3-3</p> <p>LRFD Fig. 5.9.5.1-1</p>

<p>STEP 6: MAXIMUM REINFORCEMENT</p> <p>The factored resistance (ϕ factor) of compression controlled sections shall be reduced in accordance with LRFD 5.5.4.2.1. This approach limits the capacity of over-reinforced (compression controlled) sections.</p> <p>The net tensile strain, ϵ_t, is the tensile strain at the nominal strength determined by strain compatibility using similar triangles.</p> <p>Given an allowable concrete strain of 0.003 and depth to the neutral axis $c = 6.2$ in. and a depth from the extreme concrete compression fiber to the center of gravity of the prestressing strands, $d_p = 40.7$ in.</p> $\frac{\epsilon_c}{c} = \frac{\epsilon_t}{d - c} \rightarrow \frac{0.003}{6.2} = \frac{\epsilon_t}{40.7 - 6.2}$ <p>$\epsilon_t = 0.017 > 0.005$ Therefore the section is tension controlled. $\phi = 1.0$, for flexure</p>	<p>EVAL. MANUAL C6A.5.5 EVAL. MANUAL C5.7.2.1</p> <p>LRFD 5.7.2.1 & 5.5.4.2 LRFD 5.5.4.2</p>
<p>STEP 7: MINIMUM REINFORCEMENT</p> <p>Amount of reinforcement to develop M_r equal to the lesser of $1.33M_u$ or $1.2M_{cr}$</p> $M_r = M_n = 3511 \text{ kft}$ $M_u = 1.75(586.6) + 1.25(819.3) + 1.5(78.7) = 2169 \text{ kft}$ $1.33M_u = 1.33(2169) = 2885 \text{ kft}$ $M_r > 1.33M_u \text{ (3511 kft > 2885 kft)}$ <p>Therefore, minimum reinforcement check is satisfied</p>	<p>LRFD 5.7.3.3.2 LRFD 5.7.3.2</p>
<p>STEP 8: LOAD RATING OF UNDAMAGED GIRDER RF_0;</p> <p>Assemble γ factors for both Inventory and Operating Levels:</p> <p>Inventory: $\gamma_{DC} = 1.25$; $\gamma_{DW} = 1.50$; $\gamma_{LL+IM} = 1.75$ Operating: $\gamma_{DC} = 1.25$; $\gamma_{DW} = 1.50$; $\gamma_{LL+IM} = 1.35$ Assume $P = 0$ k.</p> <p>Inventory:</p> $RF = \frac{\phi C - \gamma_{DC}DC - \gamma_{DW}DW \pm \gamma_P P}{\gamma_{LL}(LL + IM)} = \frac{3511 - 1.25(819.3) - 1.50(78.7)}{1.75(586.6)} = 2.31 \leftarrow$ <p>Operating:</p> $RF = 2.31 \frac{1.75}{1.35} = 2.99 \leftarrow$	<p>EVAL. MANUAL T6A.4.2.2-1</p> <p>EVAL. MANUAL Eq. 6A.4.2.1-1</p>

<p>STEP 9: DAMAGED CAPACITY</p> <p>Determining the damaged capacity will follow the same procedure the nominal capacity, but will include the effects of the lost strands at the damaged section.</p> $f_{ps} = f_{pu} \left(1 - k \frac{c}{d_p} \right)$ <p>$f_{pu} = 250$ ksi and $k = 0.28$ for low lax strands $d_p =$ distance from extreme compression fiber to C.G. of prestressing tendons $d_p = 45 - 4.5 = 40.5$ in</p> <p>5 strands (of 57) have been lost, therefore: $A_{ps} = 52 \times 0.08 = 4.16 \text{ in}^2$</p> $c = \frac{A_{ps} f_{ps} - A_s f_s - A'_s f'_s}{0.85 f'_c \beta_1 b + k A_{ps} \frac{f_{pu}}{d_p}} = \frac{4.16 \times 250 - 0}{0.85 \times 5.5 \times 0.78 \times 48 + 0.28 \times 4.16 \times \frac{250}{40.5}} = 5.70 \text{ in}$ <p>$a = \beta_1 c = 0.78 \times 5.70 = 4.4 \text{ in} < 6 \text{ in}$ Therefore, rectangular section behavior assumption is valid</p> $f_{ps} = 250 \left(1 - 0.28 \frac{4.4}{40.5} \right) = 242.4 \text{ ksi}$ $M_n = A_{ps} f_{ps} \left(d_p - \frac{a}{2} \right) = 4.16 \times 242.4 \left(40.5 - \frac{4.4}{2} \right) \times \frac{1}{12} = 3218 \text{ kft}$	<p>LRFD Eq. 5.7.3.1.1-1</p> <p>LRFD Eq. 5.7.3.1.1-4</p> <p>LRFD Eq. 5.7.3.2.2-1</p>
<p>STEP 10: LOAD RATING OF DAMAGED GIRDER, RF_D;</p> <p>Inventory:</p> $RF = \frac{\phi C - \gamma_{DC} DC - \gamma_{DW} DW \pm \gamma_P P}{\gamma_{LL} (LL + IM)} = \frac{3218 - 1.25(819.3) - 1.50(78.7)}{1.75(586.6)} = 2.02$ <p>Operating:</p> $RF = 2.02 \frac{1.75}{1.35} = 2.62 \text{ OK } \leftarrow$	<p>EVAL. MANUAL Eq. 6A.4.2.1-1</p>

<p>STEP 13: ASSEMBLE BEAM PROPERTIES</p> <p>Assemble geometric and material properties for the beam and FRP system. An estimate of the area of FRP (A_f) is chosen here. If the section capacity does not meet the demand after the completion of all steps in this procedure, the FRP area is iterated upon.</p>	
$E_c = 4.23 \times 10^6 \text{ psi}$ $A_{cg,C} = 886 \text{ in}^2$ $h = 45 \text{ in}$ $y_t = 22.2 \text{ in}$ $y_b = 22.8 \text{ in}$ $e = 18.3 \text{ in}$ $I_{x,C} = 255,300 \text{ in}^4$ $r = 17.0 \text{ in}$ $A_{ps} = 4.16 \text{ in}^2$ $E_{ps} = 28.5 \times 10^6 \text{ psi}$	$\epsilon_{pe} = 0.0050$ $P_e = 592,400 \text{ lb}$ $cg \text{ strands} = 4.5 \text{ in}$ $d_p = 40.5 \text{ in}$ $f_{tu} = 406 \text{ ksi}$ $\epsilon_{fu} = 0.017 \text{ in/in}$ $A_f = 0.463 \text{ in}^2 \text{ (assumed)}$ $E_f = 23.2 \times 10^6 \text{ psi}$ $d_f = 45.0235 \text{ in}$
<p>STEP 14: DETERMINE STATE OF STRAIN ON BEAM SOFFIT, AT TIME OF FRP INSTALLATION</p> <p>The existing strain on the beam soffit is calculated. It is assumed that the beam is uncracked and the only load applied at the time of FRP installation is dead load. M_D is changed to reflect a different moment applied during CFRP installation. If the beam is cracked, appropriate cracked section properties may be used. However, a cracked prestressed beam may not be a good candidate for repair due to the excessive loss of prestress required to result in cracking.</p> $\epsilon_{bi} = \frac{-P_e}{E_c A_{cg}} \left(1 + \frac{ey_b}{r^2} \right) + \frac{M_D y_b}{E_c I_g}$ $= \frac{-592400}{4.23 \times 10^6 \times 886} \left(1 + \frac{18.3 \times 22.8}{(17.0)^2} \right) + \frac{((819.3 + 78.7) \times 12000) \times 22.8}{4.23 \times 10^6 \times 255300} = -0.0002 \text{ in/in}$	
<p>STEP 15: ESTIMATE DEPTH TO NEUTRAL AXIS</p> <p>Any value can be assumed, but a reasonable initial estimate of c is $\sim 0.2h$. The value of c is adjusted to affect equilibrium.</p> $c = 0.2 \times 45 \text{ in} = 9.0 \text{ in}$	

STEP 16: DETERMINE DESIGN STRAIN OF THE FRP SYSTEM

The limiting strain in the FRP system is calculated based on three possible failure modes: FRP debonding (Eq. 10-2), FRP rupture (Eq. 10-16) and FRP strain corresponding to prestressing steel rupture (Eq. 10-17). The strain in the FRP system is limited to the minimum value obtained from (Eq. 10-2), (Eq. 10-16) and (Eq. 10-17).

FRP Strain corresponding to FRP Debonding:

$$\varepsilon_{fd} = 0.083 \sqrt{\frac{f'_c}{nE_f t_f}} = 0.083 \sqrt{\frac{5500}{1 \times 23.2 \times 10^6 \times 0.047}} = 0.0059 \text{ in/in}$$

ACI
Eq. 10-2

FRP Strain corresponding to Concrete Crushing:

$$\varepsilon_{fe} = \frac{\varepsilon_{cu}(d_f - c)}{c} - \varepsilon_{bi} = \frac{0.003 \times (45.0235 - 9.0)}{9.0} - (-0.0002) = 0.0122 \text{ in/in} \leq \varepsilon_{fd}$$

ACI
Eq. 10-16

FRP Strain corresponding to PS Steel Rupture:

$$\varepsilon_{fe} = \frac{(\varepsilon_{pu} - \varepsilon_{pi})(d_f - c)}{(d_p - c)} - \varepsilon_{bi} \leq \varepsilon_{fd}$$

ACI
Eq. 10-17

where

$$\varepsilon_{pi} = \frac{P_e}{E_p A_p} + \frac{P_e}{E_c A_c} \left(1 + \frac{e^2}{r^2} \right) = \frac{592400}{28.5 \times 10^6 \times 4.16} + \frac{592400}{4.23 \times 10^6 \times 886} \left(1 + \frac{(18.3)^2}{(17.0)^2} \right) = 0.0053 \text{ in/in}$$

ACI
Eq. 10-18

$$\varepsilon_{fe} = \frac{(0.035 - 0.0053)(45.0235 - 9.0)}{(40.5 - 9.0)} - (-0.0002) = 0.0341 \text{ in/in}$$

Therefore, the limiting strain in the FRP system is $\varepsilon_{fd} = 0.0059$ in/in and the anticipated mode of failure is FRP debonding.

STEP 17: CALCULATE THE STRAIN IN THE EXISTING PRESTRESSING STEEL

The strain in the prestressing steel can be calculated with the following expression:

$$\varepsilon_{ps} = \varepsilon_{pe} + \frac{P_e}{E_c A_c} \left(1 + \frac{e^2}{r^2} \right) + \varepsilon_{pnet} \leq 0.035$$

ACI
Eq. 10-22

Prestressing Steel Strain corresponding to concrete crushing:

$$\varepsilon_{pnet} = 0.003 \frac{(d_p - c)}{c} = 0.003 \frac{(40.5 - 9.0)}{9.0} = 0.0105 \text{ in/in}$$

ACI
Eq. 10-23a

$$\varepsilon_{ps} = 0.0059 + \frac{592400}{4.23 \times 10^6 \times 886} \times \left(1 + \frac{(18.3)^2}{(17.0)^2} \right) + 0.0105 = 0.0158 \text{ in/in} \leq 0.035$$

Prestressing Steel Strain corresponding to FRP rupture or debonding:

$$\varepsilon_{pnet} = (\varepsilon_{fe} + \varepsilon_{bi}) \frac{(d_p - c)}{(d_f - c)} = (0.0059 - 0.0002) \frac{(40.5 - 9.0)}{(45.0235 - 9.0)} = 0.0050 \text{ in/in}$$

ACI
Eq. 10-23b

$$\varepsilon_{ps} = 0.0059 + \frac{592400}{4.23 \times 10^6 \times 886} \times \left(1 + \frac{(18.3)^2}{(17.0)^2} \right) + 0.0050 = 0.0104 \text{ in/in} \leq 0.035$$

Therefore, FRP debonding represents the expected failure mode of the system and $\varepsilon_{ps} = 0.0104$ in/in.

<p>STEP 18: CALCULATE STRESS LEVEL IN THE PRESTRESSING STEEL AND FRP</p> $f_{ps} = 28500 \times \epsilon_{ps} \quad (\text{when } \epsilon_{ps} \leq 0.0076)$ <p style="text-align: center;">or</p> $f_{ps} = 250 - \frac{0.04}{\epsilon_{ps} - 0.0064} \quad (\text{when } \epsilon_{ps} \geq 0.0076)$ $\epsilon_{ps} = 0.0104 > 0.0076 \text{ therefore use } f_{ps} = 250 - \frac{0.04}{(0.0104) - 0.0064} = 239.9 \text{ ksi}$ $f_{fe} = E_f \times \epsilon_{fe} = 23.2 \times 10^6 \times 0.0059 = 136.9 \text{ ksi} \leftarrow$	<p style="text-align: center;">ACI Eq. 10-24</p> <p style="text-align: center;">ACI Eq. 10-9</p>
<p>STEP 19: CALCULATE EQUIVALENT STRESS BLOCK PARAMETERS From strain compatibility, the strain in the concrete at failure can be calculated as:</p> $\epsilon_c = (\epsilon_{fe} + \epsilon_{bi}) \frac{c}{(d_f - c)} = (0.0059 - 0.0002) \times \frac{9.0}{45.0235 - 9.0} = 0.0014 \text{ in/in}$ <p>The strain ϵ'_c corresponding to f'_c is calculated as:</p> $\epsilon'_c = \frac{1.7f'_c}{E_c} = \frac{1.7 \times 5500}{4.23 \times 10^6} = 0.0022 \text{ in/in}$ <p>Using ACI 318-08, the equivalent stress block factors can be calculated as:</p> $\beta_1 = \frac{4\epsilon'_c - \epsilon_c}{6\epsilon'_c - 2\epsilon_c} = \frac{4 \times 0.0022 - 0.0014}{6 \times 0.0022 - 2 \times 0.0014} = 0.712$ $\alpha_1 = \frac{3\epsilon'_c \epsilon_c - \epsilon_c^2}{3\beta_1 \epsilon_c'^2} = \frac{3 \times 0.0022 \times 0.0014 - (0.0014)^2}{3 \times 0.712 \times (0.0022)^2} = 0.703$	
<p>STEP 20: CALCULATE THE INTERNAL FORCE RESULTANTS</p> $c = \frac{A_p \times f_{ps} + A_f \times f_{fe}}{\alpha_1 \times f'_c \times \beta_1 \times b} = \frac{4.16 \times 239.9 + 0.463 \times 136.9}{0.703 \times (5500/1000) \times 0.712 \times 48} = 8.03 \text{ in} > 6 \text{ in} \leftarrow$ <p>c is found to be greater than the height of the flange (6 in), so c needs to be recalculated accounting for the neutral axis extending into the web. This calculation yields c = 15.2 in.</p>	<p style="text-align: center;">ACI Eq. 10-25</p>
<p>STEP 21: ACHIEVE EQUILIBRIUM The value of c calculated in Step 20 must be equal to that of the c value assumed in Step 15. If not, the value of c must be iterated upon until these values are equal.</p> <p>Upon iteration of c, flexural strength must be checked as in Step 22. If the calculated strength is not sufficient, the area of FRP reinforcement must be increased and Step 15 through Step 22 must be repeated, as is the case with this design. A_f is increased to 1.389 in^2 and the process repeated.</p> <p>By iteration, $c = 11.5 \text{ in.} \leftarrow$</p>	

STEP 22: CALCULATE THE FLEXURAL STRENGTH CORRESPONDING TO THE PRESTRESSING STEEL AND FRP COMPONENTS

The nominal capacity of the section is found as:

$$M_n = M_{np} = \psi M_{nf}$$

The corresponding contribution of prestressing steel and FRP, respectively, are found as:

$$M_{np} = A_p f_{ps} \left(d_p - \frac{\beta_1 c}{2} \right) = 4.16 \times 239.7 \times \left(40.5 - \frac{0.737 \times 11.5}{2} \right) = 36159 \text{ kin}$$

$$M_{nf} = A_f f_{fe} \left(d_f - \frac{\beta_1 c}{2} \right) = 1.389 \times 136.8 \times \left(45.0235 - \frac{0.737 \times 11.5}{2} \right) = 7750 \text{ kin}$$

$$\psi = 0.85$$

The nominal section capacity of the *repaired girder* is:

$$M_n = M_R = (36159 + (0.85)7750) \frac{1}{12} = 3562 \text{ kft} \leftarrow$$

ACI
Eq. 10-26

STEP 23: CALCULATE REPAIR RATING FACTOR, RF_R

The area of CFRP provided, A_f, is adjusted and the procedure repeated until the desired flexural capacity is achieved. M_{REP} = 3562 kft.

Inventory:

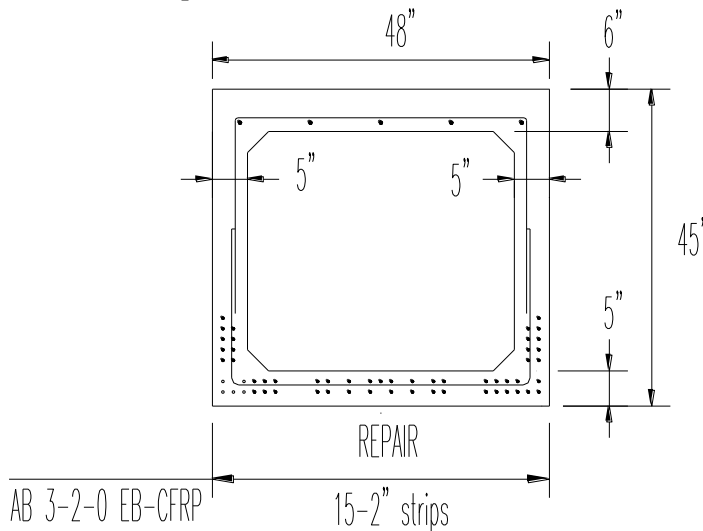
$$RF_R = \frac{\phi C - \gamma_{DC} DC - \gamma_{DW} DW \pm \gamma_P P}{\gamma_{LL} (LL + IM)} = \frac{3562 - 1.25(819.3) - 1.50(78.7)}{1.75(586.6)} = 2.36 \leftarrow$$

Operating:

$$RF_D = 2.36 \frac{1.75}{1.35} = 3.06 \leftarrow$$

STEP 24: DESIGN SUMMARY

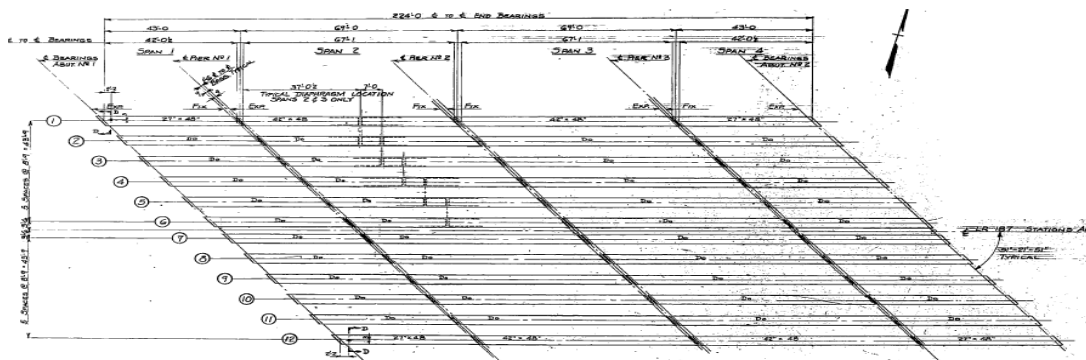
Use 15 – 2 in wide CFRP strips.



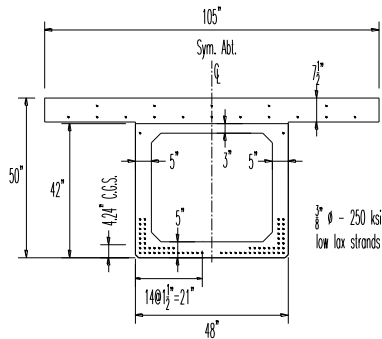
APPENDIX C – SB Prototype Design Example

Prototype Girder SB is based on the exterior girder of a decommissioned spread box (SB) girder bridge structure (Figure C1) available to the authors. The bridge, erected in 1962, was demolished and replaced in 2011; the fascia beam shown in Figure C1c was provided for eventual testing. The bridge spans 69 feet with a skew of 51.5° . Each bridge in the dual span structure consists of 6 – 48 by 42 in. box girders located 8'-9" on center and has an out-to-out dimension of 50'-8". The composite deck is 7.5 in. deep and a 0.5 in. haunch is provided making the overall SB girder depth 50 in. (Figure C1b). The primary prestressing consists of 68 - $3/8"$ diameter Grade 250 low-relaxation strands. As seen in Figure C1c, Impact damage is evident at a location above the carriageway passing beneath the bridge. This damage has been exacerbated by the fact that it is immediately beneath an active deck drain (Figure C1d). The damage shown in Figure C1 and the identification of this girder is SB 4-2-0 (see Section 2.1.3 for explanation of method of damage identification). This girder also showed significant spalling and corrosion at its pier support; the extent of this damage would likely render this span unreparable. However, for the sake of this study, this additional deterioration is not considered.

An example of the determination of capacity of the undamaged (i.e.: SB 0-0-0) and damaged (SB 6-4-0) prototype in addition to the subsequent PT-CFRP repair and assessment of the repaired capacity is provided here.



a) plan of SB prototype bridge.



b) SB prototype girder section.



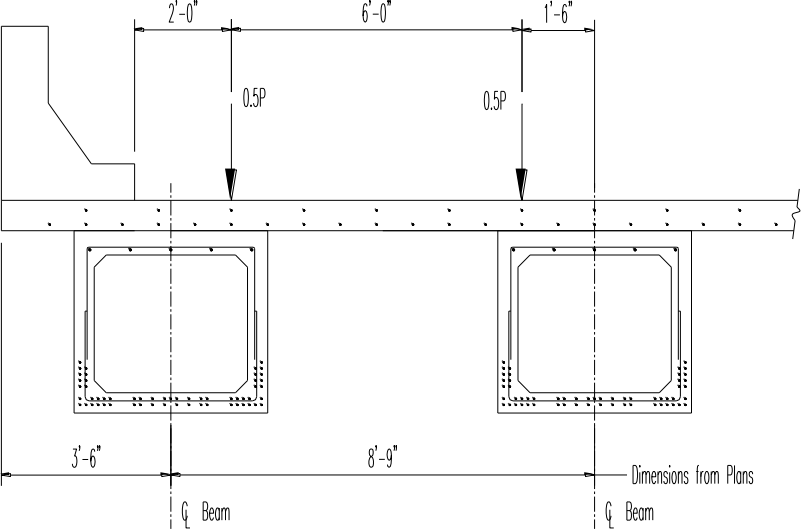
c) prototype girder *in situ* (photo from PennDOT inspection report dated August 8, 2007).



d) impact damage location (boxed location in c).

Figure C1 SB Prototype bridge and girder.

GIVEN CONDITIONS Span Length: Year Built: Concrete Compressive Strength: Prestressing Steel: Mild-reinforcing steel: Skew:	69 ft. simple span c1962 $f'_c = 5.5$ ksi (P/S beam) 3/8 in. diameter, 250 ksi low-lax strands Grade 40 0 degrees	
SECTION PROPERTIES 48 in. x 42 in. adjacent box beams: $A_{cg} = 742 \text{ in}^2$ $I_x = 181,200 \text{ in}^4$ $S_b = 9,679 \text{ in}^3$ $S_t = 7,783 \text{ in}^3$	Composite Section Properties: $A_{cg,C} = 1553 \text{ in}^2$ $I_{x,C} = 543,000 \text{ in}^4$ $S_{b,C} = 17,075 \text{ in}^3$ $S_{t,C} = 29,835 \text{ in}^3$	calculated from bridge drawings
STEP 1: DEAD LOAD ANALYSIS <i>Components and Attachment: DC (per girder)</i> Beam Self Weight: $\left(\frac{742 \text{ in}^2}{144} \times 0.150 \right) = 0.773 \text{ k / ft}$ Composite Deck Slab: $\left(\left(\frac{7.5' \times 105'}{144} + \frac{0.5' \times 48''}{144} \right) \times 0.150 \right) = 0.845 \text{ k / ft}$ Parapet (exterior): $\left(2 \times \left(\frac{42'' \times 15''}{144} + \frac{16'' \times 9''}{144} \right) \times 0.150 \right) \frac{1}{6} = 0.269 \text{ k / ft}$ Total DC: 1.887 k/ft Moment due to DC: $M_{DC} = \frac{1.887 \times 69^2}{8} = 1123.0 \text{ kft} \leftarrow$ <i>Wearing Surface: DW (per girder)</i> Asphalt thickness = 2 in.: $\left(\frac{2'' \times 59 \text{ ft}}{144} \times 0.144 \right) \frac{1}{6} = 0.197 \text{ k / ft}$ Moment due to DW: $M_{DW} = \frac{0.197 \times 69^2}{8} = 117.2 \text{ kft} \leftarrow$		

<p>STEP 2: LIVE LOAD ANALYSIS Type B cross section</p> <p>Distribution Factor for Moment – Interior Girders, g_{int} One Lane Loaded: $g_{int,m1} = \left(\frac{S}{3.0}\right)^{0.35} \left(\frac{S \times d}{12.0L^2}\right)^{0.25} = \left(\frac{8.75}{3.0}\right)^{0.35} \left(\frac{8.75 \times 48}{12.0 \times 69^2}\right)^{0.25} = 0.426$ </p> <p>Two Lanes Loaded: $g_{int,m1} = \left(\frac{S}{6.3}\right)^{0.6} \left(\frac{S \times d}{12.0L^2}\right)^{0.125} = \left(\frac{8.75}{6.3}\right)^{0.6} \left(\frac{8.75 \times 48}{12.0 \times 69^2}\right)^{0.125} = 0.659$ </p> <p>Lever Rule:</p>  <p>Using lever rule $g = 0.514$; smaller of the two is permitted to be used $g_{int} = g_{int,m2} = 0.514 \leftarrow$</p>	<p>LRFD T4.6.2.2.1-1</p> <p>LRFD T4.6.2.2.2b-1</p>
<p>Distribution Factor for Moment – Exterior Girders, g_{ext} One Lane Loaded: Using lever rule $g = 0.514$ with one lane loaded $m = 1.2$ $g_{ext,m1} = 0.514 \times 1.2 = 0.617$ </p> <p>Two Lanes Loaded: $e = 1.04 + \frac{d_e}{25} = 1.07 \geq 1.0 \quad \text{with } d_e = 0.75'$ $g_{ext,m2} = 1.07 \times 0.514 = 0.550$ $g_{ext} = g_{ext,m2} = 0.617 \leftarrow$ </p>	<p>LRFD T4.6.2.2.2d-1</p>
<p>STEP 3: MOMENT DEMAND Maximum Live Load (HL-93) Moment at MIDSPAN Design Lane Load = 381 kft Design Truck = 954 kft Design Tandem = 812 kft IM = 33%</p> <p>$M_{LL+IM} = LL + TRUCK * IM = 381 + 1.33 \times 954 = 1650 \text{ kft}$ $g \times M_{LL+IM} = 0.617 \times 1650 = 1018 \text{ kft}$</p>	<p>LRFD T3.6.2.1-1</p>

STEP 4: COMPUTE NOMINAL FLEXURAL RESISTANCE

$$f_{ps} = f_{pu} \left(1 - k \frac{c}{d_p} \right)$$

$f_{pu} = 250$ ksi and $k = 0.28$ for low lax strands

d_p = distance from extreme compression fiber to C.G. of prestressing tendons

original cg strands = 4.2 in; $d_p = 50 - 4.2 = 45.8$ in

For rectangular section behavior:

with $A_{ps} = 68 \times 0.08 = 5.44 \text{ in}^2$; $b = 105 \text{ in}$; $f'_c = 4.0 \text{ ksi}$; and $\beta = 0.85$

Assume $A_s = A'_s = 0 \text{ in}^2$.

$$c = \frac{A_{ps} f_{ps} - A_s f_s - A'_s f'_s}{0.85 f'_c \beta_1 b + k A_{ps} \frac{f_{pu}}{d_p}} = \frac{5.44 \times 250 - 0}{0.85 \times 4.0 \times 0.85 \times 105 + 0.28 \times 5.44 \times \frac{250}{45.8}} = 4.4 \text{ in}$$

$$a = \beta_1 c = 0.85 \times 4.4 = 3.7 \text{ in} < 7.5 \text{ in}$$

Therefore, rectangular behavior assumption is valid.

$$f_{ps} = 250 \left(1 - 0.28 \frac{4.4}{45.8} \right) = 243.3 \text{ ksi}$$

$$M_n = A_{ps} f_{ps} \left(d_p - \frac{a}{2} \right) = 5.44 \times 243.3 \left(45.8 - \frac{3.7}{2} \right) \times \frac{1}{12} = 4847 \text{ kft}$$

LRFD Eq.
5.7.3.1.1-1
LRFD Eq.
TC5.7.3.1.1-1

LRFD
5.7.2.2
LRFD Eq.
5.7.3.1.1-4

LRFD Eq.
5.7.3.2.2-1

<p>STEP 5: EFFECTIVE PRESTRESS Determine Effective Prestress, P_{pe}: $P_{pe} = A_{ps} \times f_{pe}$ Total Prestress Losses: $\Delta f_{pT} = \Delta f_{pES} + \Delta f_{pLT}$ immediately before transfer Effective Prestress: $f_{pe} = \text{Initial Prestress} - \text{Total Prestress Losses}$ Loss Due to Elastic Shortening, Δf_{pES}: $\Delta f_{pES} = \frac{E_p}{E_{ct}} f_{gcp}$ $f_{gcp} = \frac{P_i}{A} + \frac{P_i e^2}{I} - \frac{M_{sw} e}{I}$ Initial Prestress immediately prior to transfer = $0.7f_{pu}$. For estimating P_i immediately after transfer, use $0.90(0.7f_{pu})$. $P_i = 0.90 \times (0.7 \times 250) \times 68 \times 0.08 = 856.8$ kips $A_{cg} = 742 \text{ in}^2$; $I_x = 181,200 \text{ in}^4$; $e = 18.7 - 4.3 = 18.4$ in M_{sw} = moment due to self-weight of the member $M_{sw} = \frac{0.773 \times 69^2}{8} = 460$ kft $f_{gcp} = \frac{856.8}{742} + \frac{856.8 \times 18.4^2}{181,200} - \frac{460 \times 12 \times 18.4}{181,200} = 1.155 + 1.601 - 0.561 = 2.195$ ksi $K_1 = 1.0$ $w_c = 0.140 + 0.001f'_c = 0.140 + 0.001(5.5) \text{ kcf} = 0.146$ kcf $E_c = 33000K_1(w_c)^{1.5} \sqrt{f'_c} = 33000 \times 1.0 \times (0.146)^{1.5} \sqrt{5.5} = 4317$ ksi $E_p = 28,500$ ksi $\Delta f_{pES} = \frac{28,500}{4317} \times 2.195 = 14.5$ ksi ←</p>	<p>LRFD Eq. 5.9.5.1-1</p> <p>LRFD Eq. 5.9.5.2.3a-1</p> <p>LRFD T5.9.3-1 LRFD C5.9.5.2.3a</p> <p>LRFD 5.4.2.4 LRFD Eq. 5.4.2.4-1</p>
<p>Approximate Lump Sum Estimate of time-Dependent Losses, Δf_{pLT}: Includes creep, shrinkage and relaxation of steel. $\Delta f_{pLT} = 10.0 + \frac{f_{pi} A_{ps}}{A_{cg,C}} \gamma_h \gamma_{st} + 12.0 \gamma_h \gamma_{st} + \Delta f_{pR}$ with $H = 70\%$; $\gamma_h = 1.7 - 0.01H = 1.7 - 0.01(70) = 1.0$ $\gamma_{st} = \frac{5}{(1 + f'_c)} = \frac{5}{(1 + 5.5)} = 0.77$ Δf_{pR} = an estimate of relaxation loss = 2.5 ksi; $f_{pi} = 0.70 \times 250 = 175$ ksi $\Delta f_{pLT} = 10.0 + \frac{175 \times 5.44}{1553} (1.0)(0.77) + 12.0(1.0)(0.77) + 2.5 = 22.2$ ksi Total Prestress Losses, Δf_{pT}: $\Delta f_{pT} = \Delta f_{pES} + \Delta f_{pLT} = 14.5 + 22.2 = 36.7$ ksi ←</p>	<p>LRFD 5.9.5.3-1</p> <p>LRFD Eq. 5.9.5.3-2 LRFD Eq. 5.9.5.3-3</p> <p>LRFD Fig. 5.9.5.1-1</p>

<p>STEP 6: MAXIMUM REINFORCEMENT</p> <p>The factored resistance (ϕ factor) of compression controlled sections shall be reduced in accordance with LRFD 5.5.4.2.1. This approach limits the capacity of over-reinforced (compression controlled) sections.</p> <p>The net tensile strain, ϵ_t, is the tensile strain at the nominal strength determined by strain compatibility using similar triangles.</p> <p>Given an allowable concrete strain of 0.003 and depth to the neutral axis $c = 4.4$ in. and a depth from the extreme concrete compression fiber to the center of gravity of the prestressing strands, $d_p = 45.8$ in.</p> $\frac{\epsilon_c}{c} = \frac{\epsilon_t}{d - c} \rightarrow \frac{0.003}{4.4} = \frac{\epsilon_t}{45.8 - 4.4}$ <p>$\epsilon_t = 0.028 > 0.005$ Therefore the section is tension controlled. $\phi = 1.0$, for flexure</p>	<p>EVAL. MANUAL C6A.5.5 EVAL. MANUAL C5.7.2.1</p> <p>LRFD 5.7.2.1 & 5.5.4.2 LRFD 5.5.4.2</p>
<p>STEP 7: MINIMUM REINFORCEMENT</p> <p>Amount of reinforcement to develop M_r equal to the lesser of $1.33M_u$ or $1.2M_{cr}$</p> $M_r = M_n = 4847 \text{ kft}$ $M_u = 1.75(1018) + 1.25(1123) + 1.5(117.2) = 3361 \text{ kft}$ $1.33M_u = 1.33(3361) = 4470 \text{ kft}$ $M_r > 1.33M_u (4847 \text{ kft} > 4470 \text{ kft})$ <p>Therefore, minimum reinforcement check is satisfied</p>	<p>LRFD 5.7.3.3.2 LRFD 5.7.3.2</p>
<p>STEP 8: LOAD RATING OF UNDAMAGED GIRDER RF_0;</p> <p>Assemble γ factors for both Inventory and Operating Levels:</p> <p>Inventory: $\gamma_{DC} = 1.25$; $\gamma_{DW} = 1.50$; $\gamma_{LL+IM} = 1.75$ Operating: $\gamma_{DC} = 1.25$; $\gamma_{DW} = 1.50$; $\gamma_{LL+IM} = 1.35$ Assume $P = 0$ k.</p> <p>Inventory:</p> $RF = \frac{\phi C - \gamma_{DC} DC - \gamma_{DW} DW \pm \gamma_P P}{\gamma_{LL} (LL + IM)} = \frac{4847 - 1.25(1123) - 1.50(117.2)}{1.75(1018)} = 1.83 \leftarrow$ <p>Operating:</p> $RF = 1.83 \frac{1.75}{1.35} = 2.37 \leftarrow$	<p>EVAL. MANUAL T6A.4.2.2-1</p> <p>EVAL. MANUAL Eq. 6A.4.2.1-1</p>

<p>STEP 9: DAMAGED CAPACITY</p> <p>Determining the damaged capacity will follow the same procedure the nominal capacity, but will include the effects of the lost strands at the damaged section.</p> $f_{ps} = f_{pu} \left(1 - k \frac{c}{d_p} \right)$ <p>$f_{pu} = 250$ ksi and $k = 0.28$ for low lax strands $d_p =$ distance from extreme compression fiber to C.G. of prestressing tendons $d_p = 50 - 4.6 = 45.4$ in 10 strands (of 68) have been lost, therefore: $A_{ps} = 58 \times 0.08 = 4.64$ in²</p> $c = \frac{A_{ps}f_{ps} - A_s f_s - A'_s f'_s}{0.85f'_c \beta_1 b + k A_{ps} \frac{f_{pu}}{d_p}} = \frac{4.64 \times 250 - 0}{0.85 \times 4.0 \times 0.85 \times 105 + 0.28 \times 4.64 \times \frac{250}{45.4}} = 3.7 \text{ in}$ <p>$a = \beta_1 c = 0.85 \times 3.7 = 3.2$ in < 6 in Therefore, rectangular section behavior assumption is valid</p> $f_{ps} = 250 \left(1 - 0.28 \frac{3.7}{45.4} \right) = 244.2 \text{ ksi}$ $M_n = A_{ps} f_{ps} \left(d_p - \frac{a}{2} \right) = 4.64 \times 244.2 \left(45.4 - \frac{3.2}{2} \right) \times \frac{1}{12} = 4136 \text{ kft}$	<p>LRFD Eq. 5.7.3.1.1-1</p> <p>LRFD Eq. 5.7.3.1.1-4</p> <p>LRFD Eq. 5.7.3.2.2-1</p>
<p>STEP 10: LOAD RATING OF DAMAGED GIRDER, RF_D;</p> <p>Inventory:</p> $RF = \frac{\phi C - \gamma_{DC} DC - \gamma_{DW} DW \pm \gamma_P P}{\gamma_{LL} (LL + IM)} = \frac{4136 - 1.25(1123) - 1.50(117.2)}{1.75(1018)} = 1.43 \leftarrow$ <p>Operating:</p> $RF = 1.43 \frac{1.75}{1.35} = 1.85 \leftarrow$	<p>EVAL. MANUAL Eq. 6A.4.2.1-1</p>

<p>Service III Limit State for Inventory Level:</p> $RF = \frac{f_R - (\gamma_D)(f_d)}{(\gamma_L)(f_{LL+IM})}$ <p>Flexural Resistance:</p> $f_R = f_{pb} + \text{allowable tensile stress}$ <p>f_{pb} = compressive stress due to effective prestress</p> $P_{pe} = (175-52.1) \times 58 \times 0.08 = 570.3 \text{ kips}$ $e = 31.8 - 4.6 = 27.2 \text{ in}$ $f_{pb} = \frac{P_{pe}}{A_{eg,C}} + \frac{P_{pe}e}{S_{b,C}} = \frac{570.3}{1553} + \frac{570.3 \times 27.2}{17075} = 1.18 \text{ ksi}$ <p>Allowable Tensile Stress = $0.19\sqrt{f'_c} = 0.19\sqrt{5.5} = 0.45 \text{ ksi}$</p> $f_R = 1.18 + 0.45 = 1.63 \text{ ksi}$ <p>Dead Load Stress:</p> $f_{DC} = \frac{1123 \times 12}{17075} = 0.79 \text{ ksi}; \quad f_{DW} = \frac{117.2 \times 12}{17075} = 0.08 \text{ ksi}$ <p>Total $f_d = 0.87 \text{ ksi}$</p> <p>Live Load Stress:</p> $f_{LL} = \frac{1018 \times 12}{17075} = 0.72 \text{ ksi}$ <p>$\gamma_L = 0.80; \gamma_D = 1.0$</p> $RF = \frac{1.63 - (1.0)(0.87)}{(0.8)(0.72)} = 1.32 > 1.0 \quad \mathbf{OK} \leftarrow$	<p>EVAL. MANUAL 6A.5.4.1</p> <p>LRFD T5.9.4.2.2-1</p>
<p>Legal Load Rating:</p> <p>Although this particular structure has all rating factors greater than unity, the example is continued in order to describe a repair methodology and subsequent re-rating of the repaired structure. The repair design proceeds as follows.</p>	
<p>STEP 11: VIABILITY OF EXTERNAL REPAIRS</p> <p>The residual capacity of the unstrengthened girder (i.e.: the damaged capacity C) should safely resist an expected nominal load. For an external repair to be viable:</p> $C \geq 1.1DC - 1.1DW - 0.75(LL + IM) = 1.1(1123) - 1.1(117.2) - 0.75(1018) = 2127.7 \text{ kft}$ $4136 \text{ kft} \geq 1427.8 \text{ kft} \quad \mathbf{OK} \leftarrow$	<p>Eq. 3</p>

<p>STEP 12: DEFINE OBJECTIVE OF REPAIR</p> <p>Restore undamaged moment capacity: $M_n = 4847$ k-ft Capacity of damaged girder without repair: $M_{6.4.0} = 4136$ k-ft Capacity will be restored with the use of externally bonded CFRP plates.</p> <p>All equation, figure and table references for FRP repair design are from ACI 440.2R-08, unless otherwise noted.</p>	
<p>STEP 13: ASSEMBLE BEAM PROPERTIES</p> <p>Assemble geometric and material properties for the beam and FRP system. An estimate of the area of FRP (A_f) is chosen here. If the section capacity does not meet the demand after the completion of all steps in this procedure, the FRP area is iterated upon.</p>	
$E_c = 3.60 \times 10^6 \text{ psi}$ $A_{cg,C} = 1553 \text{ in}^2$ $h = 50 \text{ in}$ $y_t = 18.2 \text{ in}$ $y_b = 31.8 \text{ in}$ $e = 27.2 \text{ in}$ $I_{x,C} = 543,000 \text{ in}^4$ $r = 18.7 \text{ in}$ $A_{ps} = 4.64 \text{ in}^2$ $E_{ps} = 28.5 \times 10^6 \text{ psi}$ $\epsilon_{pe} = 0.0049$	$P_e = 641,700 \text{ lb}$ $cg \text{ strands} = 4.6 \text{ in}$ $d_p = 45.4 \text{ in}$ $A_f = 0.444 \text{ in}^2 \text{ (assumed using 2 strips)}$ $P_{fip} = 87,490 \text{ lb}$ $E_f = 23.2 \times 10^6 \text{ psi}$ $t_f = 0.094 \text{ in}$ $d_f = 50.047 \text{ in}$ $e_f = 31.8 \text{ in}$ $f_{fu} = 406 \text{ ksi}$ $\epsilon_{fu} = 0.017 \text{ in/in}$
<p>STEP 14: DETERMINE STATE OF STRAIN ON BEAM SOFFIT, AT TIME OF FRP INSTALLATION</p> <p>The existing strain on the beam soffit is calculated. It is assumed that the beam is uncracked and the only load applied at the time of FRP installation is dead load. M_D is changed to reflect a different moment applied during CFRP installation. If the beam is cracked, appropriate cracked section properties may be used. However, a cracked prestressed beam may not be a good candidate for repair due to the excessive loss of prestress required to result in cracking.</p> $\epsilon_{bi} = \frac{-P_e}{E_c A_{cg}} \left(1 + \frac{ey_b}{r^2} \right) + \frac{M_{SW} y_b}{E_c I_g} + \frac{-P_{fip}}{E_c A_{cg}} \left(1 + \frac{e_f y_b}{r^2} \right)$ $= \frac{-641700}{3.60 \times 10^6 \times 1553} \left(1 + \frac{27.2 \times 31.8}{(18.7)^2} \right) + \frac{((1123 + 117.2) \times 12000) \times 31.8}{3.60 \times 10^6 \times 543000} + \frac{-87490}{3.60 \times 10^6 \times 1553} \left(1 + \frac{31.8 \times 31.8}{(18.7)^2} \right) = -0.0002 \text{ in / in}$	
<p>STEP 15: ESTIMATE DEPTH TO NEUTRAL AXIS</p> <p>Any value can be assumed, but a reasonable initial estimate of c is $\sim 0.2h$. The value of c is adjusted to affect equilibrium.</p> $c = 0.1 \times 50 \text{ in} = 5.0 \text{ in}$	

STEP 16: DETERMINE DESIGN STRAIN OF THE FRP SYSTEM

The limiting strain in the FRP system is calculated based on three possible failure modes: FRP debonding (Eq. 10-2), FRP rupture (Eq. 10-16) and FRP strain corresponding to prestressing steel rupture (Eq. 10-17). The strain in the FRP system is limited to the minimum value obtained from (Eq. 10-2), (Eq. 10-16) and (Eq. 10-17).

FRP Strain corresponding to FRP Debonding:

$$\begin{aligned}\epsilon_{fd} &= 0.083 \sqrt{\frac{f'_c}{nE_f t_f}} + 0.50 \epsilon_{fu} \\ &= 0.083 \sqrt{\frac{5500}{1 \times 23.2 \times 10^6 \times 0.094}} + 0.50(0.017) = 0.0127 \text{ in/in}\end{aligned}$$

ACI
Eq. 10-2

FRP Strain corresponding to Concrete Crushing:

$$\epsilon_{fe} = \frac{\epsilon_{cu}(d_f - c)}{c} - \epsilon_{bi} = \frac{0.003 \times (50.047 - 5.0)}{5.0} - (-0.0002) = 0.0272 \text{ in/in} \leq \epsilon_{fd}$$

ACI
Eq. 10-16

FRP Strain corresponding to PS Steel Rupture:

$$\epsilon_{fe} = \frac{(\epsilon_{pu} - \epsilon_{pi})(d_f - c)}{(d_p - c)} - \epsilon_{bi} \leq \epsilon_{fd}$$

ACI
Eq. 10-17

where

$$\begin{aligned}\epsilon_{pi} &= \frac{P_e}{E_p A_p} + \frac{P_e}{E_c A_c} \left(1 + \frac{e^2}{r^2}\right) = \frac{641700}{28.5 \times 10^6 \times 4.64} + \frac{641700}{3.60 \times 10^6 \times 1553} \left(1 + \frac{(27.2)^2}{(18.7)^2}\right) = 0.0052 \text{ in/in} \\ \epsilon_{fe} &= \frac{(0.035 - 0.0052)(50.047 - 5.0)}{(45.4 - 5.0)} - (-0.0002) = 0.0334 \text{ in/in}\end{aligned}$$

ACI
Eq. 10-18

Therefore, the limiting strain in the FRP system is $\epsilon_{fd} = 0.0127$ in/in and the anticipated mode of failure is FRP debonding.

STEP 17: CALCULATE THE STRAIN IN THE EXISTING PRESTRESSING STEEL

The strain in the prestressing steel can be calculated with the following expression:

$$\epsilon_{ps} = \epsilon_{pe} + \frac{P_e}{E_c A_c} \left(1 + \frac{e^2}{r^2}\right) + \epsilon_{pnet} \leq 0.035$$

ACI
Eq. 10-22

Prestressing Steel Strain corresponding to concrete crushing:

$$\epsilon_{pnet} = 0.003 \frac{(d_p - c)}{c} = 0.003 \frac{(45.4 - 5.0)}{5.0} = 0.0242 \text{ in/in}$$

ACI
Eq. 10-23a

$$\epsilon_{ps} = 0.0049 + \frac{641700}{3.60 \times 10^6 \times 1553} \times \left(1 + \frac{(27.2)^2}{(18.7)^2}\right) + 0.0242 = 0.0294 \text{ in/in} \leq 0.035$$

Prestressing Steel Strain corresponding to FRP rupture or debonding:

$$\epsilon_{pnet} = (\epsilon_{fe} + \epsilon_{bi}) \frac{(d_p - c)}{(d_f - c)} = (0.0127 - 0.0002) \frac{(45.4 - 5.0)}{(54.047 - 5.0)} = 0.0112 \text{ in/in}$$

ACI
Eq. 10-23b

$$\epsilon_{ps} = 0.0049 + \frac{641700}{3.60 \times 10^6 \times 1553} \times \left(1 + \frac{(27.2)^2}{(18.7)^2}\right) + 0.0112 = 0.0164 \text{ in/in} \leq 0.035$$

Therefore, FRP debonding represents the expected failure mode of the system and $\epsilon_{ps} = 0.0164$ in/in.

<p>STEP 18: CALCULATE STRESS LEVEL IN THE PRESTRESSING STEEL AND FRP</p> $f_{ps} = 28500 \times \epsilon_{ps} \quad (\text{when } \epsilon_{ps} \leq 0.0076)$ <p style="text-align: center;">or</p> $f_{ps} = 250 - \frac{0.04}{\epsilon_{ps} - 0.0064} \quad (\text{when } \epsilon_{ps} \geq 0.0076)$ <p>$\epsilon_{ps} = 0.0164 > 0.0076$ therefore use $f_{ps} = 250 - \frac{0.04}{(0.0164) - 0.0064} = 246.0 \text{ ksi}$</p> $f_{fe} = E_f \times \epsilon_{fe} = 23.2 \times 10^6 \times 0.0127 = 294.6 \text{ ksi} \leftarrow$	<p>ACI Eq. 10-24</p> <p>ACI Eq. 10-9</p>
<p>STEP 19: CALCULATE EQUIVALENT STRESS BLOCK PARAMETERS From strain compatibility, the strain in the concrete at failure can be calculated as:</p> $\epsilon_c = (\epsilon_{fe} + \epsilon_{bi}) \frac{c}{(d_f - c)} = (0.0127 - 0.0002) \times \frac{5.0}{50.047 - 5.0} = 0.0014 \text{ in/in}$ <p>The strain ϵ'_c corresponding to f'_c is calculated as:</p> $\epsilon'_c = \frac{1.7f'_c}{E_c} = \frac{1.7 \times 4000}{3.60 \times 10^6} = 0.0019 \text{ in/in}$ <p>Using ACI 318-08, the equivalent stress block factors can be calculated as:</p> $\beta_1 = \frac{4\epsilon'_c - \epsilon_c}{6\epsilon'_c - 2\epsilon_c} = \frac{4 \times 0.0019 - 0.0014}{6 \times 0.0019 - 2 \times 0.0014} = 0.721$ $\alpha_1 = \frac{3\epsilon'_c \epsilon_c - \epsilon_c^2}{3\beta_1 \epsilon_c'^2} = \frac{3 \times 0.0019 \times 0.0014 - (0.0014)^2}{3 \times 0.721 \times (0.0019)^2} = 0.771$	
<p>STEP 20: CALCULATE THE INTERNAL FORCE RESULTANTS</p> $c = \frac{A_p \times f_{ps} + A_f \times f_{fe}}{\alpha_1 \times f'_c \times \beta_1 \times b} = \frac{4.64 \times 246.0 + 0.444 \times 294.6}{0.771 \times (4000/1000) \times 0.721 \times 105} = 5.5 \text{ in} \leftarrow$	<p>ACI Eq. 10-25</p>
<p>STEP 21: ACHIEVE EQUILIBRIUM The value of c calculated in Step 20 must be equal to that of the c value assumed in Step 15. If not, the value of c must be iterated upon until these values are equal.</p> <p>Upon iteration of c, flexural strength must be checked as in Step 22. If the calculated strength is not sufficient, the area of FRP reinforcement must be increased and Step 15 through Step 22 must be repeated, as is the case with this design. Therefore, A_f is increased to 0.888 in^2 (4 strips) and the process repeated.</p> <p>By iteration, $c = 5.6 \text{ in.} \leftarrow$</p>	

STEP 22: CALCULATE THE FLEXURAL STRENGTH CORRESPONDING TO THE PRESTRESSING STEEL AND FRP COMPONENTS

The nominal capacity of the section is found as:

$$M_n = M_{np} = \psi M_{nf}$$

The corresponding contribution of prestressing steel and FRP, respectively, are found as:

$$M_{np} = A_p f_{ps} \left(d_p - \frac{\beta_1 c}{2} \right) = 4.64 \times 246.0 \times \left(45.4 - \frac{0.731 \times 5.5}{2} \right) = 49512 \text{ kin}$$

$$M_{nf} = A_f f_{fe} \left(d_f - \frac{\beta_1 c}{2} \right) = 0.888 \times 293.6 \times \left(50.047 - \frac{0.731 \times 5.5}{2} \right) = 12533 \text{ kin}$$

$$\psi = 0.85$$

The nominal section capacity of the *repaired girder* is:

$$M_n = M_R = (49512 + (0.85)12533) \frac{1}{12} = 5014 \text{ kft} \leftarrow$$

ACI
Eq. 10-26

STEP 23: CALCULATE REPAIR RATING FACTOR, RF_R

The area of CFRP provided, A_f, is adjusted and the procedure repeated until the desired flexural capacity is achieved. M_R = 5014 kft.

Inventory:

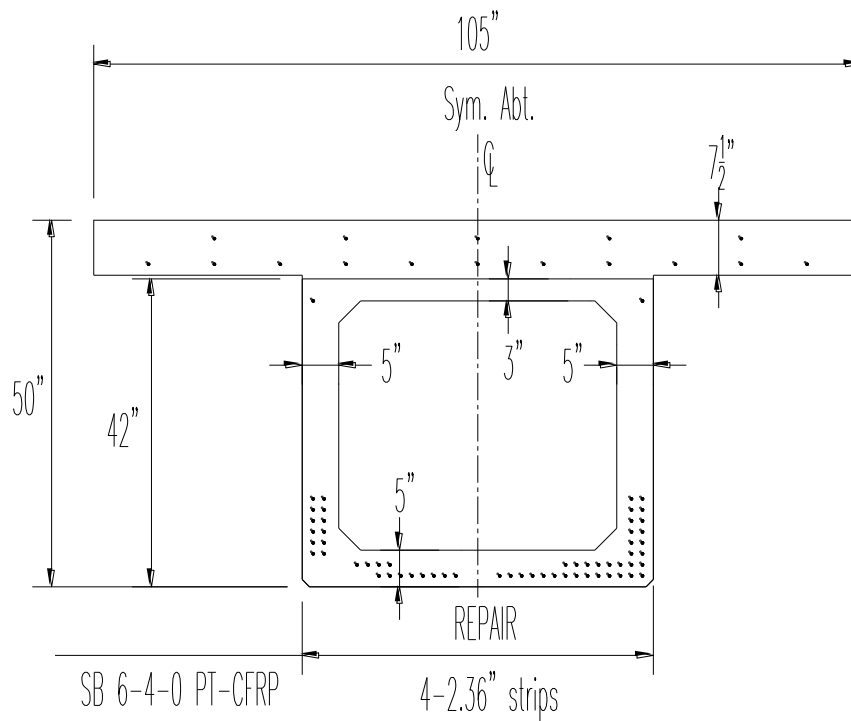
$$RF_R = \frac{\phi C - \gamma_{DC} DC - \gamma_{DW} DW \pm \gamma_P P}{\gamma_{LL} (LL + IM)} = \frac{5014 - 1.25(1123) - 1.50(117.2)}{1.75(1018)} = 1.93 \leftarrow$$

Operating:

$$RF_D = 1.93 \frac{1.75}{1.35} = 2.50 \leftarrow$$

STEP 24: DESIGN SUMMARY

Use 4 – 2.36 in wide PT-CFRP strips, stressed to 197.2 ksi (43.75 kips).



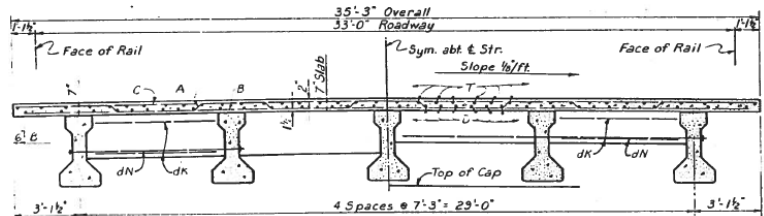
APPENDIX D1 – IB Prototype Design Example

Prototype Girder IB is based on the exterior girder of a bridge impact and repair reported by Yang et al. (2011). The bridge was erected in 1967, and impacted and repaired in 2004. The bridge, shown in Figure D1, spans 84'-8" and consists of 5 - 40 in. deep Texas 'Type C' girders (Figure D1c) spaced at 7'-3". The composite deck is 7 in. deep. The primary prestressing consists of 32 - 0.5" diameter Grade 270 low-relaxation strands, 8 of which are harped as shown in Figure D1c. The resulting strand profile results in a 10 foot length of girder having 32 straight strands at midspan. The damaged region was restricted to about an 8.5 ft length and was located near a diaphragm (Figure D1d). The damage shown in Figure D1d and the identification of this girder is IB 3-3-2.

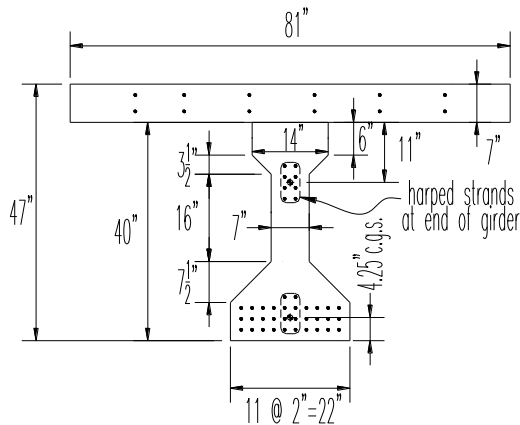
An example of the determination of capacity of the undamaged (i.e.: IB 0-0-0) and damaged (IB 3-3-2) prototype in addition to the subsequent NSM-CFRP repair and assessment of the repaired capacity is provided here. A summary of the actual repair executed for this structure, reported by Yang et al. (2011) is summarized in Section 2.2.3.2.



a) IB Prototype bridge.



b) section of IB prototype bridge.



c) IB girder section.



d) damage to exterior girder.

Figure D1 IB prototype bridge and girder (Yang et al. 2011).

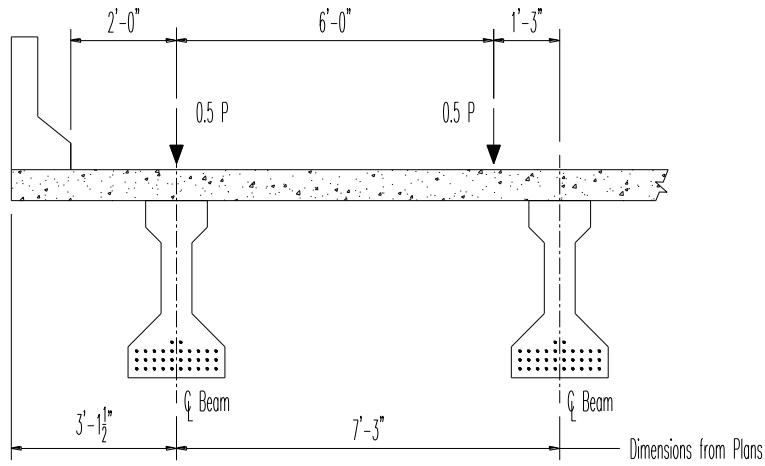
GIVEN CONDITIONS Span Length: Year Built: Concrete Compressive Strength: Prestressing Steel: Mild-reinforcing steel: Number of beams: Skew:	84'-8" c1967 6.8 ksi 1/2 in. diameter, 270 ksi 40 ksi 5 0 degrees	
SECTION PROPERTIES I girder: $A_{cg} = 495.5 \text{ in}^2$ $I_x = 82,759 \text{ in}^4$ $S_b = 4848 \text{ in}^3$ $S_t = 3609 \text{ in}^3$ $f'_c = 5.5 \text{ ksi (deck)}$ $f'_c = 6.8 \text{ ksi (girder)}$	Composite Section Properties: $A_{cg,C} = 1062.5 \text{ in}^2$ $I_{x,C} = 269,785 \text{ in}^4$ $S_{b,C} = 8655 \text{ in}^3$ $S_{t,C} = 17043 \text{ in}^3$	calculated from bridge drawings
STEP 1: DEAD LOAD ANALYSIS <i>Components and Attachment: DC1 (per girder)</i> Beam Self Weight: $\left(\frac{495.5 \text{ in}^2}{144} \times 0.150 \right) = 0.516 \text{ k/ft}$ Composite Deck Slab: $\left(\frac{7 \text{ in} \times 81 \text{ in}}{144} \times 0.150 \right) = 0.591 \text{ k/ft}$ $M = \frac{(0.516 + 0.591) \times 84.67^2}{8} = 992.0 \text{ kft}$ Diaphragm: $\left(\left(\frac{8483 \text{ in}^2 \times 8 \text{ in}}{1728} \right) 0.150 \right) = 5.891 \text{ kips}$ $M = 5.891 \times \frac{84.67}{4} = 124.7 \text{ kft}$ Moment due to DC1: $M_{DC} = 992.0 + 124.7 = 1116.7 \text{ kft} \leftarrow$ <i>Components and Attachment: DC2 (per girder)</i> Barrier: $(2 \times 0.500) \frac{1}{5 \text{ girders}} = 0.2 \text{ k/ft}$ Moment due to DC2: $M_{DC} = \frac{0.2 \times 84.67^2}{8} = 179.2 \text{ kft} \leftarrow$ <i>Wearing Surface: DW (per girder)</i> Asphalt thickness = 2 in.: $\left(\frac{2 \text{ in} \times 396 \text{ in}}{144} \times 0.144 \right) \frac{1}{5 \text{ girders}} = 0.158 \text{ k/ft}$ Moment due to DW: $M_{DW} = \frac{0.158 \times 84.67^2}{8} = 141.6 \text{ kft} \leftarrow$		

<p>STEP 2: LIVE LOAD ANALYSIS Type K cross section</p> <p>COMPUTE LIVE LOAD DISTRIBUTION FACTORS FOR INTERIOR GIRDERS <i>Compute Live Load Distribution Factors</i></p> $n = \frac{E_B}{E_D} = \frac{4.85 \times 10^3 \text{ ksi}}{4.36 \times 10^3 \text{ ksi}} = 1.11$ $e_g = 40 - 17.07 + \frac{7}{2} = 26.43$ $K_g = n(I + Ae_g^2) = 1.11(269785 + 1062.5(26.43)^2) = 1123308 \text{ in}^4$	<p>LRFD T4.6.2.2.1-1</p> <p>LRFD 4.6.2.2.1-1</p> <p>LRFD 4.6.2.2.1-2</p>
<p><i>Distribution Factor for Moment – Interior Girders, g_{int}</i> One Lane Loaded:</p> $g_{int,m1} = 0.06 + \left(\frac{S}{14}\right)^{0.4} \left(\frac{S}{L}\right)^{0.3} \left(\frac{K_g}{12.0Lt_s^3}\right)^{0.1}$ $= 0.06 + \left(\frac{7.25}{14}\right)^{0.4} \left(\frac{7.25}{84.67}\right)^{0.3} \left(\frac{1123308}{12.0(84.67)(7)^3}\right)^{0.1} = 0.473$ <p>Two Lanes Loaded:</p> $g_{int,m2} = 0.075 + \left(\frac{S}{9.5}\right)^{0.6} \left(\frac{S}{L}\right)^{0.2} \left(\frac{K_g}{12.0Lt_s^3}\right)^{0.1}$ $= 0.075 + \left(\frac{7.25}{9.5}\right)^{0.6} \left(\frac{7.25}{84.67}\right)^{0.2} \left(\frac{1123308}{12.0(84.67)(7)^3}\right)^{0.1} = 0.660$ $g_{int} = g_{int,m2} = 0.660 \leftarrow$	<p>LRFD T4.6.2.2.2b-1</p>

Distribution Factor for Moment – Exterior Girders, g_{ext}

One Lane Loaded:

Lever Rule:



Using lever rule $g = 0.586$
 with one lane loaded $m = 1.2$
 $g_{ext,m1} = 0.586 \times 1.2 = 0.703$

Two Lanes Loaded:

$$e = 0.77 + \frac{d_e}{9.1} = 0.990 \text{ with } d_e = 2.0$$

$$g_{ext,m2} = 0.990 \times 0.660 = 0.653$$

$$g_{ext} = g_{ext,m1} = 0.703 \leftarrow$$

LRFD
T4.6.2.2.2d-1

STEP 3: MOMENT DEMAND

Maximum Live Load (HL-93) Moment at MIDSPAN

Design Lane Load = 574 kft

Design Truck = 1244 kft

Design Tandem = 1008 kft

IM = 33%

$$M_{LL+IM} = LL + TRUCK * IM = 574 + 1.33 \times 1244 = 2229 \text{ kft}$$

$$g \times M_{LL+IM} = 0.703 \times 2229 = 1567 \text{ kft}$$

LRFD
T3.6.2.1-1

STEP 4: COMPUTE NOMINAL FLEXURAL RESISTANCE

$$f_{ps} = f_{pu} \left(1 - k \frac{c}{d_p} \right)$$

$f_{pu} = 270$ ksi and $k = 0.28$ for low lax strands

d_p = distance from extreme compression fiber to C.G. of prestressing tendons

original cg strands = 4.25 in; $d_p = 47 - 4.25 = 42.75$ in

For rectangular section behavior:

with $A_{ps} = 32 \times 0.153 = 4.90 \text{ in}^2$; $b = 81$ in; $f'_c = 5.5$ ksi; and $\beta = 0.78$

Assume $A_s = A'_s = 0 \text{ in}^2$.

$$c = \frac{A_{ps} f_{ps} - A_s f_s - A'_s f'_s}{0.85 f'_c \beta_1 b + k A_{ps} \frac{f_{pu}}{d_p}} = \frac{4.90 \times 270 - 0}{0.85 \times 5.5 \times 0.78 \times 81 + 0.28 \times 4.90 \times \frac{270}{42.75}} = 4.35 \text{ in}$$

$$a = \beta_1 c = 0.78 \times 4.35 = 3.39 \text{ in} < 7 \text{ in}$$

Therefore, rectangular section behavior assumption is valid

$$f_{ps} = 270 \left(1 - 0.28 \frac{4.35}{42.75} \right) = 262.3 \text{ ksi}$$

$$M_n = A_{ps} f_{ps} \left(d_p - \frac{a}{2} \right) = 4.90 \times 262.3 \left(42.75 - \frac{3.39}{2} \right) \times \frac{1}{12} = 4397 \text{ kft}$$

LRFD Eq.
5.7.3.1.1-1
LRFD Eq.
TC5.7.3.1.1-1

LRFD
5.7.2.2
LRFD Eq.
5.7.3.1.1-4

LRFD Eq.
5.7.3.2.2-1

<p>STEP 5: EFFECTIVE PRESTRESS Determine Effective Prestress, P_{pe}: $P_{pe} = A_{ps} \times f_{pe}$ Total Prestress Losses: $\Delta f_{pT} = \Delta f_{pES} + \Delta f_{pLT}$ immediately before transfer Effective Prestress: $f_{pe} = \text{Initial Prestress} - \text{Total Prestress Losses}$ Loss Due to Elastic Shortening, Δf_{pES}: $\Delta f_{pES} = \frac{E_p}{E_{ct}} f_{gcp}$ $f_{gcp} = \frac{P_i}{A} + \frac{P_i e^2}{I} - \frac{M_D e}{I}$ Initial Prestress immediately prior to transfer = $0.7f_{pu}$. For estimating P_i immediately after transfer, use $0.90(0.7f_{pu})$. $P_i = 0.90 \times (0.7 \times 270) \times 32 \times 0.153 = 832.8$ kips $A_{cg} = 495.5 \text{ in}^2$; $I_x = 82,759 \text{ in}^4$; $e = 17.07 - 4.25 = 12.82$ in M_D = moment due to self-weight of the member $M_D = \frac{0.516 \times 84.6^2}{8} = 462.4$ kft $f_{gcp} = \frac{832.8}{495.5} + \frac{832.8 \times 12.82^2}{82,759} - \frac{462.4 \times 12 \times 12.82}{82,759} = 1.681 + 1.654 - 0.860 = 2.475$ ksi $K_1 = 1.0$ $w_c = 0.140 + 0.001f'_c = 0.140 + 0.001(6.8) = 0.147$ kcf $E_c = 33000K_1(w_c)^{1.5} \sqrt{f'_c} = 33000 \times 1.0 \times (0.147)^{1.5} \sqrt{6.8} = 4850$ ksi $E_p = 28,500$ ksi $\Delta f_{pES} = \frac{28,500}{4850} \times 2.475 = 14.5$ ksi ←</p>	<p>LRFD Eq. 5.9.5.1-1</p> <p>LRFD Eq. 5.9.5.2.3a-1</p> <p>LRFD T5.9.3-1 LRFD C5.9.5.2.3a</p> <p>LRFD 5.4.2.4 LRFD Eq. 5.4.2.4-1</p>
<p>Approximate Lump Sum Estimate of time-Dependent Losses, Δf_{pLT}: Includes creep, shrinkage and relaxation of steel. $\Delta f_{pLT} = 10.0 + \frac{f_{pi} A_{ps}}{A_{cg,C}} \gamma_h \gamma_{st} + 12.0 \gamma_h \gamma_{st} + \Delta f_{pR}$ with $H = 70\%$; $\gamma_h = 1.7 - 0.01H = 1.7 - 0.01(70) = 1.0$ $\gamma_{st} = \frac{5}{(1 + f'_c)} = \frac{5}{(1 + 6.8)} = 0.64$ Δf_{pR} = an estimate of relaxation loss = 2.5 ksi; $f_{pi} = 0.70 \times 270 = 189$ ksi $\Delta f_{pLT} = 10.0 + \frac{189 \times 4.90}{1062.5} (1.0)(0.64) + 12.0(1.0)(0.64) + 2.5 = 20.7$ ksi Total Prestress Losses, Δf_{pT}: $\Delta f_{pT} = \Delta f_{pES} + \Delta f_{pLT} = 14.5 + 20.7 = 35.2$ ksi ←</p>	<p>LRFD 5.9.5.3-1</p> <p>LRFD Eq. 5.9.5.3-2 LRFD Eq. 5.9.5.3-3</p> <p>LRFD Fig. 5.9.5.1-1</p>

<p>STEP 6: MAXIMUM REINFORCEMENT</p> <p>The factored resistance (ϕ factor) of compression controlled sections shall be reduced in accordance with LRFD 5.5.4.2.1. This approach limits the capacity of over-reinforced (compression controlled) sections.</p> <p>The net tensile strain, ϵ_t, is the tensile strain at the nominal strength determined by strain compatibility using similar triangles.</p> <p>Given an allowable concrete strain of 0.003 and depth to the neutral axis $c = 4.35$ in. and a depth from the extreme concrete compression fiber to the center of gravity of the prestressing strands, $d_p = 42.75$ in.</p> $\frac{\epsilon_c}{c} = \frac{\epsilon_t}{d-c} \rightarrow \frac{0.003}{4.35} = \frac{\epsilon_t}{42.75-4.35}$ <p>$\epsilon_t = 0.026 > 0.005$ Therefore the section is tension controlled. $\phi = 1.0$, for flexure</p>	<p>EVAL. MANUAL C6A.5.5 EVAL. MANUAL C5.7.2.1</p> <p>LRFD 5.7.2.1 & 5.5.4.2 LRFD 5.5.4.2</p>
<p>STEP 7: MINIMUM REINFORCEMENT</p> <p>Amount of reinforcement to develop M_r equal to the lesser of $1.33M_u$ or $1.2M_{cr}$</p> $M_r = M_n = 4397 \text{ kft}$ $M_u = 1.75(1567) + 1.25(1116.7 + 179.2) + 1.5(141.6) = 4575 \text{ kft}$ $1.33M_u = 1.33(4575) = 6085 \text{ kft}$ <p>$M_r < 1.33M_u$ (4397 kft < 6085 kft) NO GOOD</p> $M_{cr} = S_c (f_r + f_{cpe}) - M_{dnc} \left(\frac{S_c}{S_{nc}} - 1 \right) \geq S_c f_r$ $f_r = 0.37 \sqrt{f'_c} = 0.37 \sqrt{6.8} = 0.965$ $f_{pe} = (0.70 * 270) - 35.2 = 153.8 \text{ ksi}$ $P_{pe} = A_{ps} f_{pe} = 153.8 \times 32 \times 0.153 = 753.0 \text{ kips}$ $f_{pb} = \frac{P_{pe}}{A} + \frac{P_{pe} e}{S_b} = \frac{753.0}{495.5} + \frac{753.0 \times 12.82}{4848} = 3.5 \text{ ksi}$ $M_{cr} = \frac{8758}{12} (0.965 + 3.5) - 1116.7 \left(\frac{8655}{4848} - 1 \right) = 2351 \text{ kft}$ $S_c f_r = \frac{8655}{12} (0.965) = 696 \text{ kft}$ <p>$M_{cr} > S_c f_r$ (2351 kft > 696 kft) so M_{cr} governs $1.2M_{cr} = 1.2 \times 2351 \text{ kft} = 2821 \text{ kft}$ $1.2M_{cr} < 1.33M_u$ (2821 kft < 6085 kft) Therefore $1.2M_{cr}$ governs $M_r > 1.2 M_{cr}$ (4397 kft > 2821 kft) Therefore, minimum reinforcement check is satisfied</p>	<p>LRFD 5.7.3.3.2 LRFD 5.7.3.2 LRFD 5.7.3.3.2-1</p> <p>LRFD 5.4.2.6</p>

STEP 8: LOAD RATING OF UNDAMAGED GIRDER RF_0 ;

Assemble γ factors for both Inventory and Operating Levels:

Inventory: $\gamma_{DC} = 1.25$; $\gamma_{DW} = 1.50$; $\gamma_{LL+IM} = 1.75$

Operating: $\gamma_{DC} = 1.25$; $\gamma_{DW} = 1.50$; $\gamma_{LL+IM} = 1.35$

Assume $P = 0$ k.

Inventory:

$$RF = \frac{\phi C - \gamma_{DC} DC - \gamma_{DW} DW \pm \gamma_P P}{\gamma_{LL} (LL + IM)} = \frac{4397 - 1.25(12959) - 1.50(141.6)}{1.75(1567)} = 0.94 \leftarrow$$

Operating:

$$RF = 0.94 \frac{1.75}{1.35} = 1.22 \leftarrow$$

This structure has an inventory rating factor below unity. This is not an uncommon result for older bridges - designed using the *Standard Specification* - when assessed using the LRFR approach.

The prototype bridge was designed using the AASTHO 1965 *Standard Specifications*. There are two significant differences between this design basis and the basis for LRFR assessment presented here:

1. The original *Standard Specification* design uses H20 loading whereas the LRFR approach uses HL93 loading.
2. The calculation of moment distribution factors in the *Standard Specification* may result in lower distribution factors. In the prototype structure, the distribution factor prescribed by the *Standard Specification* - $(S/5.5)/2^5 = 0.66$ - is only marginally lower than that calculated in Step 2 (above).

This issue is not the focus of this work that addresses the repair of impact damage. This work presupposes that the undamaged girder/bridge is adequate. If this is not the case, some of the external repair approaches presented in this report may be appropriate for strengthening beyond the undamaged capacity.

EVAL.
MANUAL
T6A.4.2.2-1

EVAL.
MANUAL
Eq.
6A.4.2.1-1

⁵ *Standard Specification* distribution factors apply to wheel-line load; *LRFD* distribution factors apply to entire vehicle load; thus the additional factor of 0.5 must be applied for a direct comparison to be made.

<p>STEP 9: DAMAGED CAPACITY</p> <p>Determining the damaged capacity will follow the same procedure the nominal capacity, but will include the effects of the lost strands at the damaged section.</p> $f_{ps} = f_{pu} \left(1 - k \frac{c}{d_p} \right)$ <p>$f_{pu} = 270$ ksi and $k = 0.28$ for low lax strands $d_p =$ distance from extreme compression fiber to C.G. of prestressing tendons $d_p = 47 - 4.42 = 42.58$ in 8 strands (of 32) have been lost, therefore: $A_{ps} = 24 \times 0.153 = 3.67 \text{ in}^2$</p> $c = \frac{A_{ps} f_{ps} - A_s f_s - A'_s f'_s}{0.85 f'_c \beta_1 b + k A_{ps} \frac{f_{pu}}{d_p}} = \frac{3.67 \times 270 - 0}{0.85 \times 5.5 \times 0.78 \times 81 + 0.28 \times 3.67 \times \frac{270}{42.58}} = 3.28 \text{ in}$ <p>$a = \beta_1 c = 0.78 \times 3.28 = 2.56 \text{ in} < 7 \text{ in}$ Therefore, rectangular section behavior assumption is valid</p> $f_{ps} = 270 \left(1 - 0.28 \frac{3.28}{42.58} \right) = 264.2 \text{ ksi}$ $M_n = A_{ps} f_{ps} \left(d_p - \frac{a}{2} \right) = 3.67 \times 264.2 \left(42.58 - \frac{2.56}{2} \right) \times \frac{1}{12} = 3337 \text{ kft}$	<p>LRFD Eq. 5.7.3.1.1-1</p> <p>LRFD Eq. 5.7.3.1.1-4</p> <p>LRFD Eq. 5.7.3.2.2-1</p>
<p>STEP 10: LOAD RATING OF DAMAGED GIRDER, RF_D;</p> <p>Inventory:</p> $RF = \frac{\phi C - \gamma_{DC} DC - \gamma_{DW} DW \pm \gamma_P P}{\gamma_{LL} (LL + IM)} = \frac{3337 - 1.25(12959) - 1.50(141.6)}{1.75(1567)} = 0.55$ <p>Operating:</p> $RF = 0.55 \frac{1.75}{1.35} = 0.71 \leftarrow$	<p>EVAL. MANUAL Eq. 6A.4.2.1-1</p>

<p>Service III Limit State for Inventory Level:</p> $RF = \frac{f_R - (\gamma_D)(f_D)}{(\gamma_L)(f_{LL+IM})}$ <p>Flexural Resistance:</p> $f_R = f_{pb} + \text{allowable tensile stress}$ $\text{Allowable Tensile Stress} = 0.19\sqrt{f'_c} = 0.19\sqrt{6.8} = 0.50\text{ksi}$ $f_{pb} = 3.51 \text{ ksi}$ $f_R = 3.51 + 0.50 = 4.01 \text{ ksi}$ <p>Dead Load Stress:</p> $f_{DC} = \frac{1116.7 \times 12}{4848} + \frac{179.2 \times 12}{8758} = 3.01\text{ksi}; \quad f_{DW} = \frac{141.6 \times 12}{8655} = 0.20\text{ksi}$ $\text{Total } f_D = 3.21 \text{ ksi}$ <p>Live Load Stress:</p> $f_{LL} = \frac{1567 \times 12}{8655} = 2.17\text{ksi}$ $\gamma_L = 0.80; \gamma_D = 1.0$ $RF = \frac{4.01 - (1.0)(3.21)}{(0.8)(2.17)} = 0.46 < 1.0 \quad \text{NOT OK} \leftarrow$	<p>EVAL. MANUAL 6A.5.4.1</p> <p>LRFD T5.9.4.2.2-1</p>
<p>Legal Load Rating: Although this particular structure has all rating factors below unity, the example is continued in order to describe a repair methodology and subsequent re-rating of the repaired structure. The repair design proceeds as follows.</p>	
<p>STEP 11: VIABILITY OF EXTERNAL REPAIRS The residual capacity of the unstrengthened girder (i.e.: the damaged capacity C) should safely resist an expected nominal load. For an external repair to be viable:</p> $C \geq 1.1DC - 1.1DW - 0.75(LL + IM) = 1.1(1295.9) - 1.1(141.6) - 0.75(1567) = 2756.5\text{kft}$ $3337\text{kft} \geq 2756.5\text{kft} \quad \text{OK} \leftarrow$	<p>Eq. 3</p>

<p>STEP 12: DEFINE OBJECTIVE OF REPAIR</p> <p>Restore undamaged moment capacity: $M_n = 4397$ k-ft Capacity of damaged girder without repair: $M_{3-3,2} = 3337$ k-ft Capacity will be restored with the use of near surface mounted (NSM) FRP plates.</p> <p>All equation, figure and table references for NSM repair design are from ACI 440.2R-08, unless otherwise noted.</p>	
<p>STEP 13: ASSEMBLE BEAM PROPERTIES</p> <p>Assemble geometric and material properties for the beam and FRP system. If the section capacity does not meet the demand after the completion of all steps in this procedure, the FRP area is iterated upon.</p>	
$E_c = 4.85 \times 10^6 \text{ psi}$ $A_{cg,C} = 1062.5 \text{ in}^2$ $h = 47 \text{ in}$ $y_t = 15.8 \text{ in}$ $y_b = 31.2 \text{ in}$ $e = 26.75 \text{ in}$ $I_{x,C} = 269,785 \text{ in}^4$ $r = 15.93 \text{ in}$ $A_{ps} = 3.67 \text{ in}^2$ $E_{ps} = 28.5 \times 10^6 \text{ psi}$	$\epsilon_{pe} = 0.0054$ $P_e = 564,800 \text{ lb}$ $\text{cg strands} = 4.42 \text{ in}$ $d_p = 42.58 \text{ in}$ $E_f = 23.2 \times 10^6 \text{ psi}$ $A_f = 0.470 \text{ in}^2 \text{ (assumed)}$ $\epsilon_{fu} = 0.017 \text{ in/in}$ $f_{tu} = 406 \text{ ksi}$ $d_f = 46.75 \text{ in}$
<p>STEP 14: DETERMINE STATE OF STRAIN ON BEAM SOFFIT, AT TIME OF FRP INSTALLATION</p> <p>The existing strain on the beam soffit is calculated. It is assumed that the beam is uncracked and the only load applied at the time of FRP installation is dead load. M_D is changed to reflect a different moment applied during CFRP installation. If the beam is cracked, appropriate cracked section properties may be used. However, a cracked prestressed beam may not be a good candidate for repair due to the excessive loss of prestress required to result in cracking.</p> $\epsilon_{bi} = \frac{-P_e}{E_c A_{cg}} \left(1 + \frac{e y_b}{r^2} \right) + \frac{M_D y_b}{E_c I_g}$ $= \frac{-564800}{4.85 \times 10^6 \times 1062.5} \left(1 + \frac{26.75 \times 31.17}{(15.93)^2} \right) + \frac{(1437.5 \times 12000) \times 31.17}{4.85 \times 10^6 \times 269785} = -0.000 \text{ lin/in}$	
<p>STEP 15: ESTIMATE DEPTH TO NEUTRAL AXIS</p> <p>Any value can be assumed, but a reasonable initial estimate of c is $\sim 0.2h$. The value of c is adjusted to affect equilibrium.</p> $c = 0.2 \times 47 \text{ in} = 9.4 \text{ in}$	

<p>STEP 16: DETERMINE DESIGN STRAIN OF THE FRP SYSTEM</p> <p>The limiting strain in the FRP system is calculated based on three possible failure modes: FRP debonding (Sec. 10.1.1), FRP rupture (Eq. 10-16) and FRP strain corresponding to prestressing steel rupture (Eq. 10-17). The strain in the FRP system is limited to the minimum value obtained from (Eq. 10-2), (Eq. 10-16) and (Eq. 10-17).</p> <p>FRP Strain corresponding to FRP Debonding:</p> $k_m \varepsilon_{fu} = 0.70 \times 0.0145 = 0.0102 \text{ in/in}$ <p>FRP Strain corresponding to Concrete Crushing:</p> $\varepsilon_{fe} = \frac{\varepsilon_{cu}(d_f - c)}{c} - \varepsilon_{bi} = \frac{0.003 \times (46.75 - 9.4)}{9.4} - (-0.0001) = 0.0120 \text{ in/in} \leq k_m \varepsilon_{fd}$ <p>FRP Strain corresponding to PS Steel Rupture:</p> $\varepsilon_{fe} = \frac{(\varepsilon_{pu} - \varepsilon_{pi})(d_f - c)}{(d_p - c)} - \varepsilon_{bi} \leq \varepsilon_{fd}$ <p>where</p> $\varepsilon_{pi} = \frac{P_e}{E_p A_p} + \frac{P_e}{E_c A_c} \left(1 + \frac{e^2}{r^2} \right)$ $= \frac{564800}{28.5 \times 10^6 \times 3.67} + \frac{564800}{4.85 \times 10^6 \times 1062.5} \left(1 + \frac{(26.75)^2}{(15.93)^2} \right) = 0.0058 \text{ in/in}$ $\varepsilon_{fe} = \frac{(0.035 - 0.0058)(46.75 - 9.4)}{(42.58 - 9.4)} - (-0.0001) = 0.0330 \text{ in/in}$ <p>Therefore, the limiting strain in the FRP system is $\varepsilon_{fd} = 0.0102 \text{ in/in}$ and the anticipated mode of failure is FRP debonding.</p>	<p>ACI Section 10.1.1</p> <p>ACI Eq. 10-16</p> <p>ACI Eq. 10-17</p> <p>ACI Eq. 10-18</p>
<p>STEP 17: CALCULATE THE STRAIN IN THE EXISTING PRESTRESSING STEEL</p> <p>The strain in the prestressing steel can be calculated with the following expression:</p> $\varepsilon_{ps} = \varepsilon_{pe} + \frac{P_e}{E_c A_c} \left(1 + \frac{e^2}{r^2} \right) + \varepsilon_{pnet} \leq 0.035$ <p>Prestressing Steel Strain corresponding to concrete crushing:</p> $\varepsilon_{pnet} = 0.003 \frac{(d_p - c)}{c} = 0.003 \frac{(42.58 - 9.4)}{9.4} = 0.0106 \text{ in/in}$ $\varepsilon_{ps} = 0.0054 + \frac{564800}{4.85 \times 10^6 \times 1062.5} \times \left(1 + \frac{(26.75)^2}{(15.93)^2} \right) + 0.0106 = 0.0164 \text{ in/in} \leq 0.035$ <p>Prestressing Steel Strain corresponding to FRP rupture or debonding:</p> $\varepsilon_{pnet} = (\varepsilon_{fe} + \varepsilon_{bi}) \frac{(d_p - c)}{(d_f - c)} = (0.0102 - 0.0001) \frac{(42.58 - 9.4)}{(46.75 - 9.4)} = 0.0090 \text{ in/in}$ $\varepsilon_{ps} = 0.0054 + \frac{564800}{4.85 \times 10^6 \times 1062.5} \times \left(1 + \frac{(26.75)^2}{(15.93)^2} \right) + 0.0090 = 0.0148 \text{ in/in} \leq 0.035$ <p>Therefore, FRP debonding represents the expected failure mode of the system and $\varepsilon_{ps} = 0.0148 \text{ in/in}$.</p>	<p>ACI Eq. 10-22</p> <p>ACI Eq. 10-23a</p> <p>ACI Eq. 10-23b</p>

<p>STEP 18: CALCULATE STRESS LEVEL IN THE PRESTRESSING STEEL AND FRP</p> $f_{ps} = 28500 \times \epsilon_{ps} \quad (\text{when } \epsilon_{ps} \leq 0.0086)$ <p style="text-align: center;">or</p> $f_{ps} = 270 - \frac{0.04}{\epsilon_{ps} - 0.007} \quad (\text{when } \epsilon_{ps} \geq 0.0086)$ <p>$\epsilon_{ps} = 0.0145 > 0.0086$ therefore use $f_{ps} = 270 - \frac{0.04}{(0.0149) - 0.007} = 264.9 \text{ ksi}$</p> $f_{fe} = E_f \times \epsilon_{fe} = 23.2 \times 10^6 \times 0.0102 = 236.6 \text{ ksi} \leftarrow$	<p style="text-align: center;">ACI Eq. 10-24</p> <p style="text-align: center;">ACI Eq. 10-9</p>
<p>STEP 19: CALCULATE EQUIVALENT STRESS BLOCK PARAMETERS From strain compatibility, the strain in the concrete at failure can be calculated as:</p> $\epsilon_c = (\epsilon_{fe} + \epsilon_{bi}) \frac{c}{(d_f - c)} = (0.0102 - 0.0001) \times \frac{9.4}{46.75 - 9.4} = 0.0025 \text{ in/in}$ <p>The strain ϵ'_c corresponding to f'_c is calculated as:</p> $\epsilon'_c = \frac{1.7 f'_c}{E_c} = \frac{1.7 \times 5500}{4.85 \times 10^6} = 0.0019 \text{ in/in}$ <p>Using parabolic stress-strain relationship for concrete, the equivalent stress block factors can be calculated as:</p> $\beta_1 = \frac{4\epsilon'_c - \epsilon_c}{6\epsilon'_c - 2\epsilon_c} = \frac{4 \times 0.0019 - 0.0025}{6 \times 0.0019 - 2 \times 0.0025} = 0.797$ $\alpha_1 = \frac{3\epsilon'_c \epsilon_c - \epsilon_c^2}{3\beta_1 \epsilon_c'^2} = \frac{3 \times 0.0019 \times 0.0025 - (0.0025)^2}{3 \times 0.797 \times (0.0019)^2} = 0.927$	
<p>STEP 20: CALCULATE THE INTERNAL FORCE RESULTANTS</p> $c = \frac{A_p \times f_{ps} + A_f \times f_{fe}}{\alpha_1 \times f'_c \times \beta_1 \times b} = \frac{3.67 \times 264.7 + 0.470 \times 236.6}{0.927 \times (5500/1000) \times 0.797 \times 81} = 3.3 \text{ in} < 7 \text{ in} \leftarrow$	<p style="text-align: center;">ACI Eq. 10-25</p>
<p>STEP 21: ACHIEVE EQUILIBRIUM The value of c calculated in Step 20 must be equal to that of the c value assumed in Step 15. If not, the value of c must be iterated upon until these values are equal.</p> <p>By iteration, $c = 4.9 \text{ in.} \leftarrow$</p>	

STEP 22: CALCULATE THE FLEXURAL STRENGTH CORRESPONDING TO THE PRESTRESSING STEEL AND FRP COMPONENTS

The nominal capacity of the section is found as:

$$M_n = M_{np} = \psi M_{nf}$$

The corresponding contribution of prestressing steel and FRP, respectively, are found as:

$$M_{np} = A_p f_{ps} \left(d_p - \frac{\beta_1 c}{2} \right) = 3.67 \times 264.9 \times \left(42.58 - \frac{0.711 \times 4.9}{2} \right) = 39702 \text{ kin}$$

$$M_{nf} = A_f f_{fe} \left(d_f - \frac{\beta_1 c}{2} \right) = 0.470 \times 236.6 \times \left(46.75 - \frac{0.711 \times 4.9}{2} \right) = 5005 \text{ kin}$$

$$\psi = 0.85$$

The nominal section capacity of the *repaired girder* is:

$$M_n = M_{REP} = (39702 + (0.85)5005) \frac{1}{12} = 3663 \text{ kft} \leftarrow$$

ACI
Eq. 10-26

STEP 23: CALCULATE REPAIR RATING FACTOR, RF_R

The area of NSM CFRP provided, A_f , was maximized based on geometric constraints of the bottom flange. $M_{REP} = 3663 \text{ kft}$.

Inventory:

$$RF_R = \frac{\phi C - \gamma_{DC} DC - \gamma_{DW} DW \pm \gamma_P P}{\gamma_{LL} (LL + IM)} = \frac{3663 - 1.25(1295.9) - 1.50(141.6)}{1.75(1567)} = 0.67 \leftarrow$$

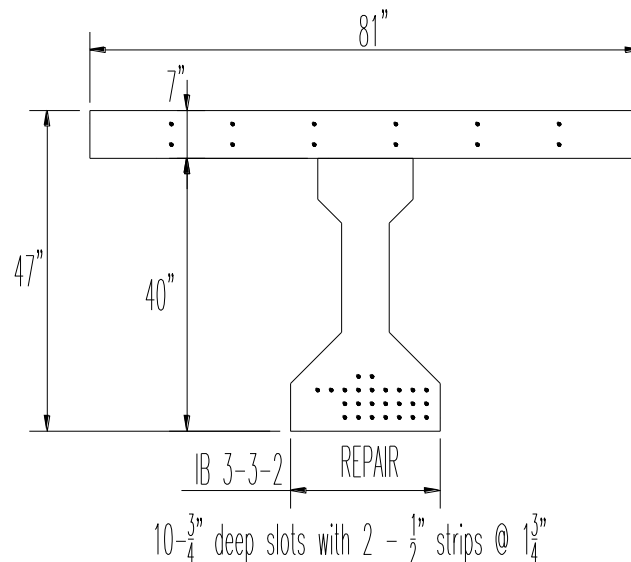
Operating:

$$RF_D = 0.67 \frac{1.75}{1.35} = 0.87 \leftarrow$$

Although this repair was not able to restore the undamaged girder capacity, it was able to restore 16% of the undamaged girder capacity.

STEP 24: DESIGN SUMMARY

Use 10 – 0.094 in wide x 0.500 in NSM CFRP strips.



APPENDIX D2 – IB 3-3-2 Hybrid Repair Design Example

The same IB prototype from Appendix D1 is used here to demonstrate the design of the hybrid repair, similar to that described by Yang et al (2011). The prototype IB structure is provided in Figure D1.

The calculations performed in the section use the properties of the IB prototype. Calculations pertaining to the demand on the girder, nominal capacity and effective prestress are the same as those in Appendix D1 (Steps 1-11). These Steps will not be repeated here; this example will commence at Step 12.

STEP 12: DEFINE OBJECTIVE OF REPAIR

Restore undamaged moment capacity: $M_n = 4397$ k-ft

Capacity of damaged girder without repair: $M_{3-3-2} = 3337$ k-ft

Strand splices are limited to 15% of the strands at any given section. Therefore, the use of strand splices will be limited to 5 (of 8) damaged strands (approximately 15% of the 32 strands in the section).

Prestressed strands will be restressed using strand splicing techniques (Section 2.3.2.4). Strand splices should be torqued to 3252 in-lbs, which induces a prestressing force of 28.9 kips in the strand (Grabb-it 2008). This torqued value corresponds to an induced prestress of $0.70f_{pu}$, sufficient to restore the *in situ* strand prestress ($0.52f_{pu}$).

Strand splicing effectively restores the strength of the strand to $0.85f_{pu}$. Therefore, at ultimate capacity, repairing 5 strands with strand splices effectively restores the equivalent of 4 complete strands ($5 \times 0.85 \sim 4$ strands). After strand splicing, the damage at this section corresponds to 4 strands total, or the 2-2-0 damage case. Therefore, the capacity of the section is calculated at this time in order to determine the capacity which must be restored by the CFRP fabric repair.

<p>STEP 13: CAPACITY AFTER STRAND SPLICE INSTALLATION</p> <p>Determining the member capacity will follow the same procedure the nominal capacity, but will include the effects of the lost strands at the damaged section and the repair of strands due to strand splicing.</p> <p>5 strands (of the 8 damaged) have been repaired and restressed due to strand splicing. However, due to the 15% reduction in capacity at ultimate, the 5 strands will be treated as equivalent to $5 \times 0.85 = 4$ strands being repaired, thus resulting in a section which has 4 strands lost. This section will be treated as a 2-2-0 damage.</p> $f_{ps} = f_{pu} \left(1 - k \frac{c}{d_p} \right)$ <p>$f_{pu} = 270$ ksi and $k = 0.28$ for low lax strands $d_p =$ distance from extreme compression fiber to C.G. of prestressing tendons $d_p = 47 - 4.4 = 42.6$ in</p> <p>4 strands (of 32) have been lost, therefore: $A_{ps} = (32-4) \times 0.153 = 4.28 \text{ in}^2$</p> $c = \frac{A_{ps} f_{ps} - A_s f_s - A_s' f_s'}{0.85 f_c' \beta_1 b + k A_{ps} \frac{f_{pu}}{d_p}} = \frac{4.28 \times 270 - 0}{0.85 \times 5.5 \times 0.78 \times 81 + 0.28 \times 4.28 \times \frac{270}{42.6}} = 3.8 \text{ in}$ <p>$a = \beta_1 c = 0.78 \times 3.8 = 3.0 \text{ in} < 7 \text{ in}$ Therefore, rectangular section behavior assumption is valid</p> $f_{ps} = 270 \left(1 - 0.28 \frac{3.8}{42.6} \right) = 263.3 \text{ ksi}$ $M_n = A_{ps} f_{ps} \left(d_p - \frac{a}{2} \right) = 4.28 \times 263.3 \left(42.6 - \frac{3.0}{2} \right) \times \frac{1}{12} = 3855 \text{ kft}$		<p>LRFD Eq. 5.7.3.1.1-1</p> <p>LRFD Eq. 5.7.3.1.1-4</p> <p>LRFD Eq. 5.7.3.2.2-1</p>
<p>STEP 14: DEFINE OBJECTIVE OF CFRP REPAIR</p> <p>Restore undamaged moment capacity: $M_n = 4397$ k-ft Capacity of damaged girder without CFRP repair: $M_{2-2-0} = 3855$ k-ft Capacity will be restored with the use of CFRP fabric.</p> <p>All equation, figure and table references for CFRP fabric design are from ACI 440.2R-08, unless otherwise noted.</p>		
<p>STEP 15: ASSEMBLE BEAM PROPERTIES</p> <p>Assemble geometric and material properties for the beam and FRP system. If the section capacity does not meet the demand after the completion of all steps in this procedure, the FRP area is iterated upon.</p>		
$E_c = 4.23 \times 10^6$ psi $A_{cg,C} = 1124.5$ in ² $h = 47$ in $y_t = 15.8$ in $y_b = 31.2$ in $e = 26.8$ in $I_{x,C} = 269,785$ in ⁴ $r = 15.9$ in $A_{ps} = 4.28$ in ² $E_{ps} = 28.5 \times 10^6$ psi $\epsilon_{pe} = 0.0049$	$P_e = 598,900$ lb cg strands = 4.4 in (based on 2-2-0 damage) $d_p = 42.6$ in (based on 2-2-0 damage) $f_{fu} = 123$ ksi $\epsilon_{fu} = 0.012$ in/in $n = 2$ layers $t_f = 0.04$ in. $A_f = 1.76$ in ² (assume using 2 layers, the entire width of the flange, 22 in.) $E_f = 10.3 \times 10^6$ psi $d_f = 47.02$ in	

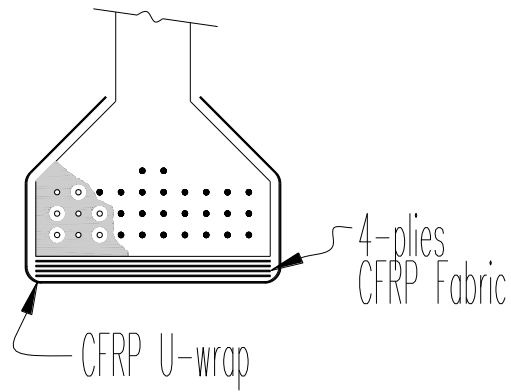
<p>STEP 16: DETERMINE STATE OF STRAIN ON BEAM SOFFIT, AT TIME OF FRP INSTALLATION</p> <p>The existing strain on the beam soffit is calculated. It is assumed that the beam is uncracked and the only load applied at the time of FRP installation is dead load. M_D is changed to reflect a different moment applied during CFRP installation. If the beam is cracked, appropriate cracked section properties may be used. However, a cracked prestressed beam may not be a good candidate for repair due to the excessive loss of prestress required to result in cracking.</p> $\epsilon_{bi} = \frac{-P_e}{E_c A_{cg}} \left(1 + \frac{e y_b}{r^2} \right) + \frac{M_D y_b}{E_c I_g}$ $= \frac{-598900}{4.23 \times 10^6 \times 1062.5} \left(1 + \frac{26.8 \times 31.2}{(15.9)^2} \right) + \frac{(1437.5 \times 12000) \times 31.2}{4.85 \times 10^6 \times 269785} = -0.000 \text{ lin/in}$	
<p>STEP 17: ESTIMATE DEPTH TO NEUTRAL AXIS</p> <p>Any value can be assumed, but a reasonable initial estimate of c is $\sim 0.1h$. The value of c is adjusted to affect equilibrium.</p> $c = 0.1 \times 47 \text{ in} = 4.7 \text{ in}$	
<p>STEP 18: DETERMINE DESIGN STRAIN OF THE FRP SYSTEM</p> <p>The limiting strain in the FRP system is calculated based on three possible failure modes: FRP debonding (Sec. 10.1.1), FRP rupture (Eq. 10-16) and FRP strain corresponding to prestressing steel rupture (Eq. 10-17). The strain in the FRP system is limited to the minimum value obtained from (Eq. 10-2), (Eq. 10-16) and (Eq. 10-17).</p> <p>FRP Strain corresponding to FRP Debonding:</p> $\epsilon_{fd} = 0.083 \sqrt{\frac{f'_c}{n E_f t_f}} = 0.083 \sqrt{\frac{6800}{2 \times 10.3 \times 10^6 \times 0.04}} = 0.0075 \text{ in / in}$ <p>FRP Strain corresponding to Concrete Crushing:</p> $\epsilon_{fe} = \frac{\epsilon_{cu} (d_f - c)}{c} - \epsilon_{bi} = \frac{0.003 \times (47.02 - 4.7)}{4.7} - (-0.0001) = 0.027 \text{ lin/in} \leq k_m \epsilon_{fd}$ <p>FRP Strain corresponding to PS Steel Rupture:</p> $\epsilon_{fe} = \frac{(\epsilon_{pu} - \epsilon_{pi})(d_f - c)}{(d_p - c)} - \epsilon_{bi} \leq \epsilon_{fd}$ <p>where</p> $\epsilon_{pi} = \frac{P_e}{E_p A_p} + \frac{P_e}{E_c A_c} \left(1 + \frac{e^2}{r^2} \right)$ $= \frac{598900}{28.5 \times 10^6 \times 4.28} + \frac{598900}{4.23 \times 10^6 \times 1062.5} \left(1 + \frac{(26.8)^2}{(15.9)^2} \right) = 0.0054 \text{ in/in}$ $\epsilon_{fe} = \frac{(0.035 - 0.0054)(4702 - 4.7)}{(42.6 - 4.7)} - (-0.0001) = 0.0332 \text{ in/in}$ <p>Therefore, the limiting strain in the FRP system is $\epsilon_{fd} = 0.0075 \text{ in/in}$ and the anticipated mode of failure is FRP debonding.</p>	<p>ACI Section 10.1.1</p> <p>ACI Eq. 10-16</p> <p>ACI Eq. 10-17</p> <p>ACI Eq. 10-18</p>

<p>STEP 19: CALCULATE THE STRAIN IN THE EXISTING PRESTRESSING STEEL</p> <p>The strain in the prestressing steel can be calculated with the following expression:</p> $\epsilon_{ps} = \epsilon_{pe} + \frac{P_e}{E_c A_c} \left(1 + \frac{e^2}{r^2} \right) + \epsilon_{pnet} \leq 0.035$ <p><i>Prestressing Steel Strain corresponding to concrete crushing:</i></p> $\epsilon_{pnet} = 0.003 \frac{(d_p - c)}{c} = 0.003 \frac{(42.6 - 4.7)}{4.7} = 0.0242 \text{ in / in}$ $\epsilon_{ps} = 0.0049 + \frac{598900}{4.23 \times 10^6 \times 10625} \times \left(1 + \frac{(26.8)^2}{(15.9)^2} \right) + 0.0242 = 0.0296 \text{ in / in} \leq 0.035$ <p><i>Prestressing Steel Strain corresponding to FRP rupture or debonding:</i></p> $\epsilon_{pnet} = (\epsilon_{fe} + \epsilon_{bi}) \frac{(d_p - c)}{(d_f - c)} = (0.0075 - 0.0001) \frac{(42.6 - 4.7)}{(47.04 - 4.7)} = 0.0067 \text{ in / in}$ $\epsilon_{ps} = 0.0049 + \frac{598900}{4.23 \times 10^6 \times 10625} \times \left(1 + \frac{(26.8)^2}{(15.9)^2} \right) + 0.0067 = 0.012 \text{ in / in} \leq 0.035$ <p>Therefore, FRP debonding represents the expected failure mode of the system and $\epsilon_{ps} = 0.0121 \text{ in/in}$.</p>	<p>ACI Eq. 10-22</p> <p>ACI Eq. 10-23a</p> <p>ACI Eq. 10-23b</p>
<p>STEP 20: CALCULATE STRESS LEVEL IN THE PRESTRESSING STEEL AND FRP</p> $f_{ps} = 28500 \times \epsilon_{ps} \quad (\text{when } \epsilon_{ps} \leq 0.0086)$ <p>or</p> $f_{ps} = 270 - \frac{0.04}{\epsilon_{ps} - 0.007} \quad (\text{when } \epsilon_{ps} \geq 0.0086)$ $\epsilon_{ps} = 0.0120 > 0.0086 \text{ therefore use } f_{ps} = 270 - \frac{0.04}{(0.0120) - 0.007} = 262.1 \text{ ksi}$ $f_{fe} = E_f \times \epsilon_{fe} = 10.3 \times 10^6 \times 0.0075 = 77.3 \text{ ksi} \leftarrow$	<p>ACI Eq. 10-24</p> <p>ACI Eq. 10-9</p>
<p>STEP 21: CALCULATE EQUIVALENT STRESS BLOCK PARAMETERS</p> <p>From strain compatibility, the strain in the concrete at failure can be calculated as:</p> $\epsilon_c = (\epsilon_{fe} + \epsilon_{bi}) \frac{c}{(d_f - c)} = (0.0075 - 0.0001) \times \frac{4.7}{47.04 - 4.7} = 0.0008 \text{ in / in}$ <p>The strain ϵ'_c corresponding to f'_c is calculated as:</p> $\epsilon'_c = \frac{1.7f'_c}{E_c} = \frac{1.7 \times 5500}{4.23 \times 10^6} = 0.0022 \text{ in / in}$ <p>Using parabolic stress-strain relationship for concrete, the equivalent stress block factors can be calculated as:</p> $\beta_1 = \frac{4\epsilon'_c - \epsilon_c}{6\epsilon'_c - 2\epsilon_c} = \frac{4 \times 0.0022 - 0.0008}{6 \times 0.0022 - 2 \times 0.0008} = 0.690$ $\alpha_1 = \frac{3\epsilon'_c \epsilon_c - \epsilon_c^2}{3\beta_1 \epsilon_c'^2} = \frac{3 \times 0.0022 \times 0.0008 - (0.0008)^2}{3 \times 0.690 \times (0.0022)^2} = 0.474$	

<p>STEP 22: CALCULATE THE INTERNAL FORCE RESULTANTS</p> $c = \frac{A_p \times f_{ps} + A_f \times f_{fe}}{\alpha_1 \times f'_c \times \beta_1 \times b} = \frac{4.28 \times 262.1 + 1.76 \times 77.3}{0.474 \times (5500/1000) \times 0.690 \times 81} = 14.7 \text{ in} \leftarrow$	<p>ACI Eq. 10-25</p>
<p>STEP 23: ACHIEVE EQUILIBRIUM</p> <p>The value of c calculated in Step 22 must be equal to that of the c value assumed in Step 17. If not, the value of c must be iterated upon until these values are equal.</p> <p>Upon iteration of c, flexural strength must be checked as in Step 24. If the calculated strength is not sufficient, the area of FRP reinforcement must be increased and Step 17 through Step 24 must be repeated, as is the case with this design. Therefore, A_f is increased to 3.520 in² (4-22in wide layers) and the process repeated.</p> <p>By iteration, c = 8.1 in. ←</p>	
<p>STEP 24: CALCULATE THE FLEXURAL STRENGTH CORRESPONDING TO THE PRESTRESSING STEEL AND FRP COMPONENTS</p> <p>The nominal capacity of the section is found as:</p> $M_n = M_{np} = \psi M_{nf}$ <p>The corresponding contribution of prestressing steel and FRP, respectively, are found as:</p> $M_{np} = A_p f_{ps} \left(d_p - \frac{\beta_1 c}{2} \right) = 4.28 \times 256.9 \times \left(42.6 - \frac{0.698 \times 8.1}{2} \right) = 43758 \text{ kin}$ $M_{nf} = A_f f_{fe} \left(d_f - \frac{\beta_1 c}{2} \right) = 3.520 \times 54.9 \times \left(47.08 - \frac{0.698 \times 8.1}{2} \right) = 8552 \text{ kin}$ $\psi = 0.85$ <p>The nominal section capacity of the <i>repaired girder</i> is:</p> $M_n = M_{REP} = (43758 + (0.85)8552) \frac{1}{12} = 4252 \text{ kft} \leftarrow$	<p>ACI Eq. 10-26</p>
<p>STEP 25: CALCULATE REPAIR RATING FACTOR, RF_R</p> <p>The area of CFRP provided, A_f, is adjusted and the procedure repeated until the desired flexural capacity is achieved. M_{REP} = 4252 kft.</p> <p>Inventory:</p> $RF_R = \frac{\phi C - \gamma_{DC} DC - \gamma_{DW} DW \pm \gamma_P P}{\gamma_{LL} (LL + IM)} = \frac{4252 - 1.25(1295.9) - 1.50(141.6)}{1.75(1567)} = 0.88 \leftarrow$ <p>Operating:</p> $RF_D = 0.88 \frac{1.75}{1.35} = 1.14 \leftarrow$ <p>Although this strand splice-CFRP fabric repair was not able to achieve an RF_R = 1.0, this repair was able restore 21% of the undamaged girder capacity.</p>	

STEP 26: DESIGN SUMMARY

Use 4 layers of 22in wide CFRP fabric.



APPENDIX D3 – IB 3-3-2 PT-Steel Design Example

The same IB prototype from Appendix D1 is used to demonstrate a PT-steel repair example. The prototype IB structure is provided in Figure D1.

The calculations performed in the section use the properties of the IB prototype. Therefore, calculations pertaining to the demand on the girder, nominal capacity and effective prestress are the same as those in Appendix D1 (Steps 1-11). These Steps will not be repeated here – this example will commence at Step 12.

<p>STEP 12: DEFINE OBJECTIVE OF REPAIR Restore undamaged moment capacity: $M_n = 4397$ k-ft Capacity of damaged girder without repair: $M_{3-3-2} = 3337$ k-ft</p> <p>Capacity will be restored with the use of post tensioned (PT) steel rods.</p>		
<p>STEP 13: ASSEMBLE BEAM PROPERTIES Assemble geometric and material properties for the beam and FRP system. If the section capacity does not meet the demand after the completion of all steps in this procedure, the FRP area is iterated upon.</p>		
<p> $E_c = 4.85 \times 10^6$ psi $A_{cg,C} = 1062.5$ in² $S_{b,C} = 8655$ in³ $I_{x,C} = 269,785$ in⁴ $h = 47$ in $y_t = 15.8$ in $y_b = 31.2$ in $r = 15.75$ in $E_{ps} = 28.5 \times 10^6$ psi $\epsilon_{pe} = 0.0049$ $A_{ps} = 4.90$ in² (undamaged) $e = 27.0$ in (undamaged) </p>	<p> $P_e = 684,460$ lb (undamaged) cg strands = 4.2 in (undamaged) $d_p = 42.6$ in $A_{ps} = 3.67$ in² (damaged) $P_e = 513,340$ lb (damaged) cg strands = 4.4 in (damaged) $e = 26.8$ in (damaged) $d_{PTsteel} = 32.0$ in (estimated) $e_{PT} = 16.2$ in </p>	

STEP 14: ESTABLISH TARGET STRESS INDUCED BY REPAIR

The goal of external steel post-tensioning is to restore the compressive stress in the bottom of the girder as intended by the original prestressed strands as well as increase the flexural capacity.

Analysis of the section after strand loss is done by sections analysis. Determine the amount of stress lost at the girder soffit due to the loss of strands:

$$\begin{aligned}
 f_{\text{loss}} &= \left(\frac{P}{A} + \frac{Pe}{S} - \frac{M_{DL}}{S} \right)_{\text{undamaged}} - \left(\frac{P}{A} + \frac{Pe}{S} - \frac{M_{DL}}{S} \right)_{\text{damaged}} \\
 &= \left(\frac{684460}{1124.5} + \frac{684460 \times 25.6}{9360} - \frac{1437.5 \times 12000}{9360} \right)_{\text{undamaged}} - \\
 &\quad \left(\frac{513340}{1124.5} + \frac{513340 \times 25.4}{9360} - \frac{1437.5 \times 12000}{9360} \right)_{\text{damaged}} \\
 &= (786.4 - 79.6) \times \frac{1}{1000} = 0.71 \text{ksi} \leftarrow
 \end{aligned}$$

It should be noted that the section modulus, S, and effective area, A, may be different for the undamaged and damaged terms particularly if the damaged girder is cracked under the influence of dead load (which is *not* the case in this example). The M_{DL} term is the moment due to girder dead load.

STEP 15: ESTABLISH REQUIRED PT FORCE

Determine the required force in the post tensioning steel needed to replace the lost strands:

$$\begin{aligned}
 f_{\text{loss}} &= \frac{P_{PT}}{A} + \frac{P_{PT}e_{PT}}{S} \\
 = 0.71 \text{ksi} &= \frac{P_{PT}}{1062.5} + \frac{P_{PT} \times 16.2}{8655} \rightarrow P_{PT} = 252.4 \text{kip} \leftarrow
 \end{aligned}$$

STEP 16: SELECT PT STEEL

PT force will be applied through high strength steel rods (Williams high strength threaded rods are selected for this example; this should not be implied as an endorsement of any kind). It is assumed that the PT steel rods will anchor a stress equal to 70% of its ultimate strength. Therefore, the area of PT steel required is:

$$A_{PT,req} = \frac{P_{PT}}{0.7 \times f_{puPT}} = \frac{252.4 \text{kip}}{0.7 \times 150 \text{ksi}} = 2.40 \text{in}^2$$

Using 1 in bars ($A = 0.85 \text{in}^2$), 3 bars will be required.

Using 1-1/4 in bars ($A = 1.25 \text{in}^2$), 2 bars will be required.

Using 1-3/8 in bars ($A = 1.58 \text{in}^2$), 2 bars will be required.

The PT steel bars will be located symmetrically about the girder web, thus multiples of two will be required for symmetry.

The nominal girder capacity (calculated in Step 17) is based on the area of steel provided. The use of two 1-1/4 in. diameter PT bars is not sufficient to restore the undamaged girder nominal capacity (despite its adequacy in restoring the lost prestressing force).

Therefore, to efficiently utilize material, two 1-3/8 in. diameter PT bars will be used in the design. The 1-3/8 in. diameter bars will be stressed to ensure the post tensioning force determined in Step 15 – 126 kips per bar or $0.53f_{pu}$ (after losses) is anchored.

STEP 17: REPAIRED CAPACITY

Determining the repaired capacity will follow the same procedure the nominal capacity, but will include the effects of the lost strands at the damaged section.

$$f_{ps} = f_{pu} \left(1 - k \frac{c}{d_p} \right)$$

For prestressed strands: $f_{pu} = 270$ ksi; $k_{ps} = 0.28$ for low lax strands; and $d_p = 47 - 4.4 = 42.6$ in; $A_{ps} = 24 \times 0.153 = 3.67 \text{ in}^2$

For high strength PT bars: $f_{pu} = 150$ ksi; $k_{PT} = 0.38$ for high strength bars (assumed Type 1 bar); and $d_{PT} = 47 - 15.0 = 32.0$ in; $A_{PT} = 2 \times 1.58 = 3.16 \text{ in}^2$

Leveraging LRFD Eq. 5.7.3.1.1-4:

$$c = \frac{A_{ps} f_{ps} + A_{PT} f_{PT}}{0.85 f'_c \beta_1 b + k_{ps} A_{ps} \frac{f_{pu}}{d_p} + k_{PT} A_{ps} \frac{f_{PT}}{d_{PT}}}$$

$$= \frac{3.67 \times 270 + 3.16 \times 150}{0.85 \times 5.5 \times 0.78 \times 81 + 0.28 \times 3.67 \times \frac{270}{42.6} + 0.38 \times 3.16 \times \frac{150}{32.0}} = 4.8 \text{ in}$$

$$a = \beta_1 c = 0.78 \times 4.8 = 3.7 \text{ in} < 7 \text{ in}$$

Therefore, rectangular section behavior assumption is valid

$$f_{ps} = 270 \left(1 - 0.28 \frac{4.8}{42.6} \right) = 261.5 \text{ ksi}$$

$$f_{PT} = 150 \left(1 - 0.38 \frac{4.8}{32.0} \right) = 141.5 \text{ ksi}$$

Leveraging LRFD Eq. 5.7.3.2.2-1:

$$M_n = A_{ps} f_{ps} \left(d_p - \frac{a}{2} \right) + A_{PT} f_{PT} \left(d_{PT} - \frac{a}{2} \right)$$

$$= \left[3.67 \times 261.5 \left(42.6 - \frac{3.7}{2} \right) + 3.16 \times 141.5 \left(36.0 - \frac{3.7}{2} \right) \right] \times \frac{1}{12} = 4532 \text{ kft}$$

STEP 18: CALCULATE REPAIR RATING FACTOR, RF_R

The area of CFRP provided, A_f , is adjusted and the procedure repeated until the desired flexural capacity is achieved. $M_R = 4532$ kft.

Inventory:

$$RF_R = \frac{\phi C - \gamma_{DC} DC - \gamma_{DW} DW \pm \gamma_P P}{\gamma_{LL} (LL + IM)} = \frac{4532 - 1.25(1295.9) - 1.50(141.6)}{1.75(1567)} = 0.98 \leftarrow$$

Operating:

$$RF_D = 0.98 \frac{1.75}{1.35} = 1.27 \leftarrow$$

Although PT steel repair was not able to achieve an $RF_R = 1.0$, this repair was able to restore the undamaged girder capacity plus an additional 3% above the undamaged girder capacity.

LRFD Eq.
5.7.3.1.1-1

STEP 19: PT STEEL ANCHORAGE

Design the bolster for the post-tensioning system. The bolster should be of sufficient capacity to anchor the induced PT forces (as determined in Step 15) and, in the event of overstress, f_{pu} of the post-tensioning bar. Therefore, in the event of overstress, the PT bar will fail prior to the bolster.

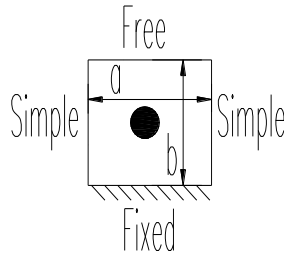
The bolster will be designed to withstand the PT bar stressed to f_{pu} (237 kips). A load factor of 1.2 will be used for the force in the PT bar, thus the anchorage will be designed for the PT force of 285 kips. A schematic of the proposed anchorage system is provided at the end of this example.

All plate stock considered in the bolster design is A36 steel ($F_y = 36$ ksi).

Design of Plate A

This plate will be designed to anchor a PT force = 285 k. Plate A is 6 in. x 6 in., the thickness needs to be determined.

The arrangement in Figure 38 suggests that Plate A can be analyzed as supported on its four edges as follows: fixed, simple, simple and free, as shown in the sketch below.



The stress in the plate may be calculated based on Table 26, Case 7a of *Roark's Formulas for Stress and Strain* (7th ed.)⁶:

$a = b = 6$ in, thus $a/b = 1$. From Table 26: $\beta_1 = 0.665$ and $\gamma_1 = 0.701$
 $q = 285.0/(6 \times 6) = 8.0$ ksi.

The maximum stress in the plate is determined as:
$$\sigma = \frac{\beta_1 q b^2}{t^2} = \frac{0.665 \times 8.0 \times 6^2}{t^2} = \frac{191}{t^2}$$

The stress in Plate A is limited to $\sigma = \phi F_y = 0.9(36) = 32.4$ ksi, thus $t \geq 2.43$ in.

Select $t = 2.5$ in. ←

The reaction at the fixed support is determined: $R = \gamma_1 q b = 0.701 \times 8.0 \times 6 = 33.6$ k/in

⁶ Young, W.C. 1989. *Roark's Formulas for Stress and Strain* (7th ed.), McGraw Hill, 763 pp.

Design of Plate B

Assume the thickness of Plate B, $t_B = 1.0$ in.

Transverse Post Tensioning

Using AASHTO LRFD (2011) Section 5.8.4.1, the nominal shear resistance of the interface plane shall be taken as (using Eq. 5.8.4.1-3):

$$V_{ni} = cA_{cv} + \mu(A_{vf}F_y + P_c)$$

Considering only the post tensioning force applied across the interface, P_c , $\mu = 0.7$ (Section 5.8.4.3); $\phi = 0.90$ (Section 5.5.4.2.1), the net compressive force, must be sufficient to resist the shear at this interface:

$$V_{ni} = 0 + 0.7(0 + P_c) = 285\text{k}$$

$$P_c = 407\text{ k}$$

Regardless of the PT member (strand or high strength bar), a maximum of $0.7f_{pu}$ can be anchored. Therefore, the area needed for this connection, $A_{TPT,req}$, is determined as follows:

$$P_c = \phi \times n \times 0.7f_{pu}$$

$$407 = 0.9 \times A_{TPT,req} \times 0.7 \times f_{pu}$$

$$A_{TPT,req} = 646 / f_{pu}$$

Using 150 ksi high strength bars: $A_{TPT,req} = 4.31$ in². Therefore, the use of 4-1.25 in diameter high strength bars ($A_{TPT} = 5.0$ in²), is sufficient.

Select 4-1.25 in diameter high strength bars $A_{TPT} = 5.0$ in². ←

Design of Plates C and D

Assume plates C and D carry 100% of the PT force and transmit this via shear to Plate B. Thus the shear capacity of the interface between C/D and B must exceed 285 k.

$$V = \phi L t 0.6 F_y \geq 285\text{ k}$$

with $L = 24$ in. (Figure 38) and $F_y = 36$ ksi, $t \geq 0.61$ in.

Select 5/8" plate for C and D

Check slenderness along leading edge of Plate C (AASHTO LRFD 6.14.2.8):

$$L_{\text{unsupported}} = 8.5\text{ in.}, t = 0.625; \lambda = 0.48 \sqrt{\frac{E}{F_y}} < 2.06 \sqrt{\frac{E}{F_y}} \dots \mathbf{OK} \leftarrow$$

Design Welds

Assuming E70XX fillet welds (1.39 k/in per sixteenth inch of weld).

The weld along Plate C/D can be determined as:

$$\frac{285.0k}{24in} = 11.9 k / in \text{ (required)}$$

$$11.9/1.39 = 8.6.$$

Use 9/16 in. fillet weld (or PJP weld) Plate C/D to A. ←

Use 3/8 in. fillet weld (or PJP weld) Plate C/D to B. ←

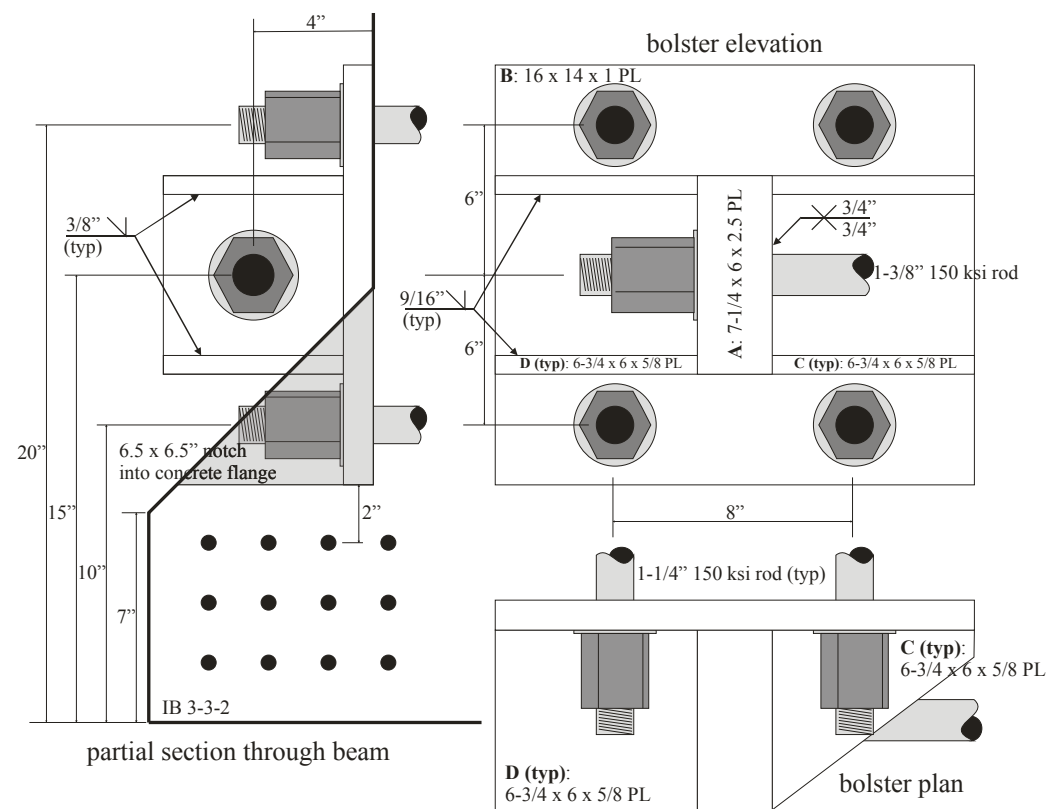
The weld along Plate B can be determined as:

$$\frac{33.6k/in}{2sides \times 1.39k/in} = 0.75 \text{ sixteenths of an inch of weld}$$

Use 3/4 in. fillet (or PJP weld) weld Plate B to A (both sides). ←

STEP 20: DESIGN SUMMARY

Use 2 – 1-3/8 in diameter, 150ksi high strength rods, stressed to $0.53f_{pu} = 126 k$.



APPENDIX E – Survey Responses

The cover letter on this page was distributed under University of Pittsburgh letterhead.

September 26, 2011

electronic transmission via NCHRP

THIS SURVEY IS DISTRIBUTED TO STATE/PROVINCIAL/JURISDICTIONAL BRIDGE ENGINEERS. IF IT IS MORE APPROPRIATE IN YOUR JURISDICTION FOR THE MAINTENANCE ENGINEERS TO RESPOND PLEASE FORWARD APPROPRIATELY

RE: REPAIR METHODS FOR IMPACT-DAMAGED PRESTRESSED CONCRETE BRIDGES – STATE OF PRACTICE SURVEY

The Structural Engineering and Mechanics Group in the Department of Civil Engineering at the University of Pittsburgh and the School of Advanced Structures at the University of Cincinnati, funded by National Cooperative Highway Research Program (NCHRP) Project 20-07, Task 307, is conducting a study aimed at establishing the state of practice for the repair of structurally damaged prestressed bridge elements.

Your assistance is requested in completing the attached survey. The objective of the survey is to establish the state of practice for the repair of structurally damaged prestressed bridge elements. This survey has been approved by NCHRP and the University of Pittsburgh Institutional Review Board and is being sent to all US State DOTs, Canadian Provincial MOTs and some other identified users.

Specifically, the survey respondent is asked to *please consider only prestressed or post-tensioned concrete bridge structures damaged once they have been placed into service in your jurisdiction. Do not consider fabrication, shipping or non-structural erection-induced damage to precast concrete elements.*

The survey responses will be tabulated and all identifying remarks stricken prior to any publication of results. In this way, presentation of the responses will be anonymous to all but the project PIs, the graduate students assisting with this project and the project oversight committee. Nonetheless, we ask that you provide your contact information so that we may “check off” your organization’s response and provide you a copy of the survey results.

We ask that you complete the survey, preferably electronically (the survey is provided in MSWord and Adobe PDF format for your convenience), and return it before **November 1, 2011** to:

Dr. Kent A. Harries, FACI, P.Eng.
kharries@pitt.edu
fax: 412.624.0135

Thank you for your assistance with this survey. Please feel free to contact me at any time.

Sincerely,

[signed]

Kent A. Harries, Ph.D., FACI, P.Eng.
Associate Professor

**State-of-Practice Survey
Repair Methods for Prestressed Concrete Bridges**

Survey completed by:

Name: _____ Title: _____
Jurisdiction: _____ email: _____
Address: _____ Telephone: _____

PLEASE RETURN COMPLETED SURVEY BEFORE NOVEMBER 1, 2011 TO:

Kent A. Harries
University of Pittsburgh
Civil and Environmental Engineering
949 Benedum Hall
Pittsburgh PA 15261
fax: (412) 624-0135
kharries@pitt.edu

Introduction

In responding to this survey, please consider only prestressed or post-tensioned concrete bridge structures damaged once they have been placed in service in your jurisdiction. Do not consider fabrication, shipping or non-structural erection-induced damage to precast concrete elements.

1. Plans and specifications for repair of damaged prestressed girders are usually prepared by (check all that apply):

22	DOT design/bridge engineer
7	DOT maintenance engineer
11	Private consultant
3	Standard details/specifications used
4	Other (please describe) _____

AR: AHTD has not yet had the opportunity to repair damaged prestressed girders once they have been put into service. AHTD has a limited number of these type bridges in its inventory.

CA: Bridge engineers who typically design only new structures are very rarely involved with the repair of existing structures. The State has four bridge maintenance design sections that are responsible for these types of repairs.

FL: Asset Maintenance Contractor

MD: The majority have been completed thru design/build process. Plans and specifications are available for review.

MT: Repairs by maintenance engineer, replacements by design engineers.

NV: Same methodology for developing repair details is used regardless of structure type. Question 3 answers applicable regardless of girder type. NDOT has not experienced damage on this structure type, in part because we have very few precast prestressed girder bridges. Survey responses not answered beyond Q 4 due to this fact.

2. Construction of repair is usually carried out by (check all that apply):

17	DOT/agency personnel
23	Private contractor
2	Other (please describe) _____

CA: DOT/agency personnel for minor patching only and private contractors for all else above minor patching.

FL: Asset Maintenance Contractor

MT: Repairs are done in-house, girder replacements are done by contractor.

TX: Most common to use contractor.

3. Rate the following factors by importance in the determination of the method or repair.

	low	moderate	high	not considered
Cost of repair	8	11	4	3
Time required to make repair	1	18	8	1
Aesthetics of repair	15	6	1	4
Interruption of service		8	17	1
Load capacity			26	1
Expected service life of repair	1	6	19	1
Maintenance required	6	10	7	2
Other, please specify:				1

4. Estimate the number of prestressed concrete bridges damaged in your jurisdiction over the last five years for the following degrees of damage:

	AK	AR	CA	FL	HI	IL	IA	KS*	LA	MD
Minor Damage	25	nr	numerous	100's	-	nr	many	3-6	10	nr
Moderate Damage	8	nr	0	50+	1	nr	14	2-4	15	nr
Significant Damage	6	nr	3	20+	1	nr	11	0-1	8	nr
Severe Damage	2	nr	1	5+	0	nr	7	0-1	5	nr
	MA	MS	MO	MT	NE	NH	NV	NJ*	NM	OK
Minor Damage	4	-	25	many	6	0	0	50	-	10
Moderate Damage	0	20	15	10	2	0	0	10	5	5
Significant Damage	3	6	5	8	2	0	0	5	5	3
Severe Damage	0	4	1	3	2	0	0	1	2	2
	PR	SD*	TX	UT	VA	WA	WI	WY*		
Minor Damage	-	3		10		5				
Moderate Damage	-	1	200	8	6	5				
Significant Damage	-	0	75	5	21	5				
Severe Damage	-	1	25	3	0	5	40			

Check here if your district does NOT track these damages:

	AK	AR	CA	FL	HI	IL	IA	KS*	LA	MD
Minor Damage	x				x	x	x		x	x
Moderate Damage	x					x			x	x
Significant Damage	x					x			x	x
Severe Damage	x					x			x	x
	MA	MS	MO	MT	NE	NH	NV	NJ*	NM	OK
Minor Damage		x	x	x		x			x	x
Moderate Damage			x			x				
Significant Damage			x			x				
Severe Damage			x			x				
	PR		SD*	TX	UT	VA	WA	WI	WY*	
Minor Damage	x			x		x		x		
Moderate Damage	x					x		x		
Significant Damage	x					x		x		
Severe Damage	x					x				

5. What actions are typically taken for the following degrees of damage (use damage definitions from Question 4)?

	no repair made	non-structural repair	load-carrying repair	replace member or structure
Minor damage	19	16		
Moderate damage	1	18	7	1
Significant damage	1	2	21	8
Severe damage	1		5	25

6. What are the typical causes of damage to prestressed concrete members that require repair action to be taken (check all that apply):

common	rare	
21	4	Vehicle impact
1	23	Corrosion occurring at unrepaired site of vehicle impact
10	13	Corrosion resulting from source other than vehicle impact
	21	Natural hazard (earthquake, hurricane/tornado, etc.)
1	21	Construction error (misplaced reinforcing steel, low strength concrete, etc.)
3	17	Nonspecific deterioration due to aging
	3	Other (please describe)

OK: strand debonding procedure has caused large spalls after beam is transported to beam site, this has not occurred in several years.

TX: Damage due to ASR.

7. In cases where repair action is eventually taken, what procedures are used to determine the extent of the damage?

commonly	rarely	
25		Visual inspection only
3	17	Non destructive evaluation (NDE/NDT); which methods are typically used?

HI: We've only used visual for the few damaged PS girders.

IA: Hammer sounding and NDT - physical load testing

NJ*: NDT has not been used in recent past, but would be considered.

SD*: Sounding with hammer.

WA: Impact hammer

3	12	Destructive evaluation; which destructive methods are typically used?
---	----	-----------------------------------------------------------------------

IA: Removal of delaminated concrete.

MD: Physically evaluate strand condition.

NE: Sounding the concrete

NM: Chip carefully around exposed tendons and stirrups to see if additional repairs are needed for the tendons and stirrups.

WA: Remove damaged portion of the girder and evaluate forces in strands.

		Other (please describe)
--	--	-------------------------

8. Briefly describe what analytical procedures are used to assess the damage and the need for repair of prestressed concrete elements (include names of software if appropriate)

AK: Engineer developed spread sheets

CA: Caltrans' proprietary CT Bridge, PS Girder, NCHRP Reports 226 and 280.

FL: If there is major damage where tendons are broken and/or there is major section loss, a load rating is performed. Based on the level of capacity loss it is determined the repair or beam replacement plan.

HI: Only if strands have visually been assessed to have section loss would be re-analyze the element for its carrying capacity and its impact to the bridge as a whole.

IL: If strands are intact we normally just determine section modulus change due to concrete loss. If strands are damaged, we run in-house developed spreadsheets to determine capacity loss due to loss of prestress.

IA: A Load Factor analysis for the operating capacity is performed. The damaged strands are considered non-effective for the analysis. The LARS software program is used to determine the remaining capacity at the location of the damage. If the damage has occurred in a high shear zone, a hand calculation of the shear capacity will be made.

KS*: Load rate VITIS/OPIS or STAAD model.

LA: LEAP-Conspan and LUSAS-Structural Analysis.

MD: SHA uses the software CONSPAN and Merlin DASH to perform load ratings of prestressed concrete bridges damages. The strand loss assumptions are made based on field conditions guidelines, like PennDOT Publication 238 Part IE, Chapter 6 Section 6.6.3.3.11 and Illinois DOT's report entitled "Inspection and Rating of PPC Deck Beam Bridges". Strengthening measures are designed to restore the members to as-built capacities when possible using externally bonded FRP products.

MA: A rerating of the damaged member(s) is made using our standard bridge rating software, AASHTOWare, Virtis, subtracting the lost section and strands. If there is enough remaining capacity, no repairs are done. If there is loss of capacity below inventory levels, the bridge is posted or the member (especially if it is an exterior member) is isolated by putting barriers on the roadway to keep Traffic off that member. In these cases, we would replace this member as part of the accident recovery process.

MS: We do not use any software to determine whether or not a prestressed concrete girder can be repaired or replaced. We visually inspect the girder and if 2 or less strands are damaged then we repair it. If 3 or more are damaged we typically replace the girder.

MT: Load rating is done using Virtis to determine the remaining capacity the beam has with the number of undamaged strands.

NE: From the analysis point of view we use rating program (LARS or Virtis). The first goal is to restore the original inventory load rating (e.i restoring the stresses to the original design) or restoring the operating capacity (e.i analyze the girder as reinforced concrete as a cracked section at ultimate ignoring the stresses this will determine the repair procedures whether splice and preload the section or splice only or just patch.

NH: Haven't had any major damage to our prestressed/post-tensioned members so haven't had to do any analytical analysis of them.

NJ*: A calculation would be performed assessing the loss of prestressing forces which has occurred due to exposed, de-bonded or broken tendons along with the loss of concrete section at the various locations of impact. The load carrying capacity would be assessed to determine what type of repair is necessary or if complete member or superstructure replacement is required.

NM: If tendons or stirrups are cut, a Virtis model is developed to determine if the load carrying capacity is affected by cut tendons or stirrups.

PR*: Damage to prestressed concrete elements is commonly assessed by visual inspection. Members (Beams) are commonly replaced by prestressed or steel beams.

OK: When strands are cut, we do analysis to determine the capacity of the beam. We use an in-house spread sheet.

SD*: Loss of strand embedment/anchorage and load capacity.

TX: We use our prestressed beam design software (PS14, PGSuper, or in-house load rating spreadsheet) to determine the operating rating or capacity for the girder assuming that the damaged strands are ineffective. If the resulting capacity has an Operating RF >1.0 or the resulting load rating >HS20, we do a non-structural repair. If the OR RF <1.0 or the OR LR <HS20, we do a structural repair to restore the capacity to RF = 1.) or LR = HS20.

UT: Use current design software to analyze with reduced prestress force to determine required extent of repair or replacement of girder.

VA: Check the effect of damage on load carrying capacity of the prestressed beam using VIRTIS or CONSPAN programs depending on the analysis needed. Load rating under the assumption that the broken/exposed strands are no longer functional. BARS and VIRTIS programs used along with long-hand analysis. Capacity analysis taking into account section loss using load rating such as VIRTIS.

WA: Long hand design/calculations, finite element modeling with SAP 2000 and verified with the PGSuper program.

WI: Primarily use in-house software & hand-calcs (if necessary) to determine need for repair.

9. Methods of repair of MINOR damage (concrete cracks and nicks; shallow spalls and scrapes not affecting tendons) used are (check all that apply):

common	rare	
22	3	Do nothing
7	11	Repaint surface
12	9	Patch concrete
	1	Other (please describe)

IA: Apply concrete sealer to spalls and scrapes.

10. Methods of repair of MODERATE damage (large concrete cracks and spalls; exposed, undamaged tendons) used are (check all that apply):

common	rare	
1	16	Do nothing
23	1	Patch concrete
17	5	Epoxy injection
22		Concrete removal/surface preparation prior to patching
17	3	Clean tendons
3	12	Installation of active or passive corrosion control measures
1		Other (please describe)

AK: Apply zinc rich coating to exposed tendons

MD: If CFRP is being installed at the site, these beams would be repaired similarly.

MA: Paint exposed tendons with epoxy paint.

NM: Corrosion is not a big issue in NM as the climate/weather is dry most of the year.

OK: Wrap with FRP.

UT: Always clean tendons, epoxy inject and patch to repair.

11. Methods of repair of SIGNIFICANT damage (exposed and damaged tendons; loss of portion of cross section) used are (check all that apply):

common rare

		Repair of tendons					
7	12	Cut tendons flush with damaged section (no tendon repair)					
	17	External post-tensioning					
6	11	Internal splices (describe below)	...is repair re-stressed?	yes	<input type="text" value="7"/>	no	<input type="text" value="3"/>
5	11	Metal sleeve splice	...is repair re-stressed?	yes	<input type="text" value="2"/>	no	<input type="text" value="5"/>
2	11	Combination splice (describe below)	...is repair re-stressed?	yes	<input type="text"/>	no	<input type="text" value="3"/>
9	11	Externally applied reinforcing material (FRP, etc.) (describe below)					
2	16	Installation of active or passive corrosion control measures					
4		Other (please describe)					

AK: Damaged sections of tendons are removed and the tendon is reattached with Grabb-it Cable Splices.

IL: We normally preload the damaged beam prior to patching to ensure patch will be in compression under live load traffic.

LA: Girder replacement.

MD: SHA has issued projects to install CFRP for repair/strengthening on several bridges.

MS: We visually inspect the girder and if 2 or less strands are damaged then we repair it. If 3 or more are damaged we typically replace the girder.

NM: Grab-It anchors have been used to resplice cut tendons. CFRP has been used as well for flexure/moment strengthening.

OK: Splice strands back together and splice.

UT: Turnbuckle type splice hand cranked tight.

		Repair of concrete					
21	1	Concrete removal/surface preparation prior to patching					
20	1	Patch concrete	...is girder preloaded to induce compression in patch?	yes	<input type="text" value="9"/>	no	<input type="text" value="8"/>
14	6	Epoxy injection					
1	2	Other (please describe)					

TX: CFRP.

9	13	Replace individual girder
3	15	Replace bridge

Please describe methods used (Question 11)

AK: See attached repair procedures

CA: Remove unsound concrete, splice and tension broken internal strands, apply vehicle preload, epoxy inject cracks, recast removed portion of bottom flange and/or web, remove vehicle preload after the concrete has reached the required strength.

HI: The only bridge which has significant damage to PS girders will be replaced. (this is NOT included in the 'replace bridge' row above.

IA: Metal sleeve is installed over restored cross section on bridges that get hit repeatedly. Void between sleeve & beam is filled by injecting epoxy resin. Sleeve provided no capacity improvement; only provides stiffness and some protection for next impact. FRP applied over restored cross section to provide confinement to repaired area. Provides no structural capacity. Occasionally, we use FRP plates for capacity improvement. Remove spalled and delaminated concrete using hand tools or 15 lb chipping hammer. If removal results in more than ½ diameter of bar or strand being exposed continue removal to min ¾" behind bar or strand. Saw cut edges of removal area ½" deep and chip square. Clean repair area by sandblast or hydroblast. Apply corrosion inhibitor to bars and strands. Patch area as either Shallow Repair (no bar/strand exposed for more than ½ diameter or patch depth < 1 ½") or Regular Repair (removal extends behind bar/strand or patch depth >1 ½"). Corrosion inhibitor added to patch materials.

IL*: Damaged area of the beam shall be cleaned of all loose and spalled concrete and sealant. Any exposed portions of the strands shall be sandblasted. Remove the existing concrete to sound concrete along the edges of the damaged area to a depth of 1" min. to 1 ½" max. Power driven pins shall be placed at 9" alternate centers along the damaged length of the beam. Where strands are exposed, place 1" x 1" x 18 gauge welded wire fabric in repair area and attach it to the pins or strands with wire ties with 1" minimum clearance between the finished surface of the new concrete and the welded wire mesh. All surfaces of existing concrete and reinforcing strands in the area to be repaired shall be coated with an epoxy-resin primer bonding agent. The repair shall be made using concrete meeting all the requirements for Class PS Concrete for precast prestressed concrete members, except the maximum size of the aggregate shall be ½". Place the lower form on the bottom of the beam and compact by vibrating (or other approved methods) the concrete mix into the voids. After accessible voids have been filled and compacted, the top vertical form shall be raised into position and the remaining voids filled and compacted. The sloping upper surface shall be finished to the configuration of the existing PPC-I Beam Flange. Note: Preload system shall be in place during the repair and curing period.

MD: Most of the SHA prestressed repair projects have been design/build for CFRP installation, where the concrete surface preparation and CFRP installation have been completed in accordance with manufacturer's recommendations, based on the contractor's selection of a manufacturer. The Contractor designs the number of layers, fiber orientation, etc. and we stipulate the minimum material properties and require that the contractor at minimum comply with NCHRP Report 609.

MA: Replace bridge if many beams are damaged with significant loss of capacity.

MT: After performing an onsite assessment and later, an analysis of the beam, and it is determined that the beam is repairable by "in-house" resources, the following basic outline for repair is followed: Saw cut ½" deep around the extent of the crushed/damaged concrete. Remove all loose and damaged concrete down to sound concrete. Repair tendons, if needed. Sandblast repair area. Form up the repair area.

Condition concrete to SSD. Preload the beam. Pour/pump repair concrete into form. 4 to 6 hours after completion of concrete pour, remove preload. Remove forms. Clean the surface of the beam along all cracks with a dry brush/rag. Blow beam/cracks clean of dust with clean compressed air. Apply epoxy injection ports to cracks. Seal cracks with epoxy paste. Inject epoxy into beam. 2 to 4 hours later, remove epoxy ports. Minor aesthetic touch up to the beam is done, but generally very little time is spent making the beam look “good”. Depending on the extent of damage, an average repair using MDT resources (MDT Maintenance personnel and equipment) will take 50 to 100+ man-hours.

NJ*: Severed tendons would typically be cut flush with the remaining sound concrete and the concrete patched in-kind if the analysis indicates that sufficient load carrying capacity remains in the damaged member. If adequate load carrying capacity does not remain, then replacement of the member is the typical option. I have never seen a member where the tendons have been repaired in NJ.

NM: Remove concrete with neat line cuts (3/4” max) around damaged area. Remove at least 3/4” around the exposed tendons and stirrups in order to get a full concrete bond around the tendons and stirrups. Preload the bridge (typically with temporary concrete barrier segments), couple the tendons and patch the concrete. Remove the barrier segments after the concrete has reached its design strength.

SD*: Removal of delaminated concrete that is unsound. Splice any cut or damaged tendons. Repair concrete spalls and delaminated areas. Apply load to girder prior to concrete repair if needed. Epoxy injection repair of cracks in girder.

TX: Most common repair for significant damage involves epoxy injection of cracks, strand splicing and re-tensioning, concrete repair with load placed on bridge, and (optional) CFRP strengthening.

UT: Turnbuckle type splice for as many tendons as room will allow. Epoxy inject and patch concrete to prevent corrosion.

WA: Grabb-it cable splice.

12. Methods of repair of SEVERE damage (damage severe enough to result in girder distortion or misalignment) used are (check all that apply):

common rare

		Repair of distortion/misalignment
	14	External post-tensioning
1	13	Jacking and re-use of damaged member
12	5	Jacking and replacement of damaged member
1	12	Provision of new/additional permanent supports (extended corbels, etc.)
1		Other (please describe)

MD: In the few instances where this level of defect has been observed, the bridges were replaced.

MS: We classify severe as 3 or more strands severed in which case the girder is replaced.

NM: For severe damage, through common sense and engineering judgment tells us to replace the damaged member rather than try and repair it. In the long run, a new member would serve better. Also, we have 2 fabricators of prestressed girders in our state, therefore the cost of a new girder is cheap.

		Repair of tendons		
2	11	Cut tendons flush with damaged section (no tendon repair)		
	13	External post-tensioning		
2	10	Internal splices (describe below)	...is repair re-stressed?	yes <input type="checkbox"/> no <input type="checkbox"/>
1	10	Metal sleeve splice	...is repair re-stressed?	yes <input type="checkbox"/> no <input type="checkbox"/>
1	10	Combination splice (describe below)	...is repair re-stressed?	yes <input type="checkbox"/> no <input type="checkbox"/>
1	12	Externally applied reinforcing material (FRP, etc.) (describe below)		
	11	Installation of active or passive corrosion control measures		
1		Other (please describe)		

MD: Replace the bridge.

MS: Girder is replaced.

NM: We do not attempt to try and repair severely damaged members.

UT: Turnbuckle type splice hand cranked tight.

		Repair of concrete		
6	8	Concrete removal/surface preparation prior to patching		
5	8	Patch concrete	...is girder preloaded to induce compression in patch?	yes <input type="checkbox"/> no <input type="checkbox"/>
5	9	Epoxy injection		
4		Other (please describe)		

MD: Replace the bridge.

MS: Girder is replaced.

NM: We do not attempt to try and repair severely damaged members.

20	2	Replace individual girder
5	12	Replace bridge

Please describe methods used (Question 12)

CA: The repair strategy used on the one structure in the last five years with severe damage was a combination of replacing the damaged exterior girders (*severe damage*) and removing and repairing damaged concrete as well as strengthening the girder with FRP reinforcement of selected interior girders (*moderate damage*).

HI: We have not had this type of damage to date. Depending on the severity and percentage of girders damage in the span(s), the individual girder would be replaced or the entire bridge replaced.

MD: In the few instances when severe defects have been observed, these bridges have been replaced.

MA: Replace bridge if many beams are damaged with significant loss of capacity.

MS: Girder is replaced not repaired.

MT: Once it is determined that the girder is not repairable, the district bridge design engineer does the design for a new girder and a project is let to an independent construction contractor.

NE: We have restored and repaired a severely damaged girder to the original inventory level by doing the following steps: preloaded the bridge /girder; splice the strands with sleeve; tensioned the strands and patch the concrete and; unload the girder.

NJ*: For this type damage, repair of the damaged members is not usually considered due to a question of reliability of the repaired member. We would typically replace a member (or maybe 2 members), if the damage is localized. If several members have been impacted, then we would typically replace the entire superstructure.

NM: Remove the portion of concrete deck over the damaged member through neat line cuts (3/4" maximum depth sawcuts). Remove and replace damaged girder with new girder. Place rebar and cast new concrete deck over new girder.

OK: Replace the girder requires deck replacement.

SD*: Same methods described for Question 11 for repair. When replacing an individual girder, diaphragm, partial deck and rail are removed. Replacement girder is put in-place, diaphragm, deck and rail replaced.

TX: For severe damage most common repair is to replace the damaged girder(s).

UT: Turnbuckle type splice for as many tendons as room will allow. Epoxy inject and patch concrete in order to prevent corrosion. Girder replacement required if damaged beyond repair.

WA: Grabb-It cable splice.

13. How well do your prescribed repair methods perform? Please identify problems and/or successes experienced in the repair of damaged prestressed concrete bridge elements in your jurisdiction.

AK: Concrete patches adhere well to existing concrete. Subsequent damage at the same location, including both spalls and cracks, penetrate through the patch interface not just along the perimeter of the previous damage. Some prestressing tendons that are exposed after multiple impacts have surface rust. In a few cases this surface rust developed small, less than one thirty second inch deep pits in the tendon.

CA: FRP strengthening combined with exterior girder replacement mentioned above not going out to bid until early 2012. The other two repair jobs in southern California have had no maintenance problems since being repaired. Both of these Significant damage repairs are considered to be a success.

FL*: We have found that FRP repairs are particularly effective. Repairs with girders loaded also works well.

HI: Only repairs we have performed on PS girders have been for concrete and not strands/tendons.

KS*: If in question remove and replace girder.

IL: Patching of PPCI beam without the benefit of preloading does not hold well under traffic. Use of FRP wraps might help in preserving the patch. Patching using preloading seems to be performing very well with patches holding without apparent further distress. One of the issues to consider is the ability to place the appropriate preloading on the beam particularly in fascia beams under a parapet where it is hard to get sufficient loading on the beam being repaired.

IA: We feel our methods are performing satisfactorily.

LA: Our most common method used recently is replacement of the existing girders when a strand has been severed.

MD: Our current practices for repairs to prestressed concrete bridges are relatively new, and therefore we have little historical records for these types of repairs. We have repaired some bridge with concrete patching only, and these repairs survived for approximately 15 years on average and did little to prevent additional spread of corrosion of the strands. As a comment to question 4, we have started categorizing beam defects and are beginning to track the condition of our inventory of prestressed structures. We have advertised several large projects to repair prestressed concrete beams and columns using concrete repairs and surface preparation in conjunction with CFRP installation.

MS: Since most of our repairs are of the patching variety they have performed well. Most often the patched girder will perform well unless the girder is struck again. We do not repair our prestressed girders that have significant damage and severed strands. We typically replace them if three or more strands are severed. All other damage is repaired by patching and epoxy injecting.

MO: The methods we use to repair moderately and significantly damaged prestressed members perform well. They allow us to put a bridge back into service at its pre-incident capacity and do not require future maintenance. For severely damaged members, our replacement philosophy eliminates any concern with a repair of such magnitude.

MT: No problems have been documented. Some beams have been hit multiple times, with no corrosion of the strands evident between impacts. Repaired areas of girders generally perform similarly to non-repaired girders when impacted.

NE: The repair was done about three years ago. So far the girder seems to function as expected. No cracks or concrete discolor is visible.

NH: Since NHDOT hasn't had any major damage to our prestressed/post-tensioned members the minor patching that has been done due to scrapes and spalls has worked well.

NJ*: Our repair methods are conservative since we don't typically attempt to repair badly damaged members using post-tensioning or splicing of tendons. That being said, we have not had any performance problems on the damaged girders that have been repaired.

NM: We have had good success repairing minor, moderate and significantly damaged girders. Repairs over 5 years old have held up well. For severely damaged girders, we replace it with a new girder. We have 2 fabricators of prestressed girders in our State; therefore the cost of replacing a girder is not significant. Repairing or replacing damaged girders is not difficult to do, especially when you have experienced design staff, construction staff and contractors doing the job for you. Prestressed girder bridges are predominant in our State.

OK: Most beam impacts produce moderate damage and just spall off a chunk of concrete usually exposing strands. We patch, apply an inhibitor product, then wrap with a Carbon FRP to keep moisture out, to keep the patch from falling on the roadway below, and to strengthen the repair. The older repairs used an E-glass FRP.

PR*: The PRHTA use to replace ONLY prestressed beams with severe damage when the rest of the bridge is in an acceptable condition. When the prestressed bridge has a low rating, the bridge is replaced.

SD*: Repairs have been successful to date. Not aware of any situations where we had to go in and fix a repair area again, unless it was damaged from another over-height impact.

TX: Our repair methods hold up very well. We've had repaired girders hit again and they not only survived but the damage was in a new location meaning our repairs were stronger than the original girder.

UT: Replacement always works well. FRP wrap seems to work well and helps keep patches in place. Patches sometimes fail. Internal splices work well. However you are limited on space, for instance if 5 tendons are cut would probably only have space to splice 3.

WA: Perform well and are durable. WSDOT has a policy in place for repair of damaged prestressed girders. See below for WSDOT Policy.

** responses from 2008 version of survey*

